

Alma Mater Studiorum – Università di Bologna

DOTTORATO DI RICERCA IN

**Scienze Chimiche**

Ciclo XXVII

Settore Concorsuale di afferenza: **03/C1**

Settore Scientifico disciplinare: **CHIM/06**

**INNOVATIVE ASYMMETRIC  
ORGANOCATALYTIC PROCESSES: EN ROUTE  
TO THE SYNTHESIS OF BIOLOGICALLY  
RELEVANT COMPOUNDS**

Presentata da: **Lorenzo Caruana**

Coordinatore Dottorato

**Prof. Aldo Roda**

Relatore

**Prof. Luca Bernardi**

Corelatore

**Prof.ssa Mariafrancesca Fochi**

ESAME FINALE ANNO 2015



**Dottorando:** *Lorenzo Caruana*  
**Tutor:** *Prof. Luca Bernardi*  
**Co-tutor:** *Prof.ssa Mariafrancesca Fochi*

*Curriculum: Scienze Chimiche*  
*Indirizzo: Metodologie di catalisi organica*

**Titolo tesi:** *INNOVATIVE ASYMMETRIC ORGANOCATALYTIC PROCESSES: EN ROUTE TO THE SYNTHESIS OF BIOLOGICALLY RELEVANT COMPOUNDS*

The PhD candidate Lorenzo Caruana has carried out his research activities at the Department of Industrial Chemistry “Toso Montanari”. Between the second and the third year of his doctorate, with the additional support of a “Marco Polo” fellowship, he spent ten months at the Department of Chemistry of the University of Aarhus (DK), joining the laboratory directed by Prof. Karl Anker Jørgensen.

During his doctorate, Lorenzo has worked on the development of new synthetic methodologies in organic chemistry, disclosing new asymmetric transformations and reactivity patterns based on the use of simple organic molecules as catalysts (asymmetric organocatalysis). His work included the discovery of new reactions, the thorough optimization of the many reaction parameters, the multi-step syntheses of complex catalysts and/or substrates, the full characterization (structural and stereochemical) of the products, as well as the performance of synthetic elaborations illustrating the usefulness of the developed methods.

Starting a PhD in organic chemistry with a different background (he had graduated in Industrial Chemistry working on silica nanoparticles), Lorenzo has shown since the beginning an outstanding resolution in learning the different aspects of organic synthesis and asymmetric catalysis. Not only was he able to master very quickly the necessary laboratory and analytical techniques, but also to tackle impending challenges with uncommon determination, coming up with his own original and innovative solutions. He has demonstrated great commitment to the research work, combined with passion, enthusiasm and creativity. Not less important, he has been able to rationalize and present his results in a very clear and understandable fashion, in both oral and written form, in both Italian and English languages. During his doctorate, Lorenzo has achieved remarkable and highly valuable results which have been the subject of several publications in highly rated international chemistry journals (JACS, ChemComm etc.). Some of these contributions have been highlighted in Synfacts, testifying their importance and impact on the scientific community. Besides, some of these disclosures were presented by Lorenzo as poster or oral communications in three international and several local conferences/summer schools. Notably, he received a “best poster” and a “best oral communication” award in two of the international events.

In addition, Lorenzo has shown very good personality and capability of working in teams. In Bologna, he has demonstrated good attitude as supervisor of less experienced undergraduate students (one bachelor and one master), whereas in Aarhus he has proven to be an exceptional co-worker for more experienced post-doctoral colleagues.

While considering Lorenzo mature and fully educated as a researcher, ready to be awarded the title of doctor of science and to take up new exciting challenges, we can certainly evaluate his PhD work as “*excellent*”.

*The Board expresses a score of excellence on the activity carried out by the candidate during the whole cycle of doctorate and considers him worthy to attain the PhD in Chemistry*

Bologna, 11/02/2015  
Prof. Luca Bernardi and Mariafrancesca Fochi



## List of publications

- Caruana, L.; Costa, A. L.; Cassani, M. C.; Rampazzo, E.; Prodi, L.; Zaccheroni, N. "Tailored SiO<sub>2</sub>-based coatings for dye doped superparamagnetic nanocomposites" *Colloids Surf. A* **2012**, *410*, 111.
- Caruana, L.; Fochi, M.; Ranieri, S.; Mazzanti, A.; Bernardi, L. "Catalytic highly enantioselective vinylogous Povarov reaction" *Chem. Commun.* **2013**, *49*, 880.
- González, P. B.; Chandanshive, J. Z.; Fochi, M.; Bonini, B. F.; Mazzanti, A.; Bernardi, L.; Locatelli, E.; Caruana, L.; Monasterolo, C.; Comes Franchini, M. "Experimental and computational investigation of the 1,3-dipolar cycloaddition of the ynamide tert-butyl N-Ethynyl-N-phenylcarbamate with c-carboxymethyl-N-phenylnitrilimine" *Eur. J. Org. Chem* **2013**, 8108.
- Fochi, M.; Caruana, L.; Bernardi, L. "Catalytic Aza-Diels-Alder reactions: the Povarov cycloaddition reaction" *Synthesis* **2014**, *46*, 135.
- Caruana, L.; Fochi, M.; Comes Franchini, M.; Ranieri, S.; Mazzanti, A.; Bernardi, L. "Asymmetric synthesis of 3,4-annulated indoles through an organocatalytic cascade approach" *Chem. Commun.* **2014**, *50*, 445.
- Caruana, L.; Kniep, F.; Johansen, T. K.; Poulsen, P. H.; Jørgensen, K. A. "A new organocatalytic concept for asymmetric  $\alpha$ -alkylation of aldehydes" *J. Am. Chem. Soc.* **2014**, *136*, 15929.
- Caruana, L.; Mondatori, M.; Corti, V.; Morales, S.; Mazzanti, A.; Fochi, M.; Bernardi, L. "Catalytic asymmetric addition of Meldrum's acid, malononitrile and 1,3-Dicarbonyls to *ortho*-quinone methides generated in situ under basic conditions" *Chem. Eur. J.* **2015**, early view DOI: 10.1002/chem.201500710.



*Polaris, ultimo astro del Piccolo Carro. Guardiamola: la sua luce viaggia nel vuoto per più di quattrocento anni, prima di raggiungere i nostri occhi (...). La luce che vediamo adesso fu irradiata quasi tredici miliardi di secondi fa. Tratteniamo il respiro per tredici secondi, moltiplichiamo per mille il tempo di questa apnea. E' un millesimo del tempo impiegato dalla luce di Polaris per arrivare a noi. La luce che irradia adesso non la vediamo. La vedrà, tra quattro secoli, chi verrà dopo di noi.*

*Ora guardate la stella del Nord, guardatela con occhi nuovi. Un giorno tra dodicimila anni, Polaris verrà rimpiazzata e in quel punto del cielo, al suo posto, vedremo Vega.*

*Salutiamo Polaris, e ringraziamola. Ha fatto un buon lavoro. Diamo il benvenuto a Vega.*

[Wu-Ming, "Anatra all'arancia meccanica"]



## Table of contents

<b>1. Introduction .....</b>	<b>11</b>
1.1. Chirality in everyday life: Nature is asymmetric.....	11
1.2. Asymmetric organocatalysis: the “third pillar” of asymmetric synthesis .....	13
1.3. Modes of activation in asymmetric organocatalysis.....	15
1.3.1. Hydrogen-bond donor catalysis.....	15
1.3.2. Chiral phosphoric acid catalysis .....	18
1.3.3. Aminocatalysis: enamine and iminium ion activation.....	20
<b>2. Aim of the Thesis .....</b>	<b>25</b>
2.1. Summary of the Thesis research.....	26
<b>3. Organocatalytic asymmetric vinylogous Povarov reaction. ....</b>	<b>31</b>
3.1. Background.....	31
3.2. Aim of the work.....	39
3.3. Results and discussion .....	40
3.3.1. Preliminary kinetic investigation of the catalytic enantioselective vinylogous Povarov reaction .....	45
3.3.2. Determination of relative and absolute configuration of adducts <b>3</b> and <b>9</b> .....	48
3.3.3. Mechanistic proposal.....	52
3.4. Experimental details .....	53
3.4.1. General methods and materials.....	53
3.4.2. Preparation of H <sub>8</sub> -BINOL derived phosphoric acid catalyst <b>4h</b> .....	54
3.4.3. General procedure for the catalytic enantioselective vinylogous Povarov reaction. ....	55
3.4.4. General procedures for elaborated products <b>6</b> , <b>7</b> , <b>8</b> , <b>9</b> .....	57
3.4.5. Crystallographic data .....	60
3.5. Conclusion .....	61
<b>4. Asymmetric organocatalytic cascade reactions in 3,4-annulation of indoles: a gateway to ergot alkaloids.....</b>	<b>63</b>
4.1. Background.....	64
4.2. Aim of the work.....	71
4.3. Organocatalytic reactions between indole derivatives <b>1</b> and enals: results and discussion.....	75
4.3.1. Determination of the absolute and relative configuration of compounds <b>3</b> and <b>6</b> and structural determination of <b>5</b> .....	82
4.3.2. Mechanistic proposals for the formation of compounds <b>3</b> and <b>5</b> .....	88
4.4. Organocatalytic reactions between indoles derivatives <b>1</b> and nitroethene: results and discussion .....	91
4.4.1. Determination of the absolute and relative configuration of compounds <b>7</b> .. ..	99
4.4.2. Mechanistic proposal for the formation of compounds <b>7</b> .....	102
4.5. Experimental details .....	105
4.5.1. General methods and materials.....	105
4.5.2. General procedures .....	106
4.6. Conclusion .....	111
<b>5. Organocatalytic asymmetric addition of active methylene compounds to <i>ortho</i>-quinone methides generated <i>in situ</i> under basic conditions.....</b>	<b>117</b>

5.1.	Background .....	118
5.2.	Aim of the work .....	125
5.3.	Results and discussion.....	127
5.3.1.	Determination of the absolute configuration of compounds <b>4</b> , <b>5</b> , <b>6</b> .....	135
5.3.2.	Mechanistic proposal and control experiments .....	136
5.4.	Experimental details .....	138
5.4.1.	General methods and materials .....	138
5.4.2.	General procedures.....	139
5.5.	Conclusion.....	141
<b>6.</b>	<b>A new organocatalytic strategy for <math>\alpha</math>-alkylation of aldehydes: asymmetric 1,6-conjugated addition of enamine-activated aldehydes to <i>para</i>-quinone methides....</b>	<b>143</b>
6.1.	Background .....	144
6.2.	Aim of the work .....	149
6.3.	Results and discussion.....	151
6.3.1.	Determination of the absolute and relative configurations of compounds <b>3</b> . .....	157
6.3.2.	Mechanistic proposal.....	158
6.4.	Experimental details.....	158
6.4.1.	General methods and materials .....	158
6.4.2.	Syntheses of starting materials <b>1</b> and <b>2</b> .....	159
6.4.3.	Synthesis of catalyst <b>4f</b> .....	160
6.4.4.	Syntheses of catalysts <b>4g</b> and <b>4h</b> .....	161
6.4.5.	Synthesis of 1-(3,5-bis(trifluoromethyl)phenyl)-3-phenethylthiourea, <b>5</b> .....	162
6.4.6.	General procedure for the organocatalytic reactions.....	162
6.4.7.	General procedure for the de- <i>tert</i> -butylation reaction sequence .....	163
6.4.8.	Crystallographic data .....	164
6.5.	Conclusion.....	164
<b>7.</b>	<b>Bibliography .....</b>	<b>167</b>

# 1. Introduction

## 1.1. Chirality in everyday life: Nature is asymmetric

A molecule is defined as *chiral* if its mirror-image is not superimposable with itself.<sup>1</sup> The majority of chiral compounds can be identified by their lack of a plan of symmetry, as well as the presence of an *asymmetric* carbon atom. These molecules (namely, their *enantiomers*) are mirror images: identical yet opposite.

Beyond this formal definition, the concept of chirality has huge implications for living organism demonstrated by the fact that essential biomolecules such as enzymes, proteins, amino-acids, sugars and nucleic-acids are chiral. However, not only biomolecules, but also other compounds we can find in everyday life are chiral. Enantiomers may look the same, but do not always behave the same and perhaps they may have significantly different biological activity. The following are some examples, from natural compounds to pharmaceuticals, in which chirality is directly involved.

### *Fragrances*

Limonene and carvone are both terpenoid compounds. Limonene takes its name from lemon but only the (*S*)-enantiomer smells of lemon, while the (*R*)-enantiomer possesses a strong smell of orange. Carvone is a component of many essential oils, (*S*)-carvone smells like caraway, its mirror image (*R*)-carvone smells like spearmint.

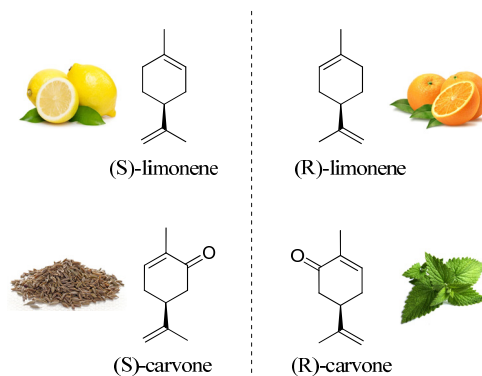


**Figure 1.**

### *Beverages*

Quinine is natural occurring alkaloid isolated from the bark of the *Cinchona* tree. Quinine has been widely exploited for its anti-malarial properties. Due to the bitter taste that possesses, quinine is also used in the preparation of “tonic waters”– which were

popularized in the British colony as malaria prophylactic – and as ingredient of chinotto beverages.

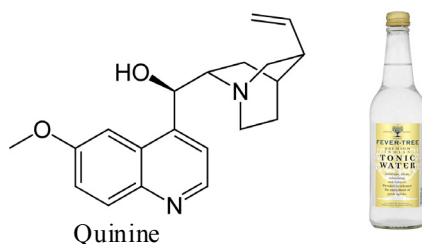


Figure 2

### *Drugs safety and effectiveness*

The activity of pharmaceuticals depends on which enantiomer is used. Since a drug must fit into the target receptor, it is often only one enantiomer that is useful. In the field of pharmacology, making the right enantiomer can be a matter of life or death. This was the case, for instance, of the drug thalidomide which was sold in 1960's to treat nausea. Yet, only one enantiomer has benefic pharmaceutical effect, while the other cause serious fetal damages. Less dramatic, but still remarkable is the case of ibuprofen, one of the most known painkiller drugs. In this case, only the (*S*)-enantiomer is responsible for the beneficial effects, whereas the (*R*)-enantiomer is not effective.

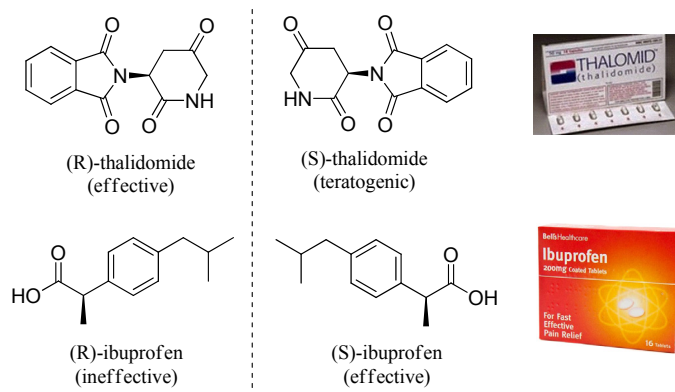


Figure 3

## 1.2. Asymmetric organocatalysis: the “third pillar” of asymmetric synthesis

The enantioselective synthesis of chiral compounds is still a primary issue for organic chemistry researchers. Most of organic compounds are chiral: from fragrances to agrochemicals, from amino acids to the double helix of DNA, whoever works in organic synthesis often needs to access to enantiomerically pure compounds. Moreover, the majority of biological receptors are chiral,<sup>2</sup> thus the wide utility of synthetic chiral molecules as single enantiomers has made asymmetric catalysis a crucial area of research.<sup>3</sup>

Throughout the second half of 20<sup>th</sup> century, enzymes and transition-metals had been considered the only classes of efficient asymmetric catalysis.<sup>4</sup> Biocatalysis lie in the use of enzymes as natural catalysts to perform organic transformations.<sup>5</sup> The main advantages of this type of catalysis include very high enantioinduction and substrate specificity. Conversely, in metal-based catalysis, the catalysts are rendered chiral by means of chiral ligands. The thus generated metal-complex catalysts are very effective even at low concentration<sup>6</sup> and are therefore well suited to industrial scale synthesis.<sup>7</sup> For these reasons, enormous progresses have been made within the field of metal-based asymmetric catalysis,<sup>8</sup> culminated in the award of Nobel Prize to Sharpless, Noyori and Knowles in 2001.

Organocatalysis relies on the use of small chiral organic molecules to catalyze organic transformations.<sup>9</sup> Organocatalysis grounds its roots into biomimetic concepts,<sup>9b</sup> in order to mimic the catalytic activity and selectivity of enzymes.<sup>10</sup> In 1970s a milestone in the area of what would become “asymmetric organocatalysis” was posed by two industrial research groups.<sup>11</sup> They published the first, highly enantioselective, catalytic aldol reaction using the simple amino acid proline as catalyst. Despite this, only few reports on the use of small organic molecules as asymmetric catalysts were published between 1968 and 1997. It seemed that these chemical studies were no interconnected to each other and there were no efforts trying to conceptualize a general organocatalytic strategy, thus the organic chemists community overlooked organocatalysis for almost thirty years.

Things began to change in the late 1990s. From that moment, organocatalysis coalesced around a small number of articles independently reported (*vide infra*). This brought the scientific community, the same that ignored most of the research on organocatalysis, to hold this field with surprising enthusiasm. The explosion of interest is certified by the

outstanding number of reports: since 2000, according to a conservative estimation, more than 7000 manuscripts have been published on this topic<sup>12</sup> (Figure 4).

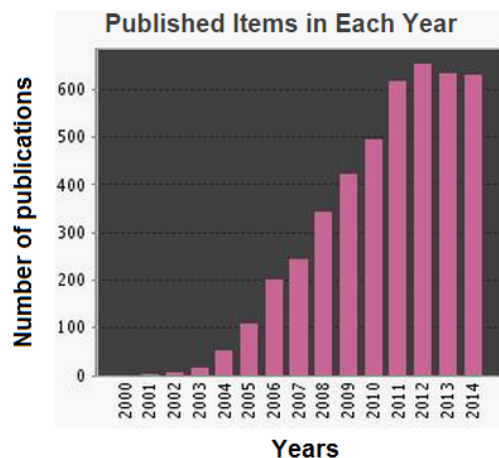


**Figure 4.** Published manuscripts on the topic of organocatalysis.

As of 1996, reports from Shi,<sup>13</sup> Denmark,<sup>14</sup> Yang,<sup>15</sup> Jacobsen<sup>16</sup> and Corey<sup>17</sup> demonstrate that small organic molecule could be effectively used as smart tools in organic synthesis. Nevertheless, only in 2000 organocatalysis was actually born by the works from Barbas, List<sup>18</sup> and MacMillan,<sup>19</sup> that led to recognize a general mode of action of organocatalysts, paving the way for a broader applicability of organocatalysis.<sup>9f</sup>

Organocatalysis, by now, has definitively matured to a recognized methodology, equal to organometallic and enzymatic catalysis and it is viewed as the third pillar of asymmetric synthesis. Organocatalysts have several important advantages, since they are usually robust, easily available, inexpensive and non-toxic. Because of their inertness towards moisture and oxygen, demanding conditions such as inert atmosphere or dry/degassed solvents are often not required. Due to the absence of transition metals, organocatalytic methods are especially appealing for the synthesis of pharmaceuticals in which hazardous metallic traces are unacceptable.<sup>9e,20</sup>

The impressive growth of research activity has brought to coin terms such as “golden age”<sup>9a</sup> or “gold rush”<sup>9b</sup> referred to organocatalysis. The large number of studies in this relatively new field of Organic Chemistry, have opened new horizon to access to complex molecular architecture, furnishing new powerful synthetic tools.<sup>20</sup> Long eclipsed by metal-based catalysis, it is now fascinating to see that organocatalysis is knowing an outright renaissance<sup>21</sup> and possibly it will remain a highly competitive research area in the years to come.

### 1.3. Modes of activation in asymmetric organocatalysis

The decisive success of organocatalysis, suddenly exploded during the past decade, arise from the identification of generic modes of activation, induction and reactivity. Generic mode of activation means that reactive species interacts with the chiral catalyst in a highly organized and predictable manner. The recognition of activation modes in organocatalysis led to the development of catalyst families that are an useful platform in developing new enantioselective reactions.<sup>9f</sup>

Based on the nature of the interaction between the catalyst and the substrate, the activation modes can be classified in covalent-based and non-covalent based.<sup>9b</sup> As regards to the non-covalent based catalysis, hydrogen-bond donor and Brønsted acid catalysis are based on interactions between the catalyst and the substrate, mimicking the working principles of enzymes.<sup>22</sup> Within the category of covalent-based activation, a prominent position is occupied by aminocatalysis that has emerged as reliable strategy to generate stereocentres at  $\alpha$ - and  $\beta$ -position of carbonyl compounds.<sup>23</sup>

The understanding of the activation approaches brought to the development of catalytic strategies in which different modes of activation can be easily combined as in the case of domino/cascade reactions.<sup>24</sup> Furthermore, different organocatalysts can be combined with other catalytic system such as metal-based<sup>25</sup> or photoredox catalysts,<sup>26</sup> reaching an extraordinary level of sophistication.

In the following paragraphs, the modes of activation encountered by facing specific synthetic challenges within my PhD studies will be described.

#### 1.3.1. Hydrogen-bond donor catalysis

Hydrogen bond plays a dominant role in biocatalysis and it is frequently exploited by enzymes in order to promote several biochemical processes. The most preeminent function is the activation of electrophile species towards nucleophilic attacks, since H-bond is able to remove the electronic density of the species which is oriented towards. Nevertheless, it must be stressed that exactly as enzymatic catalysis, H-bonding catalysis relies on the stabilization of the transition state of the reaction, induced by dipolar interaction within a confined active site.<sup>27</sup> Only recently organic chemists discovered the great potential of H-bond as a tool for the electrophilic activation in asymmetric catalysis. In 1998 and 1999 Jacobsen<sup>16</sup> and Corey<sup>17</sup> reported asymmetric Strecker

reactions using hydrogen-bonding catalysts that activate electrophile imines. This led to consolidate the concept that small chiral molecules equipped with H-bond donor moieties are able to catalyze a wide range of reactions, in enantioselective manner and with broad substrate scope. Few years later Jacobsen showed that these H-bonding based catalysts could be used for other reactions,<sup>28</sup> launching *de facto* the generic use of enantioselective H-bonding catalysis. Nowadays, compounds such as ureas, thioureas, squaramides *etc.* have emerged as privileged catalysts and numerous new asymmetric reactions have been developed on the basis of the H-bonding catalysis.<sup>22</sup>

Over the past fifteen years, the so called “bifunctional catalysts” knew a strong application in the field of asymmetric organocatalysis. These type of catalysts is characterized by the presence of a Brønsted base (usually a tertiary amine) linked through a chiral scaffold to an acid moiety which acts as H-bond donor (e.g.: alcohols, amides, sulphonamides, ureas, thioureas, squaramides, *etc.*). Most of these catalysts derive from *Cinchona* alkaloids or from *trans* 1,2-cyclohexandiamine.

*Cinchona* alkaloids are natural occurring compounds extracted from the bark of *Cinchona* tree. The structure of these catalysts consists in two pairs of pseudoenantiomers,<sup>29</sup> namely Quinine (QN) – Quinidine (QD) and Cinchonidine (CD) – Cinchonine (CN) (Figure 5).

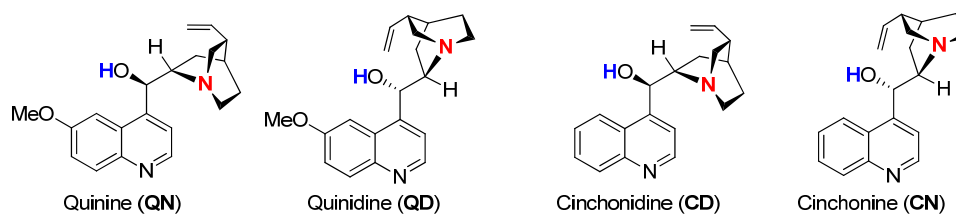


**Figure 5.** *Cinchona* alkaloids.

The tertiary amine moiety is responsible for the basic/nucleophilic activation; whereas the alcoholic group acts as acidic activator by donating a hydrogen bond. The hydroxyl group can be easily functionalized to an ester or ether moiety; on the other hand, by means of a Mitsunobu reaction, it can also be replaced with an amine moiety which is a versatile handle for the linkage to other H-bond donor as squaramides, ureas or thioureas. These latter H-bond donors are easily available; moreover, the modification of substituents on nitrogen allows the proper modulation of steric hindrance and electronic properties (Figure 6).

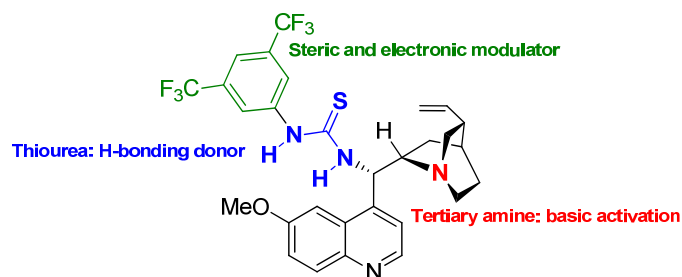
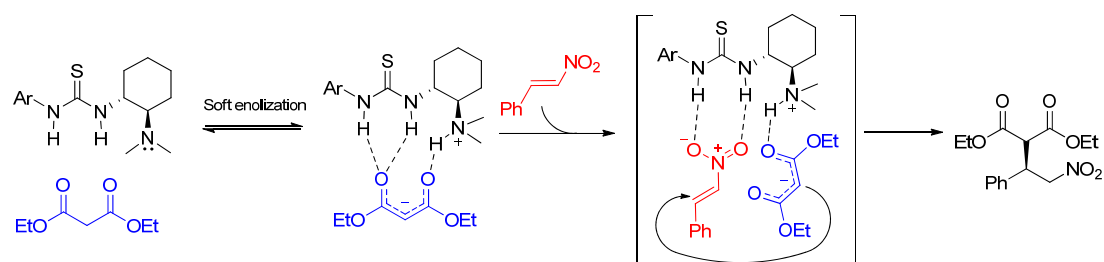


**Figure 6.** Thiourea based bifunctional catalyst derived from 9-deoxy-9-amino-*epi* Cinchona alkaloids.

The thiourea is often functionalized with a 3,5-bis(trifluoromethyl)-phenyl group in order to ensure a better catalytic activity.<sup>30</sup> In fact, this electron withdrawing moiety reduces the  $pK_a$  of N–H proton, making them more available to the hydrogen-bond donation.

The Michael addition of 1,3-dicarbonyl compounds on nitroolefin mediated by H-bonding based catalysts was developed by Takemoto in 2003.<sup>31</sup> This reaction can be taken in account as a model to understand how these catalysts can promote substrates activation and enantioselective reactions<sup>32</sup> (Scheme 1). In the first step, the nucleophile is deprotonated by the tertiary amine catalyst (soft enolization), the thus formed enolate is stabilized by multiple H-bonding between the protonated tertiary amine group and the N–H acidic proton of the thiourea. The nitroolefin (electrophile) is then coordinated to the thiourea protons, generating an ordered tertiary complex. The reaction partners are now both activated and can react to form a new C–C bond. The nitronate is finally protonated by means of a proton transfer from the tertiary amine moiety, delivering the product and releasing the catalyst.



**Scheme 1.** Reaction model for the catalytic asymmetric addition of malonate to nitroalkene

An alternative transition state model was computationally disclosed by Pápai one year later.<sup>33</sup> It consists in the coordination of the malonate to the thiourea, while the activation of the electrophile is provided by the protonated tertiary amine moiety.

Summing up, the acidic moiety of the thiourea together with the protonated tertiary amine play a key role in the stabilization of the transition state of the reaction. The

presence of H-bond generates a well-defined chiral environment which determines the preferential orientation of the reagents, therefore inducing enantioselectivity.

Another relevant H-bonding scaffold is represented by squaramides (Figure 7). Initially developed for molecular recognition, squaramides have found application in organocatalysis only since 2008.<sup>34</sup> However, compared to the closest analogous ureas and thioureas, the squaramido functionality differs in

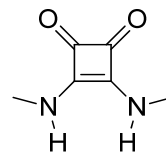


Figure 7. The squaramido moiety

five aspects:<sup>35</sup> i) duality in binding, ii) rigid structure, iii) increased H-bond spacing, iv) convergent H-bond angles and v) increased  $pK_a$ . In terms of reactivity and enantioinduction these features make the squaramides complementary to ureas and thioureas. The difference in distance and orientation of N–H bond allows to accommodate within the chiral pocket several H-bonding acceptors, providing the opportunity to choose the proper catalyst depending on the type of substrates. The insertion of chiral scaffolds derived from *Cinchona* alkaloids or from *trans* 1,2-cyclohexandiamine permits the construction of many H-bond donors, bifunctional organocatalysts which show excellent enantioinduction for a broad range of asymmetric transformations.<sup>22c</sup>

### 1.3.2. Chiral phosphoric acid catalysis

Chiral phosphoric acids belong to the category of strong Brønsted acid catalysis, in which the reactions are promoted by the partial or complete transfer of an acidic proton to the substrate, activating it for a nucleophilic attack. Independently developed in 2004 by Akiyama<sup>36</sup> and Terada,<sup>37</sup> chiral phosphoric acids have emerged as reliable catalytic systems alternative to chiral metal catalysts (Lewis acid). Since these landmark reports, several research groups have investigated the applicability of these catalysts by developing a remarkable number of organic transformations.<sup>38</sup> In particular, catalysts derived from enantiopure BINOL (1,1'-bi(2-naphthol)) are provided with some features that make them good candidates for this type of catalysis (Figure 8). In these catalysts, the active phosphoric acid moiety is installed onto the axially chiral binaphthyl backbone. Moreover, BINOL scaffold is usually modified at 3 and 3' positions with sterically demanding aryl moieties with diverse electronic properties, hence identifying the substrate recognition site. The hindered substituents shield the active site providing to the stereocontrol in asymmetric reactions. Besides the acidic proton, the phosphoryl

oxygen acts as a hydrogen-bond acceptor, giving a bifunctional attribute, conceptually similar to those encountered in H-bond catalysis.

**Binaphthyl scaffold:**

Rigid and axially chiral backbone

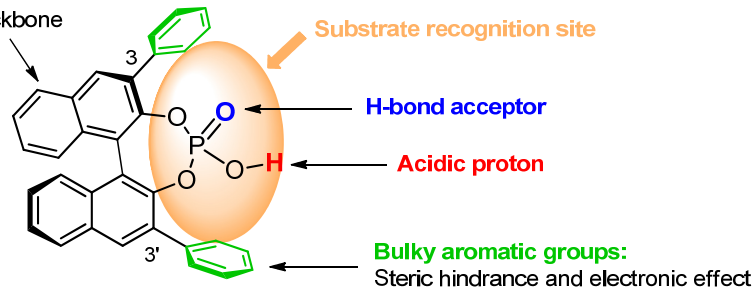
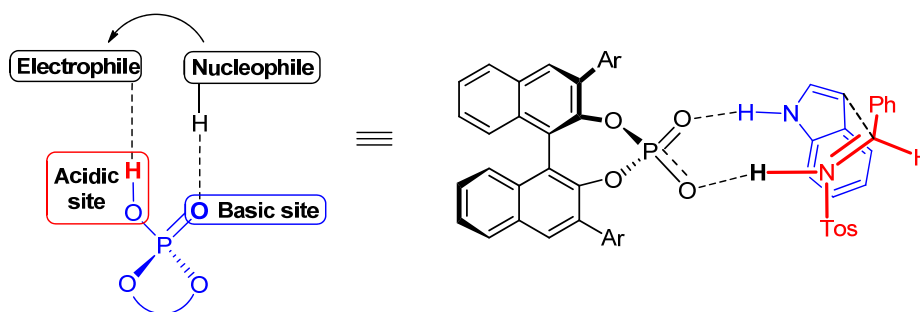


**Figure 8.** Features of chiral phosphoric acids.

The success of chiral phosphoric acids in asymmetric organocatalysis is actually ascribed to bifunctional activation, in which both Brønsted acidic and basic sites are involved in the stabilization of the transition state. The mode of action of chiral phosphoric acid was conceptualized by Goodman through computational methods.<sup>39</sup> The factors behind the stereoselection were investigated by using the Friedel-Crafts reaction between indole and different imines as a model.

On the basis of these results, the generally accepted mode of action of chiral phosphoric acids is showed in Scheme 2. It can be assumed a dual coordination in the transition state through hydrogen-bonding interactions. The bulky aryl groups guide the stereoselectivity by stereo-electronic interactions with the substrates, favouring the preferential attack of indole to one of the two faces of the imine.



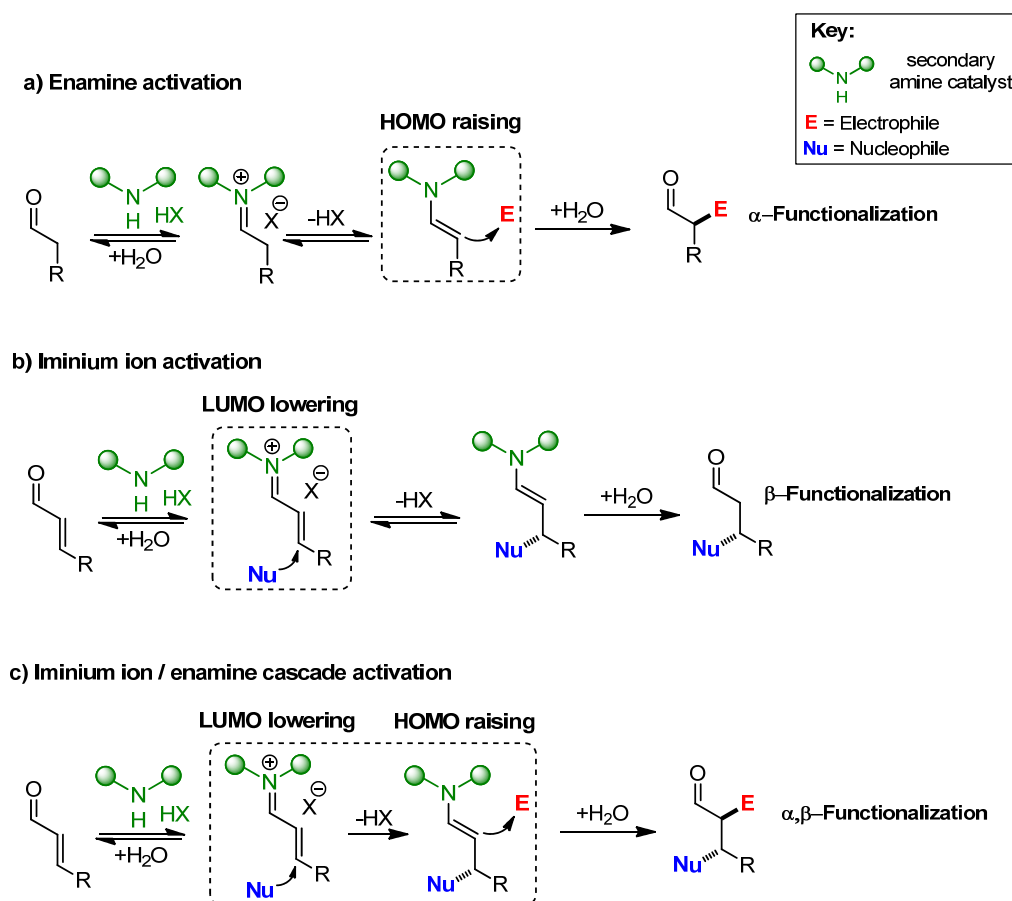
**Scheme 2.** Transition state model accounting for stereoselection in BINOL-phosphoric acids.

Finally, one last consideration about the acidity of this catalytic system. While the acidity of thioureas and other H-bond donor functionalities is rather weak,<sup>40</sup> chiral phosphoric acids are strongly acidic, with  $pK_a$  values ranging from 2 to 4 in DMSO.<sup>41</sup> Even though many evidences for hydrogen-bonding interactions have been collected, given the strong acidity of phosphoric acids, the formation of ion-pairing between a fully protonated electrophile and the phosphoric counterion cannot be excluded.<sup>42</sup>

### 1.3.3. Aminocatalysis: enamine and iminium ion activation

The use of chiral amines as catalysts for the asymmetric functionalization of carbonyl compounds is called aminocatalysis.<sup>23,43</sup> Asymmetric functionalization of carbonyl group is a cornerstone of organic chemistry,<sup>44</sup> pioneered by Hajos, Eder, Sauer, and Wiechert<sup>11</sup> in the early 1970s through the preparation of valuable intermediates for the synthesis of steroids. Nevertheless, only in 2000s as a consequence of reports from List<sup>18</sup> and MacMillan,<sup>19</sup> the possibility of employing chiral amines was conceptualized, thereby establishing the origin of asymmetric aminocatalysis and triggering the “gold rush” of organocatalysis.

Activation modes in aminocatalysis are based on covalent interaction generated upon the condensation of a chiral cyclic amine with a carbonyl group, with a mechanism that emulates the working principle of Lewis acids in carbonyl activation. The reversible condensation leads to the generation of a positive charged iminium ion intermediate in which the energy of the lowest unoccupied molecular orbital (LUMO) is lowered. In the case of isolated  $\pi$  systems, this increases the  $\alpha$ -proton acidity favouring a rapid deprotonation. The thus generated nucleophilic enamine has a higher energy of the highest occupied molecular orbital (HOMO), compared to the parent enolate. This HOMO-raising activation allowed the  $\alpha$ -functionalization of carbonyl compounds with different electrophilic species (Scheme 3a). Propagation of the HOMO-raising activation mode has led to the development of dienamine- and trienamine- based reactions, enabling  $\gamma$  and  $\epsilon$  functionalizations.<sup>45</sup> As far as conjugated  $\pi$  systems are concerned, the electronic redistribution induced by iminium ion prompts conjugated nucleophilic additions at  $\beta$ -position (Scheme 3b). The flexibility of aminocatalysis allows the combination of these activation modes.<sup>24</sup> This strategy relies on the conjugated addition of a nucleophilic species to the iminium ion, resulting in the enamine which triggers the addition of electrophiles. The iminium ion-enamine sequence is a versatile approach to accomplish a dual functionalization at  $\alpha$  and  $\beta$  positions of carbonyl compounds in a single operational step (Scheme 3c).



**Scheme 3.** Activation modes in aminocatalysis.

Diarylprolinol silyl ethers (Figure 9), independently developed by Jørgensen<sup>46</sup> and Hayashi<sup>47</sup> in 2005, are proline-derived catalysts which have proven to be very effective, promoting many kinds of reactions.<sup>43c</sup> The bulky diaryl silylether group is the key for the high enantioselectivities generally given by this catalyst. In fact, this sterically demanding moiety forces the enamine in the conformation shown, and shields one of its two faces very efficiently, thus determining the approach of the electrophile from the opposite face (Figure 10a). This mode for the enantioinduction is valid for the iminium ion activation as well. Here, the bulky fragment extends enough to shield effectively the more distant  $\beta$ -position, allowing the nucleophilic attack only from the less hindered face (Figure 10b).

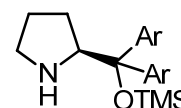


**Figure 9.** Jørgensen-Hayashi catalyst.

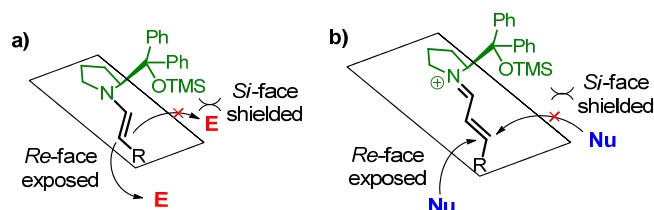


**Figure 10.** Models accounting for the enantioinduction of diphenyl silyl prolinol ethers through enamine activation (a) and iminium ion activation (b).

In both models, the efficiency of *O*-protected diaryl prolinols is related to the size of the substituents on the catalyst. Consequently, a proper modification of the aryl structure, as well as the silyl protecting group, permits a fine tuning of the catalytic stereinduction.

Within the panorama of aminocatalysis, a further prominent position is occupied by a series of imidazolidinone catalysts, also known as MacMillan's catalysts (Figure 11), and

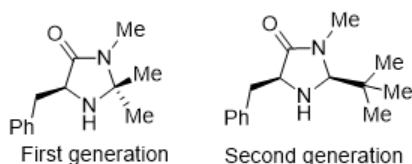


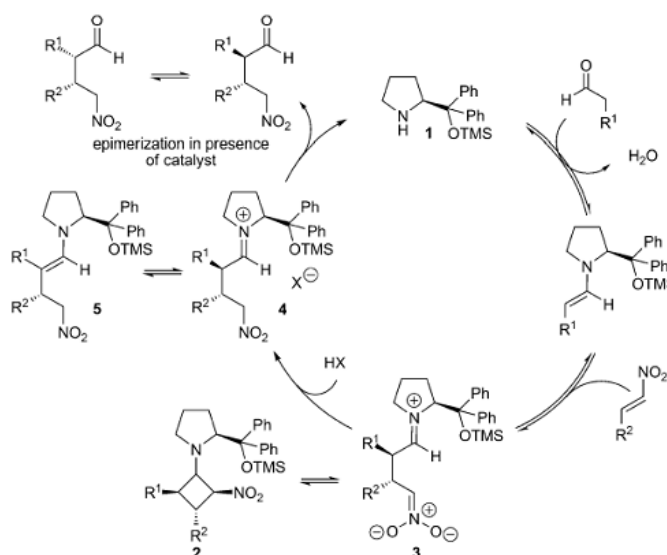
**Figure 11.** MacMillan's catalysts

derived from the amino acid phenylalanine. The first version was provided with a benzyl group and two methyl groups as sterical directing elements.<sup>19</sup>

The evolution of this catalyst results in the second generation MacMillan's catalyst.<sup>48</sup> The removal of

one methyl group makes the lone pair of electrons on nitrogen atom more accessible, resulting in faster condensation to carbonyl compounds and therefore a better catalyst activity. At the same time, replacement of the remaining methyl group with a *tert*-butyl furnishes a further element of steric control.

Recently, Michael addition reaction between enamine-activated aldehydes and nitroalkenes, originally reported by Hayashi,<sup>47</sup> has become a focus of attention. In fact, this reaction has been intensively studied from a mechanistic point of view by several group.<sup>49</sup> Initial investigations led to



**Scheme 4.** Proposed mechanism for addition of aldehydes to nitroalkenes catalyzed by diphenylprolinol trimethylsilyl ether.

conclude that the reaction follows the mechanism outlined in Scheme 4, where the cyclobutane **2** derivative is formed and the rate-determining step is the protonation of the zwitterionic intermediate **3**. These studies conducted by Seebach, Hayashi as well as by Blackmond and Pihko shed light on the mechanism. Although some controversy regarding the reaction route and the role for the observed intermediates still remains, these researches have got a detailed insight into a synthetically important reaction. These studies well demonstrate that the mechanisms of these reactions might be much more complex than it is often supposed to be.



## 2. Aim of the Thesis

The development of new synthetic routes to pharmaceutically active ingredients provided with molecular complexity serves as the basis for the challenge of treating new or existing diseases. Therefore, particular attention has been paid to drug candidates with one or more asymmetric centers. Although most complex organic molecules exist in nature as single enantiomer, the synthesis of optically active compounds is usually difficult, hence new enantioselective methods are strongly required to face this challenge. Organocatalysis is a well-recognized powerful methodology in the preparation of chiral molecules for screening and clinical trials.<sup>9e</sup> Organic catalysts are stable in air, tolerant towards moisture and usually there is no need for special equipment such as gloveboxes, dry solvents, *etc.* The preparation of many organocatalysts turns out to be relatively easy since most the chirality contained derived from naturally available sources. Finally, small organic molecules are typically non-toxic, simple to use and environmental-friendly. The benefits associated in avoiding the use of transition metals make organocatalysis a suitable methodology in the synthesis of pharmaceuticals or intermediates in which metal contamination, even in traces, is strictly forbidden.<sup>9f</sup> Organocatalysis possesses these important features, thus chemists of this field have already begun to approach chiral pharmaceutical targets.<sup>50</sup>

On this basis, the aim of this Doctoral Thesis is to capitalize the versatility of organocatalysis in the syntheses of molecules with potential biological activity, having as target the development of novel asymmetric organocatalytic transformations. During the course of my PhD studies, different types of reactions have been devised and developed. This has required to assess different families of organocatalysts, whereas sometimes it has been necessary the development of new catalytic systems. Particular attention has been devoted at the study and optimization of the reaction conditions and catalyst structure, in order to maximize yield and enantiopurity of the products as well as minimizing the catalyst loading and using the mildest conditions. The substrate scope of asymmetric reactions has always been thoroughly investigated to demonstrate the broad applicability of the proposed transformations, as well as the performance of synthetic elaborations illustrating the usefulness of the developed methods.

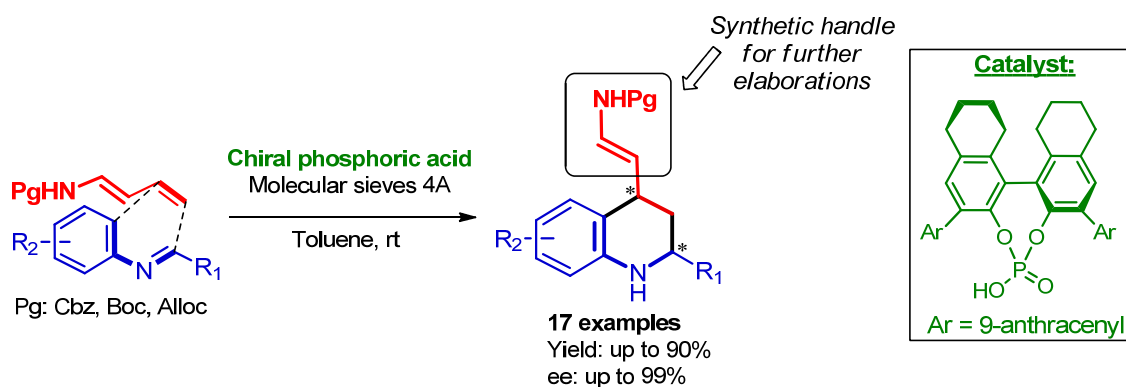
Despite conceptually distinct, the transformations detailed in the following chapters are somehow linked together by simple and recurring modes of activation, induction and reactivity, promoted by the catalysts employed. The chemical diversity of the challenges

encountered allows to get a precious overall view on organocatalysis, highlighting that enormous chemical diversity can be created by judicious choice of select catalyst.

## 2.1. Summary of the Thesis research

The followings chapters describe how the intrinsic versatility of organocatalysis and the use of different activation modes have been exploited to achieve new catalytic enantioselective processes, towards the synthesis of biologically relevant scaffolds. References can be found within each chapter.

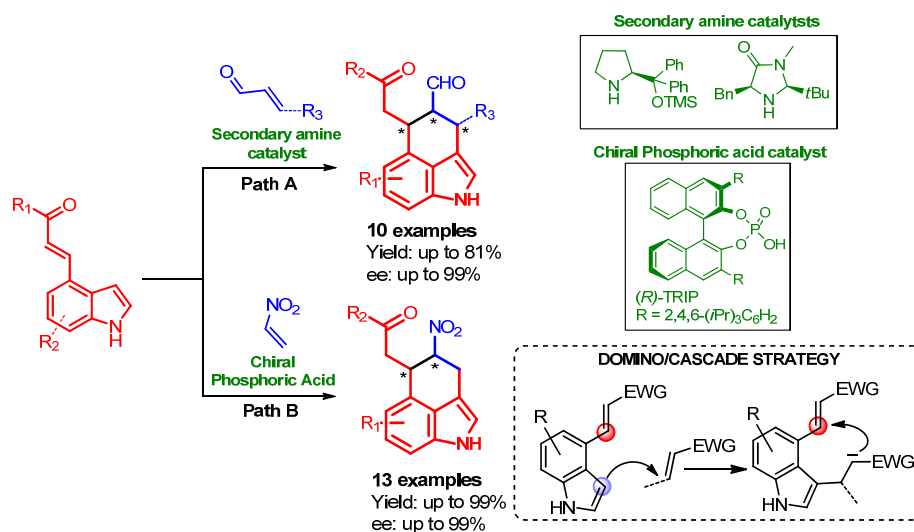
In chapter 3 the first example of asymmetric vinylogous Povarov reaction is presented (Scheme 5). The Povarov reaction is a [4+2] inverse-electron-demand cycloaddition between an electron-poor diene (typically an hetero-diene, derived from *N*-aryl imines) and an electron-rich dienophile. This transformation allows an easy access to 1,2,3,4-tetrahydroquinolines, key scaffolds in several natural and pharmaceutical compounds. Thus, it has been thoroughly investigated, even in its catalytic asymmetric version, by using several electron-rich dienophile, such as enecarbamates, vinyl ethers etc. We have found that, in the presence of chiral phosphoric acid catalyst, 1-*N*-Acyl-amino-1,3-butadienes (1-dienecarbamates) react through their terminal olefin with *N*-aryl imines (in some cases generated *in situ*), delivering the corresponding products in good yield, excellent diastereo- and enantioselectivity This process is an example of “vinylogy principle” according to which the effect of a functional group is transmitted through a conjugated  $\pi$ -system: a combination of stereo/electronic effects steers the reaction toward the vinylogous pathway, overcoming the common Diels–Alder reactivity of these dienes and also their tendency to undergo “non-vinylogous” Povarov reaction. Importantly, the obtained heterocyclic compounds possess an enecarbamate moiety which serves as a synthetic handle for further elaborations.



**Scheme 5.** Asymmetric, vinylogous Povarov reaction

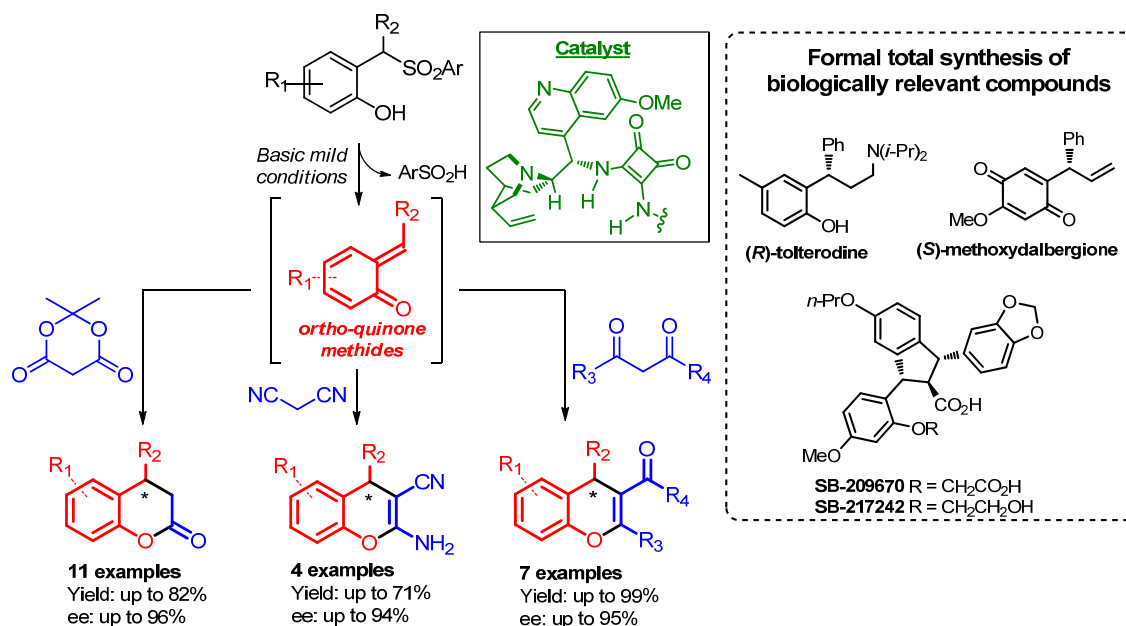
In chapter 4 domino/cascade strategies towards the synthesis of 3,4-annulated indoles are proposed. Indole and its derivatives represent probably the most important class of heterocyclic compounds due to their widespread biological and pharmaceutical activities. In particular, the tetrahydrobenzo[*cd*]indole core (3,4-ring fused) is present in many interesting natural occurring compounds such as the ergot alkaloids. Concurrently, asymmetric tandem/cascade/domino organocatalysis has recently emerged as an exceedingly powerful and useful tool for the construction of differently 1,2- and 2,3-ring-fused indole structures. However, none of the available methodology comprised the 3,4-ring fused indole. In order to approach this scaffold, indoles bearing a Michael acceptor at 4-position were synthesized. These substrates were engaged in domino reactions between two different Michael acceptors: enals and nitroethene. The reaction between indole derivatives and enals (Scheme 6, path A) is initiated by activation of acrolein through iminium ion formation with a secondary amine catalyst, followed by enamine mediated ring closure, furnishing the desired cycloadduct. Two different catalysts were employed to tailor the reactivity of the catalytic system to the enal substrates employed. On the other hand, the reaction between indole derivatives and nitroethene (Scheme 6, path B) proceeds via chiral phosphoric acid promoted Friedel–Crafts alkylation of the indole to the nitroolefin, the thus formed nitronate reacts intramolecularly with the Michael acceptor placed at the distal position of the indole derivative, delivering potential ergot alkaloids precursors. The formation of the desired cycloadducts by means of phosphoric acid catalyst was rather unexpected, therefore particularly intriguing. To get an insight on this transformation, DFT calculations have been performed and account for the observed results. Another challenge associated with the proposed transformations has been the poor nucleophilicity of indole derivatives. Careful optimization of the reaction parameters overcame the inherent low reactivity of these substrates, furnishing

highly enantioenriched 3,4-ring fused indoles, a gateway to many interesting natural occurring compounds such as ergot alkaloids, as exemplified by the formal total synthesis of 6,7-secoagroclavine.



**Scheme 6.** Synthetic strategies towards the synthesis of 3,4-ring fused indoles.

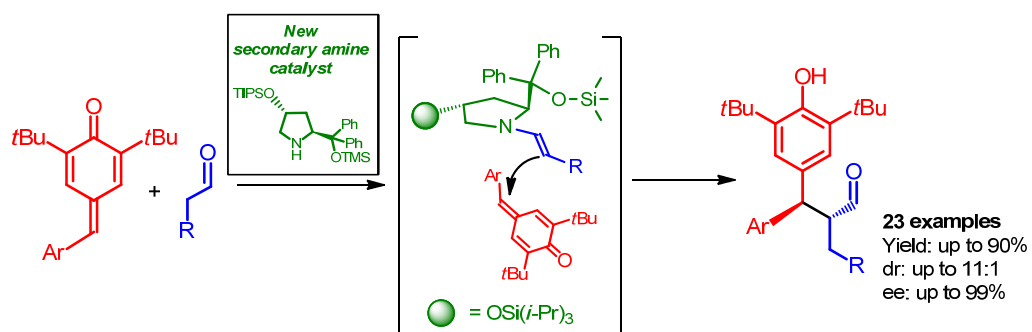
Chapter 5 deals with the development of asymmetric organocatalytic conjugate addition reactions of active methylene compounds to *ortho*-quinone methides. Due to their instability, these synthetically appealing intermediates have not been fully exploited in catalytic asymmetric settings until very recently. In this work, the intrinsic instability of *ortho*-quinone methides has been circumvented by their generation *in situ* under mild basic conditions, starting from the corresponding sulfonyl derivatives and using a squaramide based catalyst derived from natural quinine. The bifunctional catalyst is able to activate both substrates in the reaction, by means of a synergic action of the two catalytic sites, inducing high enantioselection in the addition step. The employment of different nucleophiles – *e.g.* Meldrum's acid or malononitrile – leads to the generation of 4-*H*-chromenes and chroman-2-ones in good yields and generally excellent enantioselectivities (Scheme 7). These compounds are synthetic precursors of several natural products, some of which showing interesting biological activity, or of active pharmaceutical ingredients (tolterodine) used in commercial drugs. In order to prove the synthetically usefulness of our methodology, we propose three formal total synthesis of biologically relevant compounds.



**Scheme 7.** Catalytic asymmetric addition of 1,3-dicarbonyl compounds to *o*-QMs generated *in situ*.

Finally, chapter 6 deals with what that has been called “the Holy Grail for organocatalytic chemists”, highlighting the development of a novel organocatalytic strategy for the asymmetric  $\alpha$ -alkylation of aldehydes. Addition of aldehydes to a diarylmethine moiety is a well-known example which has been thoroughly investigated in many instances. Nevertheless, the available methodologies are affected by some limitations that reduce the generality of the reaction and inhibit the possibility to generate more sophisticated structures. Prompted by the aim to generate  $\alpha$ -benzhydrylated aldehydes with more than one stereocenter, we have exploited the pronounced reactivity of *para*-quinone methides as Michael acceptors and we have developed a novel organocatalytic, asymmetric,  $\alpha$ -alkylation of aldehydes triggered by 1,6-conjugated addition of enamine to *para*-quinone methides (Scheme 8). For the first time, enamine-activated aldehydes have been reacted to these electrophiles, providing  $\alpha$ -diarylmethine-substituted aldehydes in high yield and broad substrate scope. Key to the success was the employment of a new chiral secondary amine catalyst in which the (diphenylmethyl)trimethylsilyloxy group was flanked by another bulky silyloxy moiety, placed at the C4-position of the pyrrolidine ring in a *trans* relationship. We envisaged that the (diphenylmethyl)trimethylsilyloxy group could effectively shield one face of the enamine providing enantiocontrol, while the other silyloxy moiety could sterically determine the approach of the *para*-quinone methide to the enamine, thus ensuring

diastereocontrol. With this catalytic system in hand, the stereochemistry of these reactions could be very well controlled, leading to highly diastereo- and enantioenriched products (Scheme 8).



**Scheme 8.** Organocatalytic strategy for  $\alpha$ -alkylation of aldehydes.

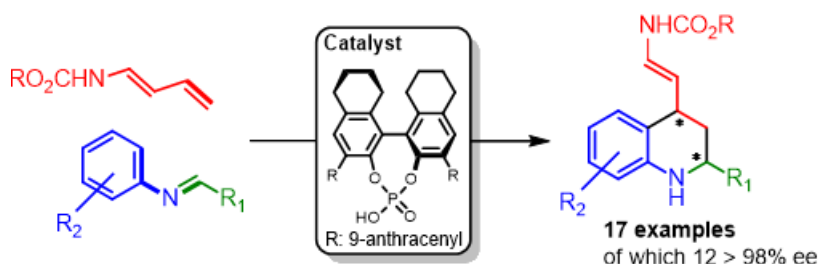
### 3. Organocatalytic asymmetric vinylogous Povarov reaction.

All the procedures and results here described are part of- and can be found in:-

- Caruana, L.; Fochi, M.; Ranieri, S.; Mazzanti, A.; Bernardi, L. “Catalytic highly enantioselective vinylogous Povarov reaction.” *Chem. Commun.* **2013**, 49, 880.

#### ABSTRACT

The Povarov reaction is a [4+2] inverse-electron-demand cycloaddition which allows an easy access to 1,2,3,4-

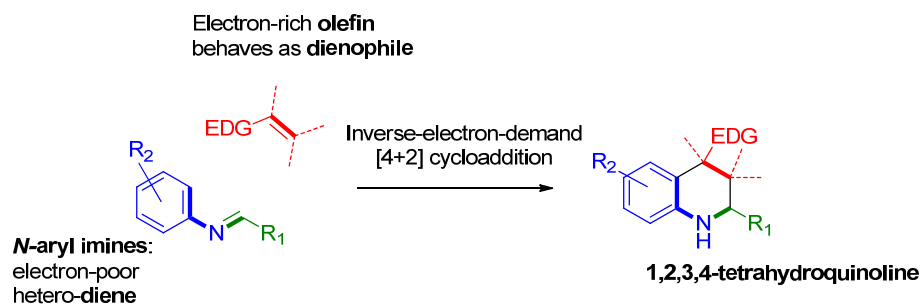


tetrahydroquinolines (THQs), key scaffolds in several natural and pharmaceutical compounds.<sup>51</sup> In this chapter, the first example of asymmetric vinylogous Povarov reaction is described. In the presence of chiral phosphoric acid catalysts, diene-1-carbamates reacted with *N*-aryl imines as dienophiles with their terminal olefins, rendering possible the development of the vinylogous version of this reaction. A combination of stereoelectronic factors steered these reactions towards the vinylogous pathway, overcoming the tendency of diene-1-carbamates to act as dienes. Employing a new (*R*)-H<sub>8</sub>-BINOL-derived catalyst, a series of imines, in some cases generated *in situ*, reacted with three differently protected 1-aminodiene affording the corresponding THQs with good yield, excellent enantioselectivity and as single diastereoisomers. The THQs obtained from this reaction bear at C4 an enecarbamate, which was subjected to various synthetic transformation.

#### 3.1. Background

In the course of investigations on the reactivity of different electron-rich olefins, in the early 1960s, Povarov and co-workers discovered that alkyl vinyl ethers and thioethers reacted with *N*-aryl imines – activated with boron trifluoride – to give 1,2,3,4-tetrahydroquinoline (THQs).<sup>52</sup> The reaction was classified by Povarov himself as a

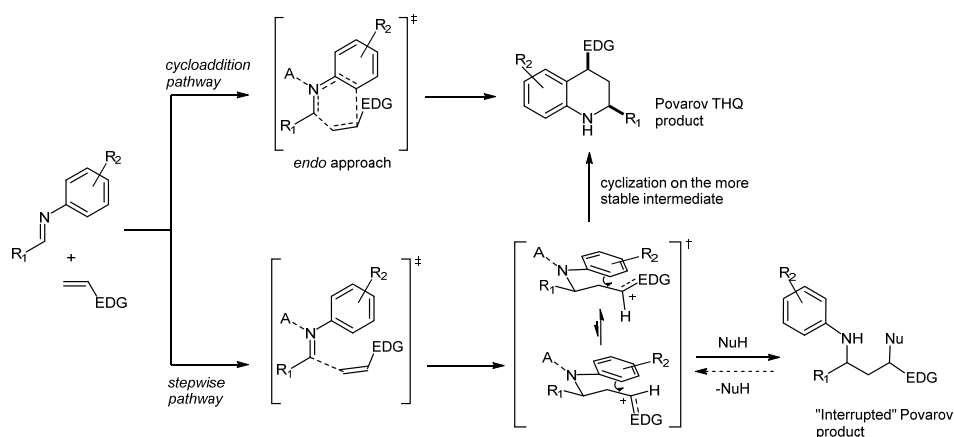
“diene-synthesis”-type reaction,<sup>53</sup> namely as a [4+2] hetero-Diels–Alder cycloaddition reaction. The requirement of Lewis acid serving to lower the LUMO of the coordinated imine, thus enhancing its electron-deficient character, the reaction was rationalized by considering a [4+2] cycloaddition between an electron-poor heterodiene and an electron-rich dienophile, with a typical inverse-electron-demand cycloaddition pathway. Nowadays, in recognition of this disclosure,<sup>53</sup> cycloadditions of *N*-aryl imines with electron-rich olefin are called Povarov reactions (Scheme 9).



**Scheme 9.** Povarov cycloaddition reaction (EDG = electron-donating group).

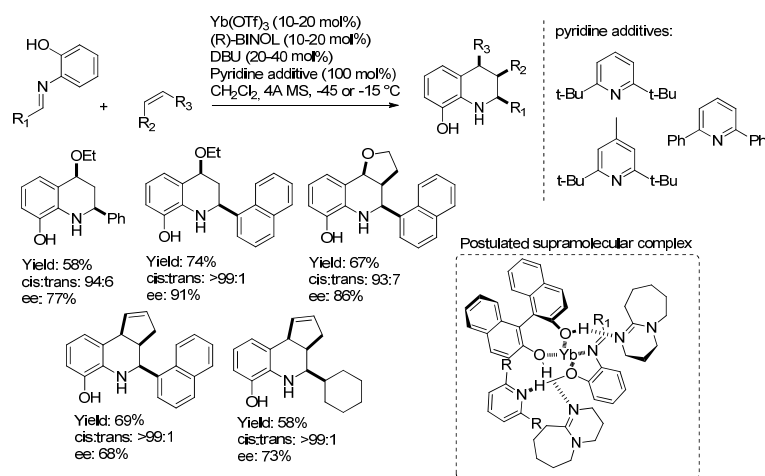
This reaction represents one of the most useful synthetic routes to access THQs (and to quinolines after oxidation), which are known to be biologically relevant scaffolds in several natural or pharmaceutical compounds.<sup>51</sup> The importance of these heterocycles has stimulated a considerable interest in the Povarov reaction, resulting in a significant advances in the last years.<sup>54</sup> Many efforts have been conducted towards the expansion of olefinic reaction partner, resulting in a variety of electron-rich dienophiles engaged in the Povarov reaction, such as vinyl (thio)ethers, enecarbamates, enamides, indoles, styrenes, vinyl indoles and ketimines just to cite few.<sup>54</sup> The Povarov reaction, due to its modular nature, has also found to be very useful in the frame of multicomponent reactions; the three-component strategy in which imines are generated *in situ*, avoids the isolation of unstable *N*-aryl imines derived from enolizable aliphatic aldehydes. Although the Povarov reaction is defined as an inverse-electron-demand aza-Diels–Alder cycloaddition, also a stepwise mechanism, namely Mannich and Friedel–Crafts reactions, must be taken in account (Scheme 10). This mechanistic hypothesis paves the way to the possible intermolecular trapping of intermediates by the addition of external nucleophiles, furnishing products derived from “interrupted” Povarov reactions. Nowadays, there is a general consensus that the reaction follows a two-step pathway, on the basis of several examples supporting this hypothesis.<sup>54c,55</sup>

As far as the stereochemistry is concerned, most Povarov reactions give, with variable selectivity, 2,4-*cis*-THQs. This relative configuration arises from an *endo* approach between diene and dienophile<sup>53</sup> or, accordingly to the more plausible stepwise pathway, the *cis* selectivity derives from the cyclization of the cationic intermediate in a chair-like transition state, where the substituents occupy the equatorial positions (Scheme 10).<sup>56</sup> Nevertheless, some exceptions to this 2,4-*cis* selectivity are reported, especially with 1,2-disubstituted olefin dienophiles.<sup>57</sup>



**Scheme 10.** Mechanistic speculations accounting for the mechanism of Povarov reaction and its interrupted version. Cycloaddition with *endo* approach, versus two-step cyclization where R<sup>1</sup> and EDG substituents occupy equatorial positions. A = Lewis or Brønsted acid activating the imine.

The first example of a catalytic enantioselective Povarov reaction was reported by Ishitani and Kobayashi in 1996,<sup>58</sup> in the frame of chiral Lewis acid catalysis. In this pioneering work, a chiral complex formed by a combination of ytterbium triflate, (*R*)-BINOL, pyridine additives and DBU catalyzed the reaction between 2-aminophenol-derived imines and vinyl ethers or cyclopentadiene, furnishing the corresponding THQs in moderate enantioselectivity but very good diastereoselectivity (Scheme 11).

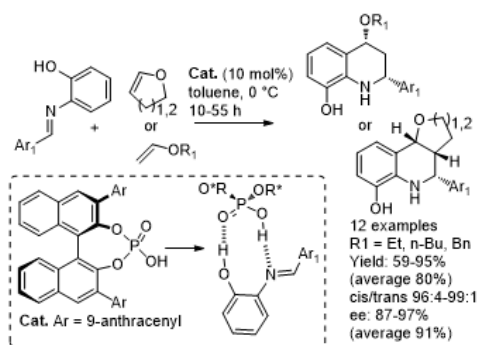


**Scheme 11.** The first catalytic enantioselective Povarov reaction.

Besides this first report, studies on asymmetric version of the Povarov reaction remained rather scarce. The scene began to change after the disclosure<sup>36,37</sup> of efficient Brønsted acid (in particular chiral phosphoric acids) for imine activation.<sup>59</sup> Due to their bifunctional behaviour (see § 1.3.2), chiral phosphoric acids activate the imine and coordinate the dienophile at the same time, leading to a highly organized transition state and ensuring high stereocontrol. The broad applicability of these catalysts in the Povarov reaction has been demonstrated by the development of numerous versions of this reaction as well as its interrupted variants.<sup>54</sup>

The first example of organocatalytic, chiral Brønsted acid catalyzed, Povarov reaction was reported by Akiyama in 2006.<sup>60</sup> In analogy with most of the chiral Lewis acid catalyzed reports, 2-aminophenol-derived imines were employed, in the presence of (*R*)-BINOL derived phosphoric acid, with different cyclic and acyclic vinyl ethers, delivering the corresponding THQs in good yield and enantioselectivity and almost perfect diastereoselectivity (Scheme 12).

Interestingly, this example represents an exception to what stated above, since the absence of acidic protons in the dienophile renders its coordination to the chiral catalyst not possible. This lack of coordination is bypassed by the presence of 2-hydroxy moiety on the imine, which allows a double coordination to the phosphoric acid, resulting in a highly ordered transition state<sup>61</sup> (Scheme 12).

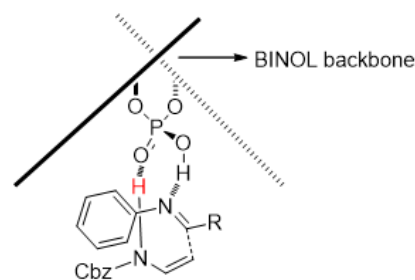


**Scheme 12.** The first example of Brønsted acid catalyzed Povarov reaction, and the double coordination of the catalyst to the imine.

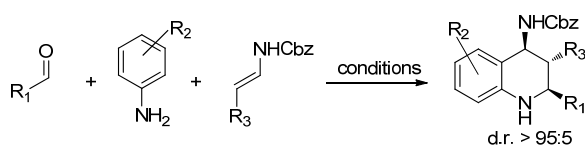
The employment of benzyl enecarbamate in the asymmetric Povarov reaction with *N*-aryl imines, catalyzed by chiral phosphoric acid has been the subject of several investigations. Most prominent results and conditions are summarized in Table 1. This reaction was disclosed by Masson and Zhu in 2009, wherein a 4-chlorophenyl substituted (*R*)-H<sub>8</sub>-BINOL-derived phosphoric acid was used as catalyst (Table 1, entry 1).<sup>62</sup> This first report described the three component reaction with benzyl *N*-vinylcarbamate, mostly limited to electron-rich anilines. The THQs obtained through this protocol were also amenable to synthetic elaborations, as demonstrated by the preparation of torcetrapib, a cholesteryl ester transfer protein inhibitor. Subsequently, another investigation from the same group expanded this protocol also to electron-poor anilines (Table 1, entry 2) and  $\beta$ -substituted (*E*)-enecarbamate (Table 1, entry 3), through simple prolongation of the

reaction time; the derived 2,3,4-substituted THQs showed an all-*trans* configuration at the stereocentres.<sup>63</sup> Recently, a different chiral phosphoric acid based on (*R*)-SPINOL scaffold,<sup>64</sup> was employed by Lin in a similar Povarov reaction.<sup>65</sup> The reaction, which was investigated with benzyl *N*-vinylcarbamate, afforded the THQ products in excellent enantioselectivity (Table 1, entry 4). Another variation of the Povarov reaction with the same carbamate but employing imines derived from fluorinated aldehydes (Table 1, entry 5) has been described by Xiao and Liu.<sup>66</sup> This reaction was catalyzed by a (*R*)-BINOL-derived phosphoric acid, delivering THQs as single 2,4-*cis*-diastereoisomers and with excellent yields and enantioselectivities. This latter study was motivated by considering the high relevance of fluoroalkyl compounds in medicinal chemistry.<sup>67</sup>

It is worth noting that in all these reactions the presence of the acidic NH in the carbamate is necessary for both reactivity and enantioselectivity, as demonstrated by several control experiments.<sup>63</sup> In fact, enecarbamates lacking NH proton did not participate productively in the catalytic reaction. It was thus further confirmed that phosphoric acids act as bifunctional catalysts by protonating/coordinating the imine – resulting in the lowering of the LUMO – and coordinating the NH of enecarbamate with its Lewis basic oxygen (Figure 12). This behaviour is in agreement with the generally accepted mode of activation of chiral phosphoric acids,<sup>39</sup> already described in § 1.3.2.



**Figure 12.** Model of activation of chiral phosphoric acid in the reaction between *N*-aryl imines and enecarbamates. The proton depicted in red is responsible for the coordination of enecarbamate.

**Table 1.** Asymmetric Povarov reaction of benyl enecarbamates, catalysed by chiral phosphoric acid.

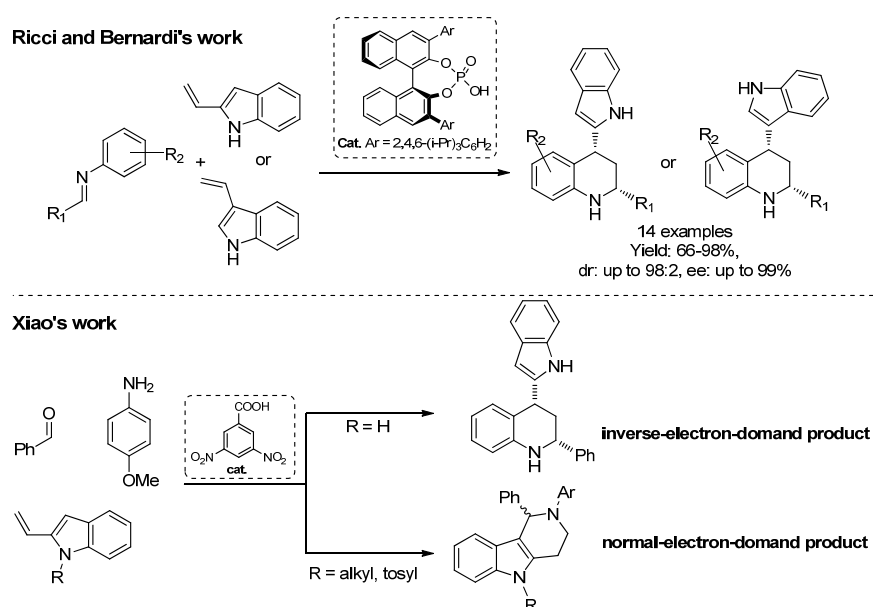
Entry	R <sup>1</sup>	R <sup>2</sup>	R <sup>3</sup>	Catalyst	Conditions	Yield	ee
1 - 17 examples REF. 62	4-ClC <sub>6</sub> H <sub>4</sub> , 4-Ph-C <sub>6</sub> H <sub>4</sub> , 4-FC <sub>6</sub> H <sub>4</sub> , 4-MeC <sub>6</sub> H <sub>4</sub> , 4-BrC <sub>6</sub> H <sub>4</sub> , 4-NCC <sub>6</sub> H <sub>4</sub> , 4-( <i>i</i> -Pr)C <sub>6</sub> H <sub>4</sub> , 4-NO <sub>2</sub> C <sub>6</sub> H <sub>4</sub> , 4-CF <sub>3</sub> C <sub>6</sub> H <sub>4</sub> , 2-furyl, <i>i</i> -PrCH <sub>2</sub> , <i>i</i> -Pr, Et, <i>n</i> -Pr, Ph	4-MeO, 4-CF <sub>3</sub> , H	H	 Cat. Ar = 4-ClC <sub>6</sub> H <sub>4</sub>	cat. 10 mol%,	57-90%	92- >99%
2 - 18 examples REF. 63	4-ClC <sub>6</sub> H <sub>4</sub> , 4-Ph-C <sub>6</sub> H <sub>4</sub> , 4-FC <sub>6</sub> H <sub>4</sub> , 4-MeC <sub>6</sub> H <sub>4</sub> , 4-BrC <sub>6</sub> H <sub>4</sub> , 4-NCC <sub>6</sub> H <sub>4</sub> , 4-( <i>i</i> -Pr)C <sub>6</sub> H <sub>4</sub> , 4-NO <sub>2</sub> C <sub>6</sub> H <sub>4</sub> , 4-CF <sub>3</sub> C <sub>6</sub> H <sub>4</sub> , 2-furyl, <i>i</i> -PrCH <sub>2</sub> , <i>i</i> -Pr, Et, <i>n</i> -Pr, Ph	4-MeO, H, 4-CF <sub>3</sub> , 4-Cl, 3-MeO	H	 Cat. Ar = 4-ClC <sub>6</sub> H <sub>4</sub>	cat. 10 mol%,	64-90%	92- >99%
3 - 14 examples REF. 63	3-MeOC <sub>6</sub> H <sub>4</sub> , 4-NO <sub>2</sub> C <sub>6</sub> H <sub>4</sub> , 2-BrC <sub>6</sub> H <sub>4</sub> , 2-furyl, PhCHCHC <sub>6</sub> H <sub>4</sub> , cyclohexyl, Et, BnOCH <sub>2</sub> , Ph	4-MeO, 4-NO <sub>2</sub> , 3-I, H	Me, <i>n</i> -Pr, <i>i</i> -Pr, (CH <sub>2</sub> ) <sub>3</sub> OTBDPS	 Cat. Ar = 4-ClC <sub>6</sub> H <sub>4</sub>	cat. 10 mol%,	48-97%	87-98%
4 - 16 examples REF. 65	4-BrC <sub>6</sub> H <sub>4</sub> , 3-BrC <sub>6</sub> H <sub>4</sub> , 2-BrC <sub>6</sub> H <sub>4</sub> , 4-ClC <sub>6</sub> H <sub>4</sub> , 4-NO <sub>2</sub> C <sub>6</sub> H <sub>4</sub> , 4-MeC <sub>6</sub> H <sub>4</sub> , 3-MeOC <sub>6</sub> H <sub>4</sub> , Ph, 1-naphthyl, <i>i</i> -Pr, cyclohexyl, <i>n</i> -pentyl, Et	4-MeO, H, 4-Br, 4-CF <sub>3</sub>	H	 Cat. Ar = 4-ClC <sub>6</sub> H <sub>4</sub>	cat. 5 mol%,	72-96%	96- >99%
5 - 12 examples, preformed imines REF.66	CF <sub>3</sub> , CF <sub>2</sub> Br, CF <sub>2</sub> Cl, CF <sub>2</sub> H, C <sub>4</sub> H <sub>9</sub> CF <sub>2</sub> , CH <sub>2</sub> CHCF <sub>2</sub> , PhCF <sub>2</sub> , 4-BrC <sub>6</sub> H <sub>4</sub> CF <sub>2</sub> , 4-MeOC <sub>6</sub> H <sub>4</sub> CF <sub>2</sub> , 4-MeC <sub>6</sub> H <sub>4</sub> CF <sub>2</sub> , 3-MeC <sub>6</sub> H <sub>4</sub> CF <sub>2</sub>	4-MeO, 4-Me	H	 Cat. Ar = 4-(2-naphthyl)C <sub>6</sub> H <sub>4</sub>	cat. 15 mol%,	81-97%	89-99%

The requirement of an NH moiety for the catalyst coordination, represents a limitation for the Povarov reaction catalyzed by chiral phosphoric acid. This restriction was overcome by Masson and Zhu, who installed a thiourea moiety on cyclic enecarbamates.<sup>68</sup> With this type of dienophile, bearing an acidic NH proton at their thiourea moiety, the reaction proceeded with good enantioselectivity in the presence of

chiral phosphoric acid as catalyst (Scheme 13). The thioureido moiety can be subsequently removed upon a two-steps synthetic procedure.

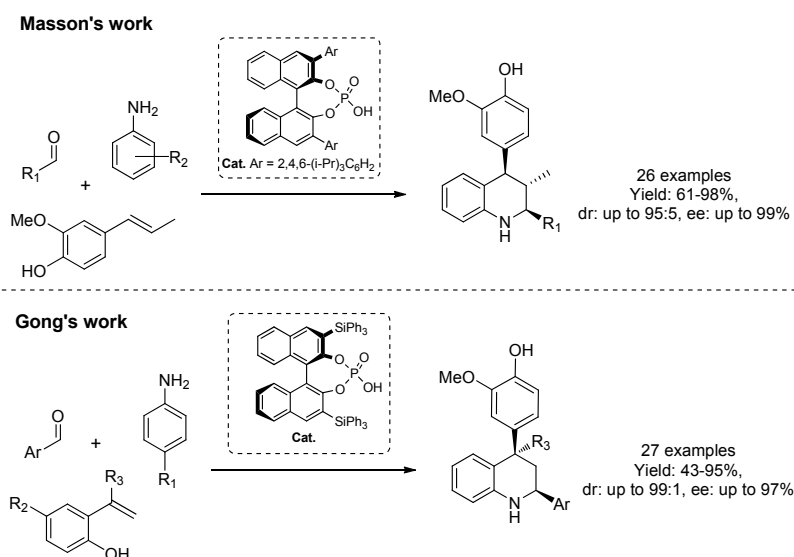
**Scheme 13.** Catalytic enantioselective Povarov reaction with cyclic enethioureas.

One class of electron-rich dienes that were found to undergo Povarov reaction are vinylindoles. In 2010, Bernardi and Ricci found that these vinyl heteroarenes reacted at their terminal double bond instead of the more common normal-electron-demand Diels–Alder reaction (Scheme 14, top).<sup>69</sup> Indeed, the indole nucleus not only renders these olefins particularly electron-rich, guaranteeing sufficient reactivity, but also offers an anchor point for catalyst coordination through its NH proton. Shortly afterwards, Xiao highlighted the double behaviour of 2-vinylindoles in the non-asymmetric reaction with *N*-aryl imines.<sup>70</sup> In the presence of acidic catalyst, 1*H*-2-vinylindoles were found to undergo Povarov reaction, whereas when *N*-substituted indoles were employed, the reaction proceeded giving the normal-electron-demand Diels–Alder products (Scheme 14, bottom). This result was rationalized by considering, once again, a possible hydrogen bond between the indole NH and the catalyst, even though electronic factors might also influence the pathway of the reaction.



**Scheme 14.** Catalytic asymmetric Povarov reaction with 2- and 3- vinylindoles (top). Double behaviour of 2-vinylindoles with *N*-aryl imines (bottom).

Hydroxystyrenes are another class of aryl-activated olefin that can undergo Povarov reaction.<sup>71</sup> Masson and co-workers focused their studies on the *E*-isomer of isoeugenol in the reaction with *in situ* generated *N*-aryl imines.<sup>71a</sup> The reaction proceeded with good results in terms of yield, diastereoselectivity – favouring the all-*trans* isomer – and enantioselectivity (Scheme 15, top). Almost simultaneously Gong and co-workers developed a similar reaction employing 2-hydroxystyrenes (Scheme 15, bottom).<sup>71b</sup>



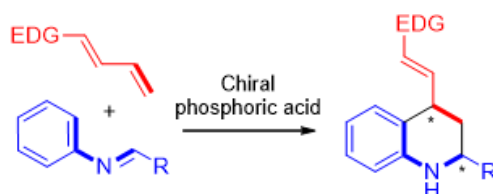
**Scheme 15.** Povarov reaction with (*E*)-isoeugenol (top). Povarov reaction with 2-hydroxystyrenes (bottom)

Although vinylindoles<sup>69,70</sup> and hydroxystyrenes<sup>71</sup> were found to undergo a Povarov reaction at their terminal double bond, in these cases the whole (hetero)aromatic moiety is the actual activating electron-donating group; therefore these reports cannot be properly considered as examples of vinylogous Povarov reactions.<sup>72</sup> Actually, the use of vinylogous reaction partners in Povarov cycloaddition has been documented marginally and only in non-enantioselective processes.<sup>72</sup> In this context, our work on the development of vinylogous Povarov reaction finds justification.

### 3.2. Aim of the work

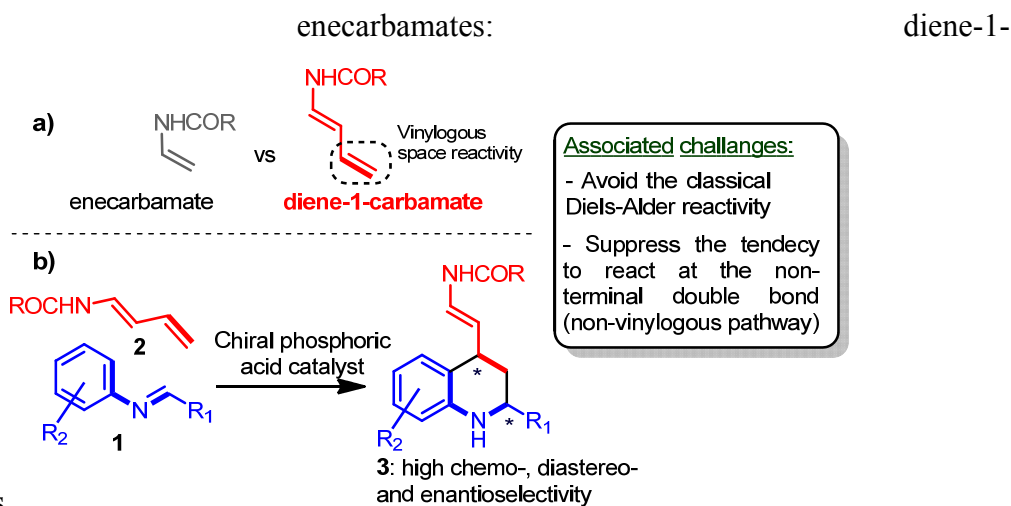
The aim of the work described in this chapter has been the realization of the first vinylogous variant of the catalytic asymmetric Povarov reaction (Scheme 16).<sup>73</sup>

To our purposes, focussing on BINOL derived phosphoric acid catalysts, we have been conscious of the requirement



**Scheme 16.** Vinylogous Povarov reaction

of a handle for dienophile coordination to the Lewis basic phosphoryl oxygen of the catalyst. Thus, we have decided to turn our attention towards the vinylogous derivatives of



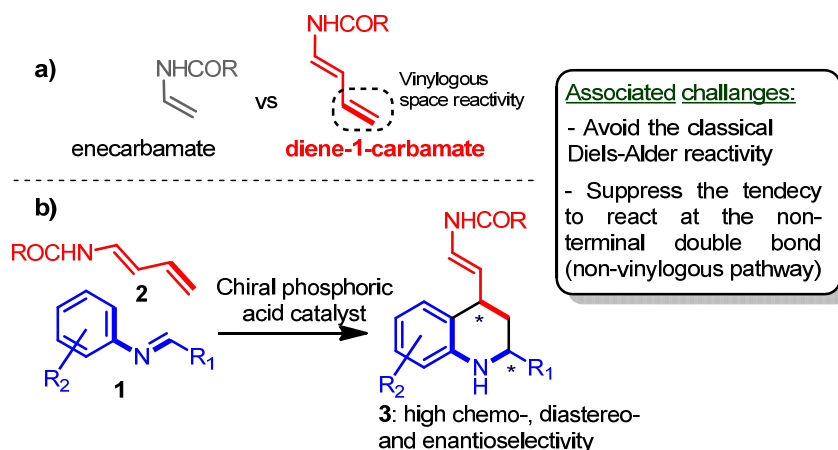
carbamates

Scheme 17a). These *N*-acyl amidodienes have been considered as potential dienophilic reaction partners, aiming at the engagement of the remote double bond, which is not directly attached to the electron-donating group, with concomitant transmission of the stereoinformation at a distant position from the anchoring point of the catalyst.

However, some synthetic challenges arise from this strategy: for instance, *N*-acyl amidodienes are known to undergo normal-electron-demand Diels–Alder cycloaddition, acting as electron-rich dienes.<sup>74</sup> Furthermore, it is note the propensity of  $\beta$ -alkyl enecarbamates to undergo Povarov reactions<sup>63</sup> despite the steric hindrance; thus, the avoidance of non-vinylogous reaction pathway has been also an important issue that has been tackled. Besides the related challenges, this work was aimed by the concept to expand the chemistry of enecarbamate towards vinylogous reactivity, hence permitting the engagement of diene-1-carbamates – as electron rich dienophile – in inverse-electron-

demand aza-Diels–Alder cycloaddition. This strategy lies in the frame of the “vinylogy principle” according to which the inductive effect of a functional group is transmitted through a double bond or a system of conjugated double bonds.<sup>75</sup> Importantly, by following our protocol, it would be possible to obtain enantioenriched 1,2,3,4-tetrahydroquinolines bearing an enecarbamate moiety at the 4-position. Given the rich chemistry of enecarbamates,<sup>76</sup> which has been considerably expanded in the frame of chiral phosphoric acid catalysis,<sup>77</sup> this moiety gives great potential for further synthetic manipulation, even in one-pot fashion.

Herein it is possible to anticipate that *N*-aryl imines **1** were reacted with diene-1-carbamates **2** in the presence of chiral phosphoric acid, giving highly diastereo- and enantioenriched 1,2,3,4-tetrahydroquinolines **3**, this reaction represents the first example of organocatalytic vinylogous Povarov reaction (Scheme 17b).



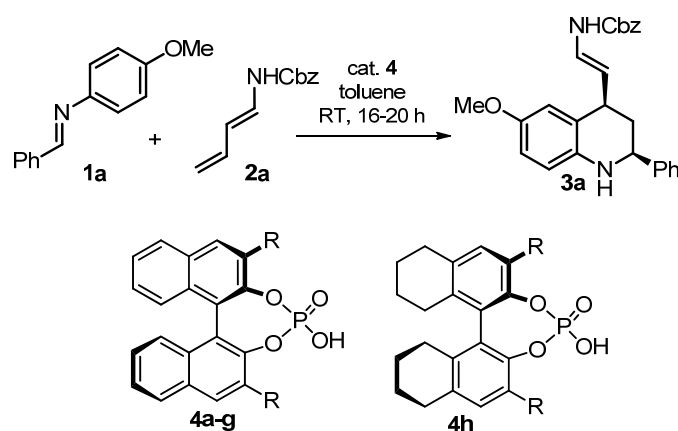
**Scheme 17.** Diene-1-carbamates enable asymmetric vinylogous Povarov reaction.

### 3.3. Results and discussion

The investigations on the asymmetric vinylogous Povarov reaction started from the screening of a series of common (*R*)-BINOL-derived phosphoric acid catalysts **4a-g** in the reaction between *N*-4-methoxyphenyl imine **1a** and *trans*-*N*-Cbz-1-amino-1,3-butadiene **2a**, in toluene as solvent (Table 2, entries 1-7). All catalysts were able to promote the reaction overnight, giving cycloadduct **3a** in low to moderate conversion and as a single *cis*-diastereoisomer. Amongst the catalyst tested, only **4b** and **4g** induced significant enantioselectivity (Table 2, entries 2 and 7). A further improvement was achieved by employing the H<sub>8</sub>-BINOL derivative of **4g**, which gave **3a** in excellent enantioselectivity (Table 2, entry 8). With this catalyst, an enhancement in catalytic

activity was observed by employing molecular sieves (MS) in the reaction (Table 2, entry 9). By using these drying agents, it was possible to decrease the catalyst loading to 1 mol%, affecting only marginally conversion and enantioselectivity (Table 2, entries 10 and 11). A further decrease to 0.3 mol% lowered the conversion (Table 2, entry 12). A preliminary reaction progress kinetic analysis<sup>78</sup> suggested that the low conversion with < 1 mol% loading is not due to insufficient catalyst activity, but rather due to deactivation of the catalyst during the reaction course. In the attempt to elucidate the causes of this deactivation, some control experiments were conducted and will be discussed afterwards.

**Table 2.** Screening of catalysts and reaction conditions in the vinylogous Povarov reaction between imine **1a** and diene-1-carbamate **2a**<sup>a</sup>

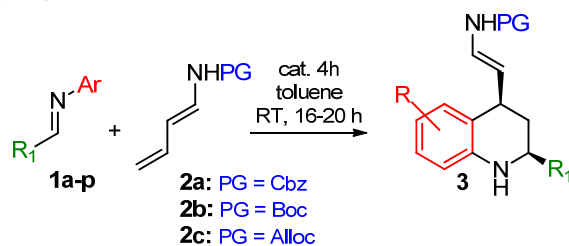


Entry	Cat. <b>4</b> (mol%)	R	MS <sup>b</sup>	Conv. <sup>c</sup> (%)	ee <sup>d</sup> (%)
1	<b>4a</b> (10)	C <sub>6</sub> H <sub>5</sub>	no	88	15
2	<b>4b</b> (10)	3,5-(CF <sub>3</sub> ) <sub>2</sub> C <sub>6</sub> H <sub>3</sub>	no	78	60
3	<b>4c</b> (10)	2,4,6-( <i>i</i> -Pr) <sub>3</sub> C <sub>6</sub> H <sub>2</sub>	no	72	13
4	<b>4d</b> (10)	4-NO <sub>2</sub> C <sub>6</sub> H <sub>4</sub>	no	57	20
5	<b>4e</b> (10)	SiPh <sub>3</sub>	no	30	10
6	<b>4f</b> (10)	9-phenanthrenyl	no	49	7
7	<b>4g</b> (10)	9-anthracenyl	no	59	92
8	<b>4h</b> (10)	9-anthracenyl	no	80	97
9	<b>4h</b> (10)	9-anthracenyl	4 Å <sup>e</sup>	84	98
10	<b>4h</b> (2.5)	9-anthracenyl	4 Å	91	98
11	<b>4h</b> (1.0)	9-anthracenyl	4 Å	85	98
12	<b>4h</b> (0.3)	9-anthracenyl	4 Å	52	95

(a) Conditions: imine **1a** (0.05 mmol), catalyst **4**, dienophile **2a** (0.06 mmol), toluene (0.20 mL), RT, overnight. In all cases, a single diastereoisomer was observed by <sup>1</sup>H NMR spectroscopy in the crude mixture. (b) 20 mg molecular sieves were employed where indicated. (c) Conversion, as determined by <sup>1</sup>H NMR spectroscopy on the crude mixture. (d) Determined by chiral stationary phase HPLC. (e) Very similar results were obtained with 3 and 5 Å MS.

The scope of the reaction was then inspected by using the optimal catalyst **4h** at 2.5 mol% loading instead of 1 mol%, in order to employ a more robust procedure. All the results are summarized in Table 3.

**Table 3.** Scope of the vinylogous Povarov reaction <sup>a</sup>.



Entry	<b>1</b>	<b>R<sub>1</sub></b>	<b>Ar</b>	<b>2</b>	<b>3-Yield<sup>b</sup> (%)</b>	<b>ee<sup>c</sup> (%)</b>
1	<b>1a</b>	C <sub>6</sub> H <sub>5</sub>	4-MeOC <sub>6</sub> H <sub>4</sub>	<b>2a</b>	<b>3a-85</b>	98
2 <sup>d</sup>	<b>1a</b>	C <sub>6</sub> H <sub>5</sub>	4-MeOC <sub>6</sub> H <sub>4</sub>	<b>2a</b>	<b>3a-70</b>	98
3	<b>1b</b>	4-BrC <sub>6</sub> H <sub>4</sub>	4-MeOC <sub>6</sub> H <sub>4</sub>	<b>2a</b>	<b>3b-83</b>	99
4	<b>1c</b>	2-BrC <sub>6</sub> H <sub>4</sub>	4-MeOC <sub>6</sub> H <sub>4</sub>	<b>2a</b>	<b>3c-90</b>	92
5	<b>1d</b>	4-MeOC <sub>6</sub> H <sub>4</sub>	4-MeOC <sub>6</sub> H <sub>4</sub>	<b>2a</b>	<b>3d-78</b>	99
6	<b>1e</b>	3,4-(MeO) <sub>2</sub> C <sub>6</sub> H <sub>3</sub>	4-MeOC <sub>6</sub> H <sub>4</sub>	<b>2a</b>	<b>3e-63</b>	99
7	<b>1f</b>	2-naphthyl	4-MeOC <sub>6</sub> H <sub>4</sub>	<b>2a</b>	<b>3f-91</b>	98
8 <sup>d</sup>	<b>1f</b>	2-naphthyl	4-MeOC <sub>6</sub> H <sub>4</sub>	<b>2a</b>	<b>3f-70</b>	>99
9	<b>1g</b>	1-naphthyl	4-MeOC <sub>6</sub> H <sub>4</sub>	<b>2a</b>	<b>3g-79</b>	89
10	<b>1h</b>	2-thienyl	4-MeOC <sub>6</sub> H <sub>4</sub>	<b>2a</b>	<b>3h-53</b>	87
11 <sup>d</sup>	<b>1i</b>	<i>i</i> -Pr	4-MeOC <sub>6</sub> H <sub>4</sub>	<b>2a</b>	<b>3i-80</b>	99
12 <sup>d</sup>	<b>1j</b>	Ph(CH <sub>2</sub> ) <sub>2</sub>	4-MeOC <sub>6</sub> H <sub>4</sub>	<b>2a</b>	<b>3j-76</b>	84
13	<b>1k</b>	C <sub>6</sub> H <sub>5</sub>	C <sub>6</sub> H <sub>5</sub>	<b>2a</b>	<b>3k-94</b>	99
14	<b>1l</b>	4-BrC <sub>6</sub> H <sub>4</sub>	C <sub>6</sub> H <sub>5</sub>	<b>2a</b>	<b>3l-74</b>	99
15	<b>1m</b>	C <sub>6</sub> H <sub>5</sub>	3,4-(MeO) <sub>2</sub> C <sub>6</sub> H <sub>3</sub>	<b>2a</b>	<b>3m-63<sup>e</sup></b>	97
16	<b>1n</b>	C <sub>6</sub> H <sub>5</sub>	4-ClC <sub>6</sub> H <sub>4</sub>	<b>2a</b>	<b>3n-25</b>	98
17	<b>1o</b>	C <sub>6</sub> H <sub>5</sub>	3-BrC <sub>6</sub> H <sub>4</sub>	<b>2a</b>	<b>3o-60<sup>f</sup></b>	99/99
18	<b>1a</b>	C <sub>6</sub> H <sub>5</sub>	4-MeOC <sub>6</sub> H <sub>4</sub>	<b>2b</b>	<b>3p-89</b>	99
19 <sup>d</sup>	<b>1a</b>	C <sub>6</sub> H <sub>5</sub>	4-MeOC <sub>6</sub> H <sub>4</sub>	<b>2b</b>	<b>3p-90</b>	98
20	<b>1a</b>	C <sub>6</sub> H <sub>5</sub>	4-MeOC <sub>6</sub> H <sub>4</sub>	<b>2c</b>	<b>3q-73</b>	99

(a) Conditions: **1a-p** (0.15 mmol), **4h** (0.00375 mmol), **2a-c** (0.18-0.30 mmol), toluene (0.60 mL), 4 Å MS (20 mg), RT, 16-20 h. A single diastereoisomer was observed by <sup>1</sup>H NMR spectroscopy in the crude mixture. (b) Isolated yield. (c) Determined by chiral stationary phase HPLC. (d) Imine formed in situ. 110 mg 4 Å MS and 5 mol% **4h** were employed. (e) The 6,7-(MeO)<sub>2</sub> regioisomer was exclusively obtained. (f) 2.8:1 diastereomeric mixture. The 7-bromo regioisomer was obtained.

Imines **1a-h** derived from different (hetero)aromatic aldehydes, could be employed with very good results (Table 3, entries 1-10). Thus, the reaction proved to be tolerant towards a broad range of different aldehydes, such as electron-rich, electron-neutral, electron-deficient and heteroaromatic. The developed protocol could be readily implemented to its three-component version, thus confirming the modular nature of Povarov reaction. In order to accomplish the multicomponent approach, it was necessary to employ a larger amount of molecular sieves and a slightly increased catalyst loading (5 mol%), to compensate the sensitivity of catalyst **4h** to water, generated during the *in situ* imine formation. Under these conditions, the products **3** were obtained with results comparable to the two-component procedure (Table 3, entries 2, 8, 19), and, more importantly, the reaction scope could be expanded to the unstable imines **1j,k** derived from enolisable aldehydes (Table 3, entries 11 and 12).

Variations at the aniline moiety in imines **1k-o** were also carried out. Imines derived from electron-neutral and electron-rich anilines afforded the corresponding cycloadducts **3k-m** in variable yields, but excellent enantioselectivities. (Table 3, entries 13-15). Interestingly, the vinylogous Povarov reaction is not only limited to electron-rich-derived imines, since **1n,o**, derived from electron-poor anilines reacted in excellent enantioselectivities, albeit in moderate yields (Table 3, entries 15 and 16).

Full regioselectivity in the cyclisation, favouring the least sterically hindered product, was observed in the reactions with imines **1m** and **1o**, substituted at 3-position of the aniline ring (Table 3, entries 15 and 17). In the case of **3m**, the reaction could in principle give two regioisomeric cycloadducts; nevertheless, from the  $^1\text{H}$  NMR analysis, it was possible to determine that the only cycloadduct formed was the 6,7-dimethoxy regioisomer **3m**, as the signals related to the aromatic protons of the 1,2,3,4-tetrahydroquinoline moiety, appeared as two singlets, and were thus indicative of a *para* relationship between these protons (Figure 13). Surprisingly, the reaction with the *N*-3-bromophenyl imine **1o** furnished the corresponding cycloadduct **3o** as a diastereomeric mixture at C2-C4, favouring the 2,4-*trans* isomer which was not even observed in any of the other examples. Also in this case,  $^1\text{H}$  NMR analysis was performed in order to understand the regiochemistry of the reaction. The signals related to the aromatic protons of the 1,2,3,4-tetrahydroquinoline moiety of the minor diastereoisomer were indicative of the *ortho/meta* relationship and not compatible with the *ortho/ortho* one; moreover, the signals related to the aromatic proton of the 1,2,3,4-tetrahydroquinoline moiety of the

major diastereoisomer appeared as a doublet of doublets and was thus indicative of a *ortho/meta* relationship with the other aromatic protons (Figure 13).

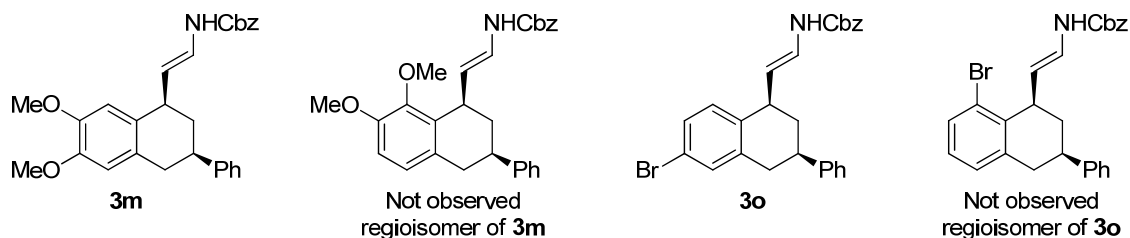
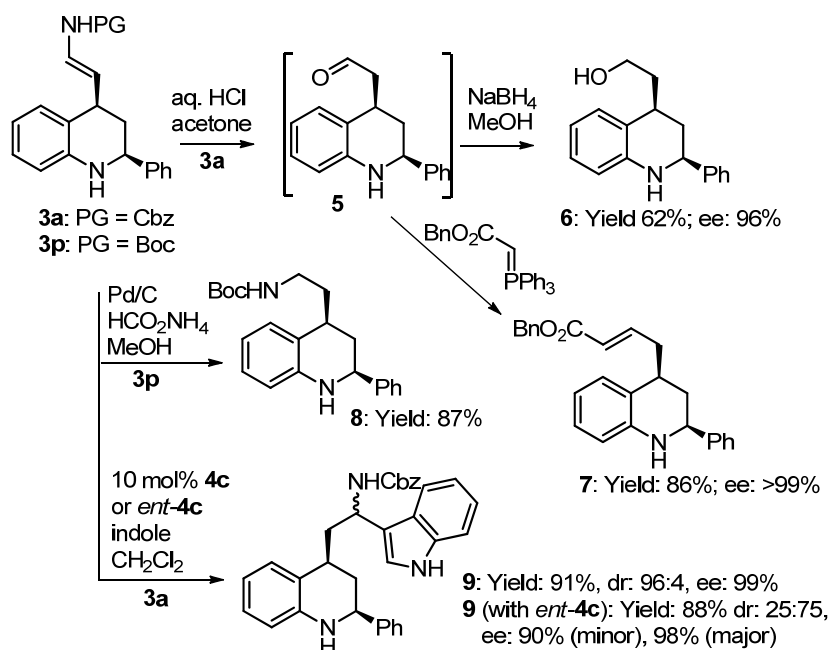


Figure 13.

Finally, the scope of the reaction was extended to dienophiles **2**. Here, different protecting groups, such as the Boc and Alloc groups in **2b** and **2c**, were successfully employed, giving comparable results to their Cbz counterpart **2a** (Table 3, entries 1 and 18-20).

Once demonstrated the broad generality of the vinylogous Povarov reaction, resulted in 17 different examples, cycloadducts **3a** and **3p** were then subjected to few synthetic elaborations at their enecarbamate moiety, summarized in Scheme 18.



Scheme 18. Synthetic elaborations on the catalytic products.

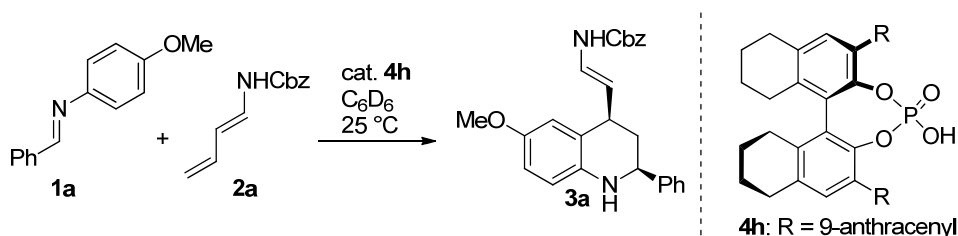
The enecarbamate moiety in **3a** was hydrolyzed in mild acidic conditions giving aldehyde **5**, which was conveniently isolated as the corresponding alcohol **6** after reduction with sodium borohydride, or as the  $\alpha,\beta$ -unsaturated ester **7** obtained by means of Wittig olefination using a stabilized phosphorous ylide. Reduction of the double bond in **3p** in the presence of ammonium formate and palladium over charcoal as catalyst,

furnished the protected primary amine **8**. In this case the Boc protected THQ **3p** was selected as starting material since the parent Cbz protected **3a** was sensitive to the hydrogenolytic conditions.

The enecarbamate moiety placed at C4 position of THQs represents a versatile handle for further synthetic elaborations. Addition of indole to the *N*-Cbz enecarbamate **3a** was efficiently carried out under chiral phosphoric acid catalysis,<sup>77b,c</sup> by using (*R*)-TRIP catalyst **4c**. The stereochemistry of the newly formed chiral centre in **9** could be partially controlled by the enantiomer of the catalyst **4c** employed. This transformation could be readily implemented in a one-pot process, affording the adduct **9** in acceptable yield but perfect diastereo- and enantioselectivity. Given the recognized importance of one-pot procedures as a new tool for organic synthesis,<sup>24</sup> this latter synthetic elaboration remarkably highlights the possibility to construct complex molecular scaffolds, with excellent control of the stereochemistry, from readily available substrates.<sup>24</sup>

### 3.3.1. Preliminary kinetic investigation of the catalytic enantioselective vinylogous Povarov reaction

The kinetics of the reaction between imine **1a** and dienophile **2a** was preliminarily studied by <sup>1</sup>H NMR using a reaction progress analysis approach (Scheme 19).<sup>78</sup>



**Scheme 19.** Vinylogous Povarov reaction between imine **1a** and **2a** used for kinetic studies.

The kinetic experiments were set up and elaborated as follows: a Schlenk tube equipped with a magnetic stirring bar was charged with 4 Å molecular sieves (70 mg). The molecular sieves were thermally activated under vacuum. After cooling to RT, the tube was filled with a N<sub>2</sub> atmosphere, then charged with the appropriate amount of imine **1a**. The appropriate amount of C<sub>6</sub>D<sub>6</sub> of a stock 0.012 M solution of catalyst **4h** in C<sub>6</sub>D<sub>6</sub> were then added. Overall, 600 μL of C<sub>6</sub>D<sub>6</sub> were employed in each experiment. The solution was stirred at 25 °C for a few minutes. The appropriate amount of dienophile **2a** was then added in one portion. After few seconds stirring to homogenize the solution, the whole mixture including the molecular sieves was transferred in a pre-dried, N<sub>2</sub>-filled NMR

tube by means of a 1 mL syringe equipped with a short and large needle. The tube was placed in a Varian 400 MHz NMR instrument at 25 °C, spinned at 16-20 Hz, and after automatic lock and shimming,  $^1\text{H}$  NMR spectra ( $n_t = 1$ ) were recorded every minute, using the automatic array pad function, until ca 70-80% conversion. From the last  $^1\text{H}$  NMR spectra recorded, it was checked that no significant decomposition of imine **1a**, dienophile **2a** or product **3a** occurred in the time frame of the analysis, nor that the reaction gave significant amounts of by-products. A preliminary control experiment carried out in the absence of catalyst **4h**, showed that background reactivity is not significant (<5% conversion after 18 h).

The spectra were collectively elaborated (phased, drift correction), and the relevant peaks integrated after baseline correction, from which the conversion at each time was determined. From the conversion, imine **2a** concentration was calculated. The resulting curve of imine vs time was plotted and fitted to a polynomial equation (ninth order) with the OriginPro 7 program. The derivative of this equation, giving the dependence of reaction rate on imine concentration, was employed for the kinetic analysis. As this curve is purely empirical, it could be used only in the range of imine concentration which was effectively employed in the experiment.

The results obtained from these experiments can be summarized as follows:

1. Reactions at different catalysts concentrations, under otherwise identical reaction conditions, to determine the order of the reaction respect to catalyst **4h**, by comparing the TOF of the experiments. TOF values were determined by dividing the reaction rate by the initial catalyst concentration used in each experiment (Figure 14).

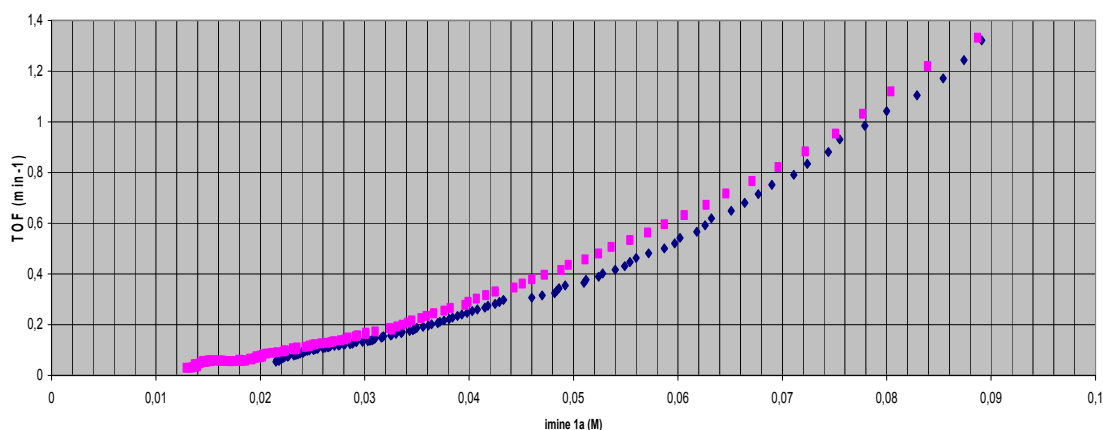


**Figure 14.** ◆:  $C_0$  [imine **1a**] 0.10 M,  $C_0$  [dienophile **2a**] 0.20 M,  $C_0$  [catalyst **4h**] 0.0020 M. ■  $C_0$  [imine **1a**] 0.10 M,  $C_0$  [dienophile **2a**] 0.20 M,  $C_0$  [catalyst **4h**] 0.0030 M.

In the plot, the two curves are roughly superimposable. It is thus possible to conclude that the reaction is approximately first order in catalyst concentration.

2. Reactions with the “same excess”. Two reactions were performed by employing the same concentration of catalyst **4h**, different starting concentration of imine **1a**, and same “excess” of dienophile **2a** in terms of concentration (Figure 15). In other words, the reaction with lower imine concentration starts exactly under the conditions (concentration of substrates and catalyst) of the other reaction at 25% conversion. This experiment shows if the activity of the catalyst is the same during the whole reaction course, or if catalyst deactivation/decomposition occurs, influencing the concentration of active catalyst which is part of the rate law (Figure 15).

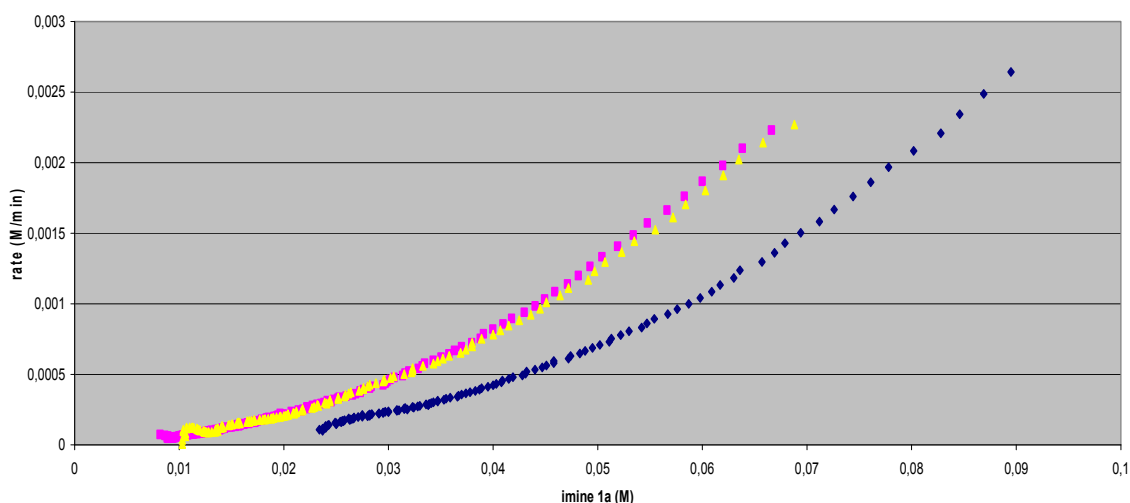


**Figure 15.** ♦:  $C_0$  [imine **1a**] 0.10 M,  $C_0$  [dienophile **2a**] 0.20 M,  $C_0$  [catalyst **4h**] 0.0020 M. ■  $C_0$  [imine **1a**] 0.075 M,  $C_0$  [dienophile **2a**] 0.175 M,  $C_0$  [catalyst **4h**] 0.0020 M. ▲  $C_0$  [imine **1a**] 0.075 M,  $C_0$  [dienophile **2a**] 0.175 M,  $C_0$  [catalyst **4h**] 0.0020 M,  $C_0$  [product **3a**] 0.025 M.

In Figure 15, the two curves ♦ (standard reaction) and ■ (reaction starting after 25% conversion) are not superimposable. Thus, catalyst deactivation/decomposition heavily occurs affecting (lowering) the reaction rate. To check if catalyst inhibition by the product was the reason for this behaviour, a third experiment ▲ was carried out under the same conditions of ■ but adding at the beginning the amount of product **3a** formed when the curve ♦ reaches 25% conversion. However, as this curve ▲ is roughly superimposable to ■ catalyst inhibition by the product is not the reason for this considerable decrease in catalyst activity with time.

Then two similar experiments were performed in the absence of molecular sieves, in order to check if these drying agents were responsible for catalyst deactivation (Figure

16). Due to the much lower activity of catalyst **4h** in the absence of molecular sieves, higher catalyst/substrates initial concentrations had to be used.

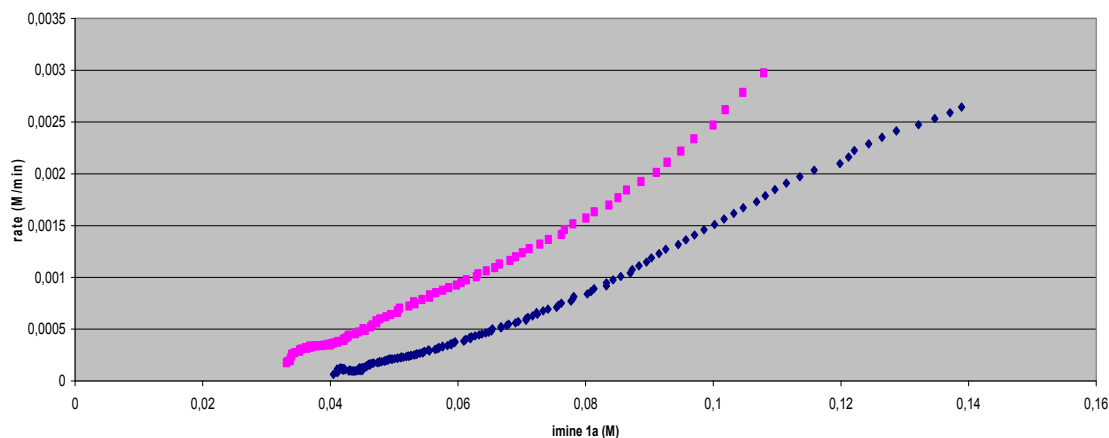


**Figure 16.** ♦:  $C_0$  [imine **1a**] 0.15 M,  $C_0$  [dienophile **2a**] 0.30 M,  $C_0$  [catalyst **4h**] 0.015 M. ■  $C_0$  [imine **1a**] 0.12 M,  $C_0$  [dienophile **2a**] 0.27 M,  $C_0$  [catalyst **4h**] 0.015 M.

As the two curves in Figure 16 are also clearly not superimposable, catalyst deactivation is not due to the presence of molecular sieves in the reaction.

From these experiments, it can be concluded that the reaction rate is approximately first order in catalyst concentration, but that catalyst deactivation heavily occurs during the course of this reaction. This prevents the determination of a rate law using the reaction progress kinetic analysis approach, which requires the same amount of active catalyst during the whole (or most of) the reaction course. This catalyst deactivation is neither due to product inhibition nor to the presence of molecular sieves.

This result suggests that the 1 mol% catalyst loading which at least has to be employed in this reaction is not due to the scarce activity of the catalyst, but rather to its decomposition, giving a crucial information on the direction to follow for decreasing the catalyst loading in this (and related) reaction.

### 3.3.2. Determination of relative and absolute configuration of adducts **3** and **9**

Compound **3k** was selected as representative compound for the determination of relative configuration by conformational analysis. The relative stereochemistry was determined by means of NMR spectroscopy. Full assignment of the  $^1\text{H}$  and  $^{13}\text{C}$  spectra was preliminarily achieved by bi-dimensional

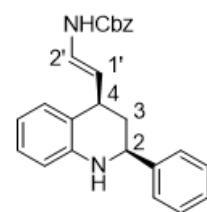


**Figure 17.** Compound **3k**.

experiments (COSY, gHSQC and gHMBC, taken in CDCl<sub>3</sub> solutions).

One of the signals of the two diastereotopic protons at C-3 appeared as a pseudo-quartet, with a large coupling constant ( $J=12.4$  Hz, H-3b in Figure 18). This implies that this proton is coupled with three hydrogens with large coupling constants, which are consistent with the geminal coupling with H-3a and with two trans-diaxial couplings with H-2 and H-4, due to a dihedral angle close to 180°.<sup>79</sup>

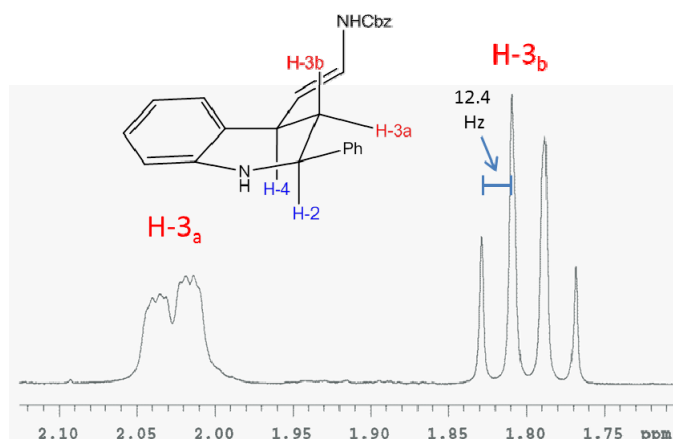


**Figure 18.** Expansion of the <sup>1</sup>H spectrum (600 MHz in CDCl<sub>3</sub>) of 3k showing the signals of the two diastereotopic hydrogens of C-3.

This clearly indicates that both H-2 and H-4 are in pseudo-axial position on the tetrahydroquinoline ring, whereas the phenyl and the ene-carbamate moiety occupy the pseudo-equatorial positions. Furthermore, the signal of H-3a (the second diastereotopic hydrogen of C-3) exhibited the same large geminal constant (12.4 Hz) and two small coupling constants due to the equatorial-axial coupling, where the dihedral angle was close to 90°.

Mono-dimensional DPGSE-NOE experiments<sup>80</sup> were acquired in order to confirm the relative stereochemistry at C-2 and C-4. On saturation of the vinylic hydrogen H-1' (trace a in Figure 19), NOE enhancement was observed for one proton at C-3 (H-3b, in pseudo-axial position) and no enhancement was observed for the other ene-carbamate proton H-2'. This confirms the *E* geometry of the double bond. The large NOE on H-3b suggests that H-1' is *anti* to H-4. On saturation of H-4, NOE were observed on H-2 (trace c in Figure 19) and on the signal of H-3a (in pseudo-equatorial position). On saturation of H-2 (trace b in Figure 19), NOE were observed for H-4 and for H-3a, thus confirming the 1-3 diaxial relationship of H-2 and H-4, already deduced from the analysis of the *J*-couplings of the <sup>1</sup>H NMR spectrum. NMR analysis thus confirmed the *cis* relative configuration of the two asymmetric centres of the 1,2,3,4-tetrahydroquinoline skeleton (thus 2*R*\*,4*S*\*), and the *E*-geometry of the exocyclic double bond.

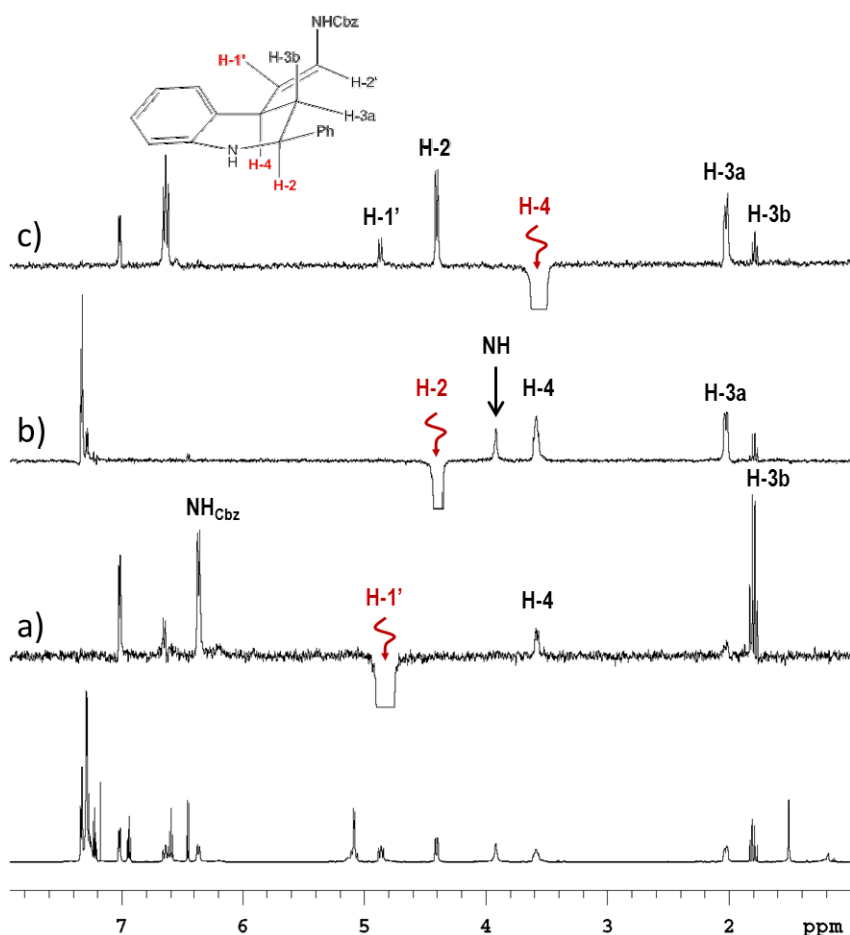


**Figure 19.** DPGSE-NOE spectra of **3k** (600 MHz in  $\text{CDCl}_3$ ). Bottom:  $^1\text{H}$ -NMR control spectrum; trace a) saturation of H-1'; trace b) saturation of H-2; trace c) saturation of H-4.

The  $^1\text{H}$  NMR spectra of the other cycloadducts **3** showed, in all cases, that the signal related to H-3b appears as a pseudo-quartet. This was consistent with a *cis* relative configuration of the two asymmetric centres. Thus, the relative configuration of all other cycloadducts **3** was deduced to be 2,4-*cis*, with the exception of the already mentioned **3o** which furnished a mixture of diastereoisomers, with the 2,4-*trans* as the major product. Having in hand the relative configuration and suitable information about the preferred conformation, the assignment of the absolute configuration was tackled by chiroptical methods.<sup>81</sup> The main pitfall of this approach is the difficulty to manage flexible molecules. About this point, the adducts **3** are not really flexible, since there is a rigid core containing the two chiral centres and strong UV chromophores close to them. Thus, chiroptical methods for the assignment of the absolute configuration of adducts **3** should be reliable. Comparison of the calculated (TD-DFT) with the experimental ECD spectrum was performed. The best simulation was obtained by the M06-2X functional, but all the simulated spectra now show a good agreement with the experimental one (Figure 20). Thus the absolute configuration could be reliably assigned as 2*S*,4*R*. This

result is in agreement with previously published Povarov reactions catalysed by similar BINIOL-derived phosphoric acid catalysts.<sup>62,63,66,68,69,71</sup>

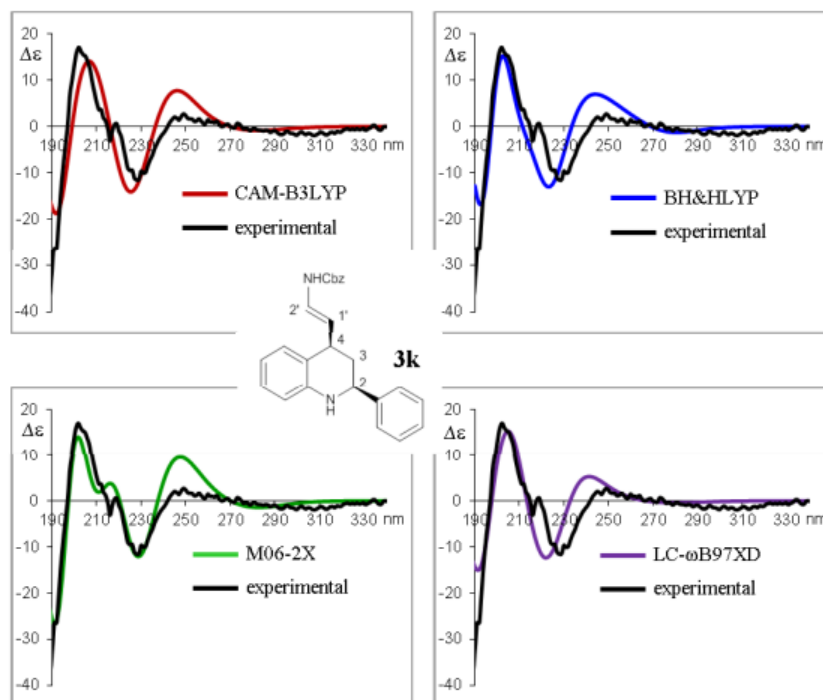


**Figure 20.** Comparison between the experimental ECD spectrum (black traces) and simulated spectra (red, blue, green and purple traces)

Along of this, after several unsuccessful attempts, suitable crystals for the determination of the absolute configuration by the anomalous dispersion X-ray method,<sup>82</sup> were obtained (for details see § 3.4.5). Thus the absolute configuration was confirmed to be as *2S,4R*. The determined relative and absolute configuration on compound **3b** by X-ray undoubtedly confirmed the relative stereochemistry already determined on **3k** by NMR analysis, as well as its absolute configuration determined with chiroptical techniques.

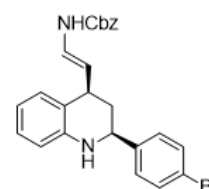
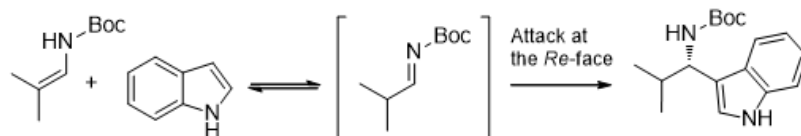


**Figure 21.** Compound **3b**.

The configuration of the chiral centre deriving from the addition of indole to the enecarbamate of cycloadduct **3a** catalysed by **4c** can be tentatively assigned on the basis



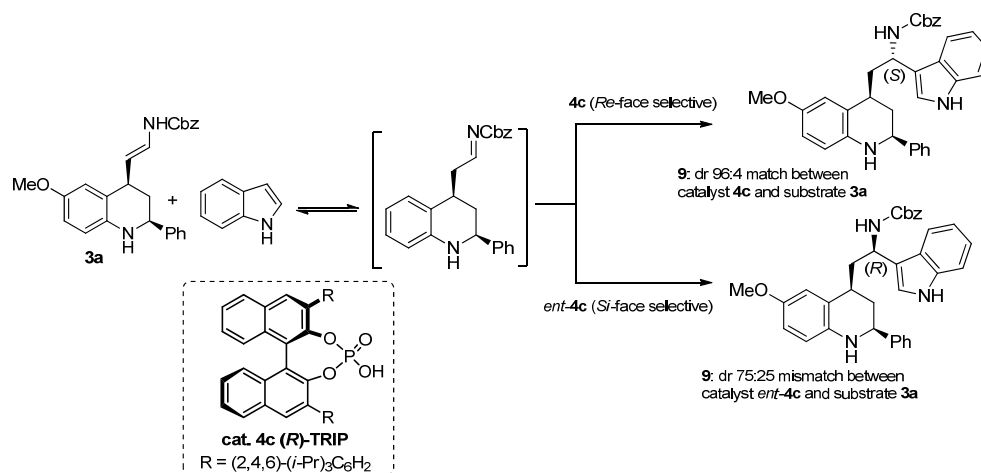
**Scheme 20.** Reported addition of indole to in situ generated N-carbamoyl imines catalysed by **4c** (ref. 83).

of the previously reported face-selectivity of catalyst (*R*)-TRIP **4c** in the reaction of indoles

with simpler enecarbamates.<sup>83</sup> In more detail, it is known that (*R*)-**4c** promotes a selective

addition of indole at the Re-face of an intermediate N-Boc imine, generated in situ from an *N*-Boc enecarbamate (Scheme 20).

It can be assumed that also in our case (*R*)-**4c** promotes the attack of indole at the same prochiral face of the intermediate *N*-Cbz imine, derived from the enecarbamate of **3a**, giving predominantly (96:4) an *S* configured product **9**. This hypothesis is confirmed by the reaction performed with *ent*-**4c** ((*S*)-**4c**), which gives predominantly (75:25) the opposite diastereoisomer of **9**. Thus, the configuration of the newly formed chiral centre in the Friedel-Crafts addition is partially controlled by the catalyst employed, with (*R*)-**4c** matching the stereochemical bias given by the pre-existing chiral centres of cycloadduct **3a**, and (*S*)-**4c** mismatching this bias (Scheme 21).

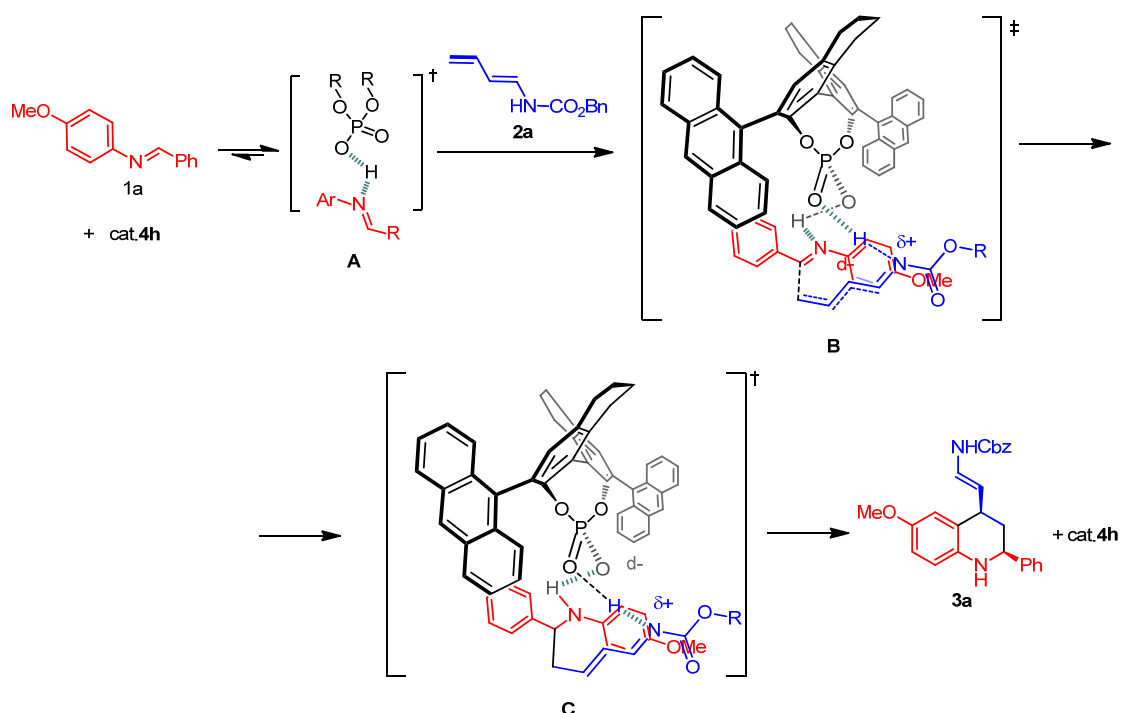


**Scheme 21.** Addition of indole to the enecarbamate of **3a** catalysed by **4c** and *ent*-**4c**.

### 3.3.3. Mechanistic proposal

To account for the observed 2*S*,4*R* absolute configuration, a reaction model involving double coordination of catalyst **4h** to both imine and dienophile can be considered (Scheme 22), on the basis of the generally accepted mode of action of BINOL derived phosphoric acid catalysts.<sup>39</sup> In particular, as shown in Scheme 22 for imine **1a** and dienophile **2a**, it can be assumed that attack of the dienophile to the imine **A**, activated by the catalyst through a hydrogen bond interaction or protonation, gives a transition state **B** wherein the phosphoryl oxygen stabilises the positive charge on the dienophile by acting as a Lewis base coordinating the carbamate proton. The large 9-anthracenyl groups guide the stereoselectivity mainly by steric interactions with the substrates, favouring attack of the dienophile at the *Si*-face of the activated imine. Presuming a two steps cycloaddition pathway, an intermediate catalyst coordinated *N*-acyl iminium ion **C** is formed first,

which then undergoes an intramolecular Friedel-Crafts reaction to give the 2*S*,4*R*-disubstituted 1,2,3,4-tetrahydroquinoline product **3a**. It could be assumed a similar reaction pathway leading to the attack at the same face of the imines **1** in all other cases, thus the absolute configuration of the remaining cycloadduct **3** has been assigned by analogy. In all cases, the reactions performed with the (*R*)-BINOL derived catalyst **4h** gave the first eluting peak as the major enantiomer.



**Scheme 22.** Proposed reaction pathway and model for enantioselectivity.

## 3.4. Experimental details

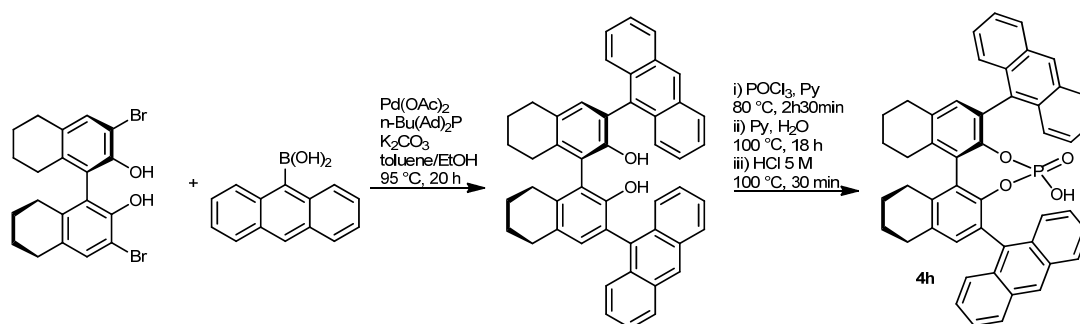
### 3.4.1. General methods and materials

$^1\text{H}$ ,  $^{13}\text{C}$  NMR spectra were recorded on a Varian AS 300, 400 or 600 spectrometer. Chemical shifts ( $\delta$ ) are reported in ppm relative to residual solvent signals for  $^1\text{H}$  and  $^{13}\text{C}$  NMR.<sup>84</sup>  $^{13}\text{C}$  NMR spectra were acquired with  $^1\text{H}$  broad band decoupled mode. Mass spectra were recorded on a micromass LCT spectrometer using electrospray (ES) ionisation techniques. Optical rotations were measured on a Perkin-Elmer 241 polarimeter. The enantiomeric excess (ee) of the products was determined by chiral stationary phase HPLC, using a UV detector operating at 254 nm.

Analytical grade solvents and commercially available reagents were used as received, unless otherwise stated. Chromatographic purifications were performed using 70-230 mesh silica. Racemic samples were prepared using diphenylphosphonic acid or  $\text{Sc}(\text{OTf})_3$

as catalyst, in  $\text{CH}_2\text{Cl}_2$  or toluene at room temperature for 24-60 h. Toluene was passed through neutral alumina before use. *N*-4-methoxyphenyl imines **1a-h** were obtained refluxing an equimolar mixture of 4-methoxyaniline and the appropriate aldehyde in EtOH for a few hours, and collected by filtration. Imines **1k-o** were obtained stirring for 48-60 h benzaldehyde and the appropriate aniline derivative in  $\text{CH}_2\text{Cl}_2$  in the presence of activated 4Å molecular sieves. Dienophiles **2a,c**<sup>85</sup> and **2b**<sup>74a</sup> were prepared by following a literature procedure. (*R*)-3,3'-Dibromo- $\text{H}_8$ -BINOL was prepared according to the literature.<sup>86</sup>

### 3.4.2. Preparation of $\text{H}_8$ -BINOL derived phosphoric acid catalyst **4h**



**Scheme 23.** Synthesis of chiral phosphoric acid **4h**.

The preparation of catalyst **4h** from 3,3'-dibromo- $\text{H}_8$ -BINOL reported below is based on ref.86b. However, both Suzuki coupling and phosphoric acid formation were substantially modified (Scheme 23). This adapted protocol, still based on the same catalyst used in ref.86b, proved to be more reliable than the original procedure, furnishing clean and well characterized products.

#### (*R*)-3,3'-Di(anthracen-9-yl)-5,5',6,6',7,7',8,8'-octahydro-[1,1'-binaphthalene]-2,2'-diol.

A Schlenk tube equipped with a magnetic stirring bar was charged with (*R*)-3,3'-dibromo- $\text{H}_8$ -BINOL (244 mg, 0.54 mmol), crude 9-anthracenyl boronic acid (600 mg),  $\text{Pd}(\text{OAc})_2$  (12.1 mg, 0.054 mmol), *n*-Bu(Ad)<sub>2</sub>P (21.2 mg, 0.059 mmol) and  $\text{K}_2\text{CO}_3$  (894 mg, 0.48 mmol). The tube was evacuated, then backfilled with  $\text{N}_2$ . Toluene (6.0 mL) and EtOH (1.7 mL) were added, the Schlenk tube was closed and screw-capped and immediately placed in an oil bath pre-warmed to 95 °C. The dark mixture was stirred at this temperature for 20 h, then cooled to RT. Sat.  $\text{NH}_4\text{Cl}$  was then added and the mixture transferred to a separating funnel with the aid of a little amount of EtOAc. The phases were separated and the aqueous phase extracted three times with  $\text{CH}_2\text{Cl}_2$ . The combined organic extracts were dried over  $\text{MgSO}_4$ , filtered and evaporated. Chromatographic purification on silica gel (*n*-hexane/ $\text{CH}_2\text{Cl}_2$  from 3:1 to 1:1) gave the title compound as a pale yellow solid in 61% yield.  $[\alpha]_{\text{D}}^{33} = +34^\circ$  (*c* = 0.385 in  $\text{CHCl}_3$ );  $^1\text{H NMR}$  ( $\text{CDCl}_3$ , 400 MHz)  $\delta$  = 8.52 (s, 2H), 8.10-8.06 (m, 2H), 8.05-8.01 (m, 2H), 7.87-7.82 (m, 2H), 7.73-7.69 (m, 2H), 7.53-7.39 (m, 6H), 7.29 (ddd, *J* = 8.8, 6.6, 1.5 Hz, 2H), 7.09 (s, 2H),

4.62 (s, 2H), 2.88-2.81 (m, 4H), 2.70 (dt,  $J_d = 18.2$  Hz,  $J_t = 6.4$  Hz, 2H), 2.64 (dt,  $J_d = 17.8$  Hz,  $J_t = 6.1$  Hz, 2H), 1.99-1.84 (m, 8H);  $^{13}\text{C}$  NMR ( $\text{CDCl}_3$ , 100 MHz)  $\delta = 149.2$ , 137.2, 133.1, 131.8, 131.6, 131.5, 130.7, 130.6, 129.9, 128.6, 128.4, 127.1, 126.5, 126.4, 125.8, 125.7, 125.2, 125.1, 122.2, 120.9, 29.2, 27.4, 23.3, 23.1; ESIMS 669  $[\text{M} + \text{Na}^+]$ .

**(R)-3,3'-Di(anthracen-9-yl)-5,5',6,6',7,7',8,8'-octahydro-[1,1'-binaphthalene]-2,2'-diyl hydrogen phosphate (4h)**

In a 100 mL round bottom flask equipped with a magnetic stirring bar, the thus obtained (R)-3,3'-di(anthracen-9-yl)-H8-BINOL (211 mg, 0.33 mmol) was dissolved in dry pyridine (0.6 mL). To this solution,  $\text{POCl}_3$  (62  $\mu\text{L}$ , 0.66 mmol) in dry pyridine (0.6 mL) was added dropwise. The mixture was then heated at 80 °C under  $\text{N}_2$  with stirring, until TLC (*n*-hexane/ $\text{CH}_2\text{Cl}_2$  1:1) indicated disappearance of the starting material (ca 2h30min). After cooling to RT, fresh pyridine (not dry, 6 mL) and water (10 mL) were added giving a white suspension. A condenser was applied to the flask, and the mixture was heated at 90 °C overnight (16 h) with vigorous stirring. After cooling to RT, 5 M aqueous HCl was added (ca 20 mL, until pH <1), and the resulting suspension was heated at 100 °C for 30 minutes with stirring. After cooling to RT, the mixture was transferred to a separating funnel, with the aid of  $\text{CH}_2\text{Cl}_2$  and water. The two phases were separated, and the aqueous phase extracted twice with  $\text{CH}_2\text{Cl}_2$ . The combined organic phases were dried over  $\text{MgSO}_4$ , filtered and evaporated under reduced pressure, leaving a residue which was purified by chromatography on silica gel ( $\text{CH}_2\text{Cl}_2/\text{MeOH}$  from 98:2 to 93:7). The fractions containing the phosphoric acid product were collected and evaporated, the residue dissolved in  $\text{CH}_2\text{Cl}_2$  and transferred in a separating funnel containing an aqueous 5 M HCl solution. The phases were separated, the aqueous phase extracted with  $\text{CH}_2\text{Cl}_2$ , the organic phases combined, dried over  $\text{MgSO}_4$ , filtered and evaporated, affording the title compound as a pale yellow solid in 63% yield.  $[\alpha]_{\text{D}}^{28} = -148$  ° ( $c = 0.335$  in  $\text{CHCl}_3$ );  $^1\text{H}$  NMR ( $\text{CDCl}_3$ , 400 MHz) [the signal at 5.00 ppm (P(O)OH integrates 3H presumably due to interactions with a water molecule]  $\delta = 8.10$  (s, 2H), 7.87 (d,  $J = 8.9$  Hz, 2H), 7.65 (d,  $J = 8.9$  Hz, 2H), 7.61 (d,  $J = 8.5$  Hz, 2H), 7.52 (d,  $J = 8.5$  Hz, 2H), 7.42-7.29 (m, 4H), 7.20-7.10 (m, 4H), 7.07 (s, 2H), 5.00 (br s, 3H), 3.07-2.95 (m, 2H), 2.94-2.86 (m, 4H), 2.64 (dt,  $J_d = 17.0$  Hz,  $J_t = 6.6$  Hz, 2H), 2.09-1.80 (m, 8H);  $^{13}\text{C}$  NMR ( $\text{CDCl}_3$ , 100 MHz) [several signals are split in doublets due to  $J_{\text{P-C}}$  coupling]  $\delta = 145.0$ , 144.9, 137.6, 134.92, 134.90, 133.4, 131.6, 131.2, 130.9, 130.4, 130.1, 128.5, 128.01, 127.98, 127.82, 127.78, 127.0, 126.3, 125.6, 124.70, 124.65, 29.3, 28.2, 22.8; ESIMS 731  $[\text{M} + \text{Na}^+]$ .

**3.4.3. General procedure for the catalytic enantioselective vinylogous Povarov reaction.**

*Two-component procedure (preformed imine)*

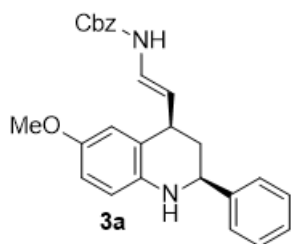
To a Schlenk tube equipped with a magnetic stirring bar, 4Å powdered molecular sieves (20 mg) were added. The molecular sieves were thermally activated under vacuum for 5

minutes and then allowed to cool to r.t. After backfilling the Schlenk tube with nitrogen, the aldimine **1a-h**, **1k-o** (0.15 mmol) was added, followed by catalyst **4h** (2.7 mg, 0.0038 mmol, 2.5 mol%), and toluene (0.60 mL). The mixture was allowed to stir for 5 minutes and then the dienophile **2a-c** (0.18 mmol or 0.30 mmol) was added in one portion. The mixture was then stirred at room temperature under a nitrogen atmosphere. After 16 h, the reaction mixture was filtered through a plug of silica gel, and the plug was washed with Et<sub>2</sub>O (4x). After concentration of solvents, the residue was analyzed by <sup>1</sup>H NMR spectroscopy to determine the diastereomeric ratio of the cycloadducts **3**. Finally, the residue was purified by chromatography on silica gel. In some cases, the residue was instead purified by dissolving it in a minimal amount of CH<sub>2</sub>Cl<sub>2</sub>, followed by precipitation with *n*-hexane, and final removal of the supernatant with a Pasteur pipette after few minutes of decantation. The enantiomeric excess of the adducts purified by precipitation was determined on their crude mixture.

*Three-component procedure (imine formed in situ).*

To a Schlenk tube equipped with a magnetic stirring bar, 4 Å powdered molecular sieves (110 mg) were added. The molecular sieves were then thermally activated under vacuum for 10 minutes and then allowed to cool to r.t. After backfilling the Schlenk tube with nitrogen, *p*-anisidine (0.15 mmol), the catalyst **4h** (5.4 mg, 0.0076 mmol, 5.0 mol%), and toluene (0.30 mL) were added, followed by the dienophile **2** (0.30 mmol). A solution of the aldehyde in toluene (0.30 mL, 0.15 mmol) was finally added, and the resulting mixture was stirred at room temperature under a nitrogen atmosphere. After 16 h, the reaction mixture was worked up and purified as in the above procedure.

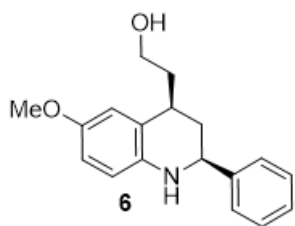
**Benzyl ((*E*)-2-((2*S*,4*R*)-6-methoxy-2-phenyl-1,2,3,4-tetrahydroquinolin-4-yl)vinyl)carbamate (**3a**)**



Following the general procedure using 0.18 mmol of dienophile **2a**, the title compound was obtained as a white solid in 85% yield, after chromatography on silica gel (*n*-hexane/EtOAc 8:2). A single diastereoisomer was observed by <sup>1</sup>H NMR in the crude mixture. The enantiomeric excess of the product was determined by chiral stationary phase HPLC (Phenomenex Lux, *n*-hexane/*i*-PrOH 70:30, 0.75 mL/min, λ = 254 nm, *t*<sub>maj</sub> = 19.4 min, *t*<sub>min</sub> = 45.1 min, 98% ee). [α]<sub>D</sub><sup>27</sup> = -45 ° (c = 0.62, CH<sub>2</sub>Cl<sub>2</sub>); <sup>1</sup>H NMR (CDCl<sub>3</sub>, 600 MHz) δ = 7.44-7.28 (m, 10H), 6.76-6.68 (m, 2H), 6.65 (dd, J = 8.4, 2.9 Hz, 1H), 6.54 (d, J = 10.1 Hz, 1H), 6.50 (d, J = 9.1 Hz, 1H), 5.18 (d, J = 12.9 Hz, 1H), 5.15 (d, J = 12.8 Hz, 1H), 4.90 (dd, J = 14.6, 10.3 Hz, 1H), 4.41 (d, J = 11.4 Hz, 1H), 3.80 (br s, 1H), 3.73 (s, 3H), 3.68-3.59 (m, 1H), 2.14-2.04 (m, 1H), 1.86 (q, J = 14.1 Hz, 1H); <sup>13</sup>C NMR (CDCl<sub>3</sub>, 150 MHz) δ = 153.5, 152.2, 144.0, 139.0, 136.0, 128.6, 128.6, 128.3, 128.2, 127.6, 126.6, 125.2, 124.9, 115.4, 114.6, 113.6, 113.5, 67.2, 56.8, 55.9, 40.3, 39.6; ESIMS 437 [M + Na<sup>+</sup>]. Using the three component procedure, the title compound was obtained in 70% yield and in 98% ee.

### 3.4.4. General procedures for elaborated products 6, 7, 8, 9

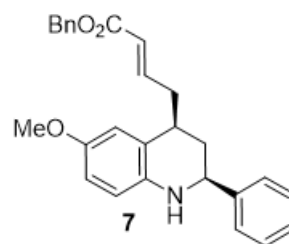
#### 2-((2*S*,4*R*)-6-Methoxy-2-phenyl-1,2,3,4-tetrahydroquinolin-4-yl)ethanol (**6**)



In a round bottomed flask, product **3a** (30 mg, 0.072 mmol) was dissolved in acetone (0.900 mL) and cooled to 0 °C. Aq. 1 M HCl (0.700 mL, 0.700 mmol) was then added in 2 min, while stirring. The resulting solution was allowed to warm to rt, and, after 4 h, quenched with saturated aqueous NaHCO<sub>3</sub>, and extracted three times with CH<sub>2</sub>Cl<sub>2</sub>; the organic layers were combined and dried over a short celite pad and the solvents were evaporated. The thus obtained crude aldehyde was dissolved in methanol (1.0 mL) and the mixture was cooled at -35 °C with a liquid nitrogen/acetone bath. Excess NaBH<sub>4</sub> (ca 15 mg) was added and the mixture was allowed to warm to -20 °C with stirring. After 15 min, the reaction was monitored by TLC (CH<sub>2</sub>Cl<sub>2</sub>/EtOAc 94:6). Since the aldehyde was still detected, additional NaBH<sub>4</sub> (ca 5 mg) was added. After additional 20 minutes the reaction was complete (TLC), and the mixture was quenched with saturated aqueous NH<sub>4</sub>Cl and extracted three times with CH<sub>2</sub>Cl<sub>2</sub>. The organic layers were combined and dried over a celite pad. After evaporation of the solvents, the crude product was purified by column chromatography (CH<sub>2</sub>Cl<sub>2</sub>/Et<sub>2</sub>O 9:1) to give the title compound as a pale yellow solid in 62% overall yield (over two steps). A single diastereoisomer was observed by <sup>1</sup>H NMR in the crude mixture, thus showing that epimerisation did not occur. The enantiomeric excess of the product was determined by chiral stationary phase HPLC (Phenomenex Lux, *n*-hexane/*i*-PrOH 70:30, 0.75 mL/min, λ = 254 nm, t<sub>maj</sub> = 11.4 min, t<sub>min</sub> = 18.8 min, 96% ee), thus showing that racemisation did not occur to a considerable extent. [α]<sub>D</sub><sup>27</sup> = -9° (c = 0.77 CH<sub>2</sub>Cl<sub>2</sub>); <sup>1</sup>H NMR (CDCl<sub>3</sub>, 400 MHz) δ = 7.44-7.28 (m, 5H), 6.82 (d, J = 2.8 Hz, 1H), 6.64 (dd, J = 8.4, 2.8 Hz, 1H), 6.51 (d, J = 8.6 Hz, 1H), 4.32 (dd, J = 11.3, 2.6 Hz, 1H), 3.86-3.69 (m, 6H), 3.29-3.19 (m, 1H), 2.35-2.19 (m, 2H), 1.81-1.69 (m, 2H); <sup>13</sup>C NMR (CDCl<sub>3</sub>, 100 MHz) δ = 152.4, 144.4, 139.6, 128.6, 127.6, 126.6, 126.0, 115.6, 113.0, 112.7, 60.5, 57.1, 55.9, 38.5, 37.9, 33.3; ESIMS 306 [M + Na<sup>+</sup>].

#### (*E*)-Benzyl 4-((2*R*,4*S*)-6-methoxy-2-phenyl-1,2,3,4-tetrahydroquinolin-4-yl)but-2-enoate (**7**)

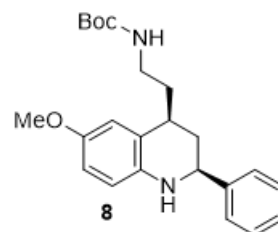
In a round bottomed flask, product **3a** (30 mg, 0.072 mmol) was dissolved in acetone (0.900 mL) and cooled to 0 °C. Aq. 1 M HCl (0.700 mL, 0.700 mmol) was then added in 2 min, while stirring. The resulting solution was allowed to warm to rt, and, after 4 h, quenched with saturated aqueous NaHCO<sub>3</sub>, and extracted three times with CH<sub>2</sub>Cl<sub>2</sub>; the organic layers were combined and dried over a short celite pad and the solvents were evaporated. The crude aldehyde was dissolved in CH<sub>2</sub>Cl<sub>2</sub> (1.0 mL) and the mixture was cooled at 0 °C with a water/ice bath. Benzyl (triphenyl-phosphoranylidene)-acetate



(41 mg, 0.100 mmol) was added under stirring. Progress of the reaction was monitored by TLC (CH<sub>2</sub>Cl<sub>2</sub>). After 1 h, the reaction was complete, and the mixture was passed over a celite pad. The crude product was purified by column chromatography (CH<sub>2</sub>Cl<sub>2</sub>/EtOAc 99:1) to give the title compound as a pale yellow solid in 86% overall yield (over two steps). A single diastereoisomer was observed by <sup>1</sup>H NMR in the crude mixture, thus showing that epimerisation did not occur, and that olefination proceeded with full *E*-selectivity. The enantiomeric excess of the product was determined by chiral stationary phase HPLC (Phenomenex Lux, *n*-hexane/*i*-PrOH 70:30, 0.75 mL/min, λ = 254 nm, t<sub>maj</sub> = 20.8min, t<sub>min</sub> = 29.5min, >99% ee), thus showing that racemisation did not occur. [α]<sub>D</sub><sup>27</sup> = -34° (c = 0.11 CH<sub>2</sub>Cl<sub>2</sub>); <sup>1</sup>H NMR (CDCl<sub>3</sub>, 400 MHz) δ = 7.49-7.27 (m, 10H), 7.08-6.95 (m, 1H), 6.77 (d, J = 2.7 Hz, 1H), 6.65 (dd, J = 8.5, 2.7 Hz, 1H), 6.53 (d, J = 8.5 Hz, 1H), 5.93 (d, J = 15.8 Hz, 1H), 5.15 (br s, 2H), 4.35 (dd, J = 11.0, 2.7 Hz, 1H), 3.75 (br s, 3H), 3.31-3.19 (m, 1H), 2.94-2.82 (m, 1H), 2.48-2.35 (m, 1H), 2.17-2.08 (m, 1H), 1.72 (q, J = 11.7 Hz, 1H); <sup>13</sup>C NMR (CDCl<sub>3</sub>, 100 MHz) δ = 165.7, 146.4, 135.0, 127.5, 127.2, 127.1, 126.7, 125.7, 122.1, 112.1, 112.0, 65.1, 55.9, 54.9, 37.5, 36.8, 34.7; ESIMS 436 [M + Na<sup>+</sup>].

***tert*-Butyl (3-((2*S*,4*S*)-6-methoxy-2-phenyl-1,2,3,4-tetrahydroquinolin-4-yl)ethyl)carbamate (8)**

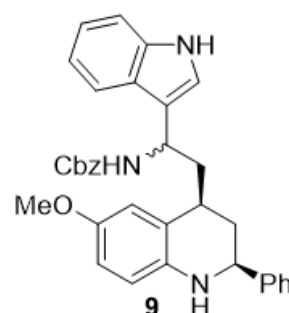
A Schlenk tube was equipped with a magnetic stirring bar and saturated with a nitrogen atmosphere. Ammonium formate (43 mg, 0.66 mmol) was added in one portion, followed by 1 mL of MeOH, activated Pd/C (10 wt %, 12 mg) and finally the product **3p** (21 mg, 0.055 mmol). The mixture was stirred at room temperature for five minutes and then warmed to 35 °C. Progress of the reaction was monitored by TLC (CH<sub>2</sub>Cl<sub>2</sub>). After 1 h, the



reaction was complete and the mixture was passed over a celite pad, diluted with CH<sub>2</sub>Cl<sub>2</sub>, and washed with water. The organic phase was dried over a short celite pad, the solvents were evaporated and the crude product was purified by column chromatography (CH<sub>2</sub>Cl<sub>2</sub>) to give the title compound as a colourless oil in 87% overall yield. The enantiomeric excess of the product was determined by chiral stationary phase HPLC (Phenomenex Lux, *n*-hexane/*i*-PrOH 80:20, 0.75 mL/min, λ = 254 nm, t<sub>maj</sub> = 18.2 min, t<sub>min</sub> = 25.4 min, 94% ee) thus showing that racemisation did not occur to a considerable extent. [α]<sub>D</sub><sup>27 °C</sup> = -13° (c = 0.60, CH<sub>2</sub>Cl<sub>2</sub>); <sup>1</sup>H NMR (CDCl<sub>3</sub>, 400 MHz) δ = 7.45-7.27 (m, 5H), 6.78 (d, J = 2.4 Hz, 1H), 6.64 (dd, J = 2.4, 8.6 Hz, 1H), 6.51 (d, J = 8.6 Hz, 1H), 4.54 (br s, 1H), 4.31 (dd, J = 2.7, 11.4 Hz, 1H), 3.76 (s, 3H), 3.27-3.05 (m, 3H), 2.27-2.08 (m, 2H), 1.82-1.60 (m, 2H), 1.43 (br s, 9H). <sup>13</sup>C NMR (CDCl<sub>3</sub>, 100 MHz) δ = 155.9, 152.4, 144.3, 139.6, 128.6, 127.6, 126.6, 125.7, 115.7, 113.1, 112.8, 79.2, 57.1, 55.9, 38.4, 38.2, 35.4, 34.2, 28.4; ESIMS 405 [M + Na<sup>+</sup>].

**Benzyl (1-(1*H*-indol-3-yl)-2-((2*S*,4*R*)-6-methoxy-2-phenyl-1,2,3,4-tetrahydroquinolin-4-yl)ethyl)carbamate (9)**

A vial equipped with a magnetic stirring bar was sequentially charged with compound **3a** (29 mg, 0.076 mmol), CH<sub>2</sub>Cl<sub>2</sub> (0.50 mL), indole (27 mg, 0.228 mmol, 3 equiv.) and catalyst **4c** (5.7 mg, 10 mol%). The vial was carefully capped, and warmed to 55 °C with stirring. After 16 h, the solution was passed through a short pad of silica, the pad washed with CH<sub>2</sub>Cl<sub>2</sub> and Et<sub>2</sub>O and the solvent evaporated, leaving a residue which was analyzed by <sup>1</sup>H NMR showing a 94:6 diastereomeric ratio, presumably at the α-NHCbz chiral



centre. Chromatographic purification on silica gel (CH<sub>2</sub>Cl<sub>2</sub>/Et<sub>2</sub>O from 100:0 to 95:5) gave the title compound as a diastereomeric mixture and as a white solid in 91% yield. The enantiomeric excess of the product was determined by chiral stationary phase HPLC (Chiralpak ADH, *n*-hexane/*i*-PrOH 70:30, 0.75 mL/min, λ = 254 nm; major diastereoisomer: *t*<sub>maj</sub> = 46.8 min, *t*<sub>min</sub> = 75.9 min, >99% ee, minor diastereoisomer: *t*<sub>maj</sub> = 35.2 min, *t*<sub>min</sub> = 66.3 min, 20% ee), thus showing that racemization did not occur.

The same title compound was also obtained in a one-pot procedure: to the catalytic reaction for obtaining **3a** (after 18 h), indole (88 mg, 0.75 mmol) and catalyst **4c** (11.3 mg, 10 mol%) were sequentially added, and the resulting mixture was heated at 80 °C for 4 h with stirring. The mixture was then filtered on short plug of silica, the plug washed several times with Et<sub>2</sub>O, and the solvents evaporated, leaving a residue which was analysed by <sup>1</sup>H NMR showing a 94:6 diastereomeric ratio, presumably at the α-NHCbz chiral centre. Chromatographic purification on silica gel (CH<sub>2</sub>Cl<sub>2</sub>/Et<sub>2</sub>O from 100:0 to 95:5) gave the title compound as a diastereomeric mixture and as a pale yellow solid in 61% yield. The enantiomeric excess of the product was determined by chiral stationary phase HPLC (Chiralpak ADH, *n*-hexane/*i*-PrOH 70:30, 0.75 mL/min, λ = 254 nm; major diastereoisomer: *t*<sub>maj</sub> = 46.8 min, *t*<sub>min</sub> = 75.9 min, 99% ee, minor diastereoisomer: *t*<sub>maj</sub> = 35.2 min, *t*<sub>min</sub> = 66.3 min, 17% ee).

<sup>1</sup>H NMR (CDCl<sub>3</sub>, 600 MHz) δ = 8.11 (br s, 1H), 7.61 (br d, *J* = 8.3 Hz, 1H), 7.44-7.39 (m, 2H), 7.38-7.26 (m, 9H), 7.18 (t, *J* = 7.7 Hz, 1H), 7.08 (br t, *J* = 7.7 Hz, 1H), 7.00 (br s, 1H), 6.86 (br s, 1H), 6.65 (dd, *J* = 8.6, 2.6 Hz, 1H), 6.54 (br d, *J* = 8.6 Hz, 1H), 5.31 (br t, *J* = 8.6 Hz, 1H), 5.15 (d, *J* = 12.2 Hz, 1H), 5.13 (d, *J* = 12.3 Hz, 1H), 5.00 (d, *J* = 9.1 Hz, 1H), 4.32 (br d, *J* = 11.1 Hz, 1H), 3.75 (s, 3H), 3.31-3.21 (m, 1H), 2.66-2.53 (m, 2H), 2.10-2.01 (m, 1H), 1.79 (q, *J* = 10.9 Hz, 1H). <sup>13</sup>C NMR (CDCl<sub>3</sub>, 150 MHz) δ = 156.1, 152.3, 144.3, 137.9, 136.6, 136.5, 128.6, 128.5, 128.1, 128.0, 127.5, 126.7, 125.8, 122.4, 120.9, 119.8, 119.4, 118.1, 115.6, 113.5, 112.5, 111.3, 66.7, 57.0, 55.9, 46.0, 42.2, 38.6, 33.4; ESIMS 554 [M + Na<sup>+</sup>].

### 3.4.5. Crystallographic data

Suitable crystal of compound **3b**, which possesses an appropriate heavy atom ( $Z > \text{Si}$  using standard Mo-K $\alpha$  radiation),<sup>87</sup> were obtained by vapour diffusion of *n*-hexane into an ethyl acetate solution.

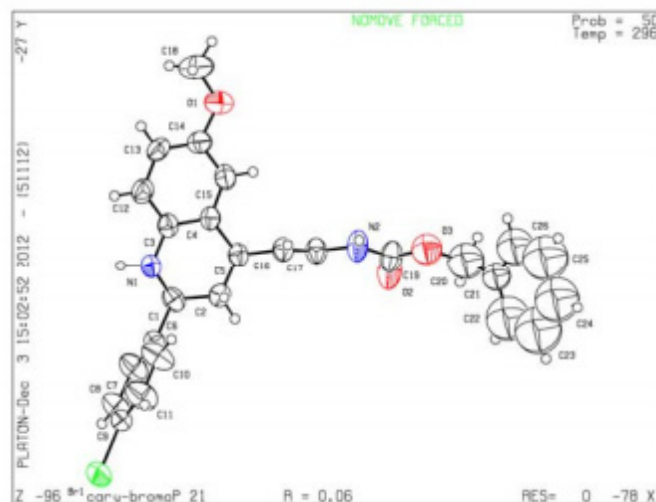
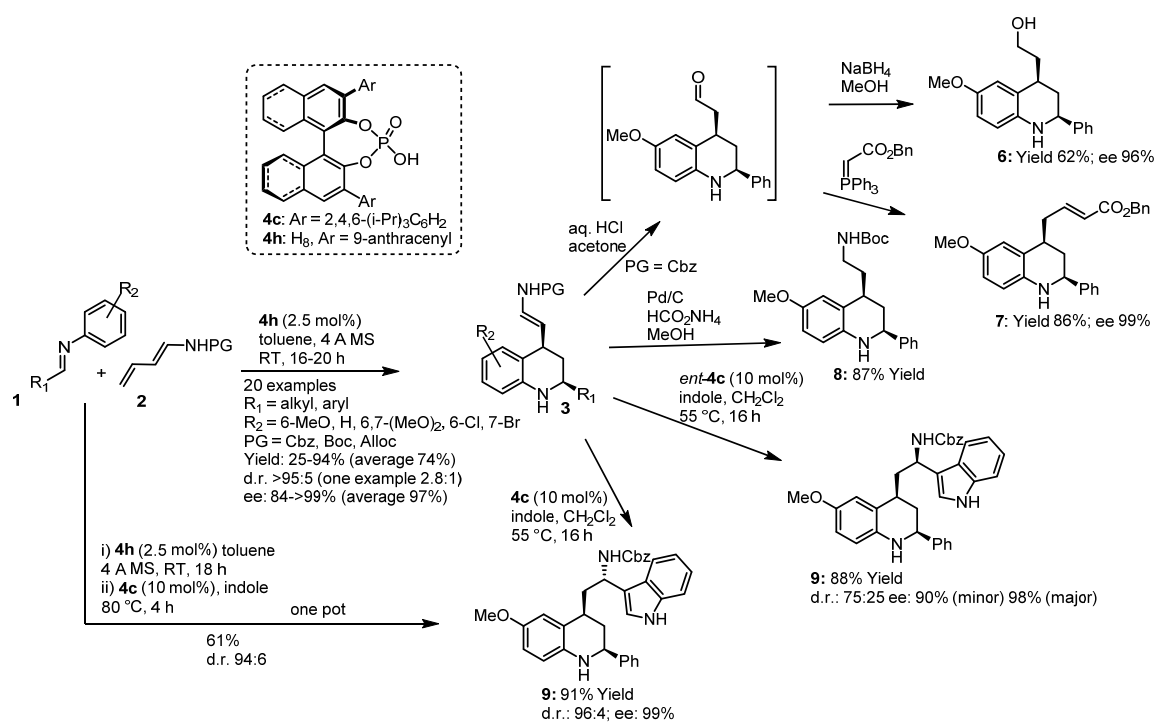


**Figure 22.** Crystallographic data for **3b**.

Molecular formula:  $\text{C}_{26}\text{H}_{25}\text{N}_2\text{O}_3\text{Br}$ ,  $M_r = 493.39$ , monoclinic, space group  $P2_1$  (No. 3),  $a = 9.5555(17)$ ,  $b = 5.0614(9)$ ,  $c = 24.813(4)$  Å,  $\beta = 92.316(2)$ ,  $V = 1199.1(4)$  Å<sup>3</sup>,  $T = 298(2)$  K,  $Z = 2$ ,  $\rho_c = 1.367$  g cm<sup>-3</sup>,  $F(000) = 508$ , graphite-monochromated MoK $\alpha$  radiation ( $\lambda = 0.71073$  Å),  $\mu(\text{MoK}\alpha) = 1.743$  mm<sup>-1</sup>, colourless rods ( $0.40 \times 0.10 \times 0.05$  mm<sup>3</sup>), empirical absorption correction with SADABS (transmission factors: 0.9179 – 0.5423), 2400 frames, exposure time 90 s,  $1.64 \leq \theta \leq 26.00$ ,  $-11 \leq h \leq 11$ ,  $-6 \leq k \leq 6$ ,  $-30 \leq l \leq 30$ , 12298 reflections collected, 4637 independent reflections ( $R_{\text{int}} = 0.0218$ ), solution by direct methods (SHELXS97) and subsequent Fourier syntheses, full-matrix least-squares on  $F_o^2$  (SHELX97), hydrogen atoms refined with a riding model except for the two NH hydrogen, that were experimentally located and refined. Data / restraints / parameters ratio = 4637 / 1 / 246,  $S(F^2) = 1.083$ ,  $R(F) = 0.0742$  and  $wR(F^2) = 0.1971$  on all data,  $R(F) = 0.0645$  and  $wR(F^2) = 0.1888$  for 4637 reflections with  $I > 2\sigma(I)$ , weighting scheme  $w = 1/[\sigma^2(F_o^2) + (0.1122P)^2 + 0.839P]$  where  $P = (F_o^2 + 2F_c^2)/3$ , largest difference peak and hole 0.998 and  $-0.0674$  e Å<sup>-3</sup>. Flack Parameter for S,R absolute configuration (C1 and C5, respectively): 0.013(19). The benzyl moiety (C20-C26) was found to be disordered over two positions, and it was isotopically refined. Crystallographic data (excluding structure factors) for the structure reported in this paper have been deposited with the Cambridge Crystallographic Data Centre as supplementary publication no. CCDC-913761.

### 3.5. Conclusion

In summary, disclosing a new vinylogous reactivity of 1-acyl-amino dienes **2** and *N*-aryl imines **1**, the first catalytic enantioselective Povarov reaction, promoted by chiral phosphoric acids, has been developed. The terminal double bond of diene **2** is not only the least sterically hindered, but also the most electron-rich of the 1,3-butadiene system;<sup>74a</sup> therefore it is possible that a combination of stereoelectronic factors steered the reaction towards the vinylogous pathway, overcoming the common Diels–Alder reactivity of dienes **2** and also their tendency to undergo “non-vinylogous” Povarov reaction despite their steric hindrance. Upon a thorough screening of chiral phosphoric acids, the new catalyst **4h** – derived from H<sub>8</sub>-BINOL phosphoric acid and bearing a 9-anthracenyl group at its 3 and 3' position – was found to promote the vinylogous reaction in excellent stereoselectivity. The catalyst activity was further enhanced by using activated molecular sieves in the reaction media. The reaction was optimized up to tolerate a low catalyst loading (up to 1 mol%). Kinetic control experiments were conducted on this reaction and demonstrated that deactivation of the catalyst occurred. This deactivation was neither due to catalyst inhibition by the product nor to the molecular sieves. The scope of the reaction was broadly demonstrated by employing several *N*-aryl imines, having different electronic properties both at the aldehyde and aniline portions. Remarkably, the organocatalytic reaction could be performed in a multicomponent fashion, where the imine was generated *in situ*. In this way, the scope of the reaction could be expanded also to imines derived from enolisable aldehydes. The Cbz-protecting group at diene **2a** could be easily replaced with Boc or Alloc group, thus demonstrating the generality of the reaction also for the diene counterpart. The relative configuration of the synthesized THQs was determined by NMR spectroscopy, whereas the absolute configuration was determined by chiroptical techniques. Relative and absolute configurations were finally confirmed by X-Ray diffraction experiments. Cycloadducts **3** were then subjected to few synthetic manipulations and, importantly, the enecarbamate moiety was exploited through an indole addition mediated by phosphoric acid; this transformation could be readily implemented in a one-pot process. All the experimental results are summarized in Scheme 24.



**Scheme 24.** Catalytic enantioselective vinylogous Povarov reaction and elaboration of the enecarbamate on the THQs.

## 4. Asymmetric organocatalytic cascade reactions in 3,4-annulation of indoles: a gateway to ergot alkaloids

The procedures and results here described are part of- and can be found in-:

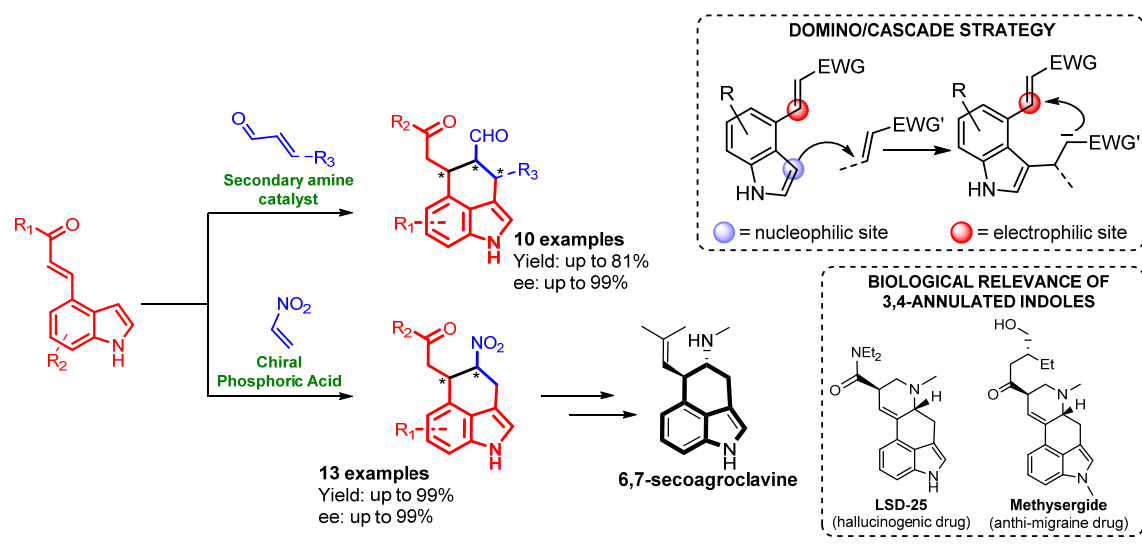
- Caruana, L.; Fochi, M.; Comes Franchini, M.; Ranieri, S.; Mazzanti, A.; Bernardi, L. “Asymmetric synthesis of 3,4-annulated indoles through an organocatalytic cascade approach.” *Chem. Commun.* **2014**, *50*, 445.
- The manuscript describing organocatalytic reactions of nitroethene with 4-substituted indoles – presented later in this chapter – is currently in preparation.

---

### ABSTRACT

Indole and its derivatives represent probably the most important class of heterocyclic compounds due to their widespread biological and pharmaceutical activities. In particular, the tetrahydrobenzo[*cd*]indole core (3,4-annulated indoles) is present in many interesting natural occurring compounds, among which ergot alkaloids.<sup>88</sup> Accordingly, various strategies have been developed for the construction of this privileged scaffold and will be briefly described in this chapter. Nevertheless, none of the available methods furnishes all carbon 3,4-ring fused indoles by means of organocatalytic strategies. We surmised that the synthetic versatility of indoles bearing Michael acceptors at 4-position could be exploited in order to tether the C3 and C4 positions of the indole nucleus, in a domino/cascade process. In fact, in these compounds, the nucleophilic position at C3 of indole is flanked by the electrophilic olefin at C4, enabling the construction of tricyclic compounds via Friedel-Crafts alkylation followed by Michael addition. These indole derivatives have been successfully engaged in the reaction between either enals or nitroethene, using secondary amine based catalysis and chiral phosphoric acid catalysis, respectively. The thus formed tricyclic compounds were obtained in excellent yields and impressive stereoselectivities. Besides the identification of the appropriate organocatalytic system, careful attention was posed in the optimization of the reactions, in order to face synthetic challenges such as the inherent low reactivity of these substrates. Furthermore, the mechanism of the reaction between 4-substituted indole derivatives and nitroethene was evaluated by DFT calculation, showing the formation of a key bicoordinated nitronate intermediate and fully accounting for the observed results.

These newly developed processes could represent a gateway to Ergot alkaloids, as exemplified by the formal total synthesis of 6,7-secoagroclavine.



## 4.1. Background

The indole scaffold is arguably one of the most significant heterocycles<sup>89</sup> due to its ubiquitous presence in numerous natural products and bioactive molecules. Important biologically active compounds – such as the essential amino acid tryptophan or the neurotransmitter serotonin – are indole-based, furthermore this scaffold is a significant component of many drugs. Hence, it is not surprising that the synthesis<sup>89</sup> and functionalization<sup>90</sup> of this structural motif has been the object of thorough research, since the first landmark report, dated 1866, regarding the preparation of the indigo dye.<sup>91</sup> Among the naturally occurring indole compounds, 3,4-ring fused indoles (those in which the 3-position of the indole is bridged to the 4-position) have been considered attractive synthetic challenges because of their significant biological activity. A remarkable example of this molecular scaffold is represented by ergot alkaloids.<sup>88</sup> From a structural point of view, ergot alkaloids are based

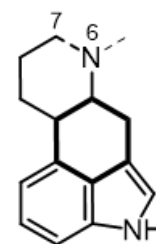


**Figure 23.** General structure of ergot alkaloids. In bold is depicted the 6-membered ring which bridges the C3 and C4 position of indole.

on a tetracyclic indole framework called ergoline, or on the related tricyclic scaffold, open among N(6) and C(7), both encompassing the 3,4-annulated motif (Figure 23). These natural compounds are produced by different species of ascomycete fungi belonging to the genus *Claviceps*, which grow especially on rye. During the Middle

Ages, the consumption of cereal contaminated by this fungus, led to epidemics of ergotism, a severe neurological disease. The activity of ergot alkaloids toward the nervous system is clearly exemplified by LSD-25 (lysergic acid diethylamide) – discovered by Hofmann in 1938 – which is one of the most potent hallucinogenic drug ever synthesized.<sup>92</sup> Since their discovery, a recreational use of these molecules raised as a result of their psychedelic properties. Despite potentially serious health consequences, justifying legal bans, these drugs marked some important cultural upheavals in society behaviour between 1960s and 1970s.<sup>93</sup> Luckily, the image of ergot alkaloids as illegal drugs or poisoning agents was gradually abandoned: nowadays, these alkaloids are considered as a highly valuable source of pharmaceuticals. In fact, ergot alkaloids-derivative are used as high potency drug, in the therapeutic treatment of various diseases. For instance, methysergide is used for the prophylaxis of migraine, whereas cabergoline (Dostinex<sup>®</sup>) found application against Parkinson disease (Figure 24).

Although these and related commercial drugs are usually prepared by semi-synthesis from

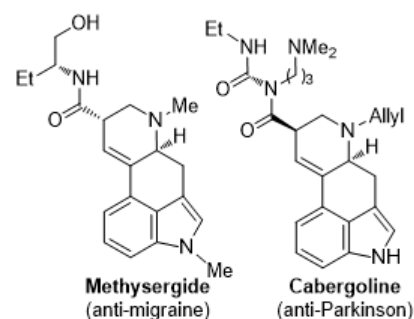
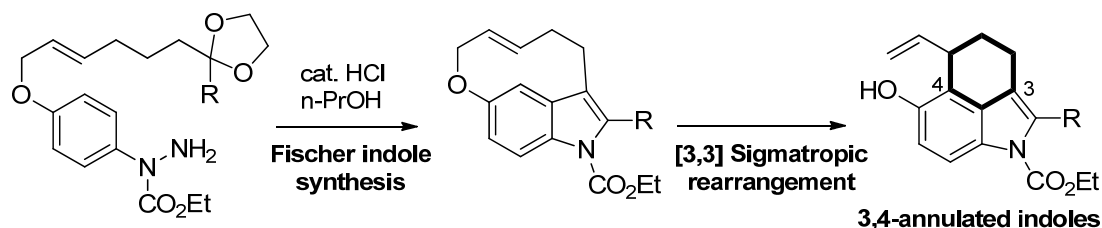


**Figure 24.**

fermentation derivatives, the importance of 3,4-annulated indoles as key framework in many medicinally useful drugs has spurred the research to the development of efficient methods to create such a structural motif starting from readily available substrates. For this reason, several members of this class of natural compounds have been the object of numerous total synthesis;<sup>94</sup> simultaneously, the construction of the challenging 1,2,3,4,5-tetrahydrobenzo[*cd*]indole scaffold has recently received substantial attention,<sup>95</sup> even in unadorned and racemic forms. In this context, those synthetic methods in which both indole and its annulated superstructure are generated in a single operation, ideally enabling a rapid access to these skeletons, should be highlighted. In fact, most of available synthetic methods are based on the introduction of functional group to the C3 or C4 positions of existing indoles, with subsequent cyclization. The main limitation of this clever strategy consists in the preparation of 4-substituted indoles – precursors of 3,4-ring fused indoles – which is found to be sometimes problematic.

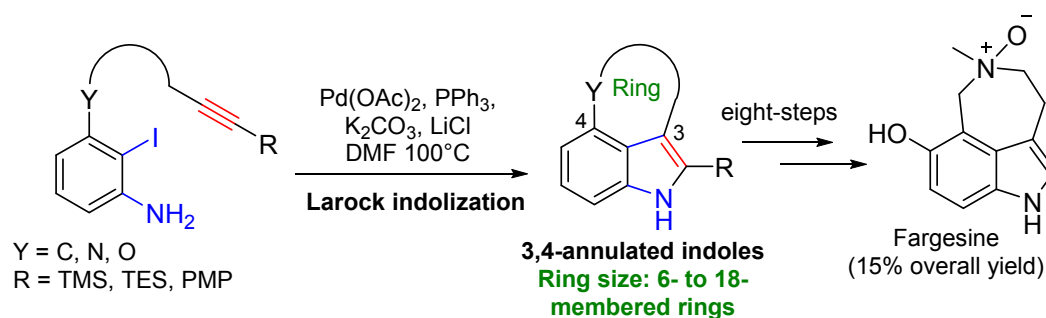
In 2012, Cho's research group exploited the famed Fischer indole synthesis to access to tricyclic benzo[*cd*]indoles.<sup>95b</sup> An intramolecular Fischer indolization of aryl hydrazides, in which a protected carbonyl group is tethered to the *para* position of aromatic ring,

furnished the corresponding indolophanes. The incorporation of a C–C double bond within the tether led to an aromatic [3,3] rearrangement, thus enabling the achievement of an all-carbon 3,4-annulated tricyclic indole scaffold, in a one-pot fashion (Scheme 25).



**Scheme 25.** Synthesis of 3,4-annulated indoles in a one-pot fashion by means of Fischer indolization and [3,3] aromatic rearrangement.

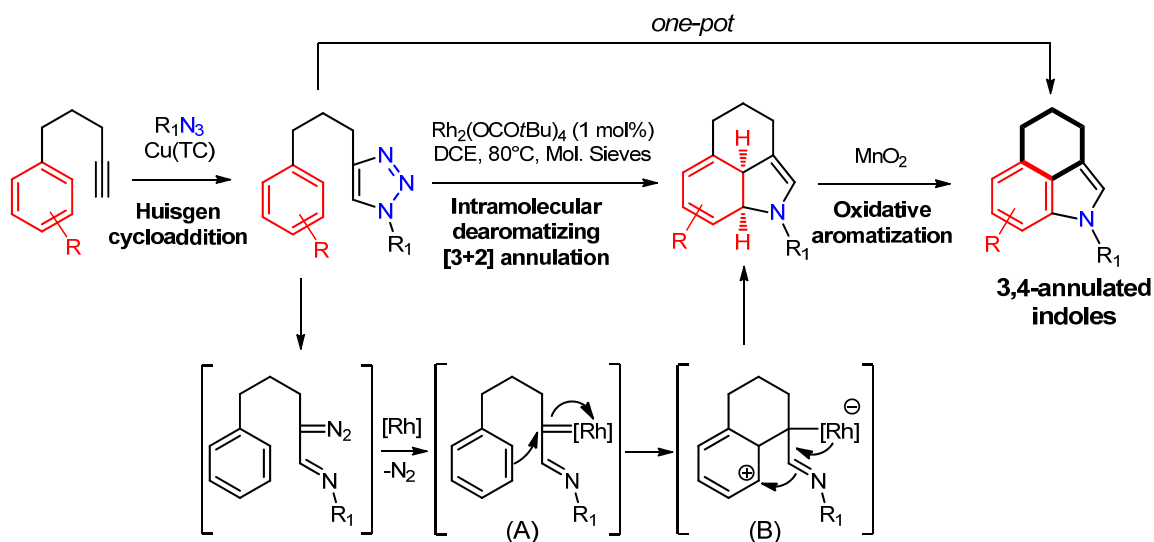
One year later, Jia and co-workers reported a general strategy for the construction of 3,4-fused tricyclic indoles through a palladium mediated Larock indolization.<sup>95c</sup> This strategy relies on the employment of 2-haloanilines bearing a side chain provided with an alkyne moiety; the reaction proceeded in the presence of palladium acetate as catalyst and triphenylphosphine as ligand. This transformation was found to be very general, affording tricyclic indoles in high yields; remarkably, the efficiency of the method was further demonstrated by the synthesis of 9-, 10-, 11-, and 18-, membered tricyclic products. Finally to probe its synthetic utility, this approach was applied to the total synthesis of natural product fargesine, which was isolated in 15% overall yield after eight-steps synthesis.



**Scheme 26.** Larock indolization as key reaction in the synthesis of 3,4-annulated indoles.

More recently, Murakami and co-workers disclosed an intramolecular dearomatizing [3+2] annulation reaction of 4-(3-arylpropyl)-1,2,3-triazoles, leading to 3,4-fused indole skeletons.<sup>95d</sup> *N*-sulfonyl-1,2,3-triazoles were readily prepared from 5-aryl-1-pentyne and sulfonyl azides by means of copper catalysed azide-alkyne cycloaddition<sup>96</sup> (Huisgen cycloaddition). The thus formed triazoles acted as 1,3-dipole equivalents in a rhodium catalysed dearomatizing [3+2] annulation, which was supposed to proceed as follow: a

reversible ring–chain tautomerization generated an  $\alpha$ -diazo imine, which immediately reacted with the rhodium catalyst to afford  $\alpha$ -imino rhodium complex (A); this electrophilic specie induced an intramolecular attack of the phenyl ring, giving the zwitterionic intermediate (B); anionic releasing of rhodium lead to cyclization at the imino nitrogen, affording the target tricyclic products (Scheme 27). Oxidative re-aromatization, mediated by manganese oxide, brought to the 3,4-annulated indole scaffold; this latter transformation could be conducted all-in-one-pot fashion.



**Scheme 27.** Construction of 3,4-annulated indole skeletons from 5-aryl-1-alkynes, by means of Huisgen cycloaddition, intramolecular dearomatizing [3+2] annulation and oxidative aromatization.

Because of their biological importance and intriguing molecular architecture, indole-containing alkaloids – particularly ergot alkaloids – have been the object of a vast number of total syntheses.<sup>94</sup> The archetype lysergic acid (Figure 25) has been the most pursued. Many recent synthetic strategies relies on pre-existing indole nucleus bearing a strategic functional group at its C4 position which serves as handle for subsequent cyclization, generating C ring (Figure 25). In 2011, this concept was clearly exemplified by Fujii and Ohno who reported an enantioselective synthesis of (+) lysergic acid, as well as (+)-lysergol and (+)-isolysergol.<sup>94f</sup> The keystone of this synthetic strategy was a palladium-catalyzed domino cyclization of an allene bearing amino and bromoindolyl groups, enabling direct construction of both C and D rings system of ergot alkaloids skeleton (Scheme 28). The axial chirality of allenes was stereospecifically transferred to

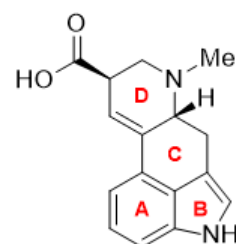
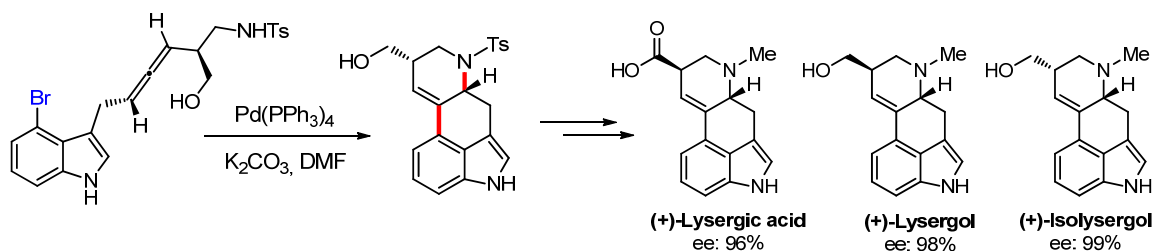


**Figure 25.** Lysergic acid

the newly formed stereocenters, resulting in the obtainment of the target ergot alkaloids in highly enantioenriched form (Scheme 28).



**Scheme 28.** Direct construction of ergot alkaloids structure motif. In blue is depicted the pre-installed functional group on C4 position of indole core. In red are depicted the new bonds formed upon Pd (0) mediated domino cyclization.

A subset of ergot alkaloids are characterized by a nitrogen-containing-seven-membered ring, namely the azepinoindole tricyclic subunit, which is exemplified by clavicipitic acid (Figure 26). Being member of the large family of 3,4-ring-fused indoles, these compounds have also emerged as target of several synthetic methods.

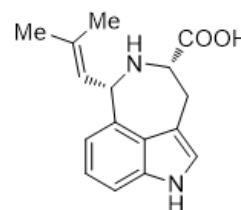
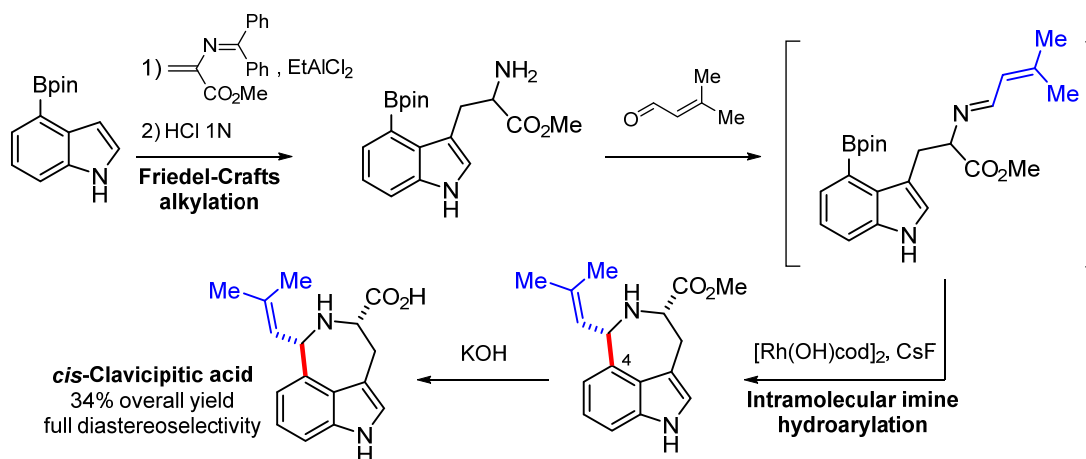


**Figure 26.** *cis*-Clavicipitic acid

Recently, Piersanti and coworkers reported a strategically approach to *cis*-clavicipitic acid by means of a rhodium(I)-catalyzed addition of 4-indolyl pinacolboronic ester to unactivated imino group as key C-C forming step.<sup>94k</sup> The tricyclic framework arose from a late-stage intramolecular Rh-catalyzed hydroarylation on the imine, obtained by condensation of 3-methylcrotonaldehyde (prenal) and 4-boronated tryptophan methyl ester (Scheme 29). This latter compound was synthesized through a Friedel–Crafts alkylation of 4-boronate indole and 2-amidoacrylate (Scheme 29). Thanks to the pinacolboronic ester as latent nucleophilic handle, the least nucleophilic C4 position of the indole core was activated towards the intramolecular prenylation, resulting in the first example of addition of pinacolboronic ester species to unactivated imine using rhodium (I) catalysis. The strategic synthetic sequence consisting in Friedel–Crafts alkylation and a Rh-catalyzed imine hydroarylation allowed the fully diastereoselective concise four-step total synthesis of *cis*-clavicipitic acid.

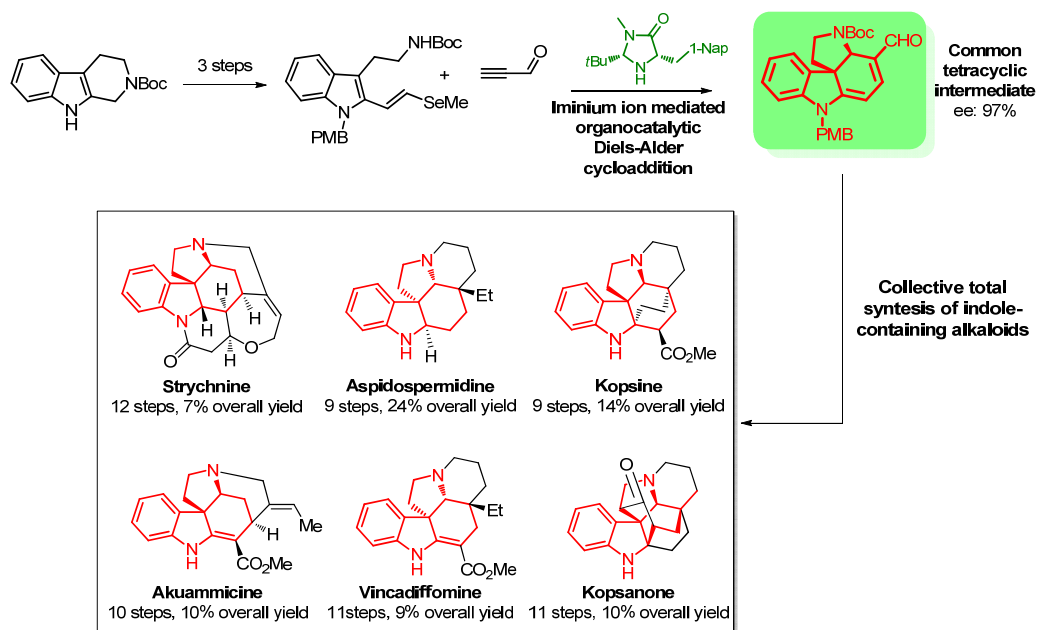


**Scheme 29.** Synthetic sequence towards *cis*-clavicipitic acid. In blue is depicted the prenyl moiety which is to be tethered to C4 position of indole, as a result of intramolecular Rh(I)-catalyzed hydroarylation (the new bond is depicted in red).

These are just few selected examples of straightforward synthetic methods, which have been adopted for the construction of 3,4-annulated indole compounds. However, different indole-containing natural products, with structures distinct from the 3,4-annulated one, are also widespread in nature and have been the subject of a plethora of synthetic studies, with organocatalytic platforms having played a key role. In this context, the development of new and efficient tandem/domino organocatalytic reactions,<sup>24,97</sup> which has occurred at a remarkably fast pace in the last ten years, has provided a real breakthrough. It is in fact possible to recognize that even if the sophistication and structural diversity of natural products have fascinated organic chemists for a long time, chemists usually adopt the so called “stop and go” approach, whereby individual transformations are conducted as stepwise processes interrupted by the isolation and purification of intermediates at each stage. By contrast, in nature the rapid conversion of simple starting materials to complex molecular scaffolds is accomplished through the use of specific enzymes, which mediate a continuous series of catalytic cascades. Following the footsteps of nature, in the last years a great amount of new “cascade”, “tandem” or “domino” reactions have been developed, especially by using small organic molecules as catalyst.<sup>24</sup> A big advantage of this strategy over classical synthesis is that at least two reactions are carried out in a single operation, under the same reaction conditions, thus avoiding time-consuming manipulations as well as the isolation of reaction intermediates. In this way molecular complexity can be achieved quickly, often accompanied by high level of stereoselectivity. Organocatalysts are particularly favorable when used in catalytic cascade reactions because they allow clear and specific modes of

activation, which can be often easily combined. Furthermore, organocatalysts are known to be tolerant to several functional groups and can be certainly employed under mild reaction conditions. The quest for “ideal syntheses” – in which complex molecular architectures could be achieved from readily available starting materials, with proper control of stereoselectivity – prompted the asymmetric organocatalysis to embrace the cascade/tandem/domino strategies with ardent enthusiasm.<sup>24,98</sup>

As far as the synthesis of natural alkaloids is concerned, the recognized benefits of asymmetric cascade/tandem/domino organocatalysis have been truly proved in many instances, particularly in the synthesis of indole-containing natural products and analogues.<sup>90,100,99</sup> For instance, MacMillan’s research group posed a milestone in the field of synthetic chemistry, by reporting an impressive collective synthesis of natural products by means of organocascade catalysis.<sup>100</sup> This concept found inspiration from Nature, wherein specific enzymes in continuous catalytic cascades rapidly produce intermediates and valuable products. Similarly, it was hypothesized that sequences of organocatalytic reactions could allow the rapid access to synthetically useful common intermediates. The implementation of the advantages of organocatalytic techniques in the framework of the total synthesis of natural products, enabled the preparation of a range of different alkaloids. The success of MacMillan’s approach was the recognition of a recurring tetracyclic intermediate with functionalities amenable to the preparation of six structurally diverse natural compounds, namely: strychnine, aspidospermidine, vincadifformine, akuammicine, kopsanone and kopsine. The key tetracyclic intermediate arose from an enantioselective organocatalyzed Diels–Alder cycloaddition between a tryptamine derivative and propynal, in the presence of an imidazolidinone catalyst, which is followed by selenide elimination, aza-Michael addition of the amine appendage to the double bond conjugated with the aldehyde, and double bond shifts; the enantioenriched product of the organocatalytic reaction was then converted to the target alkaloids after a handful of synthetic steps (Scheme 30). Notably, this organocatalytic-based approach permitted the construction of complex molecular frameworks with unprecedented levels of efficiency in terms of overall yield, step-economy and stereoselectivity, compared with the pre-existing total syntheses.<sup>100</sup>



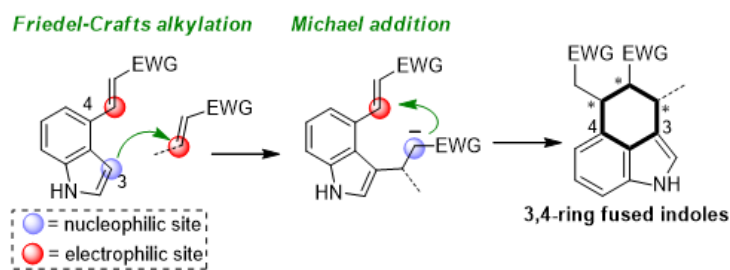
**Scheme 30.** Collective syntheses of six well-known indole alkaloids by means of an organocatalytic key reaction, leading to the tetracyclic intermediate depicted in red.

The protocol adopted by MacMillan was part of a more general strategy which exploited organocatalytic cascade reaction as a new tool in organic synthesis, inspired by the strategies used by nature to achieve complex molecules.<sup>24,97</sup>

However, even though several 1,2- and 2,3-annulated indoles have been developed by means of organocatalytic sequential reactions, related transformations giving all carbon 3,4-ring fused indoles were unreported at the outset of our studies.<sup>101</sup>

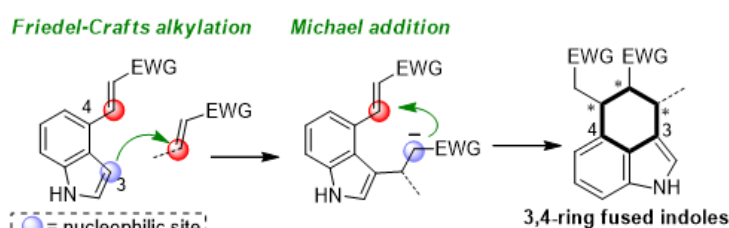
## 4.2. Aim of the work

Being fascinated by the possibility to develop a nature-inspired synthetic method and given the established importance of 3,4-annulated indoles, we have devoted our efforts to the disclosure of new synthetic routes leading to these valuable frameworks, possibly opening a gateway for the synthesis of ergot alkaloids.



**Scheme 31.** Devised organocascade strategy for the construction of 3,4-annulated indoles. (EWG = electron-withdrawing group)

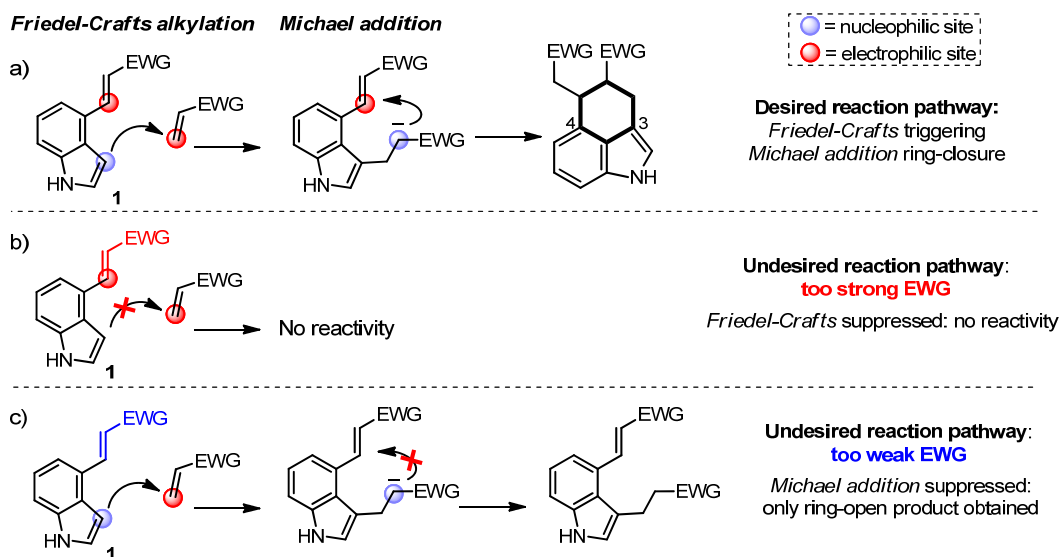
The starting point of the work has been the identification of suitable starting materials that could be productively engaged in organocatalytic cascade reactions. To this purpose, we have posed the attention on indole bearing at its 4-position a suitable Michael acceptor. This bifunctional indole has been chosen since it was recognized the synthetic versatility given by the nearby presence of two complementary reactive sites. Here, the nucleophilic C3 position is flanked by the electrophilic olefin at C4, potentially enabling the construction of the target all carbon 3,4-annulated framework through a Friedel–Crafts alkylation<sup>102</sup> triggering a Michael addition,<sup>103</sup> which terminates the cascade



sequence (

Scheme 31). On the

other hand, electron-poor olefins have appeared as good complementary reaction partners: their intrinsic electrophilic character allows attack by the nucleophilic indole, and the thus formed anionic intermediate would guide the ring-closure upon the addition to the Michael acceptor placed at C4 position of indole (Scheme 32a). Despite the simplicity of this reaction sequence, a series of not trivial issues make our approach particularly challenging. An open question was posed by the expected poor nucleophilicity of the C3 in indole **1**, caused mainly by conjugation of this carbon with the electron-withdrawing C4-acceptor, and perhaps exacerbated by steric effects. The presence of strong EWG substituent depresses considerably the reactivity of indole compared with the non-substituted one, which might result in no reactivity (Scheme 32b). On the other hand, the recourse to less electron-poor acceptor did not seem to be a viable option, since the intramolecular Michael reaction could then be suppressed, hence stopping the reaction sequence (Scheme 32c).

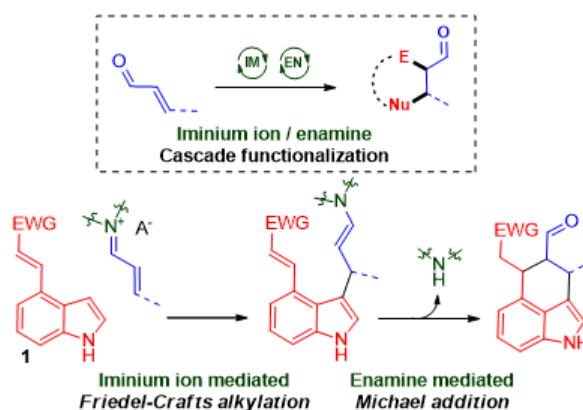


Scheme 32. Reactivity challenges with substrate 1.

Beside this, as a further complication the direct preparation of 4-substituted indole derivatives, precursor of 3,4-ring fused indoles, is normally rather difficult.<sup>104</sup> Therefore, the choice of the electron withdrawing group at C4 was limited to those installable through a very few synthetic steps from 4-formylindoles, which were chosen as suitable starting materials.

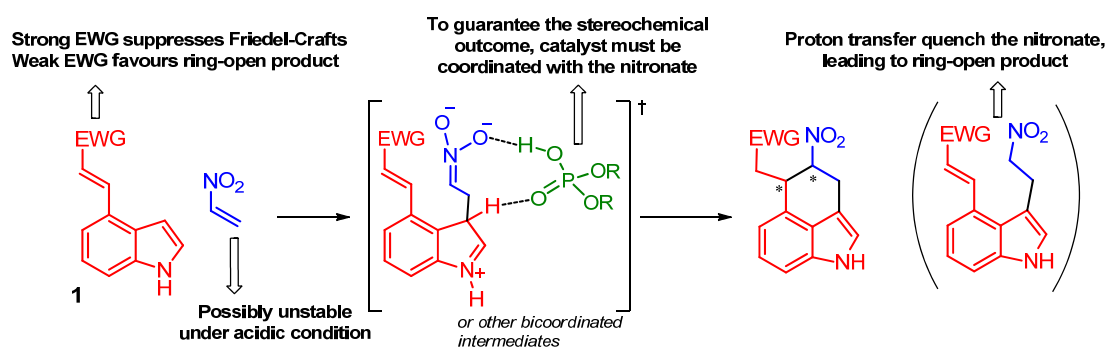
Having found in indole derivatives **1** and electron-poor olefins good candidates for the envisaged organocascade reaction, the attention was then posed towards the identification of an organocatalytic system which possesses an appropriate mode of activation, permitting the successful realization of the cascade reactions.

In particular, the merger of iminium ion and enamine catalysis,<sup>23,43,97a</sup> wherein a nucleophilic enamine is formed upon the conjugated addition to an enal activated by secondary amine catalyst, has resulted to be particularly effective in cascade processes, and was first selected to demonstrate the correctness of our plan. Thus, in our planned reaction sequence, the C3 of indoles **1** could act as nucleophile in an iminium ion

Scheme 33.  $\alpha,\beta$ -Unsaturated aldehydes enabling the organocascade reaction. EWG = electron-withdrawing group; E = electrophile; Nu = nucleophile.

promoted Friedel-Crafts<sup>105</sup> triggering an enamine-mediated intramolecular Michael addition<sup>43a106</sup> (Scheme 33).

Simultaneously, we have realized that reaction of substrates **1** with nitroethene<sup>107</sup> would provide benzo[*cd*]indoles (3,4-annulated indoles) having the nitro group at a strategic position to serve as useful precursor of ergot alkaloids. We have been confident that the recent advances in the activation of nitro compounds by means of chiral Brønsted acid catalysis, and in particular by BINOL derived phosphoric acids already described in the Chapter 3 of the Thesis<sup>108,109</sup> could not only offer a profitable solution for this transformation, but also an unprecedented diastereo- and enantio-controlled to the target tricyclic annulated compounds (Scheme 34). Nevertheless, it must be stressed that new challenges rose in association with the employment of nitroethene in combination with an acidic catalyst. Firstly, this electron-poor olefin is highly reactive and could undergo side reactions in the presence of an acidic catalyst. Secondly, the avoidance of a simple proton transfer leading to un-cyclized product was considered as a considerable challenge. In fact, Brønsted acids are very effective in promoting reactions proceeding through proton transfer from a nucleophile to an electrophile, wherein the Brønsted acid already transfer its proton to the electrophile at the early stages of the reaction, or during the transition state.<sup>38</sup> In our case, however, it is necessary that the intermediate nitronate does not get protonated, to react subsequently with the Michael acceptor at the 4-position. This latter process would in principle be favored by strong EWG Michael acceptor, but this strategy is unfeasible, as it would suppress the Friedel-Craft step. The last issue deals with the stereochemical outcome of the reaction: it was hypothesized that the catalyst should keep the coordination with the nitro-group both in Friedel-Crafts and Michael addition, in order to control the stereochemical outcome of the reaction, presumably defined in the second Michael addition step (Scheme 34).



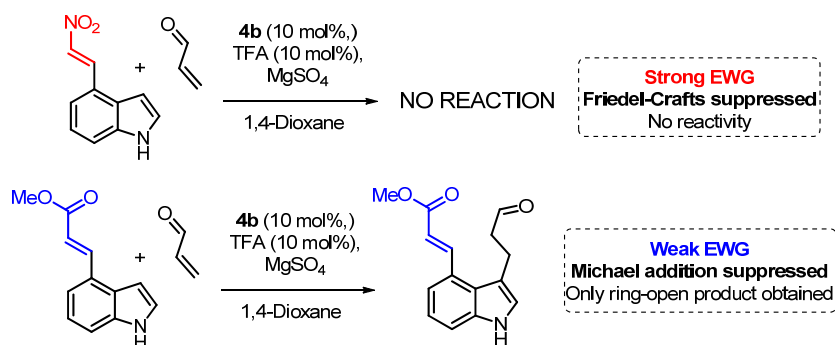
**Scheme 34.** Nitroethene enabling organocascade reaction and associated challenges.

In summary, a novel organocatalytic approach to 3,4-annulated indoles – key motif in natural relevant compounds such as ergot alkaloids – has been devised. The proposed strategy relies on a set of indole derivatives **1** which possess both nucleophilic and electrophilic active sites, which enable the cascade reactions leading to the target products. Nitroethene and  $\alpha,\beta$ -unsaturated aldehydes were selected as reaction partners given their potential effectiveness in cascade processes. The specific mode of activation for these substrates brought us to recognize in secondary amine catalysis and H-bond-donor/Brønsted acid catalysis the most suitable organocatalytic systems to achieve our goals. As anticipated, some relevant challenges are associated to this project; however we were confident that upon a careful rationalization of every single aspect of our strategy, the inherent problematic issues could have been overcome. All the obtained results and the strategies adopted to achieve them are discussed in the following paragraphs.

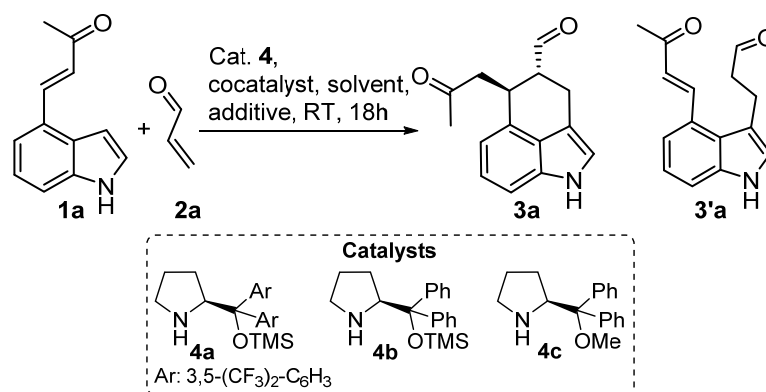
### 4.3. Organocatalytic reactions between indole derivatives **1** and enals: results and discussion

We started our work by preparing indole substrate **1**, bearing a suitable Michael acceptor at the 4-position. Being conscious that the electronic properties of the Michael acceptor could influence the reactivity of **1**, we considered  $\alpha,\beta$ -unsaturated ketones as potentially suitable substrates for the first attempts. These starting materials were easily prepared by Wittig olefination of the commercially available indole-4-carboxaldehyde (see § 4.5). Thus, considering its expected low reactivity we combined indole **1a** with the exceedingly reactive acrolein<sup>110</sup> **2a** as the enal reaction partner. Taking the published asymmetric Friedel–Crafts alkylation catalyzed by diaryl prolinol silyl ethers<sup>43c,46,47</sup> **4a** and **4b** as starting point,<sup>105</sup> we tried to apply similar reaction conditions which however, led to disappointing results (Table 4, entries 1-9). Apparently the 4-substituted indole **1a** showed an even lower reactivity than expected. Fortunately, after switching to slightly more forcing reaction conditions, by using as cocatalyst the rather strong trifluoroacetic acid (TFA), it was found that the reaction catalyzed by **4a** proceeded with promising conversion. Even though the desired 3,4-fused indole **3a** was formed as a single *trans* diastereoisomer and very good enantioselectivity, a considerable amount of ring-open product **3'a** was observed in the crude mixture (Table 4, entry 10). Speculating that water could interfere in the Michael addition step, hydrolyzing the enamine and thus stopping the reaction to **3'a**, few water-trapping agents were tested. While molecular sieves led to

a complex crude mixture, the employment of magnesium sulfate ( $\text{MgSO}_4$ ) resulted in enhanced conversion and exclusive formation of tricyclic compound **3a** (Table 4, entries 11-12). Solvent screening permitted to identify ethers as best solvents in terms of conversion and enantioselectivity. In contrast, when the reaction was performed in chloroform compounds **3a** was observed only in trace while ethanol gave a messy crude mixture (Table 4, entries 13-16). Upon selecting 1,4-dioxane as solvent and lowering the catalyst loading to 10 mol%, prolinol derived catalysts were evaluated. Diarylprolinol **4a-c** were all able to promote effectively the reaction (Table 4, entries 17-19); however, compared to its analogous, **4b** induced better enantioselectivity and was chosen for further investigations. Having found the optimized reaction conditions (Table 4, entry 18), we attempted to examine indole derivatives bearing different Michael acceptors on their C4 position. Nitroalkenes as strong EWG group did not give the Friedel–Crafts product, thus resulting not reactive; on the other hand, less electron-poor EWG as  $\alpha,\beta$ -unsaturated esters provided exclusively the open product (Scheme 35). Thus, as initially assumed the C4-substituent must possess specific electronic properties for the reaction to occur. Conversely,  $\alpha,\beta$ -unsaturated ketones as Michael acceptor group proved to be as a good compromise, hence permitting the successful outcome of both Friedel–Crafts and Michael addition.



**Scheme 35.** Influence of C4-Michael acceptor on the reaction outcome.

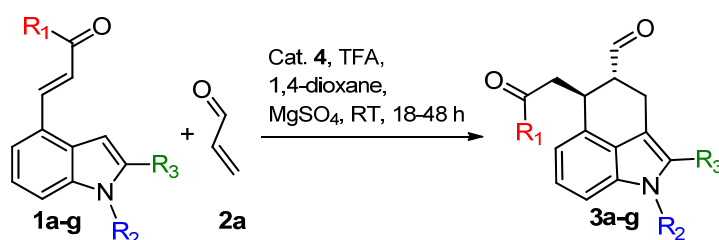
**Table 4.** Optimization of the organocatalytic reaction between **1a** and **2a**<sup>a</sup>

Entry	Solvent	Cat. (Mol %)	Coca.	Additive	3a : 3'a <sup>b</sup>	Conv. <sup>b</sup> (%)	ee <sup>c</sup> (%)
1	CH <sub>3</sub> CN	<b>4a</b> (20)	none	none	-	-	-
2	CH <sub>3</sub> CN	<b>4b</b> (20)	none	none	-	-	-
3	CHCl <sub>3</sub>	<b>4a</b> (20)	none	none	-	-	-
4	CHCl <sub>3</sub>	<b>4b</b> (20)	none	none	-	-	-
5	MTBE	<b>4b</b> (20)	Et <sub>3</sub> N	none	-	-	-
6	toluene	<b>4b</b> (20)	Schreiner's thiourea <sup>111</sup>	none	-	-	-
7	THF	<b>4a</b> (20)	CH <sub>3</sub> CO <sub>2</sub> H	none	-	trace	nd
8	THF	<b>4a</b> (20)	PhCO <sub>2</sub> H	none	-	-	-
9	THF	<b>4a</b> (20)	2-NO <sub>2</sub> PhCO <sub>2</sub> H	none	-	trace	nd
10	THF	<b>4a</b> (20)	TFA	none	57 : 43	50	98
11	THF	<b>4a</b> (20)	TFA	MS 4 Å	nd	nd <sup>d</sup>	nd
12	THF	<b>4a</b> (20)	TFA	MgSO <sub>4</sub>	> 95 : 5	85	99
13	CHCl <sub>3</sub>	<b>4a</b> (20)	TFA	MgSO <sub>4</sub>	-	<10	-
14	EtOH	<b>4a</b> (20)	TFA	MgSO <sub>4</sub>	nd	nd <sup>d</sup>	nd
15	MTBE	<b>4a</b> (20)	TFA	MgSO <sub>4</sub>	> 95:5	76	99
16	dioxane	<b>4a</b> (20)	TFA	MgSO <sub>4</sub>	> 95 : 5	100	96
17	dioxane	<b>4a</b> (10)	TFA	MgSO <sub>4</sub>	> 95 : 5	91	94
18	dioxane	<b>4b</b> (10)	TFA	MgSO <sub>4</sub>	> 95 : 5	100	99
19	dioxane	<b>4c</b> (10)	TFA	MgSO <sub>4</sub>	> 95 : 5	100	89

(a) Reaction conditions: indole derivative **1a** (0.06 mmol), catalysts **4** (10-20 mol%), cocatalyst (10-20 mol%), equimolar to the catalyst employed, acrolein **2a** (0.15 mmol), solvent (0.20 mL), RT, reaction time: 18 h. In all cases, a single diastereoisomer was observed by <sup>1</sup>H NMR in the crude mixture. When necessary, 20 mg of powdered molecular sieves (MS) 4 Å or 40 mg of MgSO<sub>4</sub> were used. (b) Conversion was determined by <sup>1</sup>H NMR and was referred to **3a**. Similarly, the ratio between **3a** and **3'a** was evaluated by <sup>1</sup>H NMR. (c) Determined by chiral stationary phase HPLC. (d) Very complex crude mixture

With the optimized condition in hand, the scope of the reaction was then inspected. Besides the simple methyl derivatives **1a**, electronically different aryl group in R<sub>1</sub> could be successfully engaged in the reaction. Variations of the ketone moiety in indoles **1a-e** afforded the tricyclic compounds **3a-e** in satisfactory yields and excellent enantioselectivities (Table 5, entries 1-5). Modifications in the indole nucleus at N1 and C2 positions in **1f** and **1g** were also tolerated furnishing **3f** and **3g** in nearly perfect enantioselectivities, although a slight decrease in yield was observed when the *N*-Me indole **1g** was employed, even at higher catalyst loading (Table 5, entries 6-7).

**Table 5.** Scope of the reaction between indoles **1** and acrolein **2a**<sup>a</sup>

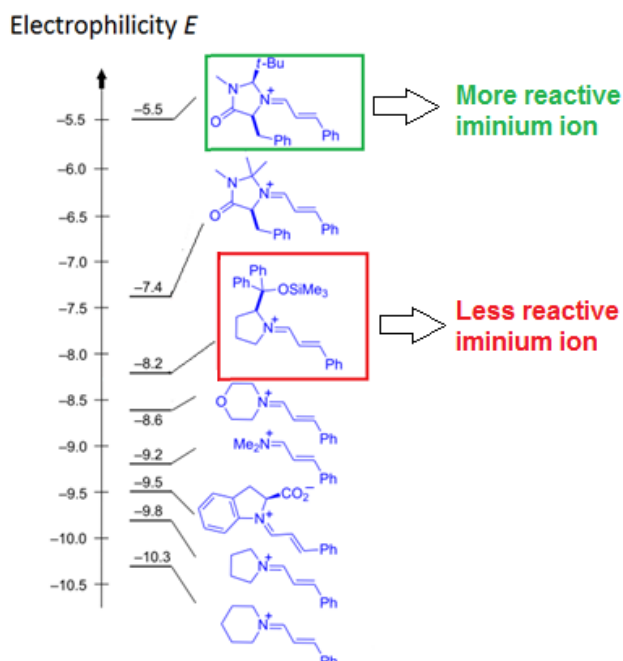


Entry	<b>1</b>	R <sub>1</sub>	R <sub>2</sub>	R <sub>3</sub>	Cat. (mol%)	<b>3</b> -Yield <sup>b</sup> (%)	ee <sup>c</sup> (%)
1	<b>1a</b>	Me	H	H	<b>4b</b> (10)	<b>3a</b> -76	98
2	<b>1b</b>	Ph	H	H	<b>4b</b> (10)	<b>3b</b> -75	98
3	<b>1c</b>	4-BrC <sub>6</sub> H <sub>4</sub>	H	H	<b>4b</b> (10)	<b>3c</b> -78	91
4	<b>1d</b>	4-MeOC <sub>6</sub> H <sub>4</sub>	H	H	<b>4a</b> (10)	<b>3d</b> -70	>99
5	<b>1e</b>	4-NO <sub>2</sub> C <sub>6</sub> H <sub>4</sub>	H	H	<b>4b</b> (10)	<b>3e</b> -71	96 <sup>d</sup>
6	<b>1f</b>	Me	H	Me	<b>4b</b> (10)	<b>3f</b> -81	>99
7	<b>1g</b>	Me	Me	H	<b>4b</b> (20)	<b>3g</b> -67	99

(a) Reaction conditions: **1a-g** (0.10 mmol), **4a** or **4b** (10-20 mol%), TFA (10-20 mol%) equimolar to the catalyst employed, acrolein **2a**, 1,4-dioxane (0.300 mL), MgSO<sub>4</sub> (50 mg), RT, reaction time: 18 h (48 h for entry 7). A single diastereoisomer was observed by <sup>1</sup>H NMR in the crude mixture. (b) Isolated yield. (c) Determined by chiral stationary phase HPLC. (d) Determined by <sup>1</sup>H NMR spectroscopy using Pirkle's alcohol as chiral shift reagent.

When it was tried to employ β-substituted aldehydes in the reaction with **1a**, under the same reaction conditions, it was observed the inability of all diarylprolinol catalysts **4a-c** in promoting the reaction (Table 6, entries 1-5). Neither the extension of the reaction time to 65 h, nor the increasing of the temperature to 70 °C, produced any valuable effect (Table 6, entries 4-5). These disappointing results, once again, highlighted the recognized poor nucleophilicity of indoles **1**, which combined with the decreased reactivity of sterically demanding β-substituted aldehydes compared to acrolein, prevented the

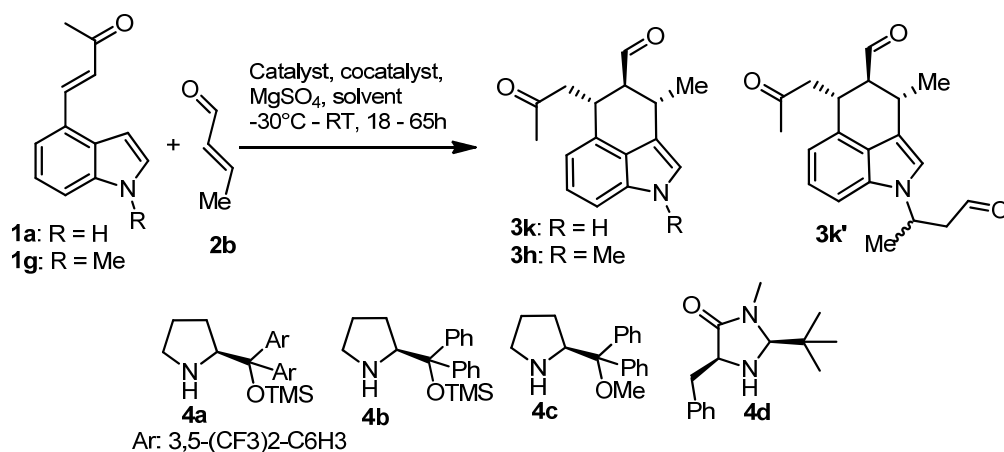
reaction from occurring. In the search of a more reactive system, we resorted to the electrophilicity scale developed by Mayr,<sup>112</sup> in which it is established that the iminium ion



**Figure 27.** Mayr electrophilicity scale. It is possible to note, highlighted in the scale, that MacMillan's catalyst-activated enals (green) are more electrophilic than the one activated by Jørgensen-Hayashi catalyst (red).

ion derived from the MacMillan second generation catalyst **4d** is about three order of magnitude more electrophilic than the one generated from prolinol **4b** (Figure 27). Therefore, we tested catalyst **4d** with crotonaldehyde **2b** using various polar and aprotic solvents (Table 6, entries 6-8), TFA as cocatalyst, at RT. The conversion increased dramatically, but besides the tricyclic target product **3k**, the related *N*-alkylated compound **3'k** was formed in not negligible amounts and moreover, the

enantiomeric excesses were unsatisfactory. No improvement was observed by replacing the cocatalyst: PTSA gave the *N*-alkylated **3'k** as the predominantly product, while 2-nitro benzoic acid did not promote the reaction at all (Table 6, entries 9-10). By using DCM/*i*-PrOH mixture as solvent, as originally reported for the reactions between indole and enals catalysed by **4d**,<sup>48</sup> the enantioselectivity was improved to encouraging values, although the ratio between **3k** and **3'k** remained poor (Table 6, entry 12). Thus, being unable to discriminate between **3k** and **3'k**, even by decreasing the amount of **2b** (Table 6, entry 13), we switched to the *N*-Me indole derivative **1g** as substrate. At RT, the reaction proceeded to complete conversion furnishing **3h** as the only product with moderate enantioselectivity (Table 6, entry 14) which was improved to a satisfactory level by decreasing the temperature to -30 °C (Table 6, entry 15).

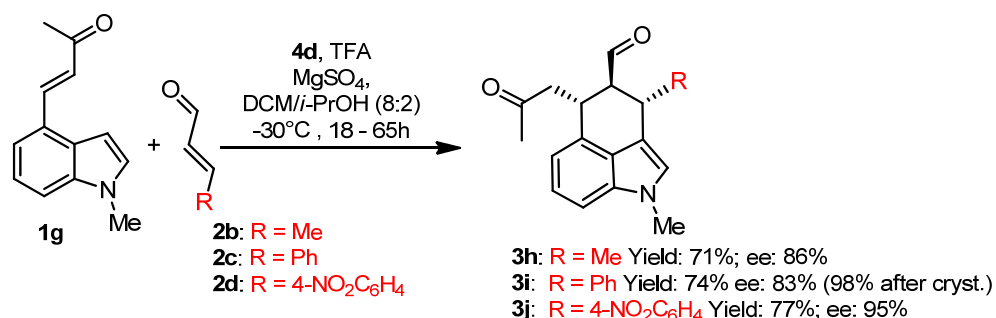
**Table 6.** Optimization of the reaction between **1** and crotonaldehyde **2b**.<sup>a</sup>

Entry	<b>1</b>	Solvent	Temp (°C)	Time (h)	Cat. (mol%)	Cocat.	<b>3k</b> : <b>3'k</b> <sup>b</sup>	Conv. <sup>b</sup> (%)	ee <sup>c</sup> (%)
1	<b>1a</b>	dioxane	RT	18	<b>4b</b>	TFA	-	< 5	-
2	<b>1a</b>	dioxane	RT	18	<b>4a</b>	TFA	-	< 5	-
3	<b>1a</b>	dioxane	RT	18	<b>4c</b>	TFA	-	< 5	-
4	<b>1a</b>	dioxane	RT	65	<b>4a</b>	TFA	-	6	nd
5	<b>1a</b>	dioxane	70	65	<b>4a</b>	TFA	-	8	nd
6	<b>1a</b>	dioxane	RT	18	<b>4d</b>	TFA	80:20	> 95	48
7	<b>1a</b>	CH <sub>3</sub> CN	RT	18	<b>4d</b>	TFA	85:15	84	38
8	<b>1a</b>	MTBE	RT	18	<b>4d</b>	TFA	90:10	94	54
9	<b>1a</b>	dioxane	RT	18	<b>4d</b>	PTSA	5:95	> 95	nd
10	<b>1a</b>	dioxane	RT	18	<b>4d</b>	2-NO <sub>2</sub> -PhCO <sub>2</sub> H	-	< 5	nd
11	<b>1a</b>	toluene	RT	18	<b>4d</b>	TFA	5:95	> 95	nd
12	<b>1a</b>	DCM/ <i>i</i> -PrOH (8:2)	RT	18	<b>4d</b>	TFA	40:60	> 95	76
13 <sup>d</sup>	<b>1a</b>	DCM/ <i>i</i> -PrOH (8:2)	RT	18	<b>4d</b>	TFA	43:57	76	80
14	<b>1g</b>	DCM/ <i>i</i> -PrOH (8:2)	RT	65	<b>4d</b>	TFA	-	> 95	78
15	<b>1g</b>	DCM/ <i>i</i> -PrOH (8:2)	-30	65	<b>4d</b>	TFA	-	94	86

(a) Reaction conditions: indole derivative **1a** or **1g** (0.10 mmol), catalyst **4** (20 mol%), cocatalyst (20 mol%), crotonaldehyde **2b** (0.25 mmol), 50 mg MgSO<sub>4</sub>, solvent (0.20 mL). In the case of entries 7 and 8 the diastereomeric ratio was evaluated to be 83:17 and 75:25 respectively; in all the other cases, a single diastereoisomer was observed by <sup>1</sup>H NMR spectroscopy in the crude mixture. (b) **3k**:**3'k** ratio and conversion were determined by <sup>1</sup>H NMR spectroscopy on the crude mixture. (c) Determined by chiral stationary phase HPLC and referred to **3k** or **3h**. (d) In this case 0.10 mmol of **2b** were used.

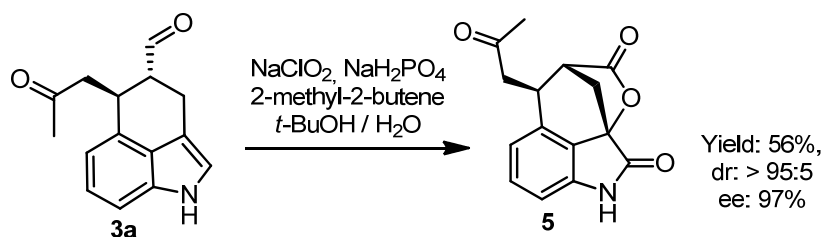
This modified protocol could also be applied to aryl β-substituted enals such as cinnamaldehyde **2c** and 4-nitro cinnamaldehyde **2d**. The corresponding tricyclic indoles **3h-j**, having three contiguous stereocenters, were obtained in good yields and

enantioselectivities. Remarkably, the moderate enantioselectivity of **3i** could be considerably enhanced upon crystallization (Scheme 36).



**Scheme 36.** Reaction scope between indole **1g** and  $\beta$ -substituted aldehydes **2b-d**.

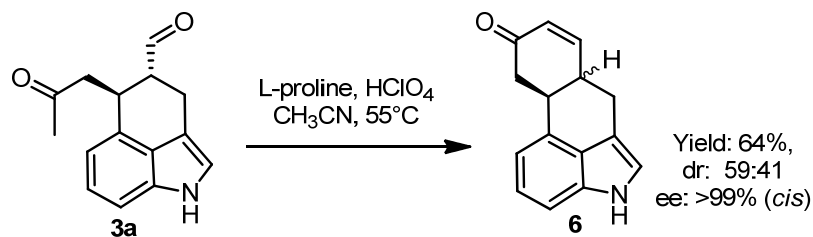
The possibility of performing synthetic manipulations in the products **3** was briefly explored. Compound **3a** was oxidized under Pinnick conditions,<sup>48</sup> namely by using NaClO<sub>2</sub> – NaH<sub>2</sub>PO<sub>4</sub> as oxidant (dihydrogen phosphate anion generates chlorous acid, the effective oxidant species) and 2-methyl-2-butene as scavenger (it quenches hypochlorous acid which is formed as by-product). Surprisingly, under these conditions that were thought to be mild, both the aldehyde moiety and the indole nucleus were oxidized, furnishing the intriguing lactone **5**. Remarkably, this compound – which presented the complex spirocyclic structure and three stereocenters, one of which was quaternary – was obtained in satisfactory yield, as a single diastereoisomer and excellent enantioselectivity (Scheme 37). A mechanistic proposal for the formation of **5** is detailed forward (see § 4.3.2).



**Scheme 37.** Oxidation of compound **3a** under Pinnick conditions.

On the other hand, Robinson annulation reaction was envisaged to tether the aldehyde moiety with the carbon  $\alpha$  to the ketone group, resulting in a tetracyclic derivative. After several unsuccessfully attempts, the reaction was performed under – old but gold – reaction conditions, as originally reported by Wiechert in the first organocatalyzed Robinson annulation.<sup>11b</sup> To our delight, L-proline was found to promote the reaction, in combination with HClO<sub>4</sub>, furnishing the tetracyclic compound **6** in satisfactory yield and

excellent enantioselectivity, despite as a mixture of diastereoisomers, due to the partial epimerization of the chiral center close to the aldehyde during the reaction (Scheme 38).



**Scheme 38.** Robinson annulation of **3a** leading to tetracyclic compound **6**.

#### 4.3.1. Determination of the absolute and relative configuration of compounds **3** and **6** and structural determination of **5**

Compound **3a** was selected as representative compound for the determination of relative configuration by conformational analysis. Full assignment of the  $^1\text{H}$  and  $^{13}\text{C}$  spectra was preliminarily achieved by bi-dimensional experiments (COSY, gHSQC and gHMBC, taken in  $\text{CDCl}_3$  solutions). The relative stereochemistry of the two stereogenic centers at C4 and C5 was determined by means of NMR spectroscopy. The two diastereotopic hydrogens belonging to C3 were found at 3.00 and 3.38 ppm whereas the two diastereotopic hydrogens belonging to C9 were found at 2.77 and 2.85 ppm (by HMBC correlation with the  $\text{C}=\text{O}$ ). The latter showed an additional coupling with the signal at 4.14 ppm (H-5). The signal of the NH (7.98 ppm) was assigned by the lack of correlation in the  $^{13}\text{C}$ - $^1\text{H}$  HSQC spectrum. DPGSE-NOE experiments<sup>80</sup> were acquired in order to assign the relative stereochemistry at C4 and C5. These centers were bearing respectively the CHO and the  $\text{CH}_2\text{COCH}_3$  substitution that could assume a *cis* or *trans* relative disposition. On saturation of the aldehyde hydrogen at 9.54 ppm, (Figure 29, trace b), NOE enhancement was observed for H-5 and for one of the diastereotopic protons at C3 at 3.38 ppm (H-3a). No enhancement was observed for the other proton H-3b, and on the two hydrogens belonging to C9. The observed NOEs suggested that the aldehyde and the  $\text{CH}_2\text{COCH}_3$  substituents lie on opposite sides of the hexa-atomic cycle. On saturation of both the diastereotopic C9 hydrogens (Figure 29, trace a), large NOEs were observed at 4.14 ppm (H-5), 2.92 ppm (H-4) and 3.00 ppm (H-3<sub>b</sub>). While the first two NOEs had to be visible independently from the relative configuration of the two stereogenic centers, the latter

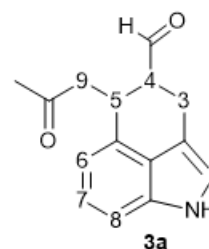


**Figure 28.** Compound **3a**

confirmed that the  $\text{CH}_2\text{COCH}_3$  moiety was on the opposite side of the cycle with respect to the CHO group. On saturation of H-5 (Figure 29, trace c), NOEs were observed on the aldehyde, on the two hydrogens at C9, but no enhancement was observed on the two hydrogens at C3. This confirms that H-5 was in a pseudo-equatorial position. Finally, on saturation of the COMe signal (not shown in figure), NOE were observed only on H-9<sub>a</sub> and H-9<sub>b</sub>, suggesting that the COMe moiety adopted a conformation that places the methyl far from the cycle. NMR analysis thus suggesting the *trans* relationship of the two stereogenic centres (thus 4*R*\*,5*S*\* relative configuration).

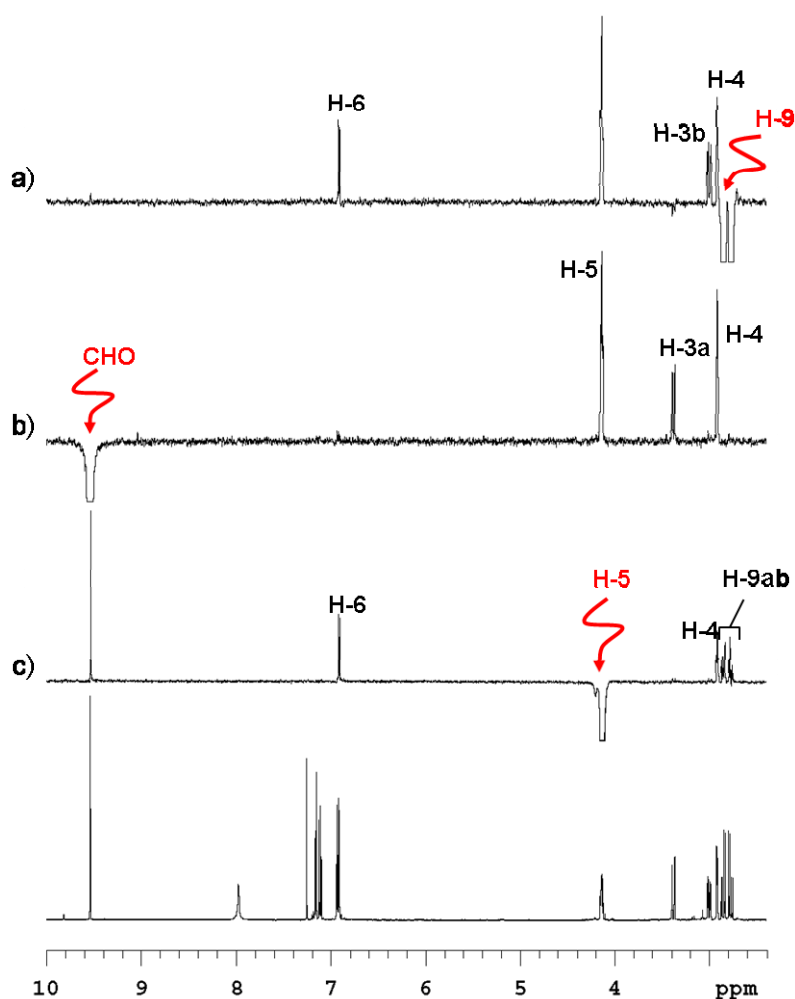


**Figure 29.** DPGSE-NOE spectra of **3a** (600 MHz in  $\text{CDCl}_3$ ). Bottom:  $^1\text{H}$ -NMR control spectrum; trace a) saturation of H-9; trace b) saturation of CHO; trace c) saturation of H-5.

We have observed only the *trans*-configured tricyclic products in all cases (**3a-g**), which can be due either to a high diastereoselectivity in the Michael reaction, or to the greater thermodynamic stability of the *trans*-adduct compared to the *cis* (i.e. product epimerization leads to the more stable *trans*-isomer after the Michael addition reaction

has taken place). Having in hand the relative configuration and suitable information about the preferred conformation, the assignment of the absolute configuration was tackled by chiroptical methods.<sup>81</sup> Comparison of the calculated (TD-DFT) with the experimental ECD spectrum was performed. The best simulation was obtained by the  $\omega$ B97-XD functional, but all the simulated spectra showed a good agreement with the experimental one. As shown in Figure 30, all the simulated spectra match well the Cotton effects at 224 nm and 270 nm when the 4*R*, 5*S* absolute configuration was assumed in the calculations. Thus the absolute configuration 4*R*, 5*S* could be assigned to **3a** with a consistent margin of confidence. The absolute configuration of the remaining compounds **3b-g** – derived from the organocatalytic reaction carried out with the same enantiomer of the catalyst **4b** – was assigned by analogy.

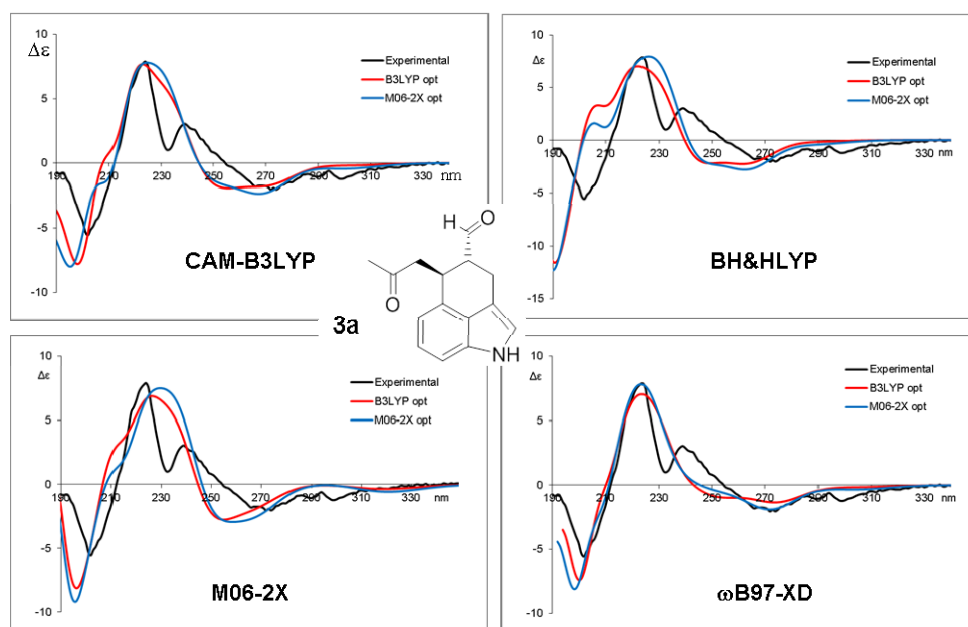


**Figure 30.** Simulations of the experimental ECD spectrum of **3a** (black traces). For each section, the black line correspond to the experimental spectrum (acetonitrile solution,  $1.5 \cdot 10^{-4}$  M, 0.2 cm path length  $\Delta\epsilon$  in  $\text{Mol L}^{-1} \text{cm}^{-1}$ ). The red lines correspond to the simulations obtained using the populations derived from B3LYP/6-31G(d) optimization. The blue lines correspond to the simulations obtained using the populations derived from M06-2X/6-31+G(d,p) optimization. The simulated spectra were vertically scaled and red-shifted by 7-14 nm to get the best match with the experimental spectrum. All the simulations are for the 4*R*, 5*S* absolute configuration.

Along of this, compound **3h** (Figure 31) was selected as representative of compounds **3h-j**, obtained when  $\beta$ -substituted enals were employed in the organocatalytic reaction catalyzed by MacMillan's catalyst **4d**. The relative configuration of compound **3h**, was determined

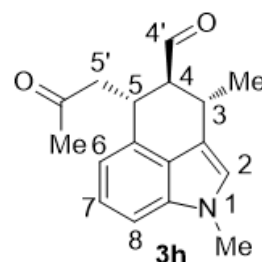


**Figure 31.** Compound **3h**

by NMR spectroscopy, after the preliminary full assignment of  $^1\text{H}$  and  $^{13}\text{C}$  spectra, achieved by bi-dimensional experiments (COSY, gHSQC and gHMBC). In particular, gCOSY spectrum showed a coupling between the aldehyde hydrogen at 9.66 ppm and the hydrogen at 2.36 ppm, allowing us to assign this signal as H-4. Moreover, this hydrogen at 2.36 ppm showed additional couplings with the signals at 4.10 and 3.52 ppm. Since the signal at 3.52 ppm was coupled with the signal of the methyl group belonging to C3 (1.36 ppm, doublet) and the signal at 4.10 ppm coupled with the two diastereotopic protons of C5' (3.09 and 2.86 ppm, two dd), we assigned the signal at 3.52 ppm to H-3 and the signal at 4.10 ppm to H-5. The signal of the proton at C4 (2.36 ppm) appeared as a triplet of doublets and exhibits two coupling constants of 9.1 Hz and one of 4.6 Hz. This implies that H-4 couples with two hydrogens with a large coupling constant and with one hydrogen with a smaller coupling constant. Moreover the aldehyde proton appeared as a doublet with one coupling constant of 4.6 Hz, that is the coupling constant with H-4. This was consistent with a coupling of H-4 with two large *trans*-diaxial coupling with H-3 and H-5, with a dihedral angle close to  $180^\circ$ . This indicated that H-3, H-4 and H-5 were in axial position of the pseudo-chair six-membered ring, while the 2-oxopropyl, the aldehyde and the methyl moieties occupied the equatorial positions (Figure 32). This assignment was confirmed by the signal of H-5, which appears as double triplet and presented two couplings of 5.7 Hz with the diastereotopic hydrogens at C6' and the same coupling of 9.1 Hz with H-4. Mono-dimensional DPGSE-NOE experiments<sup>80</sup> were acquired in order to confirm the relative stereochemistry at C3, C4 and C5. Significant NOE enhancements were observed as follows (Figure 33). On saturation of H-3, a NOE enhancement was observed for the aldehyde proton, and for H-5. On saturation of H-4, NOE enhancement was observed for the hydrogens belonging to the methyl group at C3. On saturation of H-5, NOE enhancement was observed for H-3 and for the aldehyde proton. All these experimental evidences confirmed the axial relationships between H-3, H-4 and H-5, already deduced from the analysis of the *J*-couplings of the  $^1\text{H}$  NMR spectrum, thus confirming the *trans* relative configuration of the three contiguous asymmetric centres.

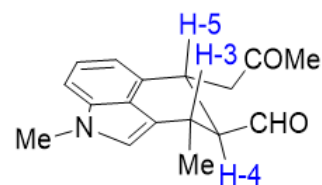


**Figure 32.** All-*trans* configuration of compound **3h**, with the pseudo-axial relationships justifying the observed large coupling constants between H-4, H-3 and H-5

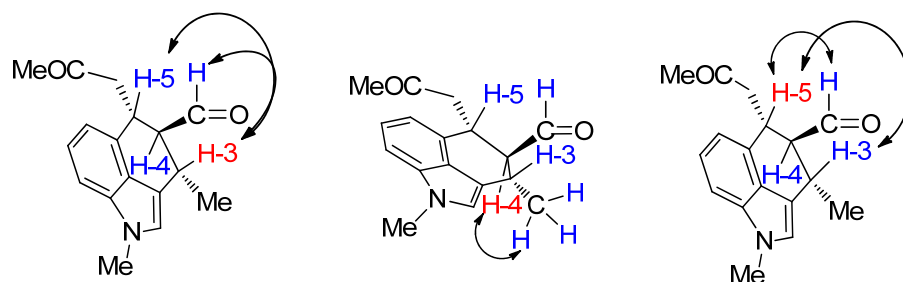
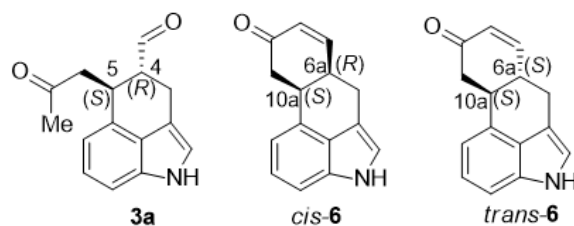


**Figure 33.** Significant NOE enhancements on saturation of the protons indicated in red.

In the case of compound **3h** the first stereocenter was generated upon the Friedel–Crafts step. Thus, the absolute configuration at C3 could be assigned as (*S*) by comparison with the already published report regarding the alkylation of indole with  $\beta$ -substituted enals, mediated by the same enantiomer of MacMillan second generation catalyst.<sup>48</sup> Having established the all *trans* relationship of the protons belonging to the stereocenters of **3h**, the absolute configuration was consequently assigned as 3*S*, 4*S*, 5*R*. Compounds **3i** and **3j** presented 3*R*, 4*S*, 5*R* absolute configuration due to the different priority of the aryl moiety at C3.

Robinson annulation of **3a** furnished tetracyclic compound **6** as a mixture of *cis* and *trans*



diastereoisomers (

Figure 34). Being compound **6** structurally constrained, the determination of its absolute configuration by means of simulations of ECD spectra and comparison with the experimental one was a straightforward technique. It must be stressed that having already established the absolute configuration of **3a**, a new assignment of the absolute

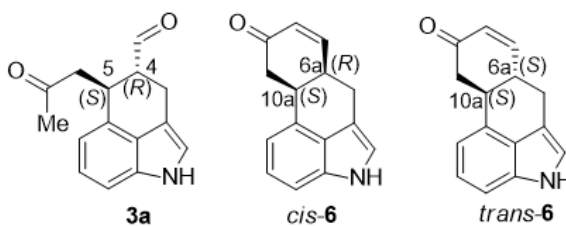


**Figure 34.** Compounds **3a** and **6**

configuration could appear an overkill, but it was not. Compound **3a** has a considerable conformational mobility, thus leaving space for some uncertainty in the precise determination of its conformations used in combination with chiroptical methods, while **6a** is rigid. The assignment of its absolute configuration is thus even more reliable. The stereogenic center at C5 of **3a** should be left unchanged, but the reaction conditions were

rather harsh (55 °C, in the presence of strong acid HClO<sub>4</sub> and L-proline, see § 4.4.2). For these reasons the independent assignment of the absolute configuration of *cis*-**6** would provide a validation about the retention of configuration at C5. Experimental ECD spectrum of *cis*-**6** agreed with all the (TD-DFT) simulations for 6a*R*, 10a*S* absolute configuration. Taking into account the different numbering of *cis*-**6**, the 10a*S* configuration matched the 5*S* configuration of the starting compound **3a**, thus confirming the retention of the stereoinformation at stereocenter C5 of **3a**

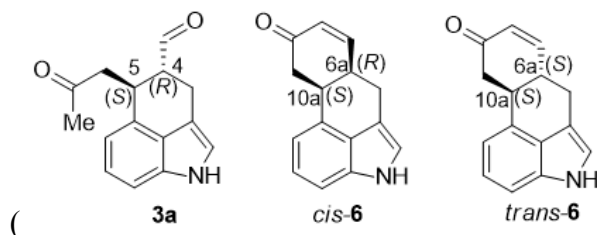


**Figure 34).**

The structure of compound **5** (Figure 35) was established by NMR experiments and mass spectrometric analysis. The ESI-mass (ESIMS) revealed a molecular mass which was not compatible with the structure of the carboxylic acid having the indole core unaltered, but on the contrary it was perfectly consistent with compound **5** (experimental ESIMS: 271 [M+Na]<sup>+</sup>). <sup>1</sup>H NMR spectrum showed only three correlated aromatic signals, no signal ascribable to the proton at C2 of indole was recognized. <sup>13</sup>C NMR revealed three signals which were compatible with C=O carbon: one carbonyl belonging to the ketone in the side chain ( $\delta = 204.6$  ppm), and two carboxyl (C4 and C2), one belonging to the lactone and one to the oxindole ( $\delta = 175.0$  and 169.9 ppm). The comparison between <sup>13</sup>C NMR, DEPT 1.0 and DEPT 1.5 experiments revealed the overall presence of seven quaternary carbons, five CH carbons (three of which aromatic), two CH<sub>2</sub> carbons and one CH<sub>3</sub> carbon. The chemical shifts of the carboxyl C2 (175.0 ppm), the quaternary C3 (78.0 ppm) and the lactone carboxyl C4 (169.9 ppm) were in agreement to those reported by Menéndez et al in the synthesis of oxindole and spyrindole structures.<sup>113</sup> In order to support the hypothesized structure of lactone **5**, a series of bidimensional NMR spectra (gCOSY, gHSQC and gHMBC) were recorded. Notably, in the gHMBC spectra, the bridged methylene (C10) was correlated with the quaternary C3 (78.0 ppm), with C5 (43.9 ppm), with the lactone carboxyl C4 (175.0

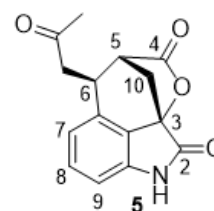
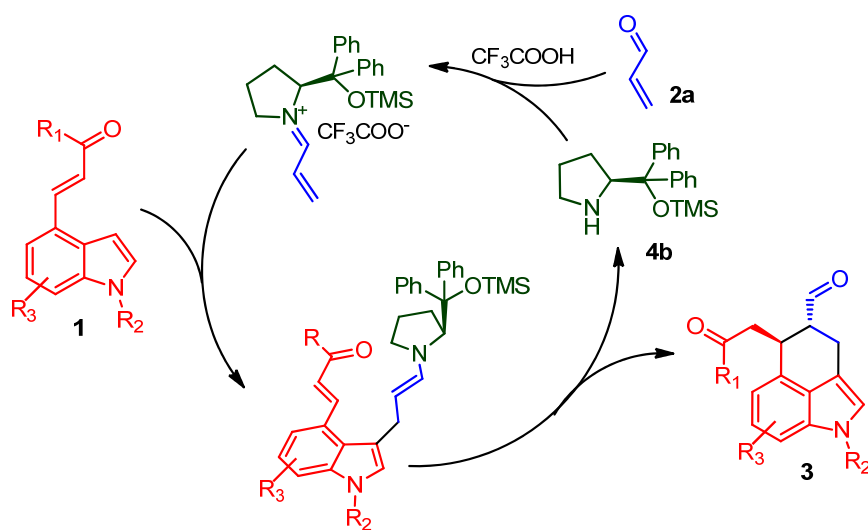


**Figure 35. Compound 5**

ppm), with an aromatic quaternary carbon at 125.9 ppm and with C6 (33.1 ppm). The set of all these experimental data led us to assign the proposed structure to compound **5**.

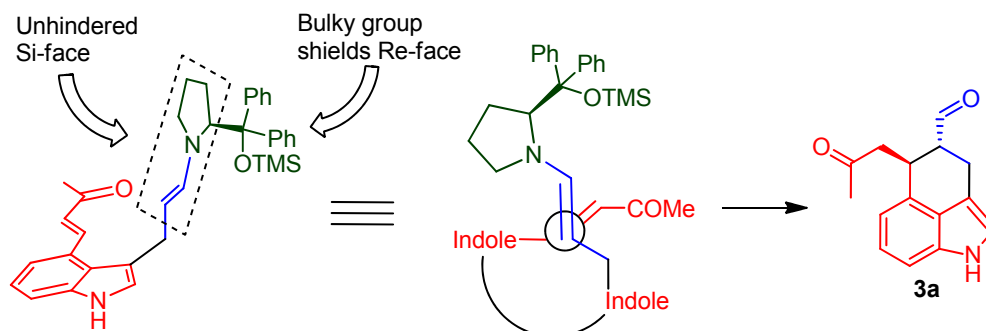
### 4.3.2. Mechanistic proposals for the formation of compounds **3** and **5**

A plausible catalytic cycle for the cascade reaction between **1** and acrolein **2a** is reported in Scheme 39. The cascade reaction is initiated by the TFA-promoted condensation of chiral amine catalyst **4b** to acrolein **2a**, resulting in the formation of an iminium ion, to which the indole derivatives **1** adds through a Friedel–Crafts alkylation. The resulting enamine subsequently undergoes an intramolecular Michael addition furnishing the tricyclic products **3** and releasing the catalyst for the next catalytic cycle.



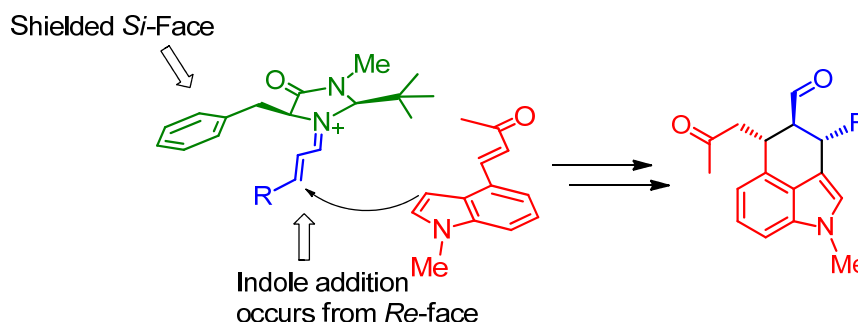
**Scheme 39.** Proposed catalytic cycle for the cascade reaction between indoles **1** and acrolein **2a**.

To account for the observed (4*R*,5*S*) absolute configuration, we refer to a transition state model in which the enantiocontrol is provided by the bulky group on the catalyst. The chiral centers are both generated in the Michael addition step, which is triggered by the Friedel–Crafts addition. In this Michael addition step it can be assumed that the electrophile will approach the enamine intermediate from the least hindered face. In the transition state the large aryl and silyloxy substituents of the catalyst keep the enamine in a *s-trans* conformation and shield the *Re*-face of the enamine. As a consequence the unhindered *Si*-face of the enamine attacks the electron-poor olefin (Scheme 40). This assumption is in line with the generally accepted models describing  $\alpha$ -functionalization of aldehydes mediated by diarylprolinol silyl ethers enamine-catalysis.<sup>43c,46,47</sup>



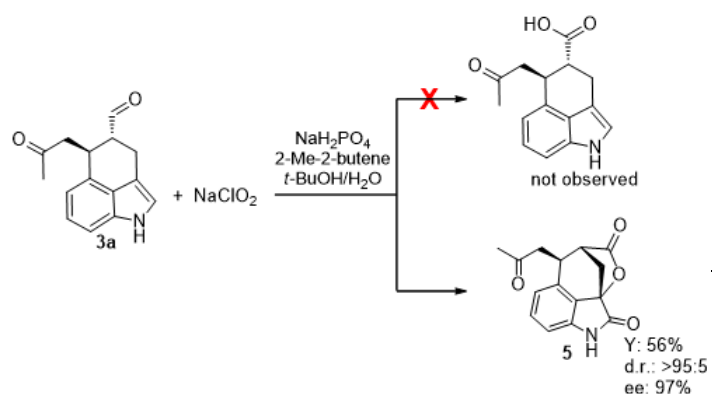
**Scheme 40.** Model accounting for the observed enantioselectivity in the enamine-mediated enantioselectivity determining step.

Concerning the explanation of the absolute configuration of **3h**, in the reaction between indole derivative **1g** and  $\beta$ -substituted enals we can hypothesize a similar catalytic cycle to that outlined in Scheme 39, in which diarylprolinol catalyst **4b** is replaced by catalyst **4d**. Contrary to the reaction between **1** and acrolein **2a**, in this reaction the first stereocenter is generated in the Friedel–Crafts step; therefore, in agreement with the report describing the enantioselective alkylation of indoles with enals catalysed by **4d**,<sup>48</sup> it can be assumed that the indole derivative **1g** attacks the iminium ion at its unshielded *Re*-face (Scheme 41), delivering, after enamine-mediated Michael addition, the products **3h-j** featuring the relative and absolute configuration shown below.



**Scheme 41.** Model for the enantioselectivity in compounds **3h-j**. The iminium ion-mediated Friedel–Crafts alkylation is the enantioselectivity-determining step.

Compound **5** was surprisingly obtained by treating **3a** under Pinnick<sup>114</sup> (or Pinnick-Lindgren<sup>115</sup>) conditions. In principle, these conditions which employ chlorous acid (*in-situ* generated by dihydrogen phosphate anion) as the oxidant species (the by-product hypochlorite should be trapped by the 2-methyl-2-butene olefin) should leave the indole core untouched,<sup>48</sup>

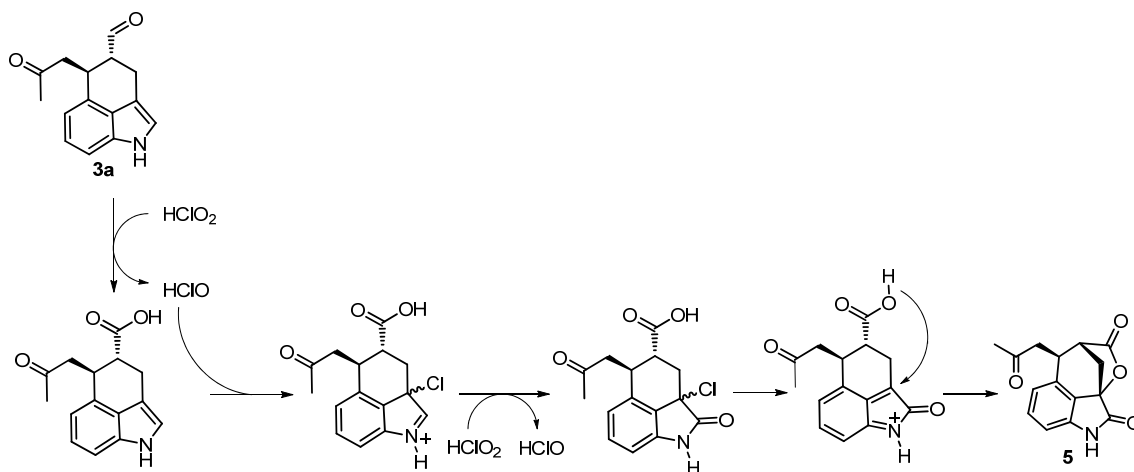


oxidizing selectively the aldehyde moiety to a carboxylic acid. However, apparently the concomitant oxidation of the indole ring occurred in compound **3a** (Scheme 42).

On the other hand, the conversion of 3-indole-propanoic acids to the corresponding spirocyclic oxindole lactones has been reported in several instances, and was found to occur under a variety of

oxidative conditions (e.g. **Scheme 42.** Oxidation of **3a** under Pinnick conditions gave spirocyclic lactone **5** instead of the expected carboxylic acid. NBS,<sup>116</sup> thallium trinitrate,<sup>117</sup> *t*-BuBr/DMSO,<sup>118</sup> oxalyl chloride/DMSO<sup>113</sup>).

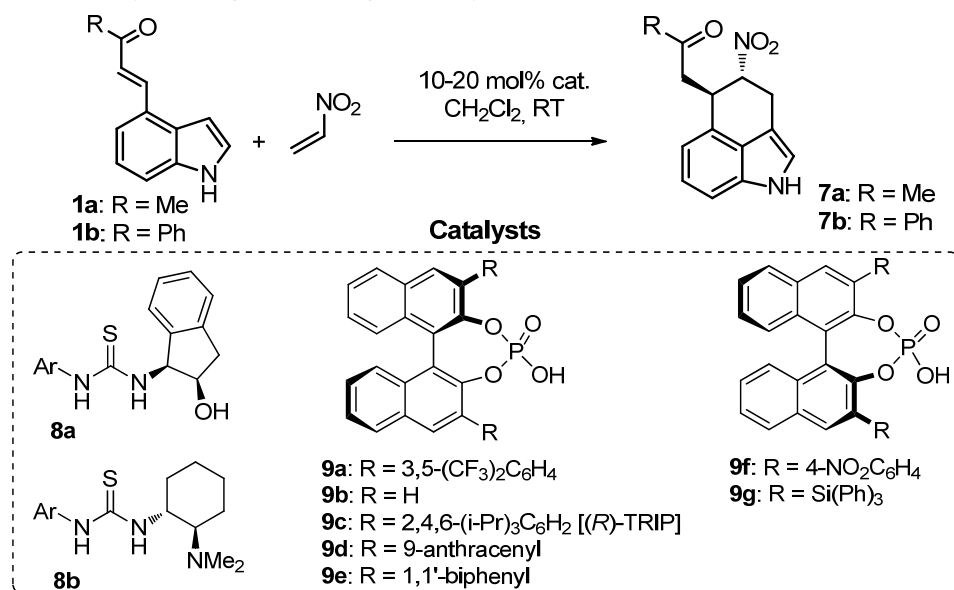
On these grounds, the proposed interpretation for the formation of compound **5** involves a first oxidation of the aldehyde moiety to the carboxylic acid by chlorite, followed by the indole oxidation and lactone formation (Scheme 43). Given the presumed inability of chlorite in oxidising the indole ring, we hypothesise that the particular structure of compound **3a** makes its indole C2-C3 bond more efficient than 2-methyl-2-butene in trapping the hypochlorite, the by-product of the first oxidative process. Regarding the mechanism of the oxidative lactonisation reaction, it can be assumed that the reaction of the indole with hypochlorite leads to a 3-chloro indolenine, which can be easily oxidized (even by chlorite) to a 3-chloro oxindole. Then, lactonisation occurs, possibly through an *ortho*-azaxylylene intermediate.



**Scheme 43.** Proposed reaction pathway leading to spirocyclic lactone **5**.

#### 4.4. Organocatalytic reactions between indoles derivatives **1** and nitroethene: results and discussion

While embarking us in the development of the organocascade reaction between indoles **1** and enals, our research group turned the attention towards nitroethene as electron-poor olefin that could be engaged in a new cascade process with derivatives **1**. As already anticipated, given the strategic position of the nitro group in the tricyclic products, this transformation would in principle allow a direct access to enantioenriched ergot alkaloids, therefore it has been considered as worthy of investigations. Despite H-bond donor catalysts has been widely used in Friedel–Crafts alkylation of indole by nitroalkenes,<sup>108</sup> preliminary experiments showed that thiourea catalysts (**8a,b**) were not able to promote any reaction between substrate **1a** and nitroethene (Table 7, entries 1-2), possibly due to the established poor nucleophilicity of indoles **1**. More acidic BINOL-derived phosphoric acid (**9a-g**) catalysts proved instead to be helpful. With these catalysts, substrate **1a** furnished the desired cascade product **7a** with moderate enantioselectivities, variable conversion and as a single *trans*-diastereoisomer (Table 7, entries 3-9). Amongst the catalysts tested, the BINOL-derived phosphoric acid **9c** was able to complete the reaction, affording **7a** with promising enantioselectivity. (Table 7, entry 5) A considerable improvement in the enantiomeric excess was achieved when indole derivative **1b** was employed in the reaction (Table 7, entry 10-16). All BINOL-derived phosphoric acid catalysts tested were found to be able to promote the cascade reaction between substrate **1b** and nitroethene, with the (*R*)-TRIP catalyst **9c** giving the best result in terms of enantioselectivity (Table 7, entry 12). It must be noted however that also the BINOL-derived catalysts **9d** and **9g** gave very good enantioselectivity in the reaction, even if slight inferior than the one obtained with **9c**. Thus, reaction between **1b** and nitroethene, catalyzed by **9c** was designated as lead reaction for the further optimization of the organocascade process.

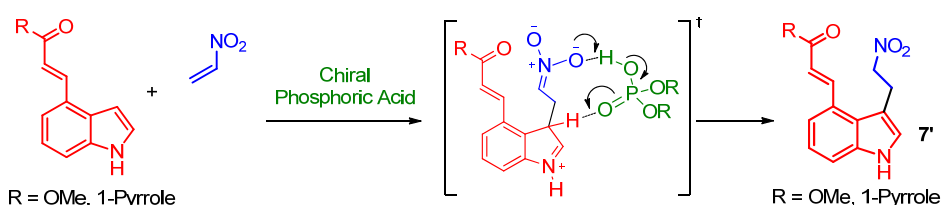
**Table 7.** Preliminary investigation on organocatalytic reaction between **1** and nitroethene.<sup>a</sup>

Entry	<b>1</b>	Cat. (mol%)	Conversion. <sup>b</sup> (%)	ee <sup>c</sup> (%)
1	<b>1a</b>	<b>8a</b>	-	-
2	<b>1a</b>	<b>8b</b>	< 5	nd
3	<b>1a</b>	<b>9a</b>	91	41
4	<b>1a</b>	<b>9b</b>	48	20
5	<b>1a</b>	<b>9c</b>	> 95	55
6	<b>1a</b>	<b>9d</b>	75	21
7	<b>1a</b>	<b>9e</b>	69	41
8	<b>1a</b>	<b>9f</b>	41	- 41
9	<b>1a</b>	<b>9g</b>	93	- 12
10	<b>1b</b>	<b>9a</b>	90	77
11	<b>1b</b>	<b>9b</b>	> 95	59
12	<b>1b</b>	<b>9c</b>	80	95
13	<b>1b</b>	<b>9d</b>	> 95	92
14	<b>1b</b>	<b>9e</b>	88	5
15	<b>1b</b>	<b>9f</b>	> 95	27
16	<b>1b</b>	<b>9g</b>	> 95	93

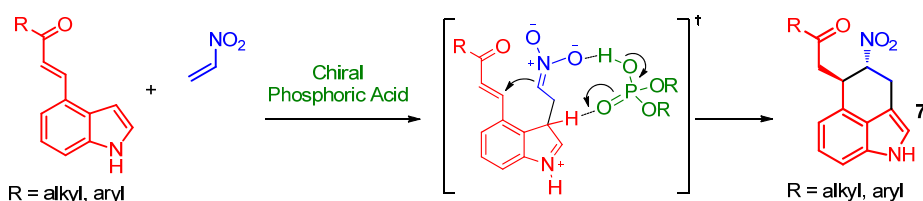
(a) Reaction conditions: indole **1a** or **1b** (0.05 mmol), nitroethene (0.075 mmol, 1 – 1.5M solution in toluene), catalysts **8a** – **8b** (0.01 mmol, 20 mol%) or catalysts **9a** – **9g** (0.005 mmol, 10 mol%), CH<sub>2</sub>Cl<sub>2</sub> (0.25 mL). Reaction time varying from 18 to 48 h. A single *trans*-diastereoisomer was observed in all reactions. (b) Determined by <sup>1</sup>H NMR analysis of the crude. (c) Determined by chiral stationary phase HPLC.

However, at this point, it should be noted that the positive results obtained with phosphoric acids as catalyst were somehow unexpected. The reaction was thought to proceed through a nitronic acid-type intermediate, formed upon the Friedel–Crafts addition and coordinated to the catalyst via H-bond. In this intermediate, proton-shift or -relay processes – “quenching” the nitronate and delivering the side product **7'** – were assumed to be very facile with an acidic catalyst such as a phosphoric acid. In fact, phosphoric acids lack a sufficiently basic moiety to have the capability of stabilizing a nitronate.<sup>119</sup> Indeed the presence of a competition between intramolecular nitro-Michael addition<sup>120</sup> and nitronate “quenching” was revealed by the exclusive formation of the open chain adducts **7'** not only in the reaction with indoles featuring a weak ester Michael acceptor, but also with indoles bearing a *N*-acyl pyrrole, which is usually an efficient acceptor for nitro-Michael reactions (Scheme 44, top).<sup>121</sup> It is also worth stressing that in the field of organocatalytic cascade reaction, only few examples deal with such type of sequential processes (H-bond promoted addition of a neutral nucleophile triggering a subsequent transformation),<sup>108d,f,122</sup> none of which involving chiral phosphoric acid. On the other hand, when indoles having a stronger Michael acceptor (e.g. the ones bearing  $\alpha,\beta$ -unsaturated ketones) were employed, the nitro-Michael pathway prevails on the nitronate “quenching” affording the tricyclic target compounds **7** (Scheme 44, bottom).

**Undesired reaction pathway: nitronate “quenching”**



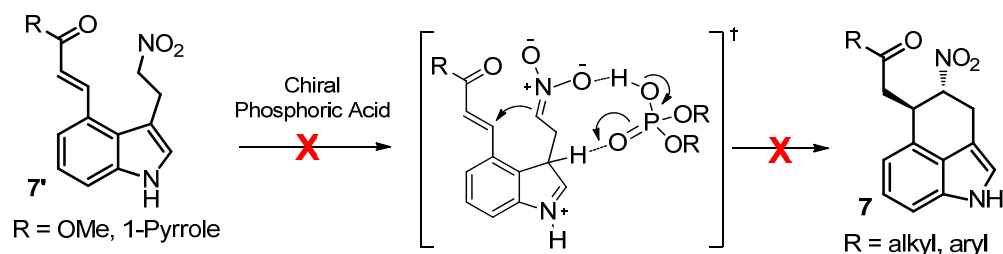
**Desired reaction pathway: nitro-Michael triggered by Friedel-Crafts**



**Scheme 44.** Comparison between nitronate “quenching” and nitro-Michael reaction pathway

For the same reason a phosphoric acid should be unable to resume undesired **7'** to target compound **7**. In principle, after the Friedel–Crafts step, the catalyst could detach and subsequently re-coordinate the non-cyclized **7'b**, promoting the nitro-Michael step. This

hypothesis was rejected since the treatment of **7'** with catalyst **9c** did not afford the tricyclic compound **7b**. This experimental evidence unequivocally remarks the predicted incapability of the catalyst to resume **7'** to **7b**, thus identifying the nitronate “quenching” as an irreversible process (Scheme 45).



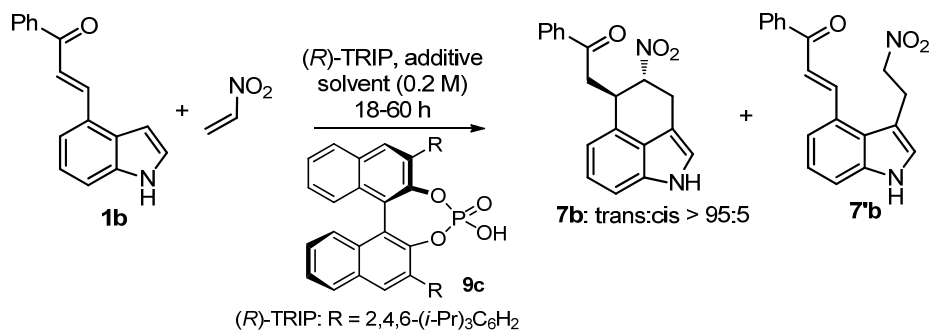
**Scheme 45.** Inability of chiral phosphoric acids to resume **7'** to **7**.

In order to rationalize the reaction pathway and get useful mechanistic insights, a computational study were carried out. The preliminary results will be discussed forward in this chapter (see § 4.4.2).

To optimize the catalytic asymmetric version of the cascade reaction, various reaction conditions have been screened, using **1b** as substrate in the reaction with nitroethene. Different solvents were initially tested (Table 8, entries 1-6), showing the necessity of employing non-coordinating solvents such as CH<sub>2</sub>Cl<sub>2</sub> or toluene in the reaction. Dichloromethane was selected for further optimization, since toluene did not efficiently solubilize substrate **1b**, and other experiments (not reported in Table 8) shown that this low solubilizing power resulted in even lower conversions with other substrates **1**. Lowering the catalyst loading to 5 mol% worsened the conversion, especially when the reaction was performed at 0 °C (Table 8, entries 7-8). Thus, drying agents were tested, in order to increase catalyst activity. Molecular sieves of different pore sizes, commonly used in phosphoric acid catalyzed reactions, were first employed (Table 8, entries 9-13). Although these drying agents did indeed increase the observed conversion, results turned out to be irreproducible, leading in some cases even to the preferential formation of the undesired side-product **7'b**. Thus, dry CH<sub>2</sub>Cl<sub>2</sub> (freshly distilled from CaH<sub>2</sub>) without additives was used as solvent, however without giving any substantial improvement (Table 8, entry 14). It was finally found that a different drying agent (MgSO<sub>4</sub>, pre-dried under vacuum at high temperature) allowed to reach full conversion in the desired product **7b**, even at 0 °C with 5 mol% catalyst loading, providing a small improvement in the enantiomeric excess of the product **7b** (Table 8, entry 15). Since a further lowering of

the catalyst loading gave insufficient conversion (Table 8, entry 16), conditions reported in entry 15 were taken as optimal to carry out the catalytic asymmetric domino reaction between **1** and nitroethene.

**Table 8.** Screening of reaction conditions between **1b** and nitroethene catalyzed by (*R*)-TRIP **PA3**<sup>a</sup>



Entry	Cat. mol%	Solvent	Additive	T (°C)	t (h)	Conv. (%) <sup>b</sup>	7b:7'b <sup>b</sup>	ee (%) <sup>c</sup>
1	10	CH <sub>2</sub> Cl <sub>2</sub>	-	RT	18	80	>9:1	95
2	10	CH <sub>2</sub> Cl <sub>2</sub>	-	RT	60	>90	>9:1	95
3	10	toluene	-	RT	60	87	>9:1	95
4	10	THF	-	RT	48	<10	-	-
5	10	EtOAc	-	RT	48	<10	-	-
6	10	CH <sub>3</sub> CN	-	RT	48	22	>9:1	nd
7	5	CH <sub>2</sub> Cl <sub>2</sub>	-	RT	48	83	>9:1	95
8	5	CH <sub>2</sub> Cl <sub>2</sub>	-	0	48	59	>9:1	96
9 <sup>d</sup>	5	CH <sub>2</sub> Cl <sub>2</sub>	4 Å MS	0	60	>90	>9:1	96
10 <sup>d</sup>	5	CH <sub>2</sub> Cl <sub>2</sub>	4 Å MS	0	60	>90	1:5	nd
11 <sup>d</sup>	5	CH <sub>2</sub> Cl <sub>2</sub>	5 Å MS	0	60	>90	>9:1	84
12 <sup>d</sup>	5	CH <sub>2</sub> Cl <sub>2</sub>	5 Å MS	0	60	>90	<1:9	-
13 <sup>d</sup>	5	CH <sub>2</sub> Cl <sub>2</sub>	3 Å MS	0	60	>90	<1:9	-
14	5	dry CH <sub>2</sub> Cl <sub>2</sub>	-	0	60	76	>9:1	97
15	5	dry CH <sub>2</sub> Cl <sub>2</sub>	MgSO <sub>4</sub>	0	60	>90	>9:1	97
16	2.5	dry CH <sub>2</sub> Cl <sub>2</sub>	MgSO <sub>4</sub>	0	60	70	>9:1	97

(a) Conditions: indole derivative **1b** (0.05 mmol), catalyst **9c** (*R*)-TRIP, nitroethene **2** (1 – 1.5 M solution in toluene, 0.075 mmol), solvent (0.25 mL). A single *trans*-diastereoisomer was observed in all cases (b) Determined by <sup>1</sup>H NMR spectroscopy on the crude mixture. (c) Determined by chiral stationary phase HPLC analysis. (d) Reaction turned out to be irreproducible, giving occasionally the open-chain product as well as the tricyclic one.

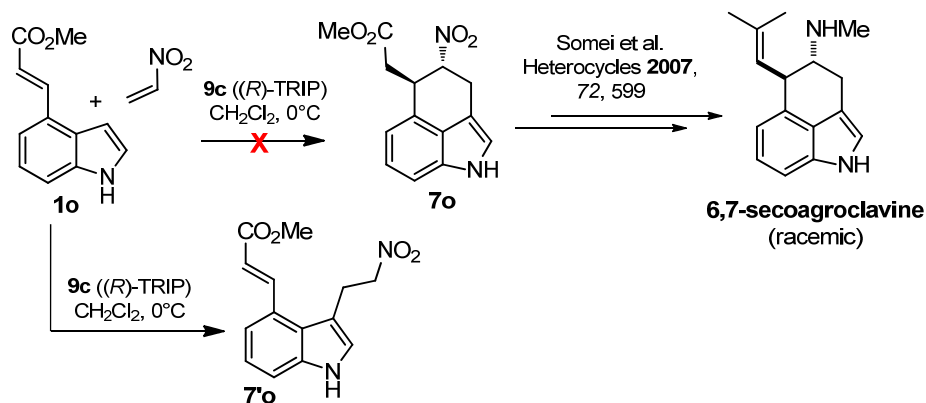
Having in hands a robust reaction protocol, the investigations on the generality of the reaction were undertaken, by varying the structure of indole substrates **1** both at the Michael acceptor and at the indole nucleus. As anticipated, the methyl ketone derivative **1a** gave only moderate enantioselectivity (Table 9, entry 1), whereas a wide range of aryl moieties either electron-rich or electron-poor, placed at the ketone portion of the molecule, were well tolerated, providing the corresponding products **7b-d,h,i** in outstanding yields, diastereo- and enantio- selectivities (Table 9, entries 2-6). However, the reaction scope was not restricted to the presence of an aryl group at the Michael acceptor. Substrate **1j** and **1k** bearing *tert*-butyl and dimethoxymethyl substituent, afforded the product **7j** and **7k** in excellent yields and enantioselectivities (Table 9, entries 7-8). Comparing these results with the ones obtained with **1a** it is possible to conclude that the steric hindrance at the acceptor is an essential feature in the achievement of good enantiocontrol in the reaction catalyzed by (*R*)-TRIP **9c**. The 2-methylindole derivative **1l** also performed very well in the reaction (Table 9, entry 9). Our organocatalytic protocol was found to proceed also with *N*-alkylated indoles **1m,n** which afforded tricyclic compound **7m,n** in very good enantioselectivities, despite slightly modified conditions were required to achieve good yields (Table 9, entries 10-11). This indicates that the N-H interaction is not involved in the stereodetermining step (see § 4.4.2). Indoles **1o** and **1p** having the weaker Michael acceptor group ester and *N*-acyl pyrrole gave, as expected, exclusively the open-chain adducts **7'o,p** (Table 9, entries 12-13). Curiously, these open-chain adducts were obtained in good yields only with molecular sieves were applied in the reaction.

**Table 9.** Scope of the catalytic enantioselective cascade reaction between indole derivatives **1** and nitroethene<sup>a</sup>

Entry	<b>1</b>	<b>R<sub>1</sub></b>	<b>R<sub>2</sub></b>	<b>R<sub>3</sub></b>	<b>7-Yield<sup>b</sup></b> (%)	<b>ee<sup>c</sup></b> (%)
1	<b>1a</b>	Me	H	H	<b>7a</b> -99	56
2	<b>1b</b>	Ph	H	H	<b>7b</b> -95	97
3	<b>1c</b>	4-BrC <sub>6</sub> H <sub>4</sub>	H	H	<b>7c</b> -99	97
4	<b>1d</b>	4-MeOC <sub>6</sub> H <sub>4</sub>	H	H	<b>7d</b> -91	97
5	<b>1h</b>	4-MeC <sub>6</sub> H <sub>4</sub>	H	H	<b>7h</b> -99	99
6	<b>1i</b>	2-naphthyl	H	H	<b>7i</b> -98	97
7	<b>1j</b>	<i>t</i> -Bu	H	H	<b>7j</b> -90	94
8 <sup>d</sup>	<b>1k</b>	CH(OMe) <sub>2</sub>	H	H	<b>7k</b> -90	98
9	<b>1l</b>	Ph	Me	H	<b>7l</b> -90	95
10 <sup>e</sup>	<b>1m</b>	Ph	H	Me	<b>7m</b> -75	96
11 <sup>f</sup>	<b>1n</b>	Ph	H	Allyl	<b>7n</b> -70	94
12 <sup>g</sup>	<b>1o</b>	OMe	H	H	<b>7'o</b> -62	-
13 <sup>g</sup>	<b>1p</b>	pyrrol-1-yl	H	H	<b>7'p</b> -94	-

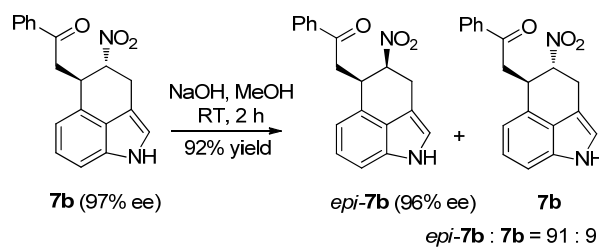
(a) Conditions: indole **1** (0.10 mmol), catalyst **9c** (*R*)-TRIP (0.005 mmol, 5 mol%), nitroethene (1.5 M toluene solution, 0.15 mmol), dry MgSO<sub>4</sub> (30 mg), CH<sub>2</sub>Cl<sub>2</sub> (0.30 mL), 0 °C, 60 h. A single *trans* diastereoisomer was obtained in all cases. (b) Isolated yield. (c) Determined by chiral stationary phase HPLC. (d) RT, 24 h. (e) 0.225 mmol of nitroethene were employed. (f) Reaction performed at RT using 7.5 mol% of **PA3** (*R*)-TRIP. (g) In the presence of 4 Å MS instead of MgSO<sub>4</sub>, RT, 24 h.

To increase the synthetic usefulness of our methodology, we thought to convert the ketone moiety of compounds **7** into a versatile ester. In fact, Somei and co-workers showed that compound *rac*-**7o**, bearing an ester group, can be converted into 6,7-secoagroclavine,<sup>94c</sup> a natural occurring ergot alkaloid isolated from *Claviceps purpurea*, after few synthetic steps. Unfortunately, our methodology was not able to directly furnish compound **7o**, as substrate **1o** gave exclusively the open-chain adduct **7'o** (Scheme 46 and Table 9, entry 12).

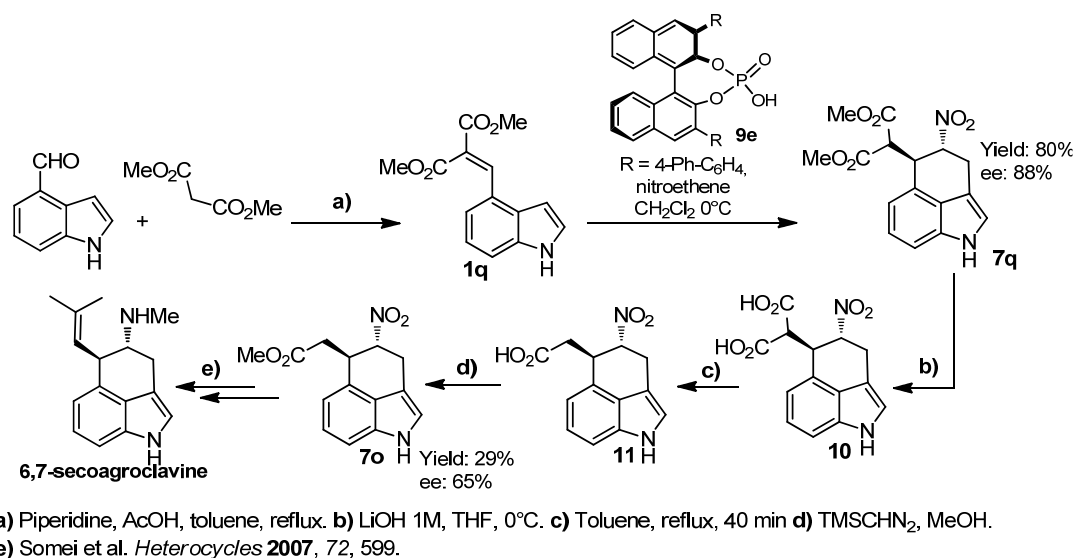


Scheme 46.

Thus, a less direct synthesis was attempted, identifying indole derivative **1q** as strategic precursor towards the obtainment of the 6,7-secoagroclavine (Scheme 48). Derivative **1q** was readily synthesized by means of Knoevenagel condensation between indole-4-carboxaldehyde and dimethyl malonate; subsequently **1q** was engaged in the organocatalytic reaction with nitroethene catalyzed by **9e**, which induced better enantioselectivity compared to (*R*)-TRIP **9c**, employed in all the reaction between **1** and nitroethene (Table 9). The ester moieties of tricyclic compound **7q** were hydrolyzed in the presence of LiOH, giving diacid **8**. Heat-promoted decarboxylation of **10** furnished the carboxylic acid **11** which was finally subjected to esterification in the presence of trimethylsilyldiazomethane and methanol, giving the target compound **7o** in 29% overall yield and moderate enantioselectivity. Unfortunately, during the hydrolysis of **7q**, we observed a partial loss of stereoinformation, possibly due to a retro-nitro-Michael reaction which takes place under basic conditions. For this reason, a thorough optimization of the hydrolysis step is currently under investigation by our research group. Although this multi-step synthetic procedure is far to be considered optimized, the obtainment of enantioenriched **7o** can be considered a promising result, paving the way for the first enantioselective formal total synthesis of 6,7-secoagroclavine. While the development of the above stated reaction sequence was in progress, we casually found that the treatment of **7b** with NaOH in MeOH caused equilibration favouring its *cis*-diastereoisomer *epi*-**7b** (Scheme 47). The more polar character of the *cis* isomer drove this epimerization in a polar medium as methanol. Importantly, equilibration

Scheme 47. Epimerization of **7b**

occurred through a selective epimerization at the  $\alpha$ -nitro stereogenic center, and not through a retro-nitro-Michael pathway that would have led to racemization. The present methodology is thus potentially able to furnish all four stereoisomers of the tricyclic benzo[*cd*]indole system in enantioenriched form.



**Scheme 48.** Synthetic sequence towards the formal total synthesis of enantioenriched 6,7-secoagroclavine.

#### 4.4.1. Determination of the absolute and relative configuration of compounds 7

As all the attempts to obtain suitable crystals for X-ray crystallography on the prepared compounds **7** were not successful, the relative and absolute configuration of these compounds were determined by a combination of conformational analysis and theoretical simulation of chiro-optical spectra.<sup>81</sup> Having in our hands a procedure that allow obtaining both diastereoisomers of the polycyclic compound **7b** and *epi-7b* (one directly by the Friedel–Craft–nitro–Michael reaction, one by selective epimerization of the  $\alpha$ -nitro carbon) it was decided to start the determination of the configuration by carrying out a conformational analysis on compound **7b**. Despite the rigidity of the heterocyclic indole core of compound **7b**, where almost all carbons of the polycyclic system lie on the same plane (Figure 36, drawn in blue) it was identified that these products could appear under various possible conformers. The main ones are depicted in Figure 36. Considering the plane where the indole lies, the  $\alpha$ -nitro carbon can be found either on the same side of the ketone (conformer #1), or on the opposite side (conformer #2).

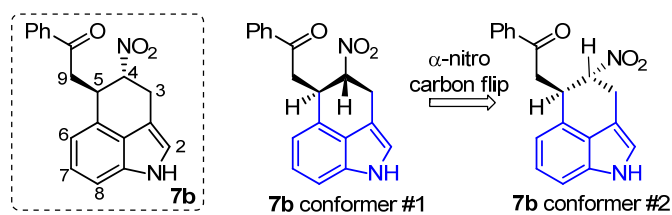


**Figure 36.** Most significant conformers of **7b**.

The relative stereochemistry of the two stereogenic centers at C4 and C5 of compound **7b** were determined by means of NMR spectroscopy, full assignment of the  $^1\text{H}$  and  $^{13}\text{C}$  spectra was preliminarily achieved by bi-dimensional experiment. Further DPGSE-NOE experiments<sup>80</sup> were acquired in order to assign the relative stereochemistry at C4 and C5. On saturation of the H-4 signal (Figure 37, trace a), NOE enhancements with similar intensity were observed for H-5, H-3', H-3'' and both the H-9 signals. On saturation of the H-5 signal (Figure 37, trace b), large NOEs were observed on H-4 and H-9 and only a small enhancement was observed for one of the H-3 hydrogens at 3.73 ppm (H-3'). The observed NOEs suggested that H-5 occupies a pseudo-equatorial position, otherwise a strong NOE should be observed on one of the H-3 signals, due to 1-3 diaxial relationship (the observation of the small NOE on H-3' is due to the presence of a second conformation with smaller population). As a confirmation, the saturation of the signal of H-3'' (in a pseudo-axial position) at 3.41 ppm yields a noticeable NOE enhancement on the H-9 hydrogens (Figure 37, trace d), that occupies a pseudo-axial position on the ring, too. All the NOE data thus agree to assign the  $4R^*,5R^*$  relative configuration (*i.e.* a *trans* relationship).

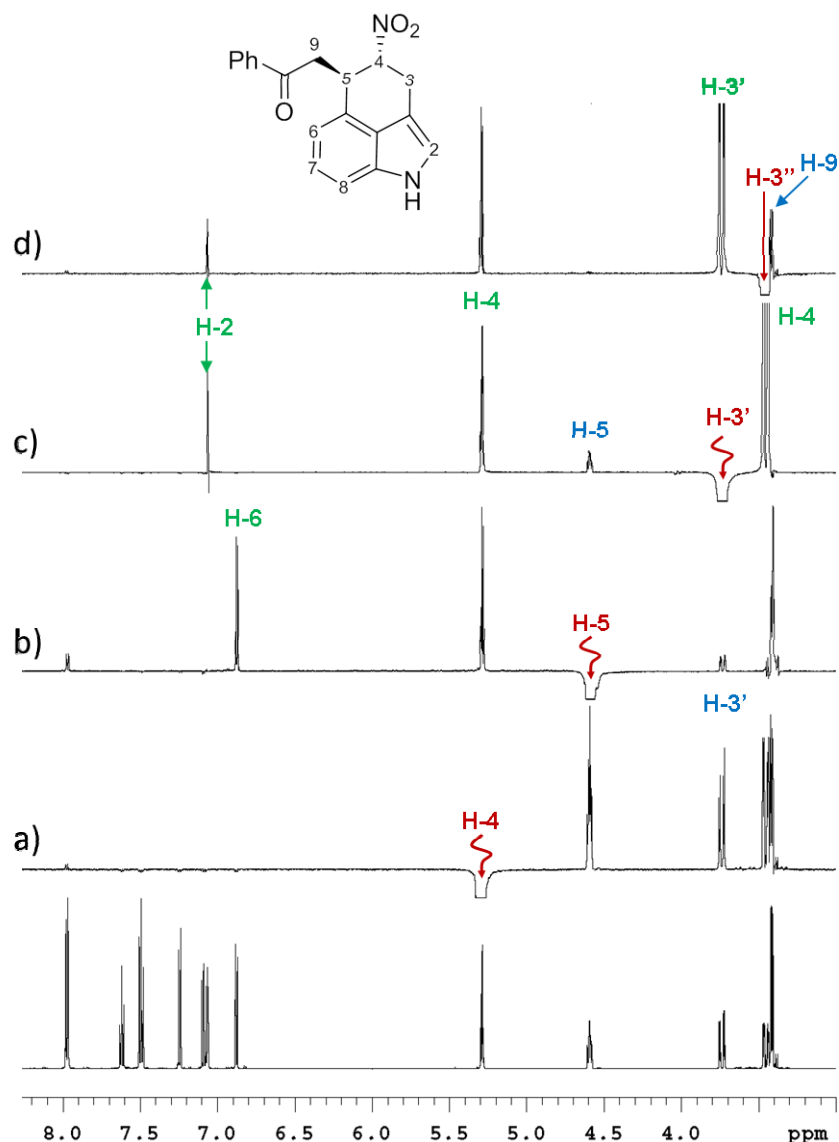


**Figure 37.** DPGSE-NOE spectra of **7b** (600 MHz in  $\text{CDCl}_3$ ,  $+25^\circ\text{C}$ ). Bottom:  $^1\text{H}$ -NMR control spectrum. Traces a-d: red labels indicate the saturation point. Green labels indicate “control” NOEs, that have to be observed to assure reliable results. Blue labels indicate diagnostic NOEs.

The determination of the absolute configuration of **7b** was instead obtained by comparing the experimental electronic circular dichroism (ECD) spectrum with the computed one. Preliminary tests were carried out in order to determine the proper distribution ratio of the different conformers of **7b**. After DFT minimization, four conformations were found to be the most stable, all of them showing the same shape of the six membered ring, corresponding to a pseudo boat conformation, with the nitro group out of the plane. Within each pair, the conformations are different in the disposition of the  $\text{CH}_2\text{COPh}$  moiety. Having in hand the relative configuration and suitable conformational analysis supporting the preferred conformations, the assignment of the absolute configuration was pursued. Simulations of the experimental ECD spectrum were performed, by using different calculation methods and the averaged conformer ratio.<sup>81</sup> As shown in Figure 38, the simulated spectra match very well

the Cotton effects at 250, 230 and 200 nm when the *4R*, *5R* absolute configuration was assumed in the calculations, therefore the absolute configuration of compound **7b** was assigned as *4R 5R*.

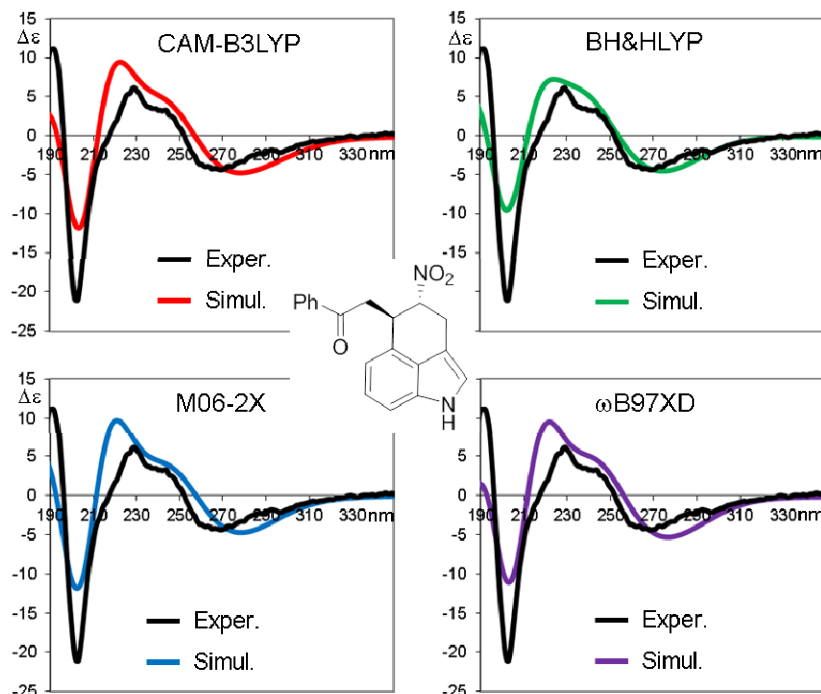


**Figure 38.** Simulations of the experimental ECD spectrum of **7b**. For each quarter, the black line correspond to the experimental spectrum (acetonitrile solution,  $1.1 \cdot 10^{-4}$  M, 0.2 cm path length,  $\square \square$  in  $\text{Mol L}^{-1} \text{cm}^{-1}$ ) and the colored line to the TD-DFT simulation (6-311++G(2d,p) basis set). The simulated spectra were vertically scaled and red-shifted by 7-14 nm to get the best match with the experimental spectrum. All the simulations are for the *4R*, *5R* absolute configuration.

As a cross check, NOE spectra and ECD analysis were carried out for the *cis*-diastereoisomer *epi-7b*, confirming the epimerization of compound **7b** occurred with inversion of stereochemistry at carbon bearing the nitro group.

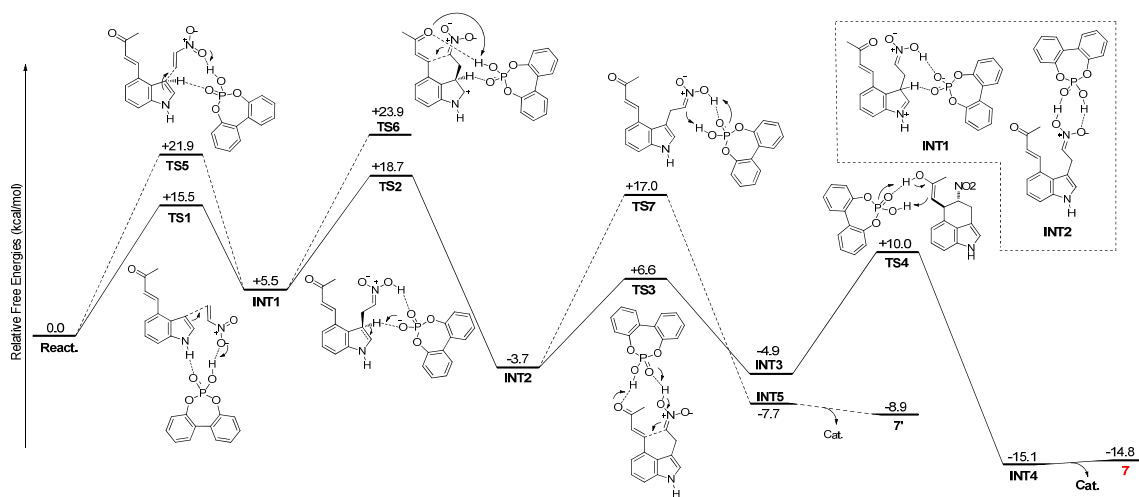
In conclusion, having established the *4R*, *5R* absolute configuration for compound **7b**, we assumed that all other compound **7** presented the same relative and absolute configuration, being afforded by the same reaction pathway.

#### 4.4.2. Mechanistic proposal for the formation of compounds **7**

As highlighted before, the formation of compounds **7** with chiral phosphoric acid is quite intriguing. To get insight about the actual pathway followed by this rather unusual acid catalyzed transformation, we turned to a computational approach. Even though a computational study on phosphoric acid catalyzed Friedel–Crafts addition of indoles to nitroalkanes had been reported,<sup>123</sup> it simply focused on the C-C bond forming step,

neglecting subsequent proton transfer events (*i.e.* rearomatization and nitronate protonation), which are crucial in this cascade process. We performed DFT calculations using the B3LYP-D functional, studying the full catalytic cycle for the reaction between nitroethene and the methyl ketone derivative **1a**, chosen as a model of substrates bearing a ketone Michael acceptor. We used the phosphoric acid derived from [1,1'-biphenyl]-2,2'-diol as a model of BINOL-derived chiral phosphoric acids (Scheme 49). First, two possibilities were found for the initial nucleophilic attack of indole on nitroethene. In the first case (**TS1**) the catalyst coordinates both the nitro-group and the indole N-H. In the second (**TS5**), it coordinates the nitro-group and the C3-H of indole. In both cases, the protonation of the nitro-group occurs concertedly with the expected C-C bond formation. The reaction occurring through **TS1** is favored by 6.4 kcal/mol over **TS5**, in line with the previously determined<sup>123</sup> pathway followed in related Friedel–Crafts processes. Importantly, both pathways lead ultimately to the same intermediate **INT1**, from which a TS (**TS6**) for the cyclization was located. However, one proton had to be manually shifted from the protonated nitro-group to the catalyst, in order to allow the protonation of the electrophilic ketone during the cyclization. Alternatively, we have found that the phosphate catalyst can promote re-aromatization of indole through C3-deprotonation (**TS2**) with a much lower energy barrier (18.7 vs 23.9 kcal/mol). This step does not occur through a H-relay process releasing the catalyst but leads instead to intermediate **INT2**. Subsequent nitro-Michael addition can occur with the catalyst coordinating both the nitro-group and the carbonyl (**TS3**), and is associated to a low energy barrier (10.3 kcal/mol). The deprotonation of the nitro-group and the protonation of the carbonyl occur concertedly with the *trans*-selective C-C bond formation. After cyclization through **TS3**, a keto-enol tautomerization is required to generate final product **7**. We have found that the catalyst can also promote this process through **TS4**. As discussed above, the formation of cyclized product **7** is in competition with the formation of side-product **7'**. This can be formed if **INT2** evolves through a nitronic acid-nitro tautomerization, instead of the cyclization. We have found that this tautomerization, when promoted by the catalyst, has a surprisingly high energy barrier of 20.7 kcal/mol (**TS7**), thus being 10.4 kcal/mol higher in energy than the TS for the cyclization (**TS3**). These results are in agreement with the exclusive formation of product **7** in the reaction on ketone-substituted indole **1b**, providing a realistic reaction picture fully justifying the observed experimental results. The reaction occurs through a nucleophilic attack of the indole **1** on nitroethene, followed by a re-aromatization occurring before the cyclization and ensuing keto-enol

tautomerism. The catalyst is involved in all steps, including the stereodetermining cyclization event, accounting for the observation of enantioenrichment in the product **7b** when an enantiopure catalyst was used. Thanks to the formation of a relatively stable catalyst-coordinated nitronic acid intermediate **INT2** and the high energy barrier associated with the tautomerisation through **TS7**, cyclisation to the desired products **7** is indeed possible, provided that a highly reactive Michael acceptor is employed (*i.e.* **TS3** energy is sufficiently low). One final consideration must be stressed on **TS4**: the free energy associated to this transition state is quite unexpectedly high for an acidic promoted keto-enol tautomerization. From this point of view, further computational investigations are currently under development.



**Scheme 49.** Free energy profile for the formation of products **7** and **7'** from the reaction between indole derivative **1a** and nitroethene. **TS1-7** are sketched on the graph.

Remarkably, this computed reaction pathway accounts for some unexpected experimental evidences. For instance, the irreproducibility of the reaction when molecular sieves were employed could be justify by considering molecular sieves able to lower the energy barrier between **INT2** and **INT5**. It must be speculated that molecular sieves have a role which goes beyond simple dehydrating agents; indeed, we hypothesize that molecular sieves, rather than lowering the energy of **TS7**, serve as external proton source, providing an alternative reaction pathway. On the other hand, the productively engagement of *N*-substituted indoles **1m,n** was rather unexpected. In contrast with simpler Friedel–Crafts reaction,<sup>123,124</sup> wherein the coordination to the indole N-H is necessary for enantioselectivity, the computed pathway of this cascade transformation predicts that this interaction is absent in the stereodetermining step (Scheme 49, **TS3**),

while it is useful for reactivity as it is related to the rate determining step (Scheme 49, TS2 vs TS5).

## 4.5. Experimental details

### 4.5.1. General methods and materials

$^1\text{H}$ ,  $^{13}\text{C}$  NMR spectra were recorded on a Varian AS 300, 400 or 600 spectrometer. Chemical shifts ( $\delta$ ) are reported in ppm relative to residual solvent signals for  $^1\text{H}$  and  $^{13}\text{C}$  NMR.<sup>84</sup>  $^{13}\text{C}$  NMR spectra were acquired with  $^1\text{H}$  broad band decoupled mode. Mass spectra were recorded on a micromass LCT spectrometer using electrospray (ES) ionisation techniques. Optical rotations were measured on a Perkin-Elmer 241 polarimeter. The enantiomeric excess (ee) of the products was determined by chiral stationary phase HPLC, using a UV detector operating at 254 nm.

Analytical grade solvents and commercially available reagents were used as received, unless otherwise stated. Chromatographic purifications were performed using 70-230 mesh silica. Analytical grade solvents and commercially available reagents were used as received, unless otherwise stated. 1H-Indole-4-carbaldehyde was purchased from Apollo Scientific. 2-Methyl-1H-indole-4-carbaldehyde,<sup>125</sup> 1-methyl-1H-indole-4-carbaldehyde<sup>126</sup> and 1-allyl-1H-indole-4-carbaldehyde<sup>126</sup> were prepared according to literature procedures. Indole substrates **1a-n** were synthesized through Wittig olefination, detailed as follows: the phosphonium salts, unless commercially available, were obtained by refluxing an equimolar mixture of triphenyl phosphine and the appropriate alkyl halides for a few hours in toluene or acetonitrile, and collected by filtration; the phosphorous ylides were then obtained by pouring a  $\text{CH}_2\text{Cl}_2$  solution of the phosphonium salts in a separating funnel containing 2N aq. NaOH; after five minutes of vigorous shaking, the organic phase was collected, dried over  $\text{MgSO}_4$ , filtered and evaporated affording the ylides; finally, the Wittig olefination between the indole-4-carbaldehyde and the appropriate phosphorous ylide<sup>94c</sup> was carried out in a toluene/1,4-dioxane mixture (8:2), at reflux temperature for 18-48 h. Indoles **1q** was synthesized through Knoevenagel condensation between indole-4-carbaldehyde and dimethyl malonate, according to a reported procedure.<sup>127</sup> Products **1a-q** were purified by column chromatography and obtained as pure *E*-isomers. Acrolein **2a** was distilled before use, cinnamaldehyde **2c** was distilled under vacuum (11 mbar, bp = 125 °C) before use, crotonaldehyde **2b** was purchased from Sigma-Aldrich as “predominantly trans” with assay >99% and was used as received. Nitroethene was obtained by dehydration of 2-nitroethanol with phthalic anhydride, according to a literature procedure;<sup>107a</sup> the nitroethene’s toluene solution of known concentration can be stored in a freezer (-25 °C) for several months without apparent degradation/changes in concentration, as checked by  $^1\text{H}$  NMR. Toluene and 1,4-Dioxane were passed through a short pad of basic alumina

before use; dichloromethane was freshly distilled over CaH<sub>2</sub>. Racemic samples of compounds **3a-g** were prepared using racemic ( $\pm$ )- $\alpha,\alpha$ -bis[3,5-bis(trifluoromethyl)phenyl]-2-pyrrolidinemethanol trimethylsilyl ether **4a** as the catalyst, in 1,4-dioxane at RT for 18-60 h. Racemic samples of compounds **3h-j** were prepared using racemic ( $\pm$ )-5-benzyl-2-tert-butyl-3-methyl-4-imidazolidinone **4d** as catalyst, in a CH<sub>2</sub>Cl<sub>2</sub>/*i*-PrOH (8:2) mixture at RT for 18-60 h. Chiral phosphoric acid **9c** (*R*)-TRIP was prepared according to a reported procedure.<sup>71a</sup> Racemic **5** was obtained by employing racemic **3a** in the oxidation reaction. Racemic *cis*-**6** for HPLC analysis was obtained by mixing a nearly equimolar mixture of the two enantiomers, obtained from the two enantiomeric products **3a** and *ent*-**3a** using L- and D-proline, respectively, in the Robinson annulation reaction. Racemic samples of **7a-d**, **7h-q** were prepared using [1,1'-biphenyl]-2,2'-diyl hydrogenphosphate as catalyst in CH<sub>2</sub>Cl<sub>2</sub> at RT for 60h. Racemic **10**, **11**, **7o** were prepared using *rac*-**7q** as starting material.

#### 4.5.2. General procedures

##### *General procedure for the catalytic asymmetric reaction of indoles 1 with acrolein 2a*

The following procedure was applied in the synthesis of compounds **3a-g**. To a vial equipped with a magnetic stirring bar, MgSO<sub>4</sub> (50 mg) was added, followed by the indole derivative **1a-g** (0.10 mmol), 1,4-dioxane (0.300 mL), catalyst **4b** (0.010 mmol) and trifluoroacetic acid (8  $\mu$ L of a 1.33 M solution of TFA in 1,4-dioxane, 0.010 mmol). The mixture was stirred for five minutes then acrolein **2a** (0.25 mmol) was added in one portion. After 18 h, the reaction mixture was filtered through a plug of silica gel, and the plug was washed with Et<sub>2</sub>O (4x). After removal of solvents, the reaction crude was analysed by <sup>1</sup>H NMR spectroscopy to determine the diastereomeric ratio of the cycloadducts. Finally, the residue was purified by chromatography on silica gel (*n*-hexane/EtOAc mixtures).

##### *General procedure for the catalytic asymmetric reaction of indole 1g with $\beta$ -substituted enals 2b-d*

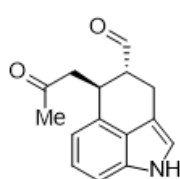
The following procedure was applied in the synthesis of compounds **3h-j**. To a vial equipped with a magnetic stirring bar, MgSO<sub>4</sub> (50 mg) was added, followed by the catalyst **4d** (0.020 mmol), a CH<sub>2</sub>Cl<sub>2</sub>/*i*-PrOH mixture (8:2, 0.200 mL) and trifluoroacetic acid (16  $\mu$ L of a 1.33 M solution of TFA in CH<sub>2</sub>Cl<sub>2</sub>/*i*-PrOH 8:2, 0.020 mmol). The vial was placed in a bath at the desired temperature, stirred for five minutes, then the  $\alpha,\beta$ -unsaturated aldehyde **2b-d** (0.25 mmol) was added in one portion. After stirring for additional five minutes, the indole derivative **1g** (0.10 mmol) was added. The resulting suspension was stirred at the same temperature for the appropriate time, then it was filtered through a plug of silica gel, and the plug was washed with Et<sub>2</sub>O (4x). After

removal of the solvents, the reaction crude was analyzed by  $^1\text{H}$  NMR spectroscopy to determine the diastereomeric ratio of the cycloadducts. Finally, the residue was purified by chromatography on silica gel (*n*-hexane/EtOAc mixtures).

*General procedure for the catalytic asymmetric reaction of indole 1 with nitroethene*

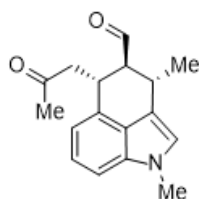
The following procedure was applied in the synthesis of compounds **7a-d**, **7h-n** and **7q**. To a Schlenk tube equipped with a magnetic stirring bar,  $\text{MgSO}_4$  (30 mg) was added. This salt was carefully thermally activated under vacuum for 5 minutes and then allowed to cool to RT. After backfilling the Schlenk tube with nitrogen, the appropriate indole derivative **1** (0.10 mmol) was added, followed by the (*R*)-TRIP catalyst **9c** (3.8 mg, 0.0050 mmol, 5.0 mol%), and  $\text{CH}_2\text{Cl}_2$  (300  $\mu\text{L}$ ). The mixture was cooled to 0  $^\circ\text{C}$  and allowed to stir for 5 minutes, then nitroethene **2** (0.15 mmol,  $x$   $\mu\text{L}$  of a 1-1.5 M toluene solution) was added in one portion. The mixture was then stirred at this temperature for 60 h, then filtered through a short plug of silica gel, and the plug washed with  $\text{Et}_2\text{O}$  (4x). After concentration of the solvents, the residue was analysed by  $^1\text{H}$  NMR spectroscopy to determine the diastereomeric ratio of the adducts **7**. Finally, the residue was purified by chromatography on silica gel, affording pure products **7**.

**(4*R*,5*S*)-5-(2-Oxopropyl)-1,3,4,5-tetrahydrobenzo[*cd*]indole-4-carbaldehyde (3a)**



Following the general procedure, the title compound was obtained as a yellow solid in 76% yield after chromatography on silica gel (*n*-hexane/EtOAc 1:1). The diastereomeric ratio was evaluated by  $^1\text{H}$  NMR of the crude mixture and was found to be >20:1. The enantiomeric excess of the product was determined by chiral stationary phase HPLC (AD-H, *n*-hexane/*i*-PrOH 80:20, 0.75 mL/min,  $\lambda = 254$  nm,  $t_{\text{maj}} = 11.9$  min,  $t_{\text{min}} = 13.2$  min, 98% ee).  $[\alpha]_{\text{D}}^{22} = -73$   $^\circ$  ( $c = 0.60$  in  $\text{CHCl}_3$ );  $^1\text{H}$  NMR ( $\text{CDCl}_3$ , 400 MHz)  $\delta = 9.53$  (s, 1H), 8.12 (br s, 1H), 7.15-7.08 (m, 2H), 6.93-6.87 (m, 2H), 4.16-4.10 (m, 1H), 3.37 (dd,  $J = 15.9, 3.0$  Hz, 1H), 3.00 (ddd,  $J = 15.9, 5.2, 1.5$  Hz, 1H), 2.93-2.89 (m, 1H), 2.84 (dd,  $J = 17.5, 6.5$  Hz, 1H), 2.77 (dd,  $J = 17.3, 7.3$  Hz, 1H), 2.12 (s, 3H);  $^{13}\text{C}$  NMR ( $\text{CDCl}_3$ , 100 MHz)  $\delta = 207.3, 204.1, 133.9, 131.1, 126.0, 123.0, 118.8, 116.4, 109.2, 109.0, 50.9, 49.0, 32.9, 30.7, 18.9$ ; MS (EI)  $m/z$ : 241 ( $\text{M}^+$ ).

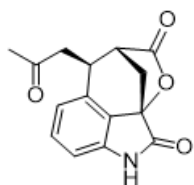
**(3*S*,4*S*,5*R*)-1,3-Dimethyl-5-(2-oxopropyl)-1,3,4,5-tetrahydrobenzo[*cd*]indole-4-carbaldehyde (3h)**



Following the general procedure and performing the reaction at 30  $^\circ\text{C}$  for 65 h, the title compound was obtained as a yellow solid in 71% yield after chromatography on silica gel (*n*-hexane/EtOAc 3:2). The diastereomeric ratio was evaluated by  $^1\text{H}$  NMR of the crude mixture and was found to be >20:1. The enantiomeric excess of the product was determined by chiral stationary phase HPLC (AD-H, *n*-hexane/*i*-PrOH

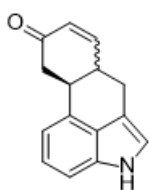
80:20, 0.75 mL/min,  $\lambda = 254$  nm,  $t_{\text{maj}} = 13.2$  min,  $t_{\text{min}} = 12.0$  min, 86% ee).  $[\alpha]_{\text{D}}^{22} = +30^{\circ}$  ( $c = 0.333$  in  $\text{CHCl}_3$ )  $^1\text{H}$  NMR ( $\text{CDCl}_3$ , 400 MHz)  $\delta = 9.66$  (d,  $J = 4.6$  Hz, 1H), 7.19-7.11 (m, 2H), 6.80 (d,  $J = 1.6$  Hz, 1H), 6.76 (d,  $J = 6.8$  Hz, 1H), 4.10 (dt,  $J = 5.7$ ; 9.1 Hz, 1H), 3.77 (s, 3H), 3.57-3.49 (m, 1H), 3.09 (dd,  $J = 18.3$ ; 5.9 Hz, 1H), 2.86 (dd,  $J = 18.3$ ; 5.9 Hz, 1H), 2.36 (td,  $J = 4.6$ ; 9.1 Hz, 1H), 2.24 (s, 3H), 1.36 (d,  $J = 6.9$  Hz, 3H);  $^{13}\text{C}$  NMR ( $\text{CDCl}_3$ , 100 MHz)  $\delta = 207.4$ , 205.3, 134.8, 131.4, 125.8, 122.6, 115.1, 113.9, 107.2, 61.3, 46.5, 32.9, 32.8, 30.5, 28.4, 19.4; MS (EI)  $m/z$ : 269 ( $\text{M}^+$ ).

**(2a*S*,5*R*,6*S*)-6-(2-Oxopropyl)-5,6-dihydro-1*H*-2a,5-methanooxepino[2,3,4-*cd*]indole-2,4-dione (5)**



To a round bottomed flask equipped with a magnetic stirring bar, compound **3a** (0.07 mmol) was dissolved in *tert*-butyl alcohol (2.5 mL) and 2-methyl-2-butene (470  $\mu\text{L}$ ) and subsequently stirred for a few minutes. To this solution was added an aqueous solution of  $\text{NaH}_2\text{PO}_4$  (120  $\mu\text{L}$  of a 0.833 M solution, 0.10 mmol) and  $\text{NaClO}_2$  (80  $\mu\text{L}$  of a 1.11 M solution, 0.09 mmol). The mixture was stirred at room temperature for 90 minutes, then the organic solvents were removed by concentrating in vacuo. The residue was diluted with 2 mL of water, then the mixture was extracted with EtOAc twice. After drying over  $\text{MgSO}_4$ , filtration and evaporation of the solvents, the crude product was purified by column chromatography (*n*-hexane / EtOAc 1 : 2) to give the title compound as a brown solid in 56% yield. A single diastereoisomer was observed in the crude mixture, thus indicating that epimerisation did not occur. The enantiomeric excess of the product was determined by chiral stationary phase HPLC (AD-H, *n*-hexane/*i*-PrOH 70:30, 0.75 mL/min,  $\lambda = 254$  nm,  $t_{\text{maj}} = 11.3$  min,  $t_{\text{min}} = 12.2$  min, 97% ee) a single enantiomer was recognized in the HPLC trace thus indicating that racemisation did not occur.  $^1\text{H}$  NMR ( $\text{CD}_2\text{Cl}_2$ , 600 MHz)  $\delta = 7.51$  (br s, 1H), 7.21 (t,  $J = 8.3$  Hz, 1H), 6.77 (d,  $J = 8.2$  Hz, 1H), 6.68 (d,  $J = 8.2$  Hz, 1H), 3.71 (dd,  $J = 2.7$ ; 8.2 Hz 1H), 3.08 (dd,  $J = 2.2$ , 5.4 Hz, 1H), 2.80 (dd,  $J = 4.8$ ; 18.4 Hz, 1 H) 2.68-2.61 (m, 2H), 2.12 (s, 3H); 2.05-2.01 (m, 1H)  $^{13}\text{C}$  NMR ( $\text{CD}_2\text{Cl}_2$ , 100 MHz)  $\delta = 204.6$ , 175.0, 169.9, 137.6, 134.2, 131.4, 125.9, 120.4, 107.7, 78.0, 47.1, 43.9, 33.1, 31.1, 29.2;  $^{13}\text{C}$  NMR DEPT 1.5 ( $\text{CDCl}_3$ , 100 MHz)  $\delta = 131.4$  (CH), 120.4 (CH), 107.7 (CH), 47.1 ( $\text{CH}_2$ ), 43.9 (CH), 33.1 (CH), 31.1 ( $\text{CH}_2$ ), 29.2 ( $\text{CH}_3$ );  $[\alpha]_{\text{D}}^{22} = +123^{\circ}$  ( $c = 0.100$  in  $\text{CH}_3\text{CN}$ ); ESIMS: 294 [ $\text{M} + \text{Na}^+$ ].

**(6a*S*,10a*S*)-6,6a,10,10a-Tetrahydronaphtho[3,2,1-*cd*]indol-9(4*H*)-one and (6a*R*,10a*S*)-6,6a,10,10a-tetrahydronaphtho[3,2,1-*cd*]indol-9(4*H*)-one (6)**

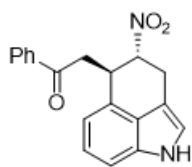


To a round bottomed flask equipped with a magnetic stirring bar, L-proline (0.07 mmol) was added, followed by 1 mL of acetonitrile, and finally  $\text{HClO}_4$  was added in one portion (38  $\mu\text{L}$  of 1.80 M solution of  $\text{HClO}_4$  in acetonitrile, 0.07 mmol) and subsequently stirred for few minutes to allow the complete solubilisation of L-proline. To this solution was added compound **3a** (0.21 mmol) and the mixture was stirred for 16 hours at 55  $^{\circ}\text{C}$ , then it was

filtered on plug of silica gel and the plug was washed several times with DCM and Et<sub>2</sub>O. The diastereomeric ratio was evaluated by <sup>1</sup>H NMR of the crude mixture and was found to be 59:41; the yield was also determined by <sup>1</sup>H NMR of the crude mixture by using 1,1,2,2-tetrachloroethane as internal standard and was found to be 64% referred to both diastereoisomers. The diastereoisomers were isolated by means of semi-preparative HPLC on a C18 column (Phenomenex® Synergi Hydro-RP) using Acetonitrile/H<sub>2</sub>O 60:40.

The minor diastereoisomer was obtained in analytically pure form and was fully characterized. The enantiomeric excess of this product was determined by chiral stationary phase HPLC (AD-H, *n*-hexane/*i*-PrOH 80:20, 0.75 mL/min, λ = 254 nm, t<sub>maj</sub> = 12.5 min, t<sub>min</sub> = 13.7 min, 99% ee), a single enantiomer was recognized in the HPLC trace thus indicating that racemisation did not occur. Full assignment of the <sup>1</sup>H and <sup>13</sup>C spectra was achieved by bi-dimensional experiments (gHSQC, gHMBC and gCOSY taken in CD<sub>3</sub>CN solutions at 45 °C) that confirms the proposed structure for compound *cis*-6. <sup>1</sup>H NMR (CD<sub>3</sub>CN, 400 MHz, 60 °C) δ = 8.93 (br s, 1H), 7.23 (d, J = 7.8 Hz, 1H), 7.12 (t, J = 7.8 Hz, 1H), 7.05 (dd, J = 3.4, 9.8 Hz, 1H), 7.00 (br s, 1H), 6.89 (d, J = 7.5 Hz, 1H), 5.88 (d, J = 10.4 Hz, 1H), 3.78-3.71 (m, 1H), 3.19 (dd, J = 5.0, 15.2 Hz, 1H), 3.10 (br s, 1H), 2.95-2.69 (m, 3H); <sup>13</sup>C NMR (CD<sub>3</sub>CN, 100 MHz, 45 °C) δ = 203.8, 154.5, 134.2, 132.0, 126.5, 122.6, 118.5, 115.3, 111.1, 103.0, 41.6, 37.0, 37.3, 29.4; [α]<sub>D</sub><sup>22</sup> = +20° (c = 0.35 in CH<sub>2</sub>Cl<sub>2</sub>); ESIMS: 246 [M + Na<sup>+</sup>].

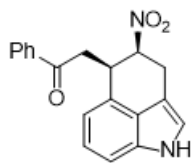
#### 1-((4*R*,5*R*)-4-Nitro-1,3,4,5-tetrahydrobenzo[*cd*]indol-5-yl)-1-phenylethanone (7b)



Following the general procedure, the title compound was obtained as a white solid in 95% yield, after chromatography on silica gel (CH<sub>2</sub>Cl<sub>2</sub>).

<sup>1</sup>H NMR analysis of the crude mixture showed the presence of a single diastereoisomer. The enantiomeric excess of the product was determined by chiral stationary phase HPLC (Chiralpak AS column, *n*-hexane/*i*-PrOH 80:20, flow 0.75 mL/min, λ 254 nm, t<sub>maj</sub> = 33.6 min, t<sub>min</sub> = 28.6 min, 97% ee). <sup>1</sup>H NMR (CDCl<sub>3</sub>, 400 MHz) δ = 8.06 (br s, 1H), 7.96-7.93 (m, 2H), 7.62-7.56 (m, 1H), 7.50-7.44 (m, 2H), 7.21 (br d, J = 8.0 Hz, 1H), 7.14 (br t, J = 8.0 Hz, 1H), 6.96-6.93 (m, 1H), 6.83 (d, J = 7.1 Hz, 1H), 5.24 (dt, J<sub>t</sub> = 5.8 Hz, J<sub>d</sub> = 4.4 Hz, 1H), 4.65 (q, J = 6.2 Hz, 1H), 3.79 (dd, J = 16.0, 5.7 Hz, 1H), 3.43 (dd, J = 18.1, 6.0 Hz, 1H), 3.40 (ddd, J = 16.2, 4.3, 1.1 Hz, 1H), 3.33 (dd, J = 18.1, 7.1 Hz, 1H); <sup>13</sup>C NMR (CDCl<sub>3</sub>, 100 MHz) δ = 197.2, 136.5, 133.7, 133.5, 129.6, 128.8, 128.1, 124.8, 123.6, 118.9, 116.0, 109.5, 107.3, 85.4, 41.9, 36.9, 25.1; [α]<sub>D</sub><sup>25</sup> = -107 (c = 0.586 in CH<sub>2</sub>Cl<sub>2</sub>); ESIMS = 343 (M + Na<sup>+</sup>).

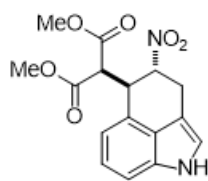
#### (1-((4*S*,5*R*)-4-nitro-1,3,4,5-tetrahydrobenzo[*cd*]indol-5-yl)-1-phenylethanone) (*epi*-7b)



In a vial equipped with a magnetic stirring bar, compound **3a** (0.072 mmol, 97% ee) was dissolved in MeOH (200  $\mu$ L), and the resulting solution cooled to 0  $^{\circ}$ C with stirring. A NaOH solution in MeOH (268  $\mu$ L of a solution prepared dissolving 96 mg NaOH in 1.5 mL of MeOH, 0.43 mmol, 6 equiv.) was added, the reaction allowed to warm to RT.

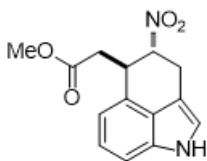
After 2 h stirring, it was judged by TLC (*n*-hexane/Et<sub>2</sub>O 3/7) that the diastereomeric mixture had reached the equilibrium composition. The mixture was diluted with Et<sub>2</sub>O, sat. aq. NH<sub>4</sub>Cl was added, the phases separated, and the aqueous phase extracted with EtOAc (3 x). The combined organic extracts were dried by filtration on a Celite<sup>®</sup> plug, evaporated and analysed by <sup>1</sup>H NMR spectroscopy, which showed a 91:9 diastereomeric ratio favouring the *cis*-isomer. The product was purified by chromatography on silica gel (*n*-hexane/EtOAc 35:65), affording an analytically pure sample of the title compound as a white solid accompanied by its diastereomeric mixture with the starting **3a** (overall 92% yield). The enantiomeric excess of the product was determined by chiral stationary phase HPLC (Chiralpak ADH column, *n*-hexane/*i*-PrOH 80:20, flow 0.75 mL/min,  $\lambda$  254 nm,  $t_{\text{maj}}$  = 23.2 min,  $t_{\text{min}}$  = 20.4 min, 96% ee), showing that epimerisation occurred without racemisation, under these conditions. Optical rotation was not measured due to the very small amount of pure compound available. <sup>1</sup>H NMR (acetone-*d*<sub>6</sub>, 600 MHz)  $\delta$  = 10.07 (br s, 1H), 8.01 (br d, *J* = 8.3 Hz, 1H), 7.60 (br t, *J* = 8.3 Hz, 1H), 7.49 (br t, *J* = 8.4 Hz, 1H), 7.21 (d, *J* = 8.3 Hz, 1H), 7.16 (br s, 1H), 7.02 (br t, *J* = 8.3 Hz, 1H), 6.86 (br d, *J* = 8.3 Hz, 1H), 5.32 (br quint, *J* = 4.0 Hz, 1H), 4.60 (br quint, *J* = 4.0 Hz, 1H), 3.67 (ddd, *J* = 15.9, 9.2, 1.7 Hz, 1H), 3.62 (br dd, *J* = 15.5, 7.4 Hz, 1H), 3.59 (dd, *J* = 15.9, 4.9 Hz, 1H), 3.36 (br dd, *J* = 17.6, 3.9 Hz, 1H); <sup>13</sup>C NMR (acetone-*d*<sub>6</sub>, 150 MHz)  $\delta$  = 198.7, 138.7, 135.6, 134.6, 131.9, 130.2, 129.6, 126.9, 124.0, 121.1, 117.0, 111.2, 108.9, 87.0, 41.0, 38.5, 31.1, 26.1; ESIMS = 343 (M + Na<sup>+</sup>).

#### Dimethyl 2-((4*R*,5*R*)-4-nitro-1,3,4,5-tetrahydrobenzo[*cd*]indol-5-yl)malonate (**7q**)



Following the general procedure, but using 10 mol% of catalyst **9e** and two equiv. of nitroethene, the title compound was obtained as a white solid in 80% yield, after chromatography on silica gel (CH<sub>2</sub>Cl<sub>2</sub>). <sup>1</sup>H NMR analysis of the crude mixture showed the presence of a single diastereoisomer. The enantiomeric excess of the product was

determined by chiral stationary phase HPLC (Chiralpak AD-H column, *n*-hexane/*i*-PrOH 90:10, flow 0.75 mL/min,  $\lambda$  254 nm,  $t_{\text{maj}}$  = 46.2 min,  $t_{\text{min}}$  = 53.0 min, 88% ee). <sup>1</sup>H NMR (CDCl<sub>3</sub>, 400 MHz)  $\delta$  = 8.06 (br s, 1H), 7.20 (br d, *J* = 8.3 Hz, 1H), 7.11 (br t, *J* = 8.0 Hz, 1H), 6.96 (br s, 1H), 6.91 (br d, *J* = 7.0 Hz, 1H), 5.22 (q, *J* = 3.4 Hz, 1H), 4.80 (dd, *J* = 20.9, 3.4 Hz, 1H), 3.90 (dd, *J* = 17.8, 3.0 Hz, 1H), 3.80 (s, 3H), 3.61 (s, 3H), 3.57 (d, *J* = 10.5 Hz, 1H), 3.34 (br dd, *J* = 17.5, 4.3 Hz, 1H). <sup>13</sup>C NMR (CDCl<sub>3</sub>, 100 MHz)  $\delta$  = 167.8, 167.5, 133.9, 125.4, 124.5, 123.2, 119.3, 117.8, 110.4, 106.5, 83.1, 55.8, 53.1, 52.6, 40.2, 23.5.  $[\alpha]_{\text{D}}^{25}$  = +87 (c = 0.52 in CH<sub>2</sub>Cl<sub>2</sub>);

**Methyl 2-((4R,5R)-4-nitro-1,3,4,5-tetrahydrobenzo[cd]indol-5-yl)acetate (7o)**

In a vial equipped with a magnetic stirring bar, compound **7q** (1 equiv.) was dissolved in THF (0.1 M), then LiOH (4 equiv.) was added at -20 °C and the mixture was stirred for 3 h, then it was allowed to reach room temperature. The reaction was quenched with water and KHSO<sub>4</sub> 0.5 M was added to acidify the mixture. The crude mixture was then extracted three times with EtOAc, then dried over MgSO<sub>4</sub>, filtered on Celite<sup>®</sup>, and evaporated. The crude was dissolved in toluene and heated at 100°C for 45 min. Afterwards, the solvent was evaporated and the residue was dissolved in a mixture of toluene/MeOH 1:1, then TMSCHN<sub>2</sub> (1 equiv.) was added at 0 °C and the mixture was stirred at room temperature. After 3 h the solvents were evaporated and the residue was directly purified on chromatography on silica gel (CH<sub>2</sub>Cl<sub>2</sub>), affording the title compound in 29% overall yield, and as a mixture 9:1 of diastereoisomers. The enantiomeric excess of the product was determined by chiral stationary phase HPLC (Chiralpak AS column, *n*-hexane/*i*-PrOH 80:20, flow 0.75 mL/min, λ 254 nm, *t*<sub>maj</sub> = 19.2 min, *t*<sub>min</sub> = 24.0 min, 65% ee). <sup>1</sup>H NMR (CDCl<sub>3</sub>, 400 MHz) δ = 8.02 (br s, 1H), 7.23 (dr d, J = 8.2 Hz, 1H), 7.17 (br t, J = 7.4 Hz, 2H), 6.98 (br s, 1H), 6.94 (br d, J = 7.14 Hz, 1H), 5.18 (dt, J<sub>T</sub> = 6.4 Hz, J<sub>D</sub> = 4.4 Hz, 1H), 4.35 (q, J = 6.7 Hz, 1H), 3.75 (dd, J = 15.7, 6.4 Hz, 1H), 3.72 (s, 3H), 3.43 (ddd, J = 16.0, 4.3, 0.9 Hz, 2H), 2.80 (dd, J = 16.6, 6.2 Hz, 1H), 2.76 (dd, J = 16.6, 6.4 Hz, 2H). <sup>13</sup>C NMR (CDCl<sub>3</sub>, 100 MHz) δ = 171.5, 133.7, 128.6, 123.6, 118.8, 115.8, 109.7, 107.3, 85.4, 52.0, 37.9, 37.1, 25.4.

**4.6. Conclusion**

The functionalization of indole nucleus is a fascinating area that still has a tremendous impact on organic synthesis.<sup>90</sup> Remarkable attention must be focussed on 3,4-annulated indoles which are the key structural motif of ergot alkaloids, a class of natural occurring compounds whose biological and pharmaceutical importance has been widely recognized.<sup>88</sup> Alongside this, the concept of “cascade reactions” has strongly merged with the asymmetric organic synthesis, gaining a great deal of interest in recent years as useful and nature-inspired tool for the efficient construction of complex chiral molecular structure, from simple and readily available starting materials.<sup>24</sup> For these reasons, our research group has moved towards the disclosure of new organocatalytic cascade approaches leading to the high valuable 3,4-ring fused indole scaffold. To build a molecular architecture between the C3 and C4 positions of indole following an organocatalytic approach, we have exploited the synthetic versatility of readily available

indoles bearing at their C4 a suitable Michael acceptor: in these compounds, the nucleophilic position at C3 of indole is flanked by the electrophilic olefin at C4, enabling the construction of tricyclic compounds via Friedel-Crafts alkylation<sup>102,105</sup> followed by Michael addition,<sup>103,106</sup> by using either  $\alpha,\beta$ -unsaturated aldehydes or nitroethene. Despite the conceptual simplicity, this approach has been sprinkled of intriguing synthetic challenges such as the expected low reactivity of this type of indole derivatives, in which the nucleophilicity of C3 is partially “quenched” by the conjugation with the Michael acceptor. Being conscious that too strong Michael acceptor would suppress the Friedel-Crafts reactivity, whereas too weak Michael acceptor would result unable to promote the triggered Michael addition, we have considered  $\alpha,\beta$ -unsaturated ketones Michael acceptor as a good compromise. Indeed, although an initial reluctance, after carefully optimization, indole derivatives **1** were reacted with the exceedingly reactive acrolein **2a** as enal partner,<sup>110</sup> in the presence of Jørgensen-Hayashi catalyst<sup>43c</sup> **4b**, TFA as cocatalyst and MgSO<sub>4</sub> as additive. The reaction proceeded through the Friedel-Crafts alkylation of indole by the iminium ion activated enal, triggering an enamine mediated ring closure. The reaction proved to be tolerant towards a broad range of indole derivatives, bearing different substituents both at the keto group of the Michael acceptor and on the indole nucleus. The corresponding tricyclic compounds **3a-g** were obtained with excellent results in terms of yields, diastereo- and enantioselectivities. Once moved to  $\beta$ -substituted enals, we have faced once again with the poor nucleophilicity of indoles derivatives **1**: every attempt to extend the optimized reaction conditions with acrolein to  $\beta$ -substituted enals failed, showing the inability of diarylprolinol derived catalysts in promoting this reaction. In search of a more reactive catalytic system, we turned to use imidazolidinone catalyst **4d** (MacMillan’s second generation catalyst)<sup>48</sup> which generate an iminium ion three orders of magnitude more reactive than diaryl prolinol type catalysts.<sup>112</sup> Under these re-optimized reaction conditions, also  $\beta$ -substituted aldehyde were productively engaged in our cascade protocol, affording compounds **3h-j**. Remarkably this latter 3,4-annulated indoles possess three contiguous stereocenters whose stereochemistry is perfectly controlled. The possibility of performing synthetic manipulation in products **3** was briefly explored. Treatment of **3a** under Pinnick conditions<sup>48</sup> oxidized both the aldehydes and the indole core, furnishing the intriguing lactone **5**; on the other hand a Robinson annulation reaction<sup>11b</sup> rendered the tetracyclic derivative **6** as a mixture of diastereoisomers (Scheme 50).

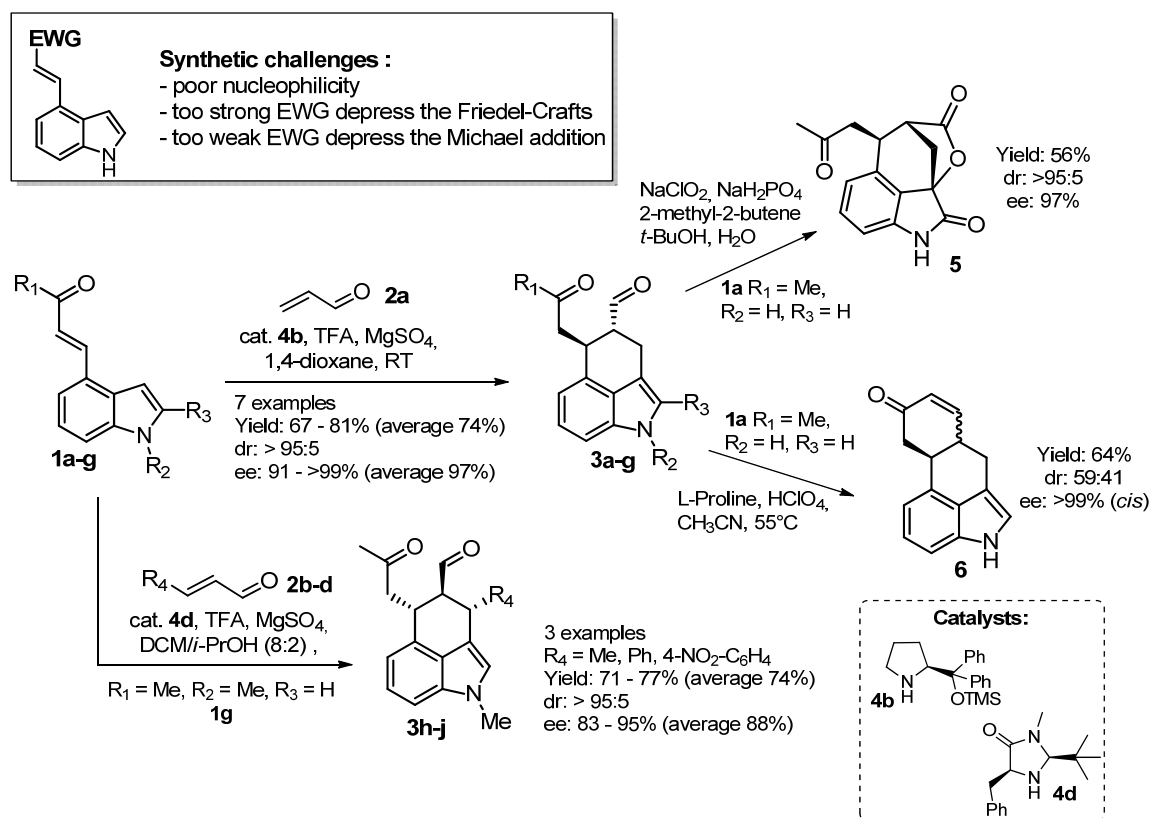
The quest for a reaction partner which could allow a direct access to ergot alkaloids have prompted us to develop a further organocascade approach between indoles **1** and this nitro-olefin. Quite surprisingly, the reaction between indoles **1** and nitroethene<sup>107</sup> was found to be promoted by chiral phosphoric acid catalysts, affording the corresponding tricyclic compounds **7** which present the same atom connectivity of ergot alkaloids. Upon a thorough screening of phosphoric acid catalysts and reaction conditions, we identified **9c** (*R*)-TRIP able to promote the reaction with perfect stereocontrol; moreover, the use of MgSO<sub>4</sub> as additive was found to have a positive influence on the reproducibility and reactivity. With the well-optimized reaction conditions different tests were carried out, generally obtaining very good results. Indole derivatives bearing aryl substituents at their ketone-fragment gave excellent results in terms of yields and stereoselectivities, confirming the suitability of this compounds in our protocol. The derivatization of these compounds on the *N*-indole position did not prevent the successful occurrence of the reaction: upon a slight modification of the reaction conditions, *N*-alkyl indole substrates furnished the corresponding products with very good results. Moving to non-aromatic keto substrates provided satisfactory results only when hindered substituents were placed on the Michael acceptor group. Ester derivatives and some of their surrogates were also tested, however these substrates were not suitable for the cascade cyclization, as the only products detected were the open-chain **7'**. In order to demonstrate the synthetic usefulness of our procedure, we developed a synthetic sequence for the obtainment of compound **7o** which is a precursor of the ergot alkaloid 6,7-secoagroclavine. Despite this latter process is currently under optimization, since better enantioselectivity has to be devised, the obtainment of enantioenriched **7o** allow us to claim the first formal total synthesis of enantioenriched 6,7-secoagroclavine<sup>94c</sup> by means of an organocatalytic reaction as cornerstone in the synthetic sequence. While the development of this synthetic sequence was ongoing, it was found that a clean epimerization occurred under strongly basic conditions. This transformation can be considered as a “lucky strike” since, in principle, allows to access to both diastereoisomers of the products with the same catalytic enantioselective procedure (Scheme 51).

The exclusive obtainment of tricyclic compound **7** in the presence of chiral phosphoric acid catalyst was very intriguing. Computational investigations of the acid catalyzed cascade reaction, showed that rearomatization of the indole core precedes the nitro-Michael step and that a key bicoordinated nitronate intermediate is formed. Here the

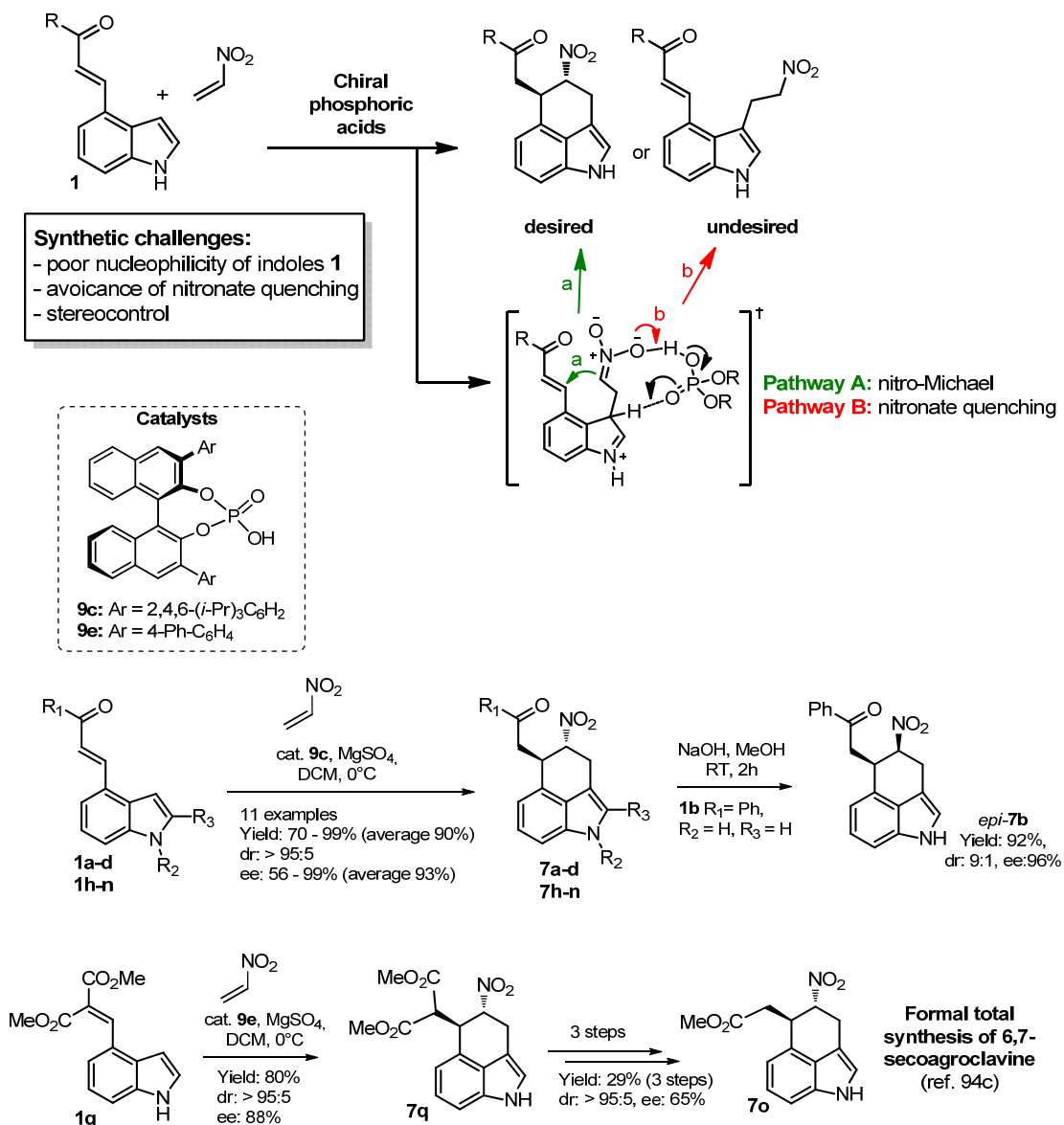
reaction can proceed through the stereoselective nitro-Michael pathway,<sup>120</sup> or simply lead to nitronate protonation when indole derivatives bearing weak Michael acceptor were employed. Importantly, this mechanistic proposal fully accounts for the observed experimental results.

The absolute and relative configuration were unambiguously assigned on compounds **3a**, **3h**, **6**, **7b** and *epi-7b* by means of NMR analysis and comparison of simulated ECD spectra with the experimental one.

In summary, we have introduced 4-substituted indoles **1** as useful substrates for asymmetric organocatalytic cascade reactions, resulting in a new synthetic route to 3,4-annulated indoles. The employment of these substrates in related transformation bring us to access to ergot alkaloids through the formal total synthesis of enantioenriched 6,7-secoagroclavine.



**Scheme 50.** Catalytic enantioselective organocascade reaction between indoles **1** and enals **2**, giving 3,4-annulated indoles **3**, related synthetic elaborations and associated challenges.



**Scheme 51.** Catalytic enantioselective organocascade reaction between indoles **1** and nitroethene, giving 3,4-annulated indoles **7** and associated challenges. The related synthetic elaboration allowed the access to enantioenriched ergot alkaloid.



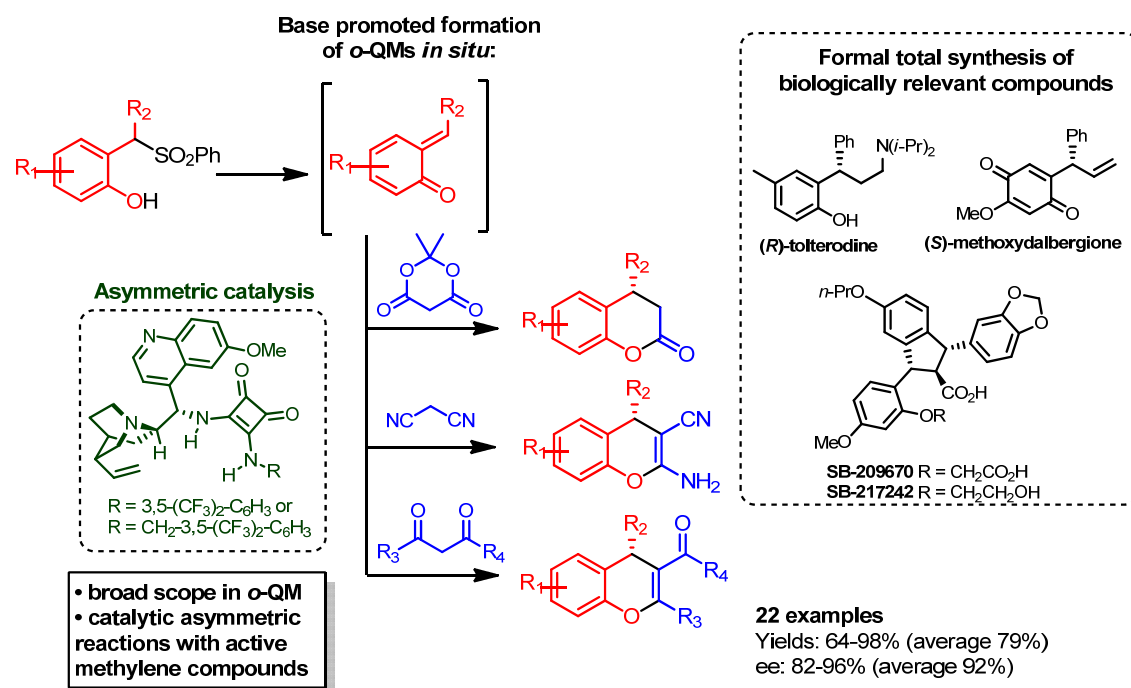
## 5. Organocatalytic asymmetric addition of active methylene compounds to *ortho*-quinone methides generated *in situ* under basic conditions

The procedures and results here described are part of- and can be found in-:

- Caruana, L.; Mondatori, M.; Corti, V.; Morales, S.; Mazzanti, A.; Fochi, M.; Bernardi, L. “Catalytic asymmetric addition of Meldrum’s acid, malononitrile and 1,3-dicarbonyls to *ortho*-quinone methides generated *in situ* under basic conditions.” *Chem. Eur. J.* **2015**, early view DOI: 10.1002/chem.201500710.
- 

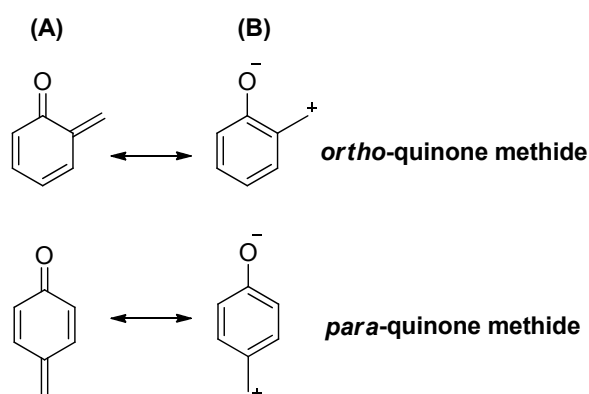
### ABSTRACT

This chapter deals with the development of a new approach to the utilization of highly reactive and unstable *ortho*-quinone methides (*o*-QMs) in organocatalytic asymmetric settings. Due to their instability, these synthetically appealing intermediates have begun to be exploited in asymmetric settings only recently.<sup>128,154</sup> Our approach relies on enantioselective reaction catalyzed by bifunctional organocatalysts in which the transient *o*-QM intermediates are generated *in situ* from 2-sulfonylalkyl phenols through base promoted elimination of sulfinic acid. The use of mild Brønsted basic conditions for transiently generation of *o*-QMs is unprecedented, and allows to overcome the intrinsic instability of these intermediates, hence permitting the productively engagement of different methylene nucleophiles such as Meldrum’s acid, malononitrile, and 1,3-dicarbonyl compounds. The catalytic transformations give new and general entries to enantioenriched 3,4-dihydrocoumarines, 4*H*-chromenes and xanthenones. These frameworks are synthetic precursors of several natural products (some of which showing interesting biological activity) and active pharmaceutical ingredients used in commercial drugs. In order to testify the importance and usefulness we propose the formal total syntheses of three biologically relevant compounds: (*R*)-tolterodine (antimuscarinic drug), (*S*)-4-methoxydalbergione (allergen of *Dalbergia Nigra*) and SB-209670 / SB-217242 (potent endothelin antagonists).



## 5.1. Background

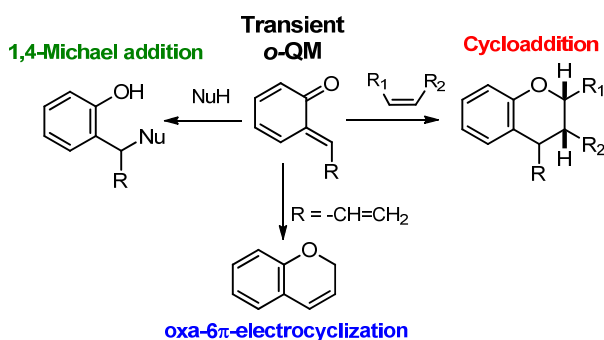
Quinone methides display a cyclohexadiene core featuring an exocyclic methylene and a carbonyl residue, mainly disposed at *ortho* or *para* position. The 1,2- and 1,4-quinone methides (namely *ortho*- and *para*-quinone methides, respectively) are formally neutral molecules (Scheme 52, A) however, the zwitterionic aromatic resonance structures (Scheme 52, B) are highly relevant, rendering these molecules highly polarized and thus reactive at those sites. *ortho*- and *para*-Quinone methides can be considered as Michael acceptors however, compared



**Scheme 52.** Resonance structures of quinone methides

to the classic enones, the reactivity of quinone methides is much more pronounced. In fact, while addition of nucleophiles to simple Michael acceptor results in a small decrease in the stability of the system due to the loss of conjugation and simultaneous formation of enolic intermediate, addition of nucleophiles to quinone methides results in a large increase in the  $\pi$ -stabilization energy due to the formation of a fully aromatic ring;

this provides a considerable driving force that exceedingly enhances the reactivity of quinone methides. The combination of these features confers a distinctive reactivity to quinone methides.<sup>129</sup> While *para*-quinone methides only react in 1,6-Michael addition of nucleophiles; *ortho*-quinone methides possess a greater charge dipole which make them less stable, more reactive and perhaps give them more intriguing chemistry which let *o*-QMs to emerge as highly useful and versatile intermediates. The reactivity of *o*-QMs is expressed by three typical reaction pathways (Scheme 53): not only the 1,4-Michael type



**Scheme 53.** The three typical reaction pathways of *o*-QMs

addition with various nucleophiles but also, cycloadditions with  $2\pi$  partners and oxa- $6\pi$ -electrocyclizations are possible.<sup>128</sup> The latter two reaction pathways result in benzopyran subunits which are valuable scaffolds in the frame

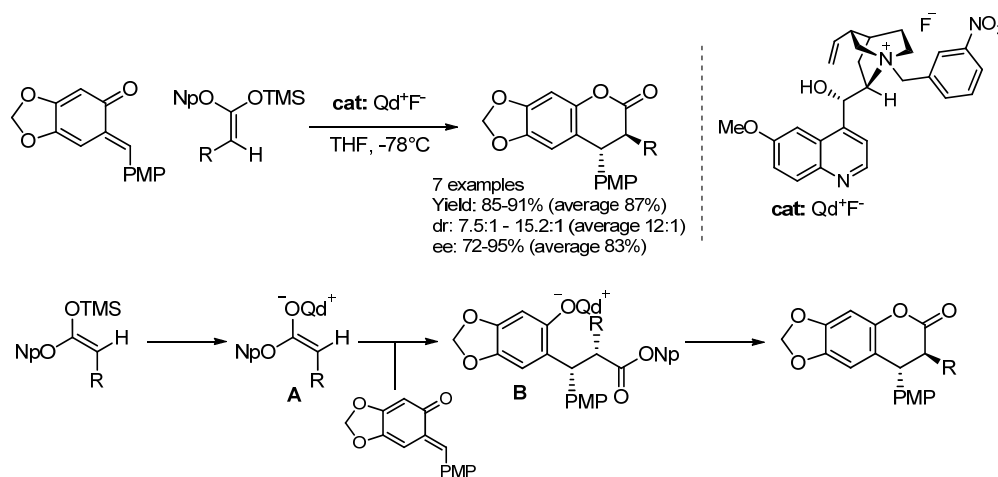
of the synthesis of complex natural products.<sup>128d</sup>

From a historical perspective *o*-QMs were first invoked by Fries in 1907,<sup>130</sup> but only many decades later more direct evidences of their existence were collected, first by using low-temperature IR spectroscopy<sup>131</sup> and later by X-Ray diffraction experiments in which *o*-QMs were entrapped in an iridium complex.<sup>132</sup> Despite their transiency, *o*-QMs (and their *para*-substituted counterparts *p*-QMs) are relatively common moieties in biological settings.<sup>129b</sup> QMs are often proposed as biosynthetic intermediates, and several natural compounds contain these moieties. More importantly, the biological activity/toxicity featured by many natural/synthetic molecules is attributed to the reactivity of (transiently generated) QMs sub-units, acting as powerful alkylating agents towards biological targets. These observations have not only inspired a number of natural product syntheses based on QM intermediates,<sup>128d</sup> but have also spurred very active research areas dealing with the control/sensing of biological processes through the generation of reactive QMs *in situ*.<sup>128b,g</sup>

Being labile intermediates, *o*-QMs have been termed as “ephemeral”, “elusive” intermediates, and even as a “synthetic enigma”.<sup>128</sup> The marked reactivity of quinone methides was historically seen as deterrent to their employment in organic synthesis. In fact, reports describing the utilization of QMs in catalytic asymmetric settings have been scarce until very recently,<sup>128c</sup> highlighting the challenge of taming their high reactivity

and instability. Significant breakthrough have exploited the possibility of stabilizing the electron-poor triene core of QMs by electron donating substituents, up to point their isolation have become possible.<sup>133</sup>

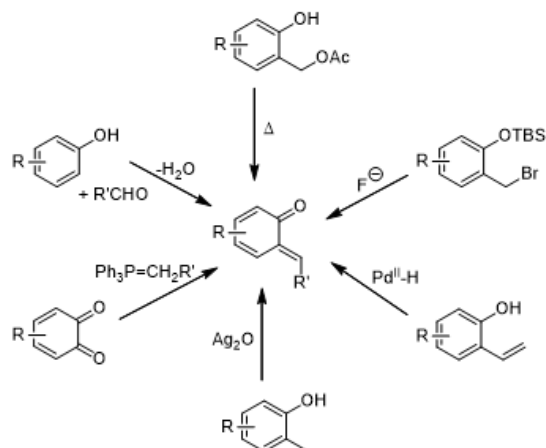
The first remarkable application of stabilized *ortho*-quinone methides in organocatalytic asymmetric fashion was reported by Lectka in 2008, describing an enantioselective [4+2] cycloaddition of stable *o*-QMs to silyl ketene acetals. Chiral cinchona alkaloid-derived tetraalkylammonium fluoride behaved as a precatalyst to generate the ketene enolate *in situ*. The proposed mechanism, shown in Scheme 54, involves fluoride ion-promoted desilylation of the ketene acetal, forming the ion-paired ketene enolate A. This species, regioselectively attacks the *o*-QM at the methide group to produce intermediate B, with the restoration of aromaticity acting as driving force. Subsequently B undergoes lactonization to form the desired cycloadduct product and releasing 2-naphtoxide. The tetraalkylammonium fluoride organocatalyst was termed as “precatalyst” since the fluoride anion was sacrificed to initiate the reaction. Thus, the ammonium ion of the catalyst could form ion pairs with the ketene enolate, effecting on the enantioselectivity by electronic effects rather than by steric bulk.



**Scheme 54.** Enantioselective reaction of stabilized *ortho*-quinone methide with ketene enolate using chiral ammonium fluoride precatalyst.

Other remarkable examples of the utilization of stabilized *o*-QMs in asymmetric catalysis involve NHC activation of enals aldehydes, resulting in [4+3] cycloaddition reactions.<sup>134</sup> However, the requirement of stabilized substrates clearly represents an inherent limitations in the scope of these protocols. In order to move around this restriction, various synthetic methodologies for the *in situ* generation of *o*-QMs have been developed which turned to be intimately linked with the manner in which *o*-QMs are to be utilized. Stepping back to the general utilization of *o*-QM in organic chemistry, the most common

methods for their generation is the elimination of a stable molecule from the benzylic position, to generate the methylene and  $\alpha$ -carbonyl functionalities with concomitant



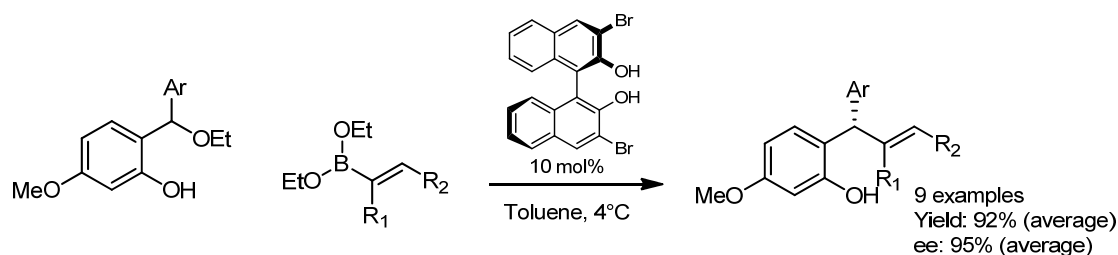
**Scheme 55.** Some methods for the generation of *o*-QMs

dearomatization. This process may be induced thermally or by addition of a nucleophile, base or acid.<sup>128d,e,f</sup> Other classic *o*-QMs generation routes include tautomerization (which may be induced thermally, photolytically, or via Pd<sup>II</sup>-hydride), benzylic oxidation, Wittig olefination of an *ortho*-quinone, or by aldol condensation (Scheme 55).<sup>128d,e,f</sup>

More challenging aim is to push the boundaries towards conditions

compatible with both formation of reactive *ortho*-quinone methide and asymmetric catalysis; indeed, only very recently organocatalytic methods combining chiral catalysts with catalytic asymmetric transformation of *o*-QM generated in situ, have strongly emerged.<sup>134,135,137,138,139,140,141,142,143,154</sup>

In 2012, Schaus and co-workers described the asymmetric addition of aryl- or alkenyl-boronates to *o*-QMs, generated from 2-hydroxybenzyl alcohols or 2-hydroxybenzyl ethers under mild acidic conditions (Scheme 56).<sup>135</sup> The boronate was found to be acidic enough to promote the QM formation in the presence of BINOL derived catalyst. The thus formed highly reactive *o*-QMs were trapped by nucleophilic boronates before dimerization or polymerization side-reactions could occur. The hydroxyl group was crucial for reactivity, as its absence resulted in no product, in accordance with the occurrence of *o*-QM intermediate in the reaction. Despite successfully, this approach – exploiting the *in situ* formation of a reactive intermediate – was limited to the presence of electron-donating group placed at the *para* position of the exocyclic methylene. In fact, electron-donating substituents at that position are able to stabilize both the *o*-QM intermediate (by inductive and resonance effects) and to facilitate its formation;<sup>128b</sup> emphasizing once again the difficulty of the applications of *o*-QMs in asymmetric catalysis.



**Scheme 56.** Organocatalytic enantioselective addition of boronates to *in situ* formed *o*-QMs.

How the BINOL-derived chiral diol could effectively promote the reaction was not completely clear since Goodman and co-workers performed computational investigations.<sup>136</sup> The DFT calculations suggested that asymmetric boronate addition to *o*-QMs, proceeded via a Lewis acid catalyzed process through a closed six-membered transition state (Figure 39). The BINOL-derived catalyst underwent an exchange process with the initial boronate ligands, loss of both ligands resulted in a more Lewis acidic boron which is the active species in the reaction.

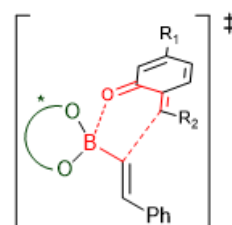
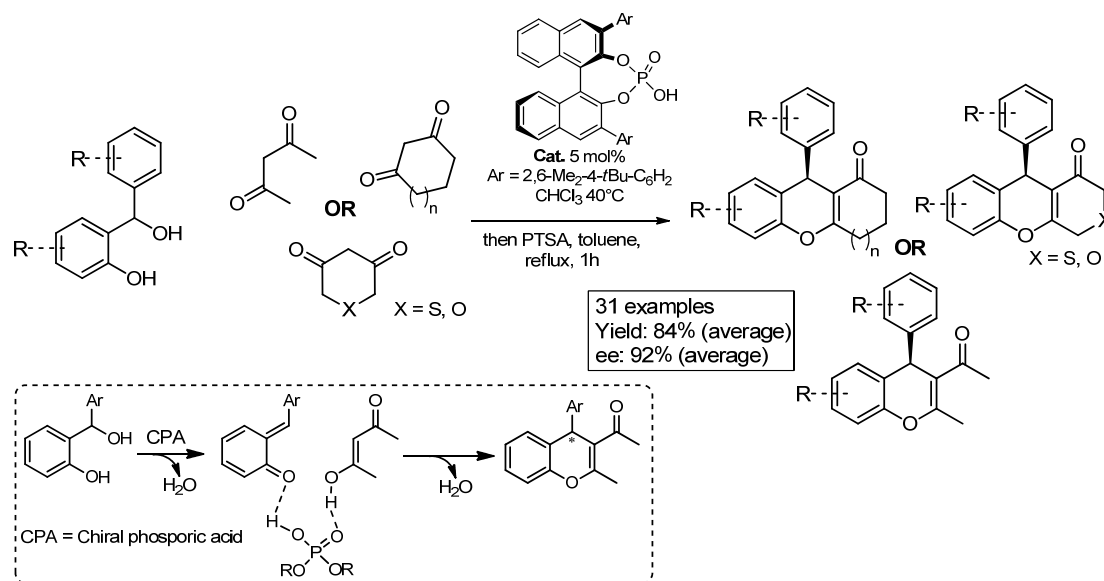


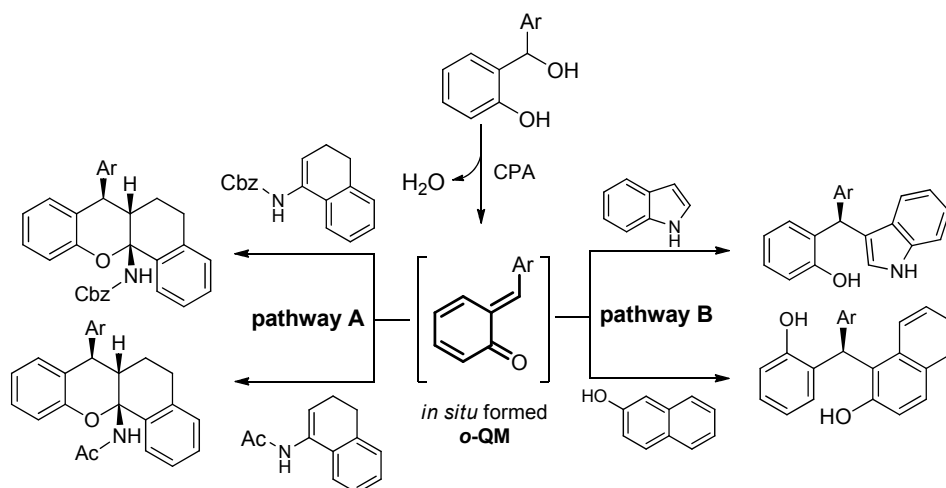
**Figure 39.** Transition state model for the reaction between vinyl boronate and *o*-QMs. In green is highlighted the chiral diol condensated to the boronate, whereas in red is highlighted the six-membered transition state.

Beyond the aforementioned example of alcohol elimination of 2-alkoxyalkyl phenols, generating the *o*-QMs, the challenging task related to the transient formation of *o*-QMs intermediates, has been recently met with other approaches. Available examples include palladium-catalyzed oxidative addition to *ortho*-hydroxy styrenes,<sup>137</sup> desilylation – halide elimination of *O*-silyl 2-haloalkyl phenols<sup>138</sup> and pyrones,<sup>139</sup> and dehydration of the corresponding benzylic alcohols.<sup>140</sup> The latter approach, wherein chiral Brønsted acid catalysts promote both dehydration and addition to the thus formed *o*-QM, has proven to be particularly flexible and has been very recently applied to a broad range of nucleophilic reaction partners. In this context, Schneider's group has devoted many research efforts to the employment of these substrates in asymmetric transformations, catalyzed by chiral phosphoric acids.<sup>141</sup> The first example of its kind dealt with a catalytic enantioselective process for the synthesis of 4*H*-chromenes. A sequence of conjugate addition of  $\beta$ -diketones to *in situ* generated *ortho*-quinone methides, followed by cyclodehydration reaction furnished 4-aryl-4*H*-chromanes in excellent yields and high enantiopurity. A BINOL-based phosphoric acid was employed as Brønsted acid catalyst which converted *ortho*-hydroxy benzyhydril alcohols into hydrogen-bonded *o*-QMs and effected the formation of a new C-C bond in high enantioselectivity (Scheme 57).<sup>141a</sup>



**Scheme 57.** Chiral phosphoric acid catalyzed, conjugate addition of 1,3-dicarbonyls to *in situ* generated *ortho*-quinone methides.

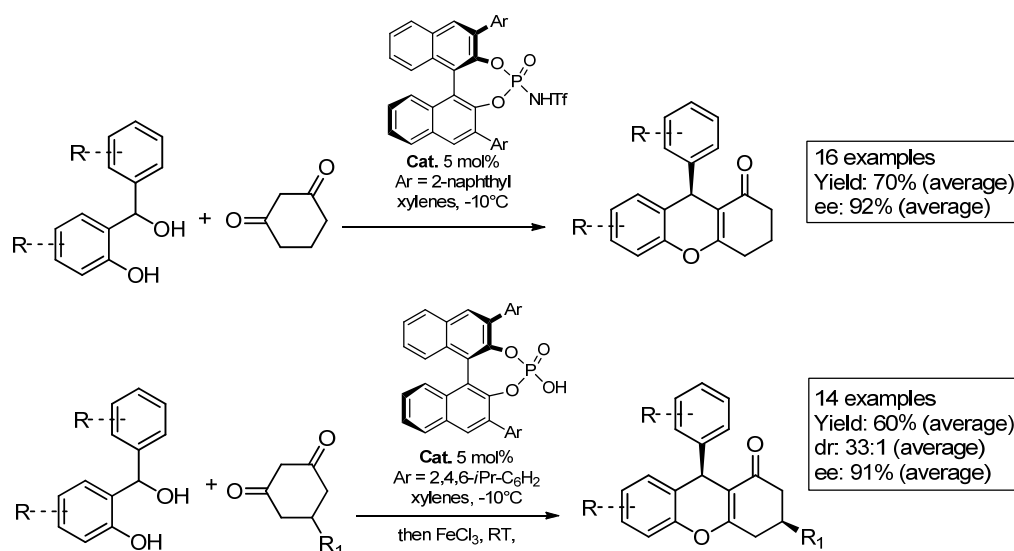
The conjugated addition was not limited to 1,3-dicarbonyls, but could be instead extended to other nucleophilic reaction partners such as enecarbamate/enamides<sup>141b</sup> or electron-rich aromatic ring (*e.g.* indoles or naphthols).<sup>141c</sup> In the first case the conjugate addition triggered the *N,O*-acetalization, giving rise to acetamido-substituted tetrahydroxanthenes (Scheme 58, pathway A); whereas in the second, only the conjugated addition took place delivering diarylindolylmethanes or triarylmethanes (Scheme 58, pathway B).



**Scheme 58.** Chiral phosphoric acid (CPA) catalyzed reaction of *o*-QMs with enecarbamates/enamides (pathway A) and with indoles or  $\beta$ -naphthols (pathway B).

Almost simultaneously, the acidic *in situ* generation of *o*-QMs from diaryl hydroxybenzylic alcohols, permitting the productive engagement of these unstable and highly reactive intermediates was independently developed by Rueping<sup>142</sup> and Sun<sup>143</sup>

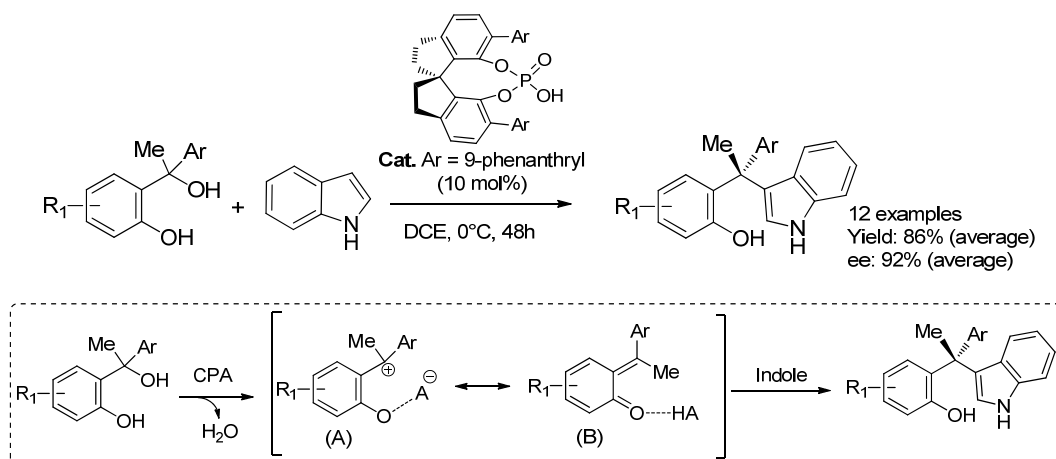
research groups. Rueping and co-workers described an enantioselective synthesis of tetrahydroxanthenones by means of asymmetric Brønsted acid catalysis. A BINOL-based *N*-triflylphosphoramidate was able to promote the *in situ* generation of *o*-QMs and their subsequent reaction with 1,3-cyclohexanedione to provide the desired tetrahydroxanthenes with excellent stereoselectivity. In addition, BINOL-based phosphoric acid was found to promote the reaction between *o*-QMs and 5-monosubstituted 1,3-dicarbonyl substrates. In this latter case the desymmetrization afforded products containing two distant stereocenters (Scheme 59). Once again, the acidic organocatalyst both promoted the formation of *o*-QMs and their engagement in the asymmetric reaction via a transition state in which the reactive species are both coordinated.



**Scheme 59.** Chiral phosphoric acid catalyzed, conjugate addition of cyclohexanedione to *in situ* generated *ortho*-quinone methides (top). Desymmetrization of 5-monosubstituted cyclohexanedione with *in situ* generated *ortho*-quinone methides, affording tetrahydroxanthenes embedding two distant stereocenters (bottom).

Few months later, Sun and co-workers extended this protocol by employing tertiary diaryl hydroxybenzylic alcohols in the reaction with indole, catalyzed by chiral phosphoric acid.<sup>143</sup> This transformation is worth noting since affords products bearing an all-carbon quaternary stereocenter which is known to be a particularly challenging structural element to assemble.<sup>144</sup> The reactions described by Sun were effective for a range of tertiary alcohols as long as electron-rich phenols bearing a methyl group at the benzylic position were employed; whereas 2- or 4-substituted indoles could not be used possibly due to the steric hindrance close to the reactive 3-position. A set of control

experiments established that the phenolic hydroxyl-group is crucial for the reactivity, as well as the N-H moiety of indole which permitted the catalyst coordination. The proposed mechanism involves the protonation of the tertiary alcohol and subsequent H<sub>2</sub>O elimination. This leads to the formation of carbocation (A), the resonance form of a H-bond coordinated *o*-QMs (B). These structures were considered two extreme forms of the real reaction intermediate in terms of electron density. The stereoselection performed by the chiral phosphoric acid could be explained either considering an ion-pair (in A) or hydrogen-bonding (in B), to form the all-carbon quaternary stereocenter (Scheme 60).



**Scheme 60.** Enantioselective construction of all-carbon quaternary stereocenters from indoles and tertiary hydroxylbenzyl di-aryl alcohols (CPA = chiral phosphoric acid).

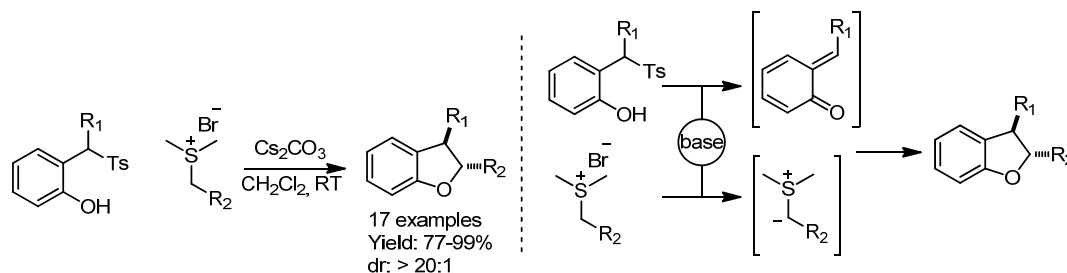
The employment of *ortho*-quinone methides in asymmetric syntheses has been knowing a flurry of interest. With this growth, the variety of ways in which these intermediate are generated has also diversified and it seems that a kind of “domestication” is to be reached, spurring the researchers to deploy “elusive” and “ephemeral” *ortho*-quinone methide in a range of asymmetric transformations.

## 5.2. Aim of the work

The strategies for the *in situ* generation of *ortho*-quinone methides have conferred to these species high synthetic potentials, even though the embracing of these methodologies with asymmetric organocatalysis has emerged only recently.

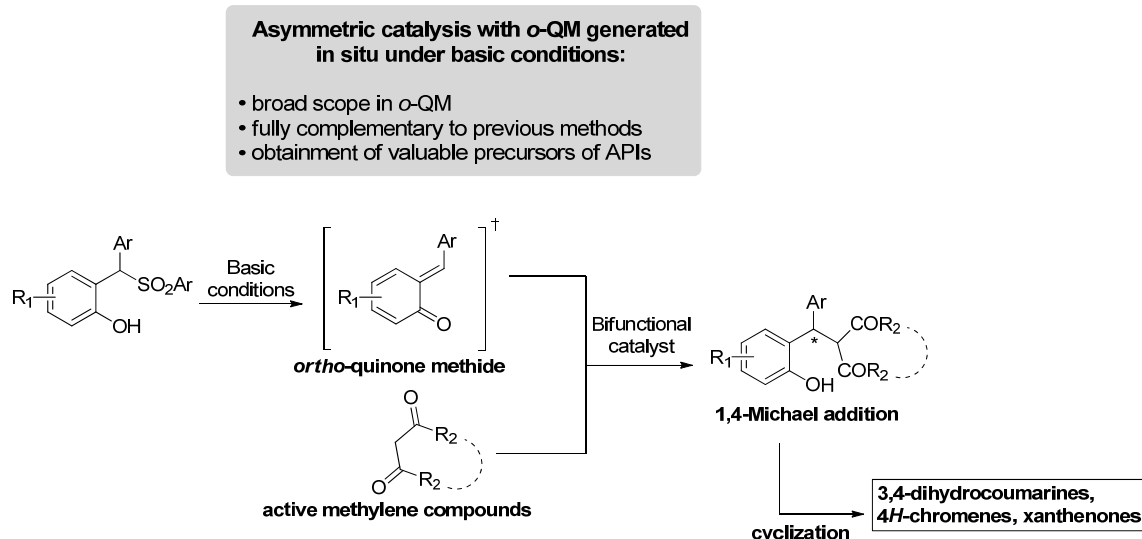
Our attention was drawn by a report proposed by Zhou and co-workers,<sup>145</sup> describing the generation of *o*-QMs under mild basic conditions and their employment in a nucleophilic addition with sulfur ylides, affording 2,3-dihydrobenzofurans in high diastereoselectivity.

Zhou and co-workers used 2-tosylalkylphenols as precursors of *o*-QMs which are generated upon the basic-promoted elimination of tosyl sulfonic acid (Scheme 61).



**Scheme 61.** Strategy for the generation of *o*-QMs under basic conditions (Zhou and co-workers).

Inspired by this novel strategy, and on the basis of the literature data for asymmetric transformation involving the generation of transient species through sulfonyl elimination,<sup>146</sup> we have aimed to the development of a novel strategy for the generation of *o*-QMs under basic conditions, in the enantioselective reaction with active methylene compounds, promoted by H-bond donor organocatalyst bearing a Brønsted basic sites (*e.g.* *Cinchona* derived catalysts).<sup>22</sup> It has been envisaged that the high variability in *o*-QMs structure will be provided by their *in situ* production, whereas the unprecedented exploitation of Brønsted basic conditions for both *o*-QM generation (from 2-(arylsulfonyl)alkyl phenols) and enantioselective reaction will give to our approach a fully complementary scope to other methodologies based on the acidic generation of *o*-QMs. In accordance with our envisioned approach, we expect that not only the previously reported 1,3-diketones or 3-ketoesters might be employed, but also substrates that require a basic activation such as Meldrum's acid or malononitrile could find a fruitful application in the asymmetric transformation. The cyclization at the phenolic oxygen will eventually follow the nucleophilic addition, delivering 3,4-dihydrocoumarins, 4*H*-chromenes and xanthenones, possessing a stereocenter at the benzylic position (Scheme 62). These privileged scaffolds<sup>147</sup> might serve as useful precursors in the synthesis of natural products as well as active pharmaceutically ingredients (APIs).

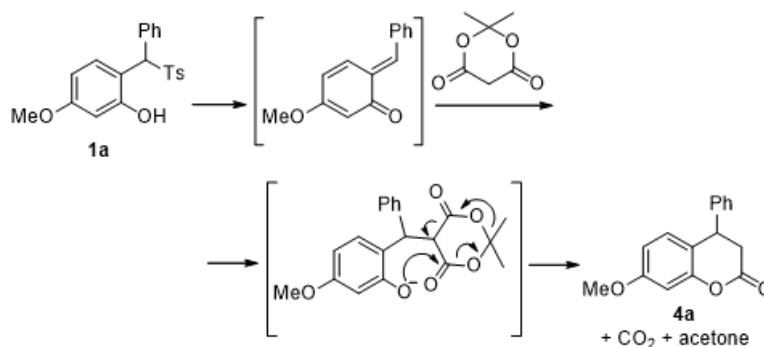


**Scheme 62.** Basic conditions and bifunctional catalysts promote the *in situ* generation of *ortho*-quinone methide, in the reaction with active methylene compounds.

### 5.3. Results and discussion

At the outset of this work, we explored combinations of bifunctional organocatalyst, inorganic bases and various common active methylene compounds in the reaction with the 5-methoxysalicylaldehyde derived sulfone **1a**. It was envisioned that the electron-donating methoxy group would favor the formation of the *o*-QMs and stabilize it. Indeed, encouraging reactivity

was observed with Meldrum's acid, which furnished the 3,4-dihydrocoumarin **4a**, resulting from the cyclization and



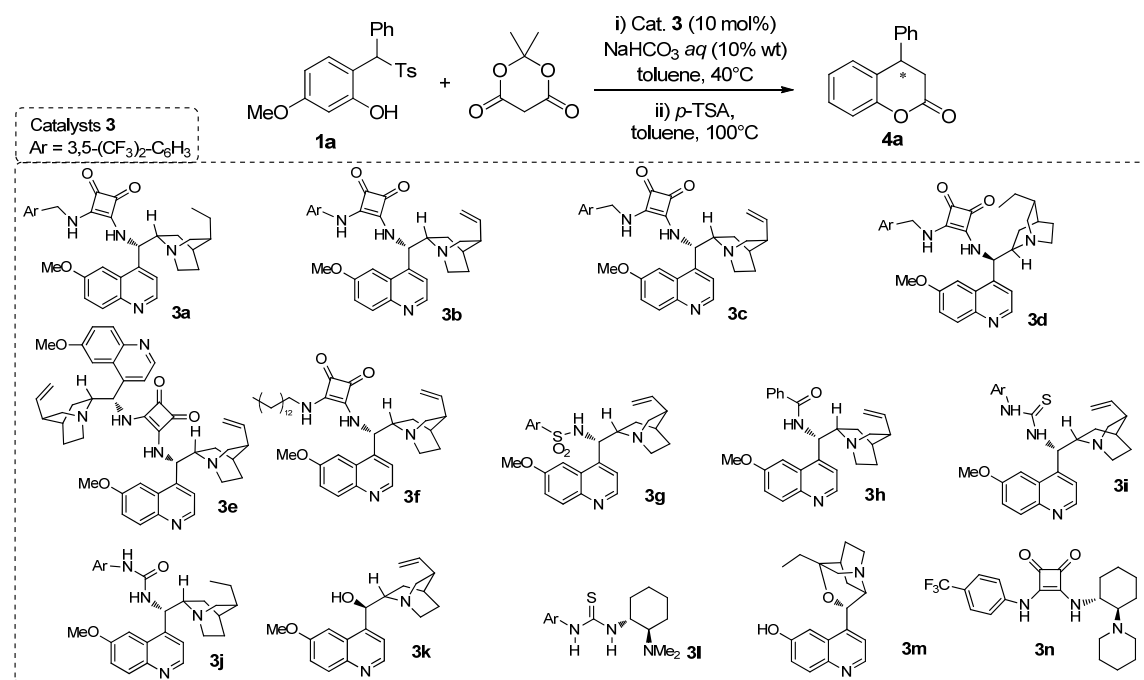
subsequent decarboxylation of the intermediate adduct

**Scheme 63.** Addition of Meldrum's acid on **1a** and ensuing cyclization/decarboxylation leaving **4a**.

(Scheme 63).<sup>128b, 135.</sup> The investigations were continued by screening a broad range of H-bond donor catalysts in the reaction between **1a** and Meldrum's acid at 40 °C, using aqueous sodium bicarbonate as basic additive and toluene as solvent. The crude mixtures were always treated with PTSA, in order to ensure lactonization to **4a** of the corresponding open-chain carboxylic acid, sometimes observed in the crude. This

preliminary results pointed to 9-amino(9-deoxy)*epi* (dihydro)quinine squaramide catalysts<sup>34,35</sup> **3a** and **3b** which performed best amongst the catalysts tested (Table 10).

**Table 10.** Preliminary catalysts screening in the reaction between **1a** and Meldrum's acid.<sup>a</sup>



Entry	Cat. <b>3</b>	Time (h)	Conversion <sup>b</sup> (%)	ee <sup>c</sup> (%)
1	<b>3a</b>	24	>95	87
2	<b>3b</b>	24	>95	92
3	<b>3c</b>	17	>95	85
4	<b>3d</b>	19	>95	-66
5	<b>3e</b>	22	>95	7
6	<b>3f</b>	22	>95	85
7	<b>3g</b>	22	67	racemic
8	<b>3h</b>	22	85	-14
9	<b>3i</b>	22	>95	74
10	<b>3j</b>	22	>95	83
11	<b>3k</b>	22	>95	29
12	<b>3l</b>	17	>95	-70
13	<b>3m</b>	22	59	-16
14	<b>3n</b>	22	>95	-48

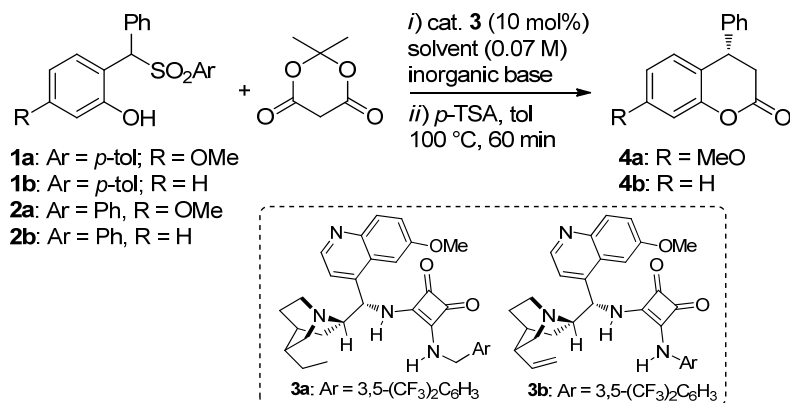
(a) Conditions: i) Sulfone **1a** (0.05 mmol), Meldrum's acid (0.10 mmol), cat. **3** (0.005 mmol, 10 mol%), toluene (0.71 mL), NaHCO<sub>3</sub> aq (1.00 mmol, 10 wt% aqueous solution), 40 °C, then HCl aq 0.1 M, filtration on Celite®, evaporation; ii) toluene, PTSA (0.005 mmol), 100 °C, 1 h. (b) Determined by <sup>1</sup>H NMR after the first step (considering **4** + carboxylic acid). (c) Determined by chiral stationary phase HPLC.

A series of control experiments revealed the non-trivial role of the inorganic base. In fact, when the reaction was carried out in the absence of the basic additive, the conversion value of **1a** coincided with the catalyst loading (10 or 20 mol%), thus suggesting that the

inorganic base served to regenerate the catalyst permitting its turnover, whereas the organocatalyst **3** is also responsible for the generation of the reactive *o*-QMs<sup>148</sup> (a detailed discussion will be addressed in § 5.3.2). Indeed, the importance of the inorganic base was demonstrated by the results shown in Table 11, entries 1-4. While lower enantioselectivities with bases stronger than bicarbonate could be attributed to a background racemic reaction, the lower conversions observed with non-aqueous bases were ascribed to their poor efficiency in catalyst regeneration. Using aqueous NaHCO<sub>3</sub>, an increase in conversion and enantioselectivity was observed at 40 °C, using the aniline derived catalyst **3b** (Table 11, entry 5 and Table 10, entry 1). Even though better results could be obtained using DCE as solvent (Table 11, entry 6), we faced with great disappointment when we purified product **4a** to determine the yield of the reaction, which resulted unacceptably low. A large number of experiments directed at its improvement through changing the various reaction parameters (solvent, catalyst loading and type, temperature, concentration, reaction time, type and amount of inorganic base, order and rate of the additions, excess of Meldrum's acid), proved to be unfruitful. Furthermore, the reaction with the unsubstituted sulfone **1b**, lacking the stabilizing methoxy group, proved to be sluggish, with only 61% conversion reached after prolonged reaction time, even when using 5 equiv. of Meldrum's acid (Table 11, entry 7). The unsatisfactory results obtained with these two sulfones **1** were ascribed to two opposite reasons,<sup>128b</sup> which we thought give enough merit to the definition of *o*-QMs as a "synthetic enigma"<sup>128a</sup>. In the case of the methoxy derivative **1a**, the rapid formation of the *o*-QM intermediate, accompanied by its plausibly poor reactivity, caused its accumulation in the reaction medium. Thus, degradation competed with the desired enantioselective addition, resulting in low yield. In the case of the unsubstituted derivative **1b**, decomposition was not an issue, since the highly reactive *o*-QM formed only in small amounts. However, its formation was so disfavored that conditions compatible with the sensitive catalytic asymmetric step could not be devised. Pleasingly and unexpectedly, we discovered a solution applicable to both cases, observing that a very subtle change at the aryl group of the sulfone, swapping the *p*-tolyl for a phenyl, gave a surprisingly dramatic improvement over its leaving group ability. In fact, there is usually no difference in reactivity between these two sulfones;<sup>146</sup> however, the unsubstituted phenyl sulfone **2b** fully converted even at RT, affording the product **4b** in good yield and improved enantioselectivity (Table 11, entry 8). On the other hand, the opportunity of producing the sensitive methoxy substituted *o*-QM intermediate from

sulfone **2a** at RT, instead of 40 °C, was sufficient to avoid most of the degradation pathway, resulting in improved yield of the corresponding product **4a** (Table 11, entry 9).

**Table 11.** Selected optimization results in the reaction between sulfones **1** or **2** and Meldrum's acid



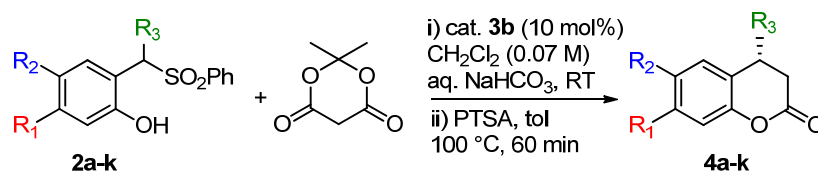
Entry	1,2	Solvent	Base (equiv.)	3	T (°C)	t (h)	Conv. (%) <sup>b</sup>	ee (%) <sup>c</sup>
1	<b>1a</b>	toluene	NaHCO <sub>3</sub> aq. 10% (10)	<b>3a</b>	RT	24	<b>4a-41</b>	72
2	<b>1a</b>	toluene	K <sub>2</sub> CO <sub>3</sub> aq. 5% (10)	<b>3a</b>	RT	24	<b>4a-44</b>	48
3	<b>1a</b>	toluene	Na <sub>2</sub> CO <sub>3</sub>	<b>3a</b>	RT	24	<b>4a-30</b>	69
4	<b>1a</b>	toluene	Na <sub>2</sub> CO <sub>3</sub>	<b>3a</b>	RT	24	<b>4a-29</b>	80
5	<b>1a</b>	toluene	NaHCO <sub>3</sub> aq. 10% (10)	<b>3b</b>	40	22	<b>4a- &gt;95</b>	92
6	<b>1a</b>	DCE	NaHCO <sub>3</sub> aq. 10% (10)	<b>3b</b>	40	18	<b>4a- &gt;95 (47)<sup>d</sup></b>	93
7 <sup>e</sup>	<b>1b</b>	DCE	NaHCO <sub>3</sub> aq. 10% (10)	<b>3b</b>	40	96	<b>4b-61</b>	92
8 <sup>e</sup>	<b>2b</b>	DCM	NaHCO <sub>3</sub> aq. 10% (10)	<b>3b</b>	RT	70	<b>4b- &gt;95</b>	93
9 <sup>e</sup>	<b>2a</b>	DCM	NaHCO <sub>3</sub> aq. 5% (10)	<b>3b</b>	RT	20	<b>4a- &gt;95 (76)<sup>d</sup></b>	94

(a) Conditions: *i*) sulfone **1** or **2** (0.05 mmol), Meldrum's acid (0.10 mmol), cat. **3** (0.005 mmol, 10 mol%), solvent (0.75 mL), inorganic base, then HCl aq. 0.1 M, filtration of the organic phase on Celite<sup>®</sup>, evaporation; *ii*) toluene, cat. PTSA, 100 °C, 60 min. (b) Determined by <sup>1</sup>H NMR after the first step (considering **4** + carboxylic acid). (c) Determined by chiral stationary phase HPLC. (d) Yield of product **4** purified by chromatography on silica gel. Reactions performed on 0.10 scale. (e) 5 equiv. of Meldrum's acid were used.

Having found in phenyl sulfones **2** suitable substrates for the organocatalytic transformation with Meldrum's acid, the scope of the reaction was inspected by using aqueous sodium bicarbonate as stoichiometric base, dichloromethane as solvent and performing the reaction at room temperature. Sulfones **2a-f**, having substituents with

different electronic properties at the phenolic ring, performed very well in the reaction, affording the corresponding 3,4-dihydrocoumarines **4a-f** in good yields and enantioselectivities (Table 12, entries 1-6). As previously mentioned, the substituents on the phenolic ring play a major role on the stability/reactivity of the *ortho*-quinone methide. Substrates lacking the stabilizing electron-donating group might form only minimal amount of *o*-QMs which, however, would be too reactive to be compatible with the organocatalytic conditions. Nonetheless, our methodology was successfully extended to electron-neutral and even electron-deficient substrates (Table 12, entries 2 and 5), furnishing the corresponding adducts with results comparable to the ones obtained with electron-rich substrate. These results clearly demonstrated the non-obvious tolerance of our approach to a range of electronically different *o*-QMs. Curiously, the highly electron-rich substrate **2f** required increased catalyst loading to reach satisfactory values of enantioselectivity. In this case it could be envisioned that the resulting *o*-QMs would be so stable that is formed in substantial amounts, giving a background racemic reaction. Fortunately, increase the catalyst loading to 20 mol% a satisfactory result could be achieved even with substrate (Table 12, entry6)

Then, we assessed variations at the benzylic substituent, which also can influence to the behavior of the *o*-QM. Once again both electron-donating and withdrawing groups at this aromatic substituent were well tolerated, as the corresponding adducts **4g-k** were obtained with good results (Table 12, entries 7-11).

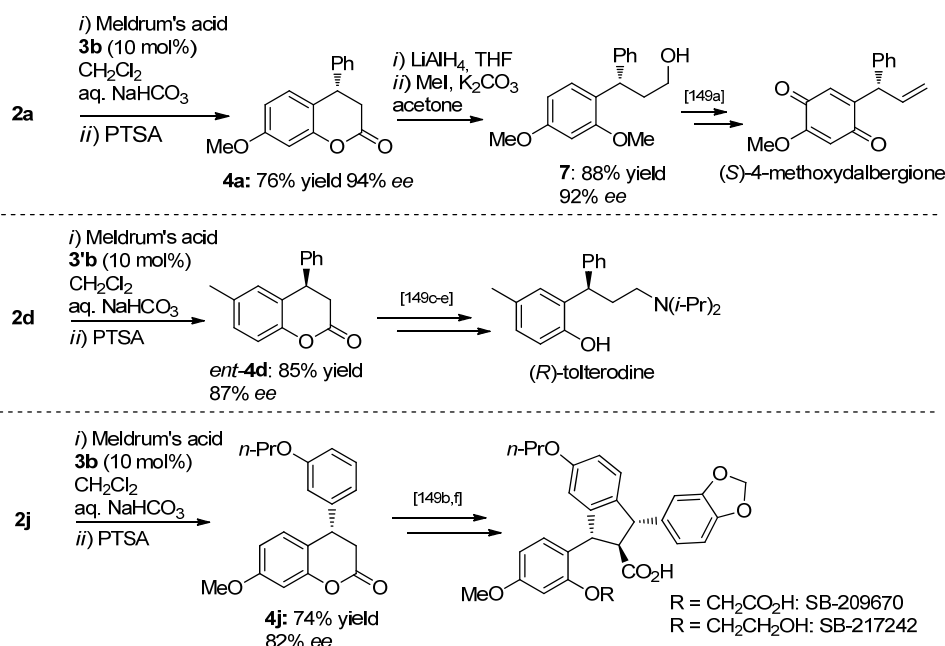
**Table 12.** Scope of the organocatalytic asymmetric reaction between sulfones **2** (precursors of *o*-QMs) and Meldrum's acid.<sup>a</sup>

Entry	<b>2</b>	R <sub>1</sub>	R <sub>2</sub>	R <sub>3</sub>	4-Yield <sup>b</sup> (%)	ee <sup>c</sup> (%)
1	<b>2a</b>	OMe	H	Ph	<b>4a-76</b>	94
2	<b>2b</b>	H	H	Ph	<b>4b-83</b>	93
3	<b>2c</b>	Me	H	Ph	<b>4c-77</b>	95
4 <sup>d</sup>	<b>2d</b>	H	Me	Ph	<b>4d-82</b>	96
5	<b>2e</b>	H	Br	Ph	<b>4e-76</b>	93
6 <sup>e</sup>	<b>2f</b>	O(CH <sub>2</sub> )O		Ph	<b>4f-76</b>	88
7	<b>2g</b>	H	H	4-(MeO)C <sub>6</sub> H <sub>4</sub>	<b>4g-79</b>	88
8	<b>2h</b>	H	H	4-ClC <sub>6</sub> H <sub>4</sub>	<b>4h-82</b>	95
9	<b>2i</b>	H	Me	4-ClC <sub>6</sub> H <sub>4</sub>	<b>4i-81</b>	95
10	<b>2j</b>	H	Me	3-( <i>n</i> PrO)C <sub>6</sub> H <sub>4</sub>	<b>4j-74</b>	82
11	<b>2k</b>	H	Me	2-(MeO)C <sub>6</sub> H <sub>4</sub>	<b>4k-70</b>	92

(a) Reaction conditions: *i*) sulfone **2** (0.10 mmol), Meldrum's acid (0.50 mmol), cat. **3b** (0.010 mmol, 10 mol%), CH<sub>2</sub>Cl<sub>2</sub> (1.42 mL), aq. NaHCO<sub>3</sub> (5% or 10%, 5.0 mmol), RT, 18-72 h then HCl aq. 0.1 M, filtration of the organic phase on Celite®, evaporation; *ii*) toluene, cat. PTSA, 100 °C, 60 min. (b) Isolated yield. (c) Determined by chiral stationary phase HPLC. (d) This reaction was also performed with catalyst **3'b** derived from quinidine, quasi-enantiomeric to **3b**. (e) In this case 20 mol% of **3b** was used. When 10 mol% of catalyst was used product **4f** was obtained in 66% yield and 76% ee.

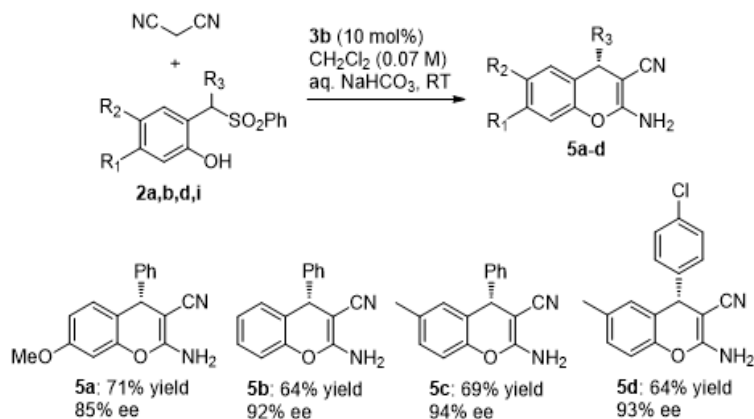
4-Aryl-3,4-dihydrocoumarins **4** are highly valuable intermediates in the synthesis of biologically active compounds.<sup>149</sup> Thus, the present methodology, allowing the obtainment of enantioenriched 3,4-dihydrocoumarins, might serve as a useful synthetic platform. For instance, reduction of the lactone moiety in compound **4a** followed by methylation gave the alcohol **7** with preserved enantioenrichment; the latter compound could be converted in two steps into (*S*)-methoxydalbergione,<sup>135,149a</sup> a natural quinone product isolated from *Dalbergia* tropical plant (Scheme 64, top). On the other hand, by using the pseudo-enantiomeric quinidine catalyst **3'b**, compound *ent*-**4d** was readily obtained even if with slightly decreased enantioselectivity. This 3,4-dihydrocoumarin is the key intermediate in several syntheses of (*R*)-tolterodine,<sup>149c,d,e</sup> the active ingredient of the commercial antimuscarinic drug Detrol® (Scheme 64, middle). Finally, compound **4j**

is the precursor of the potent endothelin antagonists SB-209670 and SB-217242<sup>149b,f</sup> (Scheme 64, bottom).



**Scheme 64.** Formal total syntheses of biologically active compounds by means of organocatalytic key-step reaction.

Then, we studied the reaction with other nucleophiles amenable to activation by catalysts **3**. Performing the reaction under the same conditions used for Meldrum's acid, we were pleased to discover that

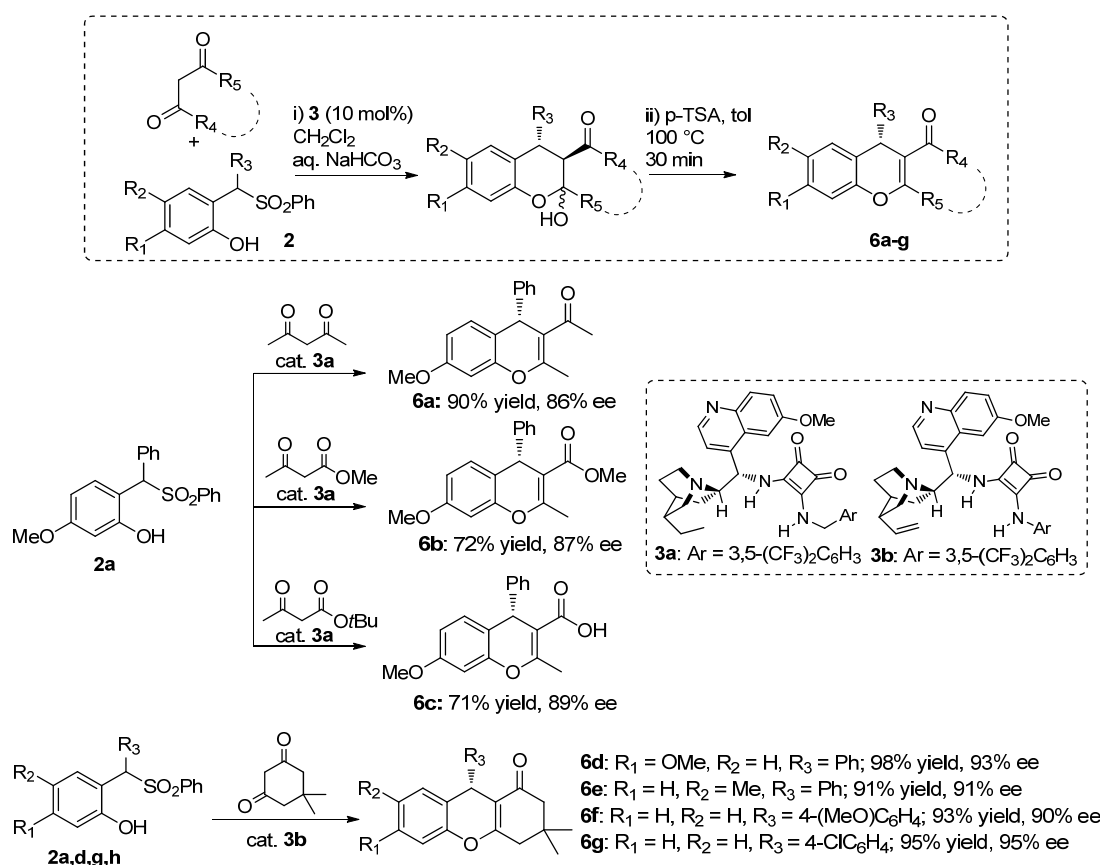


**Scheme 65.** Organocatalytic asymmetric additions of malononitrile to *o*-QMs in situ generated from sulfones **2**

malononitrile reacted well with various *o*-QM precursors **2** (Scheme 65). The initial adducts cyclized spontaneously, without requiring any additional treatment, furnishing cleanly the corresponding 4*H*-chromenes **5a-d**. Also in this case, the reaction proved to be tolerant to various substituents at the aromatic rings. Interestingly, the products **5** feature a specific 2-amino-4*H*-4-arylchromene-3-carbonitrile framework, which was found to possess some promising apoptosis inducing activity.<sup>150</sup> The present method

represents the first general catalytic enantioselective approach to this class of *4H*-chromenes.

We have also explored the reaction with 1,3-diketones and 1,3-ketoesters (Scheme 66). In these reactions, an equilibrating diastereomeric mixture of hemiacetal adducts was obtained in the crudes, which could be dehydrated to *4H*-chromenes and xanthenones **6** by treatment with PTSA. These acidic conditions caused ester cleavage in the case of product **6c** derived from *tert*-butyl acetoacetate. The reactions with acetylacetone and 3-ketoesters proved to be somewhat less robust compared to the previous nucleophiles explored, with good results being obtained only with the methoxy substituted sulfone **2a**. Furthermore, better enantioselectivities were obtained by using the benzylamine substituted catalyst **3a**. In contrast, excellent reactivity and tolerance to various substitution patterns was regained in the reactions with dimedone, which afforded the corresponding xanthenones **6d-g** with nearly quantitative yields and excellent enantioselectivities.

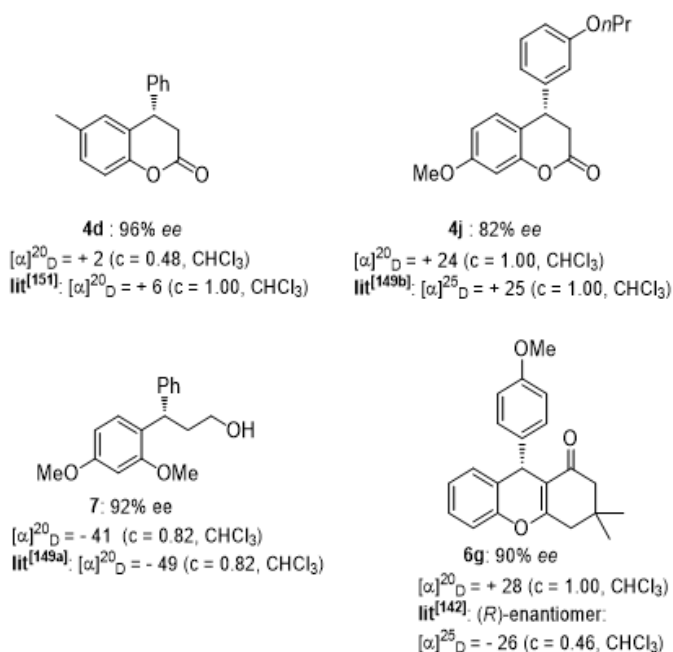


**Scheme 66.** Organocatalytic asymmetric additions of 1,3-diketones and 3-ketoesters to *o*-QMs in situ generated from sulfones **2**

### 5.3.1. Determination of the absolute configuration of compounds **4**, **5**, **6**

The absolute configuration of compounds **4d**,<sup>151</sup> **4j**,<sup>149b</sup> **7**<sup>149a</sup> (derived from **4a**) and **6g**<sup>142</sup> was determined by comparison of the specific rotations ( $[\alpha]_D^{20}$ ) with reported literature data, as shown in Figure 40.

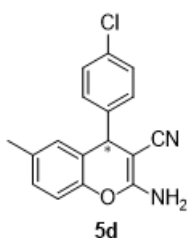
Due to the structural difference of the nucleophile employed, we also decided to determine the absolute configuration of compounds **5**. Their absolute configuration was determined



**Figure 40.** Optical specific rotations of **4d**, **4j**, **7**, **6g**.

by a combination of conformational analysis and theoretical simulations of chiro-optical spectra, namely by comparison of calculated (TD-DFT) with experimental ECD spectra.<sup>81</sup> To this purpose, compound **5d** was selected as representative compound. The best simulation was obtained using M06-2X functional, that simulates correctly also the relative intensities of the peaks. The very good agreement of all the simulations with the experimental spectrum reliably assigns the (*S*) absolute configuration to **5d**. As shown in Figure 41, all the simulated spectra match well the Cotton effects when the (*S*) absolute configuration was assumed in the calculations.

In summary, we determined the absolute configuration of products **4a,d,j**, **5d**, **6g**, which was found to be (*S*) in all cases, irrespectively of the nucleophile and the *o*-QM precursor employed in the reaction. Therefore, since we have used the same catalyst **3b** (or the closely related **3a**) in the other catalytic reactions, we can safely assign (*S*) absolute configuration also to the remaining compounds **4-6**.



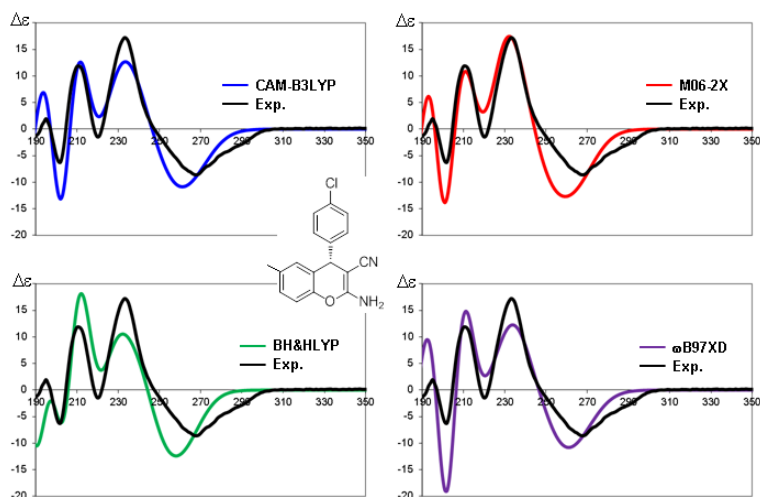
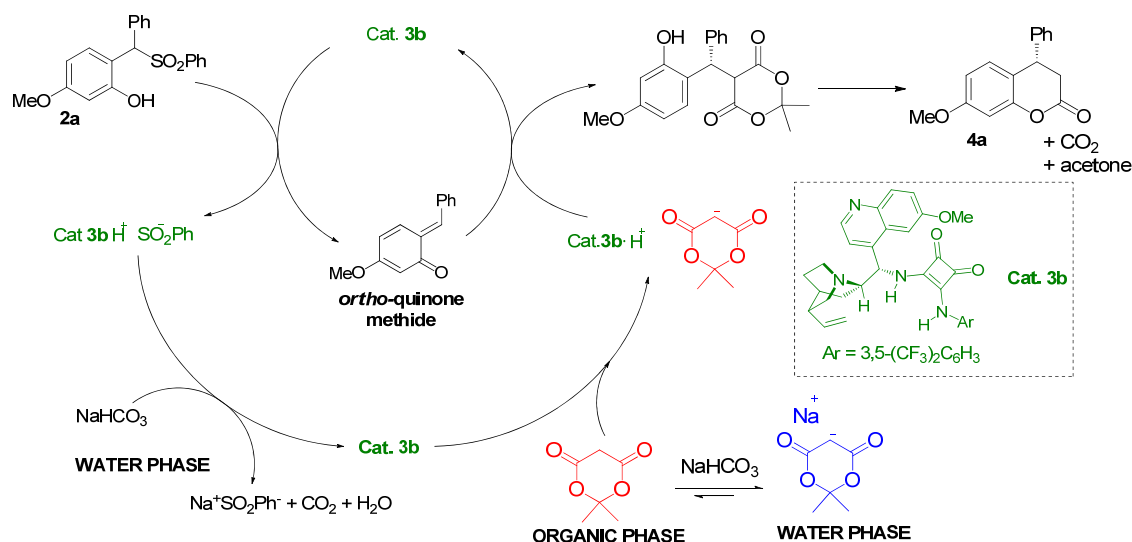


**Figure 41.** TD-DFT simulated spectra calculated for **5d** using four different functionals (CAM-B3LYP, BH&HLYP, M06-2X,  $\omega$ B97-XD) and the same 6-311++G(2d,p) basis set. For each case the first 50 excited states were calculated, and the spectrum was obtained using a 0.20 eV line width at half height. The simulated spectra were shifted by 8-12 nm to match the experimental

### 5.3.2. Mechanistic proposal and control experiments

In order to get an insight on the reaction pathway followed by the catalytic reactions, few control experiments were carried out. In a first control experiment, a reaction between sulfone **2a** (0.10 mmol) and Meldrum's acid (0.50 mmol) was performed using catalyst **3b** (0.02 mmol) in  $\text{CD}_2\text{Cl}_2$  as solvent (1.42 mL) and in the absence of the inorganic base (the aqueous solution of  $\text{NaHCO}_3$  was replaced with 1.68 mL of water). After 24 h,  $^1\text{H-NMR}$  analysis of the organic phase revealed approximately 20% of conversion to **4a**. This experimental evidence suggests that the tertiary amine moiety of the bifunctional catalyst **3b** is responsible for the generation of the *ortho*-quinone methide from **2a**, accounting for the conversion observed in the absence of  $\text{NaHCO}_3$ . Therefore, it is plausible that – under the standard reaction conditions – the mild inorganic base has the main role of regenerating the catalyst by acid neutralization, thus allowing catalyst turnover, rather than forming the quinone methide intermediate. On this basis, we propose the reaction pathway outlined in Scheme 67, wherein in the presence of bifunctional catalyst **3b**, sulfone **2a** is readily deprotonated generating the transient *o*-QM upon sulfinic acid elimination, while the inorganic base restores the protonated catalyst to the active form **3b**. Although less likely, it is also possible that the ion pair formed by the catalyst and Meldrum's acid is involved in the generation of the *o*-QM (i.e. deprotonated Meldrum's acid acts as a base).



**Scheme 67.** Proposed reaction pathway.

This proposal is in line with previous findings dealing with the formation of *N*-carbamoyl imines from  $\alpha$ -amido sulfones in reactions catalysed by a Cinchona alkaloid<sup>148a</sup> and phase-transfer catalysts.<sup>148b,c</sup> In the latter case, it was established that the deprotonated nucleophile acted as the base.

Alongside this, an intriguing aspect of this reaction is that Meldrum's acid (pKa = ~4.9 in water) should be completely deprotonated under the basic (excess aq. NaHCO<sub>3</sub>) reaction conditions, and thus present as sodium salt only in the aqueous phase. To verify this, we evaluated the distribution of Meldrum's acid between the aqueous and organic phases under the reaction conditions. Meldrum's acid (0.25 mmol) was dissolved in CD<sub>2</sub>Cl<sub>2</sub> (0.75 mL) in presence of bibenzyl as internal standard (0.125 mmol); 0.81 mL of a 5 wt% aqueous solution of NaHCO<sub>3</sub> (0.50 mmol) was added, and the mixture stirred for 30 min. The aqueous phase was removed and the organic phase was analyzed by <sup>1</sup>H-NMR spectroscopy. Comparison between the signals of the internal standard with the signals of Meldrum's acid allowed to establish that approximately only 1 mol% of Meldrum's acid is present in the organic phase, hence confirming that most of Meldrum's acid has been deprotonated by NaHCO<sub>3</sub> and moved to the aqueous phase. A similar result was obtained by performing the experiment in the presence of catalyst **3b**, although quantification of the amount of Meldrum's acid present was less feasible in this case, due to the presence of the catalyst signals.

It can thus be concluded that Meldrum's acid is only marginally present in the organic media in the non-deprotonated form. Nevertheless, albeit in low amount, Meldrum's acid is activated by catalyst **3b** within the organic phase and can react with the previously in

situ generated *o*-QM, delivering the addition product and finally **4a**. As the reaction proceeds, Meldrum's acid distributes from aqueous towards the organic phase, ensuring a very low but constant concentration of nucleophile. It is worth to note that both reactive species are present in small amount in the reaction media, thus justifying the large excess of nucleophile (5 equiv.) employed in the optimized reaction protocol, as well as the long reaction times (up to 72 h) usually required.

Similarly, we assessed the distribution of malononitrile and acetylacetone between the aqueous and organic phases: in the first case, we estimated 25 mol% of residual malononitrile in the organic phase; while, as far as acetylacetone is concerned, 75 mol% of this substrate is present in the organic solvent. While Meldrum's acid has a pKa compatible with a complete protonation by NaHCO<sub>3</sub> and its consequent distribution into the aqueous phase, in the case of malononitrile and acetylacetone the non-negligible solubility of these compounds in water can be invoked to justify their partial removal from the organic phase.

## 5.4. Experimental details

### 5.4.1. General methods and materials

<sup>1</sup>H, <sup>13</sup>C NMR spectra were recorded on a Varian Mercury 400 or Inova 600 spectrometer. Chemical shifts (δ) are reported in ppm relative to residual solvent signals for <sup>1</sup>H and <sup>13</sup>C NMR.<sup>84</sup> <sup>13</sup>C NMR spectra were acquired under <sup>1</sup>H broadband decoupling. Chromatographic purifications were performed using 70-230 mesh silica. Mass spectra were recorded on a micromass LCT spectrometer using electrospray (ES) ionisation techniques or using electron impact (EI) ionisation techniques. Optical rotations were measured on a Perkin-Elmer 241 polarimeter. The electronic circular dichroism (ECD) spectra were recorded on a Jasco J-810 spectropolarimeter. The enantiomeric excess (*ee*) of the products was determined by chiral stationary phase HPLC, using a UV detector operating at 234 nm. The absolute configuration of the products was assigned as described in the relevant section.

Analytical grade solvents and commercially available reagents were used as received, unless otherwise stated. The 6-hydroxybenzo[*d*][1,3]dioxole-5-carbaldehyde used for the preparation of sulfone **2f** was prepared from sesamol by modifying a literature procedure.<sup>152</sup> Sulfones **2a-k** were easily prepared according to a modified literature procedure;<sup>145</sup> except for sulfones **2a** and **2f**, which were purified by column chromatography, all other sulfones were obtained cleanly without purifications. Catalysts **3a**, **3b** and **3'b** were prepared following reported procedures.<sup>34,153</sup> Racemic samples were

prepared by using an excess (5 equiv.) of  $K_2CO_3$  in presence of a catalytic amount (0.1 equiv.) of tetrabutylammonium bromide (TBABr).

### 5.4.2. General procedures

*General procedure for the organocatalytic reaction of Meldrum's acid or dimedone with sulfones 2 (Method A)*

To a vial equipped with magnetic stirring bar, catalyst **3b** (0.010 mmol) was added, followed by sulfones **2a-k** (0.10 mmol), Meldrum's acid or dimedone (0.50 mmol), DCM (1.42 mL) and  $NaHCO_3$  *aq* (1.00 mmol, 1.68 mL of a 5 wt% aqueous solution). The mixture was stirred at room temperature until TLC analysis showed complete conversion of the corresponding sulfone (approximately 24 h for **2a** and **2f**, 96 h for the remaining sulfones), then the reaction was quenched with HCl 0.1 M. Afterwards the mixture was extracted three times with DCM and the organic layers were passed through a short plug of Celite<sup>®</sup> and  $MgSO_4$ . The solvents were removed, the crude was dissolved in toluene (1.0 mL) and PTSA monohydrate (ca 0.01 mmol) was added. The mixture was stirred at 100 °C for 1 h, then directly purified by column chromatography on silica gel (*n*-Hexane/EtOAc mixtures) to afford the corresponding 3,4-dihydrocoumarines **4a-k** or the tetrahydro-1*H*-xanthen-1-ones **6d-g**.

*General procedure for the organocatalytic reaction of malononitrile with sulfones 2 (Method B)*

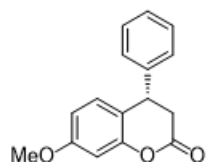
To a vial equipped with magnetic stirring bar, catalyst **3b** (0.010 mmol) was added, followed by sulfones **2a,b,d,i** (0.10 mmol), malononitrile (0.50 mmol), DCM (1.42 mL) and  $NaHCO_3$  *aq* (1.00 mmol, 0.84 mL of a 10 wt % aqueous solution). The mixture was stirred at room temperature until TLC analysis showed complete conversion of the corresponding sulfone (approximately 16 h for **2a**, 96 h for the remaining sulfones), then the reaction was quenched with HCl 0.1 M. Afterwards the mixture was extracted three times with DCM and the organic layers were passed through a short plug of Celite<sup>®</sup> and  $MgSO_4$ . After evaporation of the solvents, the crude reaction mixture was finally purified by column chromatography on silica gel (DCM or *n*-Hexane/EtOAc mixtures) to afford the corresponding 2-amino-4*H*-4-arylchromene-3-carbonitriles **5a-d**.

*General procedure for the organocatalytic reaction of acetylacetone or 3-ketoesters with sulfones 2 (Method C)*

To a vial equipped with magnetic stirring bar, catalyst **3a** (0.010 mmol) was added, followed by sulfone **2a** (0.10 mmol), acetylacetone or the appropriate 3-ketoester (0.50 mmol), DCM (1.42 mL) and  $NaHCO_3$  *aq* (1.00 mmol, 0.84 mL of a 10 wt% aqueous solution). The mixture was stirred at room temperature until TLC analysis showed complete conversion of the corresponding sulfone (approximately 24 h), then the reaction was quenched with HCl 0.1 M. Afterwards the mixture was extracted three times with

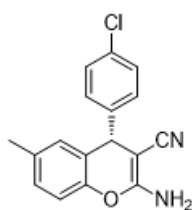
DCM and the organic layers were passed through a short plug of Celite<sup>®</sup> and MgSO<sub>4</sub>. The solvents were removed, the crude was dissolved in toluene (1.0 mL) and PTSA monohydrate (ca 0.01 mmol) was added. The mixture was stirred at 100°C for 30 min., then directly purified by column chromatography on silica gel (*n*-Hexane/EtOAc mixtures) to afford the corresponding 4*H*-chromenes **6a-c**.

#### (*S*)-7-Methoxy-4-phenylchroman-2-one (**4a**)



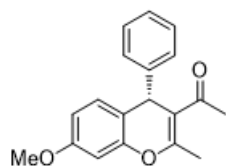
Following the general procedure (method A), but using NaHCO<sub>3</sub> *aq* (10 wt%) as inorganic base, the title compound was isolated by column chromatography (*n*-Hexane/EtOAc 5:1) in 76% yield as white solid. **<sup>1</sup>H-NMR** (CDCl<sub>3</sub> 400MHz) δ = 7.37-7.27 (m, 3H), 7.17-7.13 (m, 2H), 6.87 (d, *J* = 8.3 Hz, 1H), 6.69 (d, *J* = 2.7 Hz, 1H), 6.64 (dd, *J* = 8.5, 2.5 Hz, 1H), 4.29 (t, *J* = 6.8 Hz, 1H), 3.80 (s, 3H), 3.07 (dd, *J* = 15.7, 6.0 Hz, 1H), 2.99 (dd, *J* = 15.8, 7.8 Hz, 1H). **<sup>13</sup>C NMR** (CDCl<sub>3</sub> 100MHz) δ = 167.6, 160.0, 152.5, 140.7, 129.1, 128.9, 127.6, 127.5, 117.6, 110.7, 102.5, 55.5, 40.1, 37.3; **EI-MS** [*M*<sup>+</sup>]: 254; [*α*]<sub>D</sub><sup>20</sup> = +36 (*c* = 0.75 in CHCl<sub>3</sub>). The *ee* was determined by chiral stationary phase HPLC (Chiralpak AD-H, *n*-Hexane/*i*-PrOH 90:10, flow = 0.75mL/min, λ = 234 nm, *t*<sub>maj</sub> = 17.8 min, *t*<sub>min</sub> = 16.2 min, *ee* = 94%).

#### (*S*)-2-Amino-4-(4-chlorophenyl)-6-methyl-4*H*-chromene-3-carbonitrile (**5d**)



Following the general procedure (method B), the title compound was isolated by column chromatography (*n*-Hexane/EtOAc 2:1) in 64% yield as white solid. **<sup>1</sup>H-NMR** (CDCl<sub>3</sub> 400MHz) δ = 7.29 (br d, *J* = 9.0 Hz, 2H), 7.13 (br d, *J* = 8.3 Hz, 2H), 7.00 (d, *J* = 8.4 Hz, 1H), 6.90 (d, *J* = 8.4 Hz, 1H), 6.71 (s, 1H), 4.68 (s, 1H), 4.62 (br s, 2H), 2.21 (s, 3H); **<sup>13</sup>C NMR** (CDCl<sub>3</sub> 100MHz) δ = 159.3, 146.5, 143.2, 134.8, 133.0, 129.6, 129.3, 129.1, 129.0, 121.8, 119.7, 116.1, 60.3, 40.5, 20.7; **ESI-MS** [*M* - *H*]<sup>-</sup>: 295; [*α*]<sub>D</sub><sup>20</sup> = -33 (*c* = 0.567 in acetone). The *ee* was determined by chiral stationary phase HPLC (Chiralcel OD, *n*-Hexane/*i*-PrOH 90:10, flow = 0.75mL/min, λ = 234 nm, *t*<sub>maj</sub> = 18.0 min, *t*<sub>min</sub> = 22.0 min, *ee* = 93%).

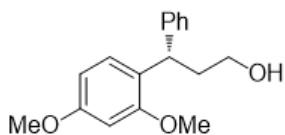
#### (*S*)-1-(6-Methoxy-3-methyl-1-phenyl-1,4-dihydronaphthalen-2-yl)ethanone (**6a**)



Following the general procedure (method C), but performing the reaction at 10 °C, the title compound was isolated by column chromatography (*n*-Hexane/EtOAc 5:1) in 90% yield as white solid. **<sup>1</sup>H-NMR** (CDCl<sub>3</sub> 400MHz) δ = 7.29-7.21 (m, 4H), 7.18-7.13 (m, 1H), 6.99 (d, *J* = 8.3 Hz, 1H), 6.57 (dd, *J* = 8.4, 2.6 Hz, 1H), 6.54 (d, *J* = 2.6 Hz, 1H), 4.95 (s, 1H), 3.75 (s, 3H), 2.44 (s, 3H), 2.15 (s, 3H); **<sup>13</sup>C NMR** (CDCl<sub>3</sub> 100MHz) δ = 199.2, 159.1, 158.7, 149.6, 146.0, 129.5, 128.9, 127.5, 126.8, 116.9, 114.4, 111.4, 101.1, 55.4, 41.7, 30.1, 20.0; **EI-MS**: [*M*<sup>+</sup>] 294; [*α*]<sub>D</sub><sup>20</sup> = +20 (*c* = 0.75 in CHCl<sub>3</sub>). The *ee* was

determined by chiral stationary phase HPLC (Chiralpak AD-H, *n*-Hexane/*i*-PrOH 90:10, flow = 0.75mL/min,  $\lambda$  = 234 nm,  $t_{\text{maj}}$  = 11.2 min,  $t_{\text{min}}$  = 9.5 min, *ee* = 86%).

### Synthesis of (*S*)-3-(2,4-dimethoxyphenyl)-3-phenylpropan-1-ol (7)



In an oven dried vial filled with nitrogen, compound **2a** (0.125 mmol, 1 equiv) was dissolved in dry THF (0.40 mL). The solution was cooled to 0 °C and LiAlH<sub>4</sub> (0.275 mmol, 2.2 eq., 118  $\mu$ L of a 2.3 M solution in 2-Me-THF) was added. The reaction mixture was warmed to room temperature and stirred for 1 h; then the reaction was carefully quenched with HCl 1 M and extracted with EtOAc (3x). The organics were washed with water, brine and finally dried over MgSO<sub>4</sub>. After filtration, the solvents were removed, the crude was dissolved in acetone (1.00 mL) and placed in a round bottom flask. Afterwards K<sub>2</sub>CO<sub>3</sub> (0.187 mmol, 1.5 equiv) was added, followed by methyl iodide (0.138 mmol, 1.1 equiv) The mixture was refluxed overnight, then was cooled to room temperature and 10 mL of water were added. The product was extracted twice with EtOAc and the organic layers were washed with water, brine and dried over MgSO<sub>4</sub>. After filtration and removal of solvents, the title compound **7** was obtained in spectroscopically pure form without further purification as yellowish oil in 88% yield (2 steps). <sup>1</sup>H-NMR (CDCl<sub>3</sub> 400MHz)  $\delta$  = 7.29 (m, 4H), 7.20-7.15 (m, 1H), 7.08 (d, J = 9.4 Hz, 1H), 6.49-6.45 (m, 2H), 4.55 (t, J = 8.4 Hz, 1H), 3.79 (s, 3H), 3.77 (s, 3H), 3.64-3.52 (m, 2H), 2.36-2.27 (m, 1H), 2.24-2.15 (m, 1H); <sup>13</sup>C NMR (CDCl<sub>3</sub> 100MHz)  $\delta$  = 159.1, 157.8, 144.8, 128.5, 128.2, 128.0, 125.9, 125.3, 104.5, 98.6, 61.2, 55.5, 55.3, 38.5, 37.8;  $[\alpha]_{\text{D}}^{20}$  = -41 (c = 0.82, in CHCl<sub>3</sub>). The *ee* was determined by chiral stationary phase HPLC (Chiralpak AD-H, *n*-Hexane/*i*-PrOH 80:20, flow = 0.75mL/min,  $\lambda$  = 234 nm,  $t_{\text{maj}}$  = 18.3 min,  $t_{\text{min}}$  = 10.6 min, *ee* = 92%).

## 5.5. Conclusion

The first example of an organocatalytic asymmetric reaction with *o*-QMs which exploit Brønsted basic conditions for the *in situ* generation of these challenging intermediates has been disclosed. The reactive *o*-QMs have been generated from the corresponding sulfones derivatives **2** and were productively engaged with Meldrum's acid as nucleophilic partner in the presence of 9-amino(9-deoxy)*epi* quinine squaramide as the catalyst, together with sodium bicarbonate as stoichiometric inorganic base. A series of control experiments allowed us to delineate a plausible catalytic cycle in which the bifunctional catalysts derived from *Cinchona* alkaloids is responsible for the *in situ* generation of the electrophilic intermediate, while the role of the inorganic base was found to be the regeneration of the catalyst, hence permitting its turnover. Remarkably,

our protocol could be readily applied to substrates devoid of electron-donating group and therefore able to stabilize the deriving *o*-QMs. This outcome confers broad applicability to our approach, furnishing different substituted 4-aryl-3,4-dihydrocoumarines **4** with excellent yields and enantioselectivities. Furthermore, the usefulness of our strategy was testified by the formal syntheses of tolterodine (an antimuscarinic drug), methoxydalbergione (a natural quinone), and SB-209670/SB-217242 (endothelin antagonists), from the catalytic products.<sup>135,149</sup>

The scope of the reaction was also extended to different nucleophilic reaction partners: malononitrile could be engaged in the reaction, under the same conditions employed for Meldrum's acid, furnishing enantioenriched compounds **5**, whose 2-amino-4*H*-4-chromenes-3-carbonitrile framework is a biologically valuable scaffold.<sup>150</sup> Finally, also 1,3-diketones (*e.g.* acetylacetone and dimedone) and 3-ketoesters (*e.g.* methyl- and *tert*-butyl acetoacetate) underwent the organocatalytic reaction with the *in situ* generated *o*-QMs, affording the corresponding 4*H*-chromenes with good results.

While this project was in progress, other examples dealing with the asymmetric transformation of *in situ* generated *o*-QMs appeared on the scientific literature,<sup>154</sup> remarking once again the great appeal related to the intriguing chemistry of these intermediates. Nevertheless, with the exception of one paper which is based on the same concepts outlined in this chapter, and which appeared in the literature after the submission of our work, we think that our strategy can be considered fully complementary to the other contributions, giving a new and versatile asymmetric entry to 3,4-dihydrocoumarines, 4*H*-chromenes and xantenones. In fact, not only the Brønsted basic generation of *o*-QMs was unprecedented, allowing us to exploit a basic catalyst for the enantioselective reaction; but also it was demonstrated the broad scope of our protocol towards different nucleophilic partners such as Meldrum's acid, which possesses greater synthetic potential,<sup>149</sup> but has never been used before in these kinds of transformations.

## 6. A new organocatalytic strategy for $\alpha$ -alkylation of aldehydes: asymmetric 1,6-conjugated addition of enamine-activated aldehydes to *para*-quinone methides.

The procedures and results here described are part of- and can be found in-:

- Caruana, L.; Kniep, F.; Johansen Kiilerich, T.; Poulsen, H. P.; Jørgensen, K. A. “A new organocatalytic concept for asymmetric  $\alpha$ -alkylation of aldehydes”. *J. Am. Chem. Soc.* **2014**, *136*, 15929.

This work was carried out at the Department of Chemistry, University of Aarhus, Denmark, supported by “Marco Polo” fellowship of the University of Bologna, Italy. The author of this Doctoral Thesis gratefully acknowledges.

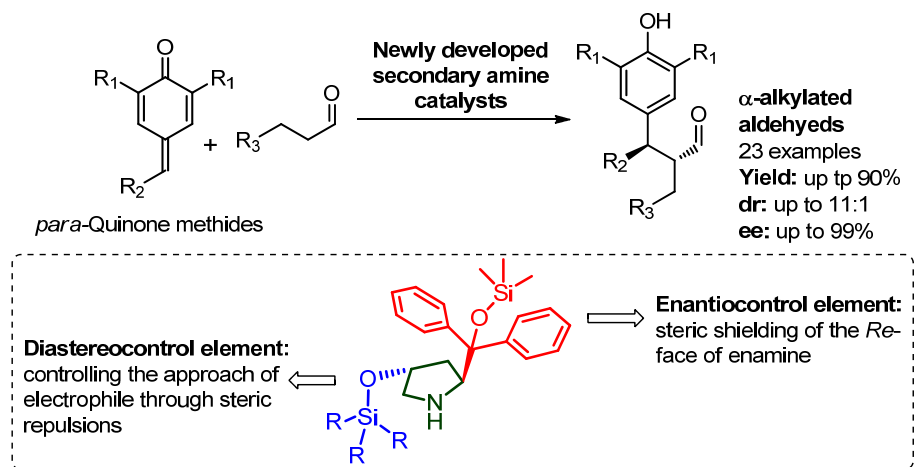
---

### ABSTRACT

Organocatalytic  $\alpha$ -alkylation of aldehydes is recognized as a challenging goal in organic chemistry.<sup>155</sup> After the development of amino-based catalysts,<sup>23,43</sup> enamine activation of aldehydes has emerged as a reliable strategy to achieve asymmetric  $\alpha$ -alkylated compounds.<sup>3</sup> Addition of aldehydes to a diarylmethine moiety is a well-known example which has been thoroughly investigated. For instance, diaryl alcohols<sup>156</sup> and diaryl halides<sup>157</sup> can be employed for *in-situ* generation of benzhydryl carbocations which react with an enamine-activated aldehyde, in a S<sub>N</sub>1-type mechanism. Nevertheless, the requirement of highly stabilized and symmetrical carbocations constitutes a limitation of these protocols, hence reducing the generality of the reaction and inhibiting the possibility to generate more sophisticated structures.

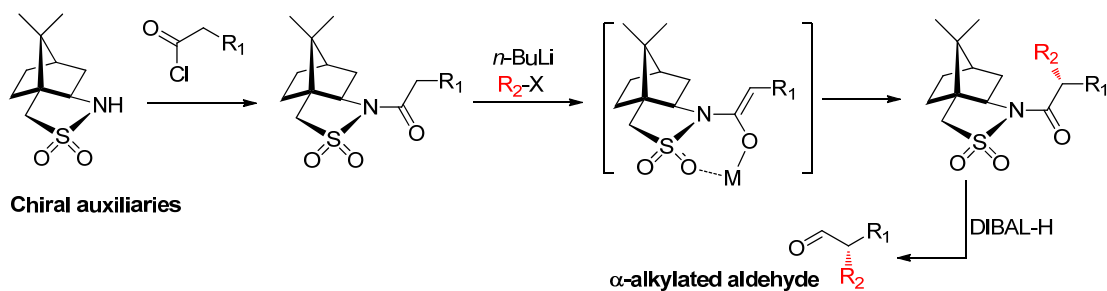
Prompted by the aim to generate  $\alpha$ -benzhydrylated aldehydes with more than one stereocenter, we have exploited the pronounced reactivity of *para*-quinone methides<sup>129</sup> as Michael acceptors and we have developed a novel organocatalytic, asymmetric  $\alpha$ -alkylation of aldehydes triggered by 1,6-conjugated addition of enamine to *para*-quinone methides. In order to take on the challenge of both diastereo- and enantiocontrol, we designed a new generation secondary amine catalyst in which the (diphenylmethyl)trimethylsiloxy group was flanked by another bulky silyloxy moiety, placed at the C4-position of the pyrrolidine ring and in trans relationship. We envisaged that the (diphenylmethyl)trimethylsiloxy group could effectively shield one face of the enamine providing enantiocontrol, while the other silyloxy moiety could sterically determine the approach of the *para*-quinone methide to the enamine, thus ensuring diastereocontrol. Under these optimized conditions the desired functionalized aldehydes

were obtained in high yields, excellent enantioselectivities and good diastereoselectivities under mild conditions



## 6.1. Background

At the beginning of 21<sup>st</sup> century, the pioneering works of List<sup>18</sup> on enamine activation and MacMillan<sup>19</sup> on iminium ion activation of carbonyl compounds triggered the so called “gold rush” of aminocatalysis.<sup>23</sup> Since then an enormous number of organocatalytic transformations promoted by primary or secondary amines have been developed with excellent outcomes.<sup>9,23,43</sup> Some topics have particularly attracted the attention of chemists involved in this research field, one of which was certainly the  $\alpha$ -alkylation of aldehydes.<sup>155</sup> This transformation represents one of the most effective routes to establish new stereocenters and C-C bonds in organic reactions. In general, the classic (and so far most successful) approach to the  $\alpha$ -alkylation of carbonyl compounds has involved the formation of metal enolates and treatment with different alkyl halides by a S<sub>N</sub>2 mechanism; this strategy can be rendered asymmetric by the use of stoichiometric amounts of chiral auxiliaries, as exemplified in Scheme 68.<sup>158</sup>



**Scheme 68.** Oppolzer's strategy for asymmetric alkylation of aldehydes mediated by chiral auxiliaries, through the formation of metal enolates (Oppolzer, 1989 see ref. 159a)

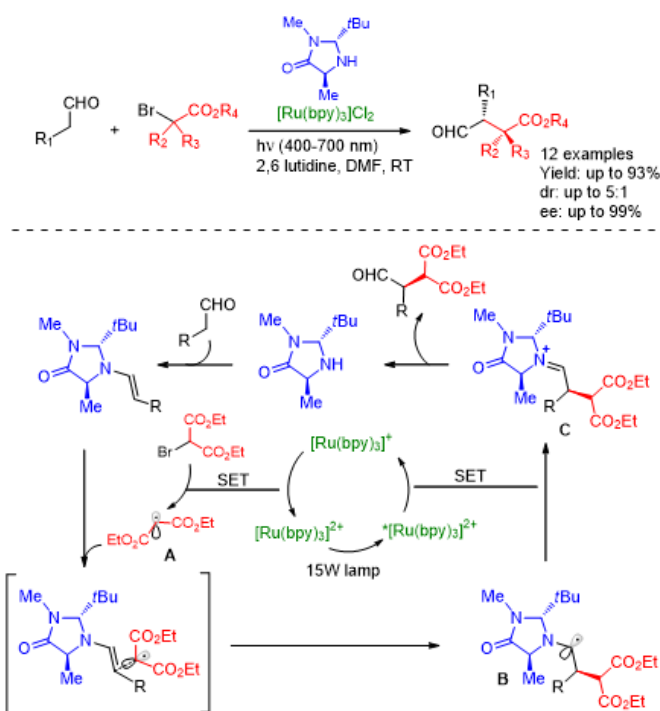
After the advent of organocatalysis, it became clear that the enamine-activation of aldehydes promoted by secondary amine catalysts, could be a straightforward approach to achieve  $\alpha$ -alkylated derivative. However, the difficulties surrounding development of suitable methodologies have brought the  $\alpha$ -alkylation of aldehydes to become a “Holy Grail” of organocatalysis.<sup>159</sup> Indeed, the reason that  $\alpha$ -alkylation of aldehydes is such a challenging goal is due to the potential occurrence of side reactions, including *N*- or *O*-alkylation of the catalyst or undesired self-aldolization. Despite the aforementioned difficulties, significant advances have been recently reached, providing new strategies for the direct asymmetric  $\alpha$ -alkylation of aldehydes.<sup>23,155</sup> (Scheme 69).

MacMillan and co-workers described starting from 2008 the  $\alpha$ -alkylation of aldehydes by way of single electron transfer (SET) using a dual catalytic system, namely an imidazolidinone secondary amine and a photoredox catalysts.<sup>160</sup> The reaction pathway was rationalized by two intertwined catalytic cycles (Scheme 69). Initiation of the reaction occurs through application of a suitable light source (*e.g.* a household 15W fluorescent light bulb),

which excites the photoredox catalyst  $[\text{Ru}(\text{bpy})_3]^{2+}$  to a higher energy state  $^*[\text{Ru}(\text{bpy})_3]^{2+}$ . This

excited species oxidizes a sacrificial quantity of (in situ generated) enamine, creating a reduced ruthenium complex  $[\text{Ru}(\text{bpy})_3]^+$ . The latter enters into a productive catalytic cycle by single electron transfer to the electron-deficient

organohalide substrate, regenerating  $[\text{Ru}(\text{bpy})_3]^{2+}$  and forming, by loss of halide anion, a radical A, which reacts with the enamine. This last step leads to an  $\alpha$ -alkylated amino radical B, which through SET to excited  $^*[\text{Ru}(\text{bpy})_3]^{2+}$  provides iminium C, closing the

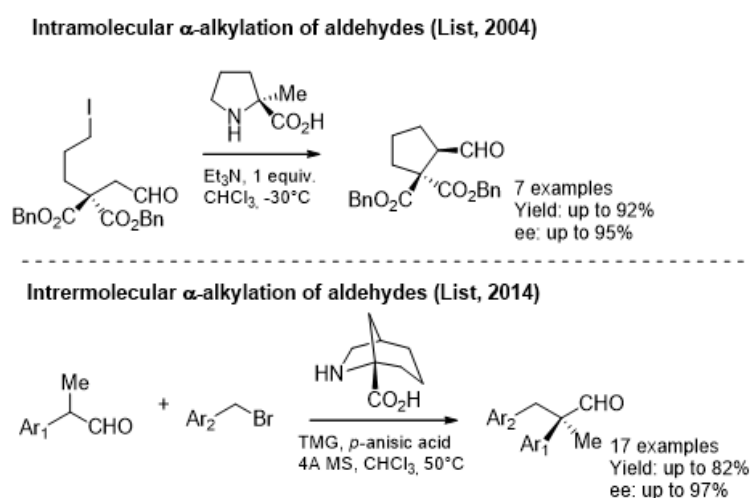


**Scheme 69.** Merging of organo- and photoredox-catalytic systems

photoredox catalytic cycle; the subsequent hydrolysis of C affords the alkylated aldehydes. This chemistry represents a modern, elegant and efficient strategy for the  $\alpha$ -alkylation of aldehydes,<sup>161</sup> even though it requires electrophilic organohalide partners that contain a radical-stabilizing group. Besides, the cost of ruthenium-based photocatalysts needs also to be considered.

A more conventional approach had been already reported by List and co-workers, describing the intramolecular  $\alpha$ -alkylation reaction of haloaldehydes using proline-based enamine catalysis (Scheme 70, top).<sup>162</sup> Interestingly, the  $\alpha$ -geminal methyl substitution in the proline catalyst increased the enantioselectivity of the reaction, either by increasing the population of the *anti*-conformer of the *trans*-enamine, or by minimizing the enamine-(re)formation from the cyclized product. The intermolecular version of this reaction remained elusive until 2014, when the same group described the catalytic asymmetric  $\alpha$ -benzylation of aldehydes (Scheme 70, bottom).<sup>163</sup> Racemic  $\alpha$ -branched aldehydes were converted into the corresponding products in a dynamic kinetic asymmetric transformation. A sterically demanding bicyclic proline analogue catalyzed this reaction, delivering aldehydes with a quaternary center in  $\alpha$ -position in high enantioselectivity.

The broad time span between these two reports highlights the difficulties in the development of intermolecular version  $\alpha$ -alkylation of aldehydes via an  $S_N2$  mechanism.

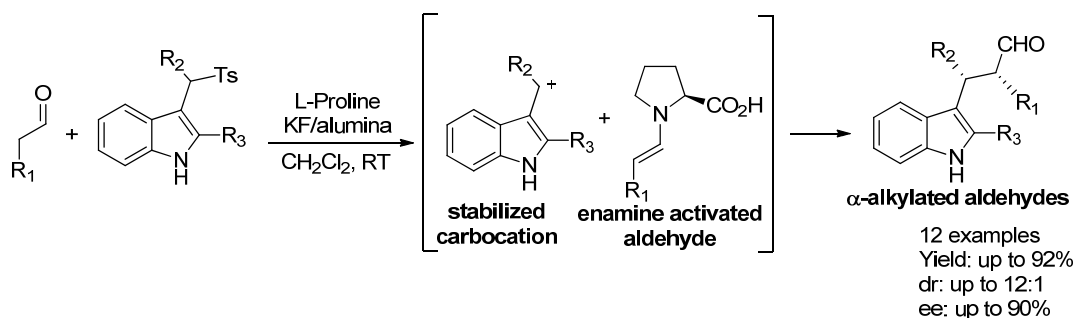


**Scheme 70.** Intramolecular and intermolecular  $\alpha$ -alkylations of aldehydes described by List's group.

Indeed, the catalyst-alkylation reaction, as well as the tendency of aldehydes to undergo self-aldolization and racemization provide intrinsic complications for this type of reactions. In order to overcome these problems, the authors utilized  $\alpha$ -branched aldehydes, as the corresponding products are stable and do not undergo racemization. Concomitantly, the reaction was performed in an acid/base “buffer system” (*i.e.* TMG and *p*-anisic acid) in order to accelerate the enamine formation through mild acid

catalysis, neutralize the hydrogen halide acidic by-product and finally suppress the *N*-alkylation of the catalyst.

While the  $S_N2$   $\alpha$ -alkylation of aldehydes is a significant challenge, the  $S_N1$ -based organocatalytic approach was devised in 2008 by Melchiorre and Petrini, reporting the first intermolecular  $\alpha$ -alkylation of aldehydes.<sup>164</sup> Key for the success was the employment of 3-(1-arylsulfonylalkyl)indoles, substrates amenable to generate highly stabilized carbocations. In this transformation, a stabilized carbocation was generated upon the elimination of a tosyl group, mediated by KF supported on basic alumina; the resulting intermediate reacted with the enamine derived from the condensation of L-proline to the aldehyde. The subsequent hydrolysis of the catalyst afforded the  $\alpha$ -alkylated product in excellent results in term of yields and enantioselectivities, while the diastereoselectivity was only moderate in some cases (Scheme 71).

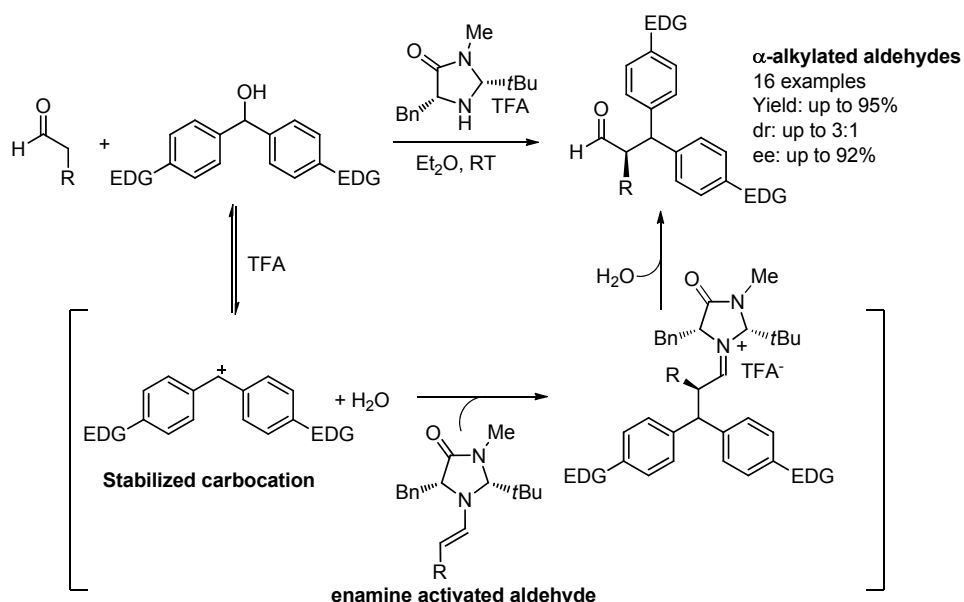


**Scheme 71.** Melchiorre's strategy for  $\alpha$ -alkylation of aldehydes: stabilized carbocations, derived from 3-(1-arylsulfonylalkyl)indoles, reacted with enamine-activated aldehydes.

Subsequently, other groups have contributed additional methods for the asymmetric  $\alpha$ -alkylation of aldehydes, combining enamine catalysis with the generation of cationic species as reactive partners. In particular, the enantioselective addition of aldehydes to diarylmethine moieties represents one of the most explored possibilities to install alkyl substituents at the  $\alpha$ -position of the carbonyl center. In this context, the use of diaryl alcohols for the *in situ* generation of a reactive carbocation has been pioneered by Cozzi et al.<sup>156a</sup> This work merges two concepts: namely enamine catalysis and Mayr's electrophilicity/nucleophilicity scale.<sup>112</sup> The Mayr scale provided inspirational reading material for this  $S_N1$ -type chemistry, categorizing a broad range of nucleophiles and electrophiles as a function of two parameters namely nucleophilic parameter *N* and electrophilic parameter *E*. The second order reaction rate constant *k* in a reaction between a nucleophile and an electrophile is related to those parameters *N* and *E* and to a nucleophile-dependent slope parameter *s* and can be formulated as follow:

$$\log(k) = s(N+E)^{165}$$

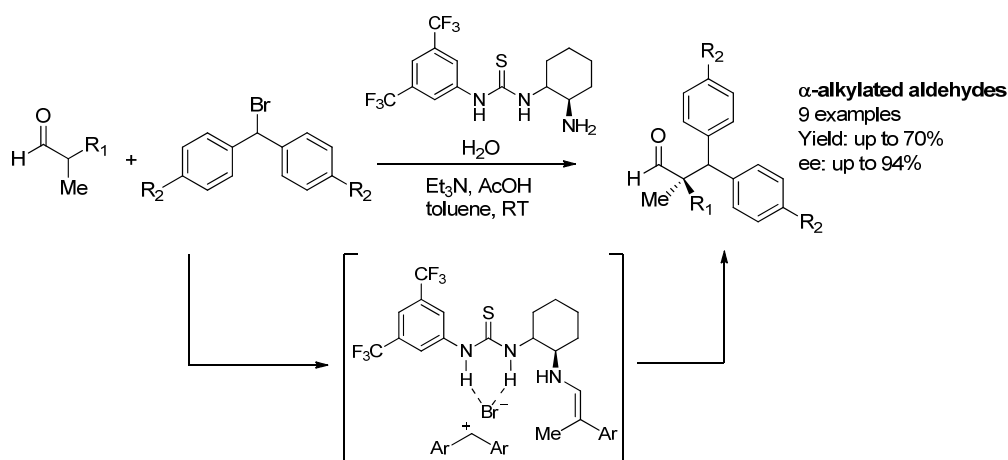
Several  $S_N1$ -type reactions can be rationally designed using the Mayr scale of reactivity. To design carbenium ion reactions, however, it is important to consider both the electrophile and the nucleophile; indeed, a reaction cannot be observed if an unsuitable nucleophile is used. Mayr has established a predictive ‘rule of thumb’ ( $N + E > -5$ )<sup>166</sup> for a successful reaction between an electrophile and a nucleophile, ignoring steric effects. Cozzi and co-workers hypothesized that highly nucleophilic enamine-activated aldehydes, could be reacted with stabilized carbocation generated upon water elimination from the corresponding diaryl alcohols; the addition of strong acids such as trifluoroacetic acid (TFA) was crucial for carbocation formation. MacMillan’s catalysts showed high efficiency and gave the alkylated products in satisfactory enantioselectivities, albeit moderate diastereoselectivities (Scheme 72). This elegant methodology, allowing the direct enantioselective  $\alpha$ -alkylation of aldehydes, paved the way for a new avenue for the realization of this important reaction, by following Cozzi’s strategy.<sup>156</sup> Nevertheless, this methodology was limited by the nature of alcohol, which must be able to generate a stable carbocation. Thus, only substrates bearing electron-donating substituents on the phenyl ring could be productively engaged in the organocatalytic transformation.



**Scheme 72.** Cozzi’s strategy for  $\alpha$ -alkylation of aldehydes: stabilized carbocations, derived from diaryl alcohols, reacted with enamine-activated aldehydes.

Similarly, Jacobsen and co-workers developed another protocol for the  $\alpha$ -alkylation of aldehydes by means of hydrogen-bond catalysis and anion binding.<sup>157</sup> The authors took

advantage of the anion binding properties of thioureas to promote the anion abstraction from a neutral precursor (*i.e.* a diaryl bromide), generating a reactive carbocation. The thus formed electrophilic species was reacted with  $\alpha$ -branched aldehydes to furnish the alkylated product. The best catalyst was a primary thiourea, which induced good reactivity and enantioselectivity. The primary amine forms the enamine intermediate with the  $\alpha$ -branched aldehydes, while the thiourea moiety has the crucial role of activating the electrophile and promote the enantioinduction (Scheme 73). The proposed mechanism proceeds via a carbocation associated to the catalyst, once again in an  $S_N1$ -like mechanism.



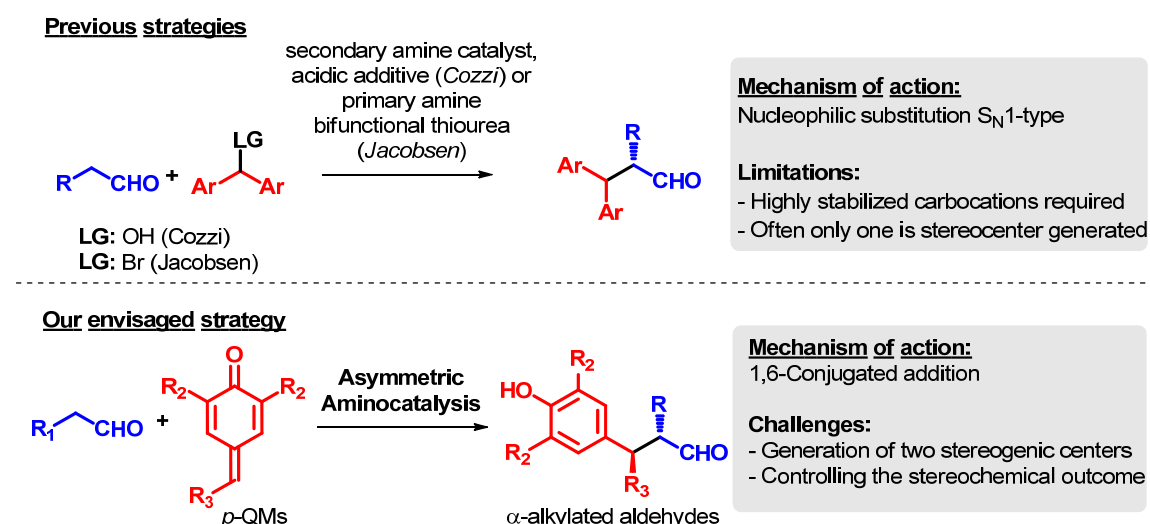
**Scheme 73.** Jacobsen's strategy for  $\alpha$ -alkylation of aldehydes: stabilized carbocations, derived from diaryl bromide (upon anion abstraction), reacted with enamine-activated aldehydes.

Despite these latter reports, some issues related to the preparation of alpha-alkylated aldehydes through enamine catalysis still remained elusive. A major limitation of the reactions proceeding via a  $S_N1$ -like mechanism is the requirement of highly stabilized carbocation for the reaction to occur; thus limiting the scope of the reaction to diaryl substrates bearing strong electron-donating group on the phenyl ring. Moreover, the simultaneous formation of diarylmethine stereocenter, applying unsymmetrically substituted benzhydryl carbocations, and the control of the diastereoselectivity in these kind of reaction still remained an unsolved challenge.<sup>156a,c,f,164</sup>

## 6.2. Aim of the work

In the  $\alpha$ -alkylation proceeding via a  $S_N1$ -like mechanism, the precursor of the reactive carbocation must be symmetrically substituted with electron-donating moiety. This requirement not only reduces the synthetic versatility of the approach, but restricts to only one possible stereocentres on the alkylated product. In order to overcome these

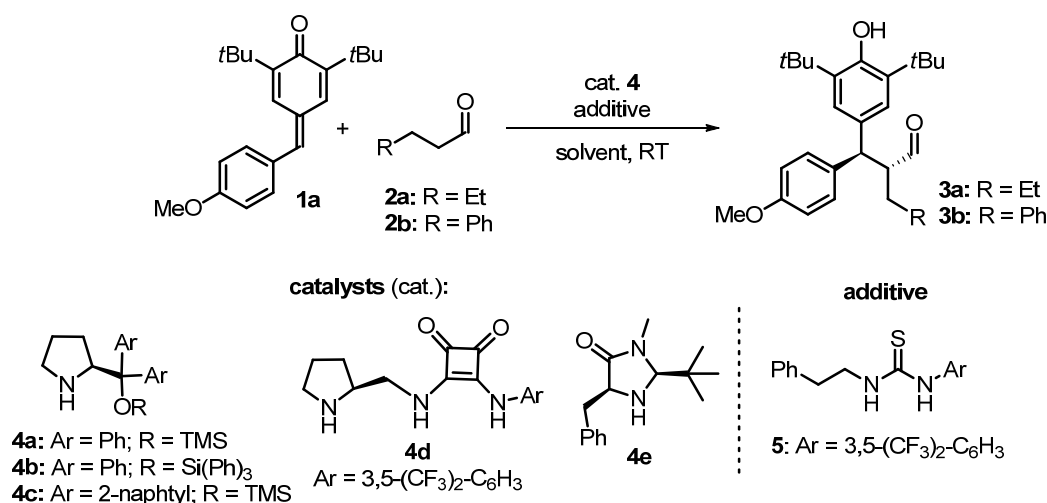
limitations, we reasoned that the  $\alpha$ -alkylation of aldehydes with unsymmetrically substituted benzhydryl moieties and the consequent formation of two contiguous stereocenters might be feasible by applying *p*-QMs as electrophile. Thus, stimulated by the aim of adorning the  $\alpha$ -position of aldehydes with a diarylmethine stereocenter, while generating two contiguous asymmetric centers, we have envisaged a novel organocatalytic protocol for the  $\alpha$ -alkylation of aldehydes based on the enamine-mediated 1,6-conjugated addition<sup>167</sup> of aldehydes to *para*-quinone methide (*p*-QMs) (Scheme 74).<sup>129</sup> As discussed in Chapter 5, the aromatization of the cyclohexatriene ring constitutes the driving force of the 1,6-conjugated addition of nucleophiles to these substrates, thus we expect a suitable reactivity with enamine-activated aldehydes. In addition, reports describing the organocatalytic addition reactions to *p*-QMs are surprisingly scarce.<sup>168</sup> Despite the conceptual simplicity of this strategy, we were concerned about some issues related to the stereochemical outcome of the reaction, especially concerning the diastereocontrol. Given the absence of a closed transition state in which the *syn* and *anti* conformations are thermodynamically very different, here an open transition state is involved and the outcome of the reaction only depends on the size and steric repulsions of the substituents in the reactants. Thus the diastereocontrol of this transformation appeared particularly challenging



**Scheme 74.** Comparison between previous strategies and our strategy for the  $\alpha$ -alkylation of aldehydes.

### 6.3. Results and discussion

*para*-Quinone methide **1a** was readily synthesized through a Knoevenagel-type reaction between 2,6-di-*tert*-butyl phenol and *p*-anisaldehyde in the presence of stoichiometric amount of piperidine (see §6.4.2). The presence of the bulky and electron-donating *tert*-butyl groups was found to be crucial for the stability of the *p*-QM, allowing its isolation. We started our investigation by screening a series of secondary amine catalysts in the reaction of *para*-quinone methide **1a** with pentanal **2a** in CH<sub>2</sub>Cl<sub>2</sub> as solvent. Amongst the catalysts tested (Table 13, entries 1-5), only catalyst **4a** was able to complete the reaction in 24 h, delivering the product **3a**, in good conversion and high enantioselectivity, but only with poor diastereoselectivity. No improvement in diastereoselectivity was observed using different solvents (Table 13, entries 6-11). Next we realized that by the employment of hydrocinnamaldehyde **2b**, product **3b** was obtained in excellent enantioselectivity and a slightly better diastereoselectivity (Table 13, entries 12). Thus, **2b** was chosen as the most suitable aldehyde for further screenings. Interestingly, the readily available thiourea **5** could be used as a Lewis-acidic additive to accelerate the reaction, affording **3b** in high conversion without erosion of enantioselectivity. This increased reactivity may be presumably explained by considering an activation of **1a** via H-bond interaction between the carbonyl group of the *p*-QM and the thioureido moiety of **5**. However, the diastereomeric ratio (dr) was not influenced by this thiourea additive (Table 13, entries 13).

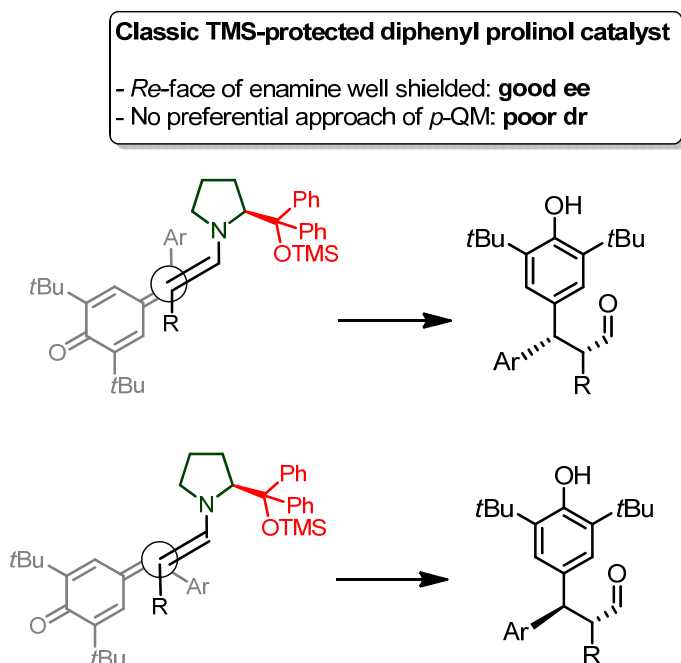
**Table 13.** First optimization of the organocatalytic reaction between *p*-QM **1a** and aldehydes **2**.<sup>a</sup>

Entry	<b>2</b>	Solvent	Cat. (mol%)	Additive (mol%)	Conversion <sup>b</sup> (%)	dr <sup>b</sup>	ee <sup>c</sup> (%)
1	<b>2a</b>	CH <sub>2</sub> Cl <sub>2</sub>	<b>4a</b> (20)	-	95	1.4:1	91
2	<b>2a</b>	CH <sub>2</sub> Cl <sub>2</sub>	<b>4b</b> (20)	-	58	1.2:1	88
3	<b>2a</b>	CH <sub>2</sub> Cl <sub>2</sub>	<b>4c</b> (20)	-	77	2.0:1	90
4	<b>2a</b>	CH <sub>2</sub> Cl <sub>2</sub>	<b>4d</b> (20)	-	31	1.1:1	nd
5	<b>2a</b>	CH <sub>2</sub> Cl <sub>2</sub>	<b>4e</b> (20)	-	55	1.2:1	nd
6	<b>2a</b>	Toluene	<b>4a</b> (20)	-	22	1.8:1	77
7	<b>2a</b>	THF	<b>4a</b> (20)	-	65	1.2:1	86
8	<b>2a</b>	MeCN	<b>4a</b> (20)	-	>95	1.2:1	66
9	<b>2a</b>	MeOH	<b>4a</b> (20)	-	91	1.4:1	36
10	<b>2a</b>	CHCl <sub>3</sub>	<b>4a</b> (20)	-	82	1.5:1	92
11	<b>2a</b>	EtOAc	<b>4a</b> (20)	-	75	1.3:1	88
12	<b>2b</b>	CH <sub>2</sub> Cl <sub>2</sub>	<b>4b</b> (20)	-	75	1.8:1	99
13	<b>2b</b>	CH <sub>2</sub> Cl <sub>2</sub>	<b>4b</b> (20)	<b>5</b> (20)	>95	1.7:1	99

(a) Reaction conditions: *p*-QM **1a** (0.05 mmol), aldehydes **2a** or **2b** (0.075 mmol), catalysts **4** (0.01 mmol), additive **5** (0.01 mmol), solvent (0.200 mL), reaction time: 24 h. (b) Determined by <sup>1</sup>H NMR of the crude reaction mixture. (c) Determined by Chiral Stationary Phase UPC<sup>2</sup> and referred to the major diastereoisomer.

At this stage, it seemed that the diastereoselectivity of the reaction could not be improved only by variation of the reaction conditions. In order to understand the origin of the low diastereoselectivity, an epimerization test was carried out by treating the major diastereoisomer of **3b** with 20 mol% of (±) **4a**. No epimerization was observed after 48 h. Hence, the catalyst cannot form an enamine species with the alkylated aldehyde which would lead to loss of stereoinformation at the α-carbon atom. On this experimental

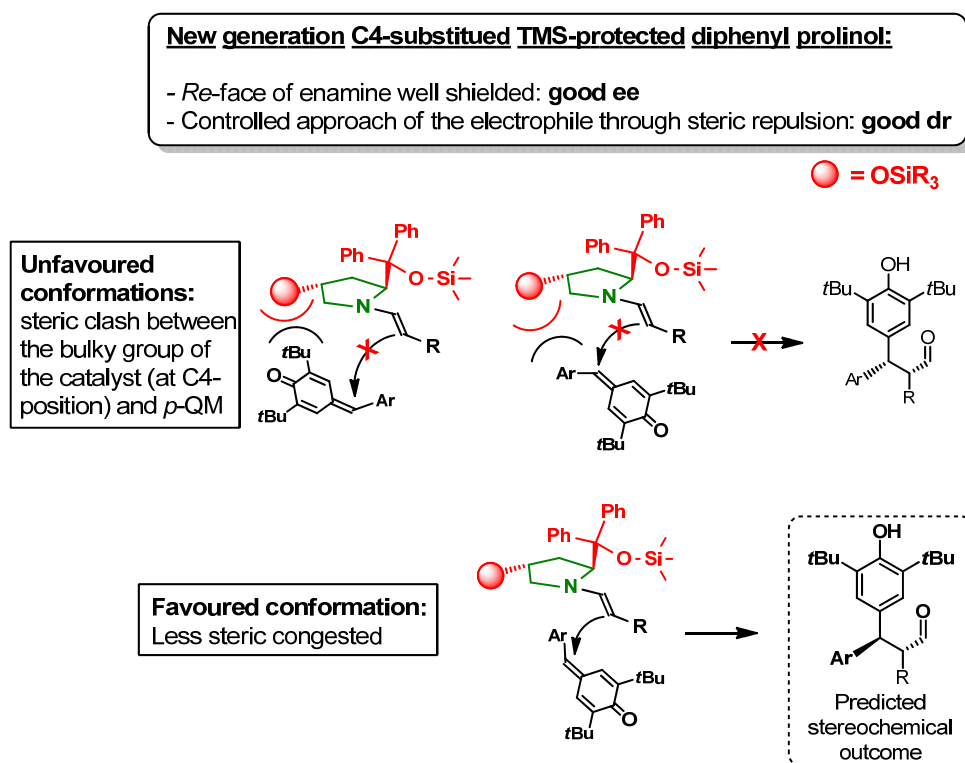
evidence, it was hypothesized that an uncontrolled approach of the *p*-QM to the enamine-activated aldehyde might justify the lack of diastereoselectivity at the benzhydrylic stereocenter. On the basis of the generally accepted mode of enantioinduction of diaryl prolinols catalysts,<sup>43c</sup> the bulky (diphenylmethyl)-TMS group on the catalyst shields the *Re* face of the enamine, allowing the *p*-QM to approach only from the less hindered face, and providing for the enantiocontrol. However, given the planarity of *p*-QM as well as the significant distance between the bulky *t*Bu group and the prochiral benzhydryl center, in combination with the lack of sterical elements blocking a preferential conformation, both the configuration that will lead to the *syn* and *anti* product are equally probable, delivering a mixture of diastereoisomer at the benzhydrylic stereocenter (Scheme 75).



**Scheme 75.** Model accounting for the observed low diastereoselectivity in the reaction between *p*-QMs **1** and enamine-activated aldehydes by Jørgensen-Hayashi catalyst. An antiperiplanar TS is considered.

With the aim to tackle the challenge to improve the diastereoselectivity of this reaction, we synthesized a new set of secondary amine catalysts (see § 6.4.3 and 6.4.4 for details). Here, the (diphenylmethyl)trimethylsilyloxy group was flanked by another bulky silyloxy moiety, placed at the C4-position of the pyrrolidine ring and in a trans relationship. We envisaged that the (diphenylmethyl)trimethylsilyloxy group could effectively shield one face of the enamine providing enantiocontrol, while the other silyloxy moiety could

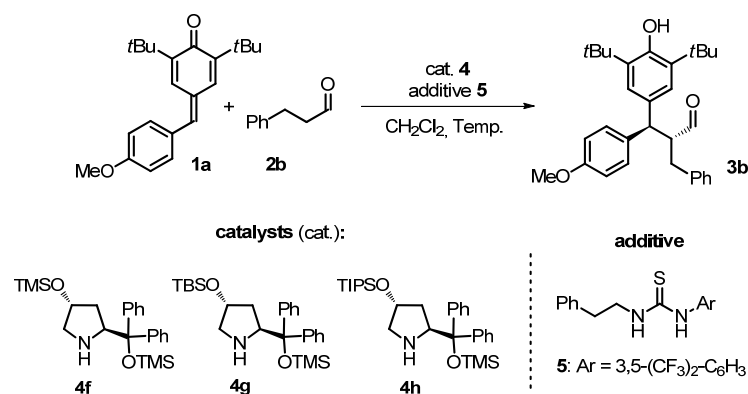
sterically determine the approach of the *para*-quinone methide to the enamine, thus ensuring diastereocontrol (Scheme 76).



**Scheme 76.** Plausible mode of stereoinduction in the reaction between *p*-QMs **1** and enamine-activated aldehydes by means of newly developed C4-substituted TMS-protected diphenyl prolinol catalyst.

Gratifyingly, the use of catalyst **4f** led to a promising enhancement of the diastereoselectivity, still maintaining high enantioselectivity (Table 14, entry 1).

Speculating that a protection group larger than trimethylsilyl (TMS) at the peripheral C4-hydroxy group could have an even more positive influence on the diastereoselectivity, we installed a *tert*-butyl(dimethyl)silyl group (TBS) as well as a tri(isopropyl)silyl group (TIPS) at this site. To our delight, catalysts **4g** and **4h** could indeed further improve the diastereoselectivity, while the enantioselectivity remained excellent (Table 14, entries 2, 3). The sterically most demanding catalyst **4h** was superior to catalysts **4f** and **4g**. With this catalyst a further enhancement of the diastereomeric ratio was achieved by reducing the temperature to 4 °C, although an additional decrease to -35 °C led to a low conversion even after prolonged time. (Table 14, entries 4, 5). Finally, by increasing the amount of thiourea **5** to 30 mol%, we were able to lower the loading of the aminocatalyst to 10 mol% upon prolonged reaction time to 48 h (Table 14, entry 6).

**Table 14.** Final optimization of the organocatalytic reaction between *p*-QM **1a** and aldehyde **2b**.<sup>a</sup>

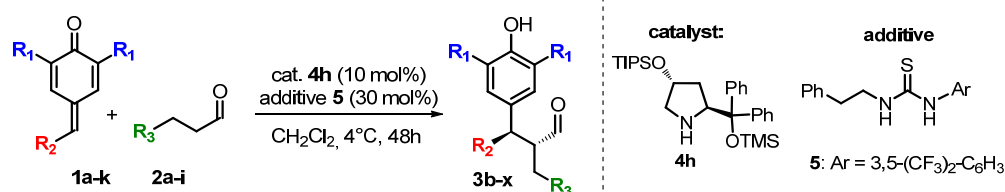
Entry	Cat. (mol%)	Additive (mol%)	T (°C)	Conversion <sup>b</sup> (%)	dr <sup>b</sup>	ee <sup>c</sup> (%)
1	<b>4f</b> (20)	<b>5</b> (20)	RT	90	4.7:1	99
2	<b>4g</b> (20)	<b>5</b> (20)	RT	>95	5.1:1	99
3	<b>4h</b> (20)	<b>5</b> (20)	RT	>95	6.8:1	99
4	<b>4h</b> (20)	<b>5</b> (20)	4	>95	7.8:1	99
5 <sup>d</sup>	<b>4h</b> (20)	<b>5</b> (20)	-35	45	9.6:1	99
6 <sup>e</sup>	<b>4h</b> (10)	<b>5</b> (30)	4	>95	7.9:1	99

(a) Reaction conditions: *p*-QM **1a** (0.05 mmol), aldehyde **2b** (0.075 mmol), catalysts **4** (10-20 mol%), additive **5** (20-30 mol%), dichloromethane (0.200 mL), reaction time: 24 h. (b) Determined by <sup>1</sup>H NMR of the crude reaction mixture. (c) Determined by Chiral Stationary Phase UPC<sup>2</sup> and referred to the major diastereoisomer. (d) Reaction time: 72 h. (e) Reaction time: 48 h.

With the optimized reaction conditions in hand, the scope of the reaction was investigated. A broad set of *para*-quinone methides **1a-f** bearing electron-rich, electron-neutral and electron-deficient aromatic moieties were reacted with hydrocinnamaldehyde **2b**, affording the corresponding  $\alpha$ -alkylated aldehydes **3b-g** in good yield and high diastereo- and enantioselectivity (Table 15, entries 1-6). It is notable that the heteroaromatic substituted *p*-QMs **1g-i** also reacted smoothly and afforded the corresponding  $\alpha$ -alkylated aldehydes **3h-j** with similar yields and comparable stereoselectivities as their aromatic analogues (Table 15, entries 7-9). Due to decomposition of the *para*-quinone methide, the reaction of **1j**, in which R<sub>2</sub> is a methyl substituent, afforded product **3k** in lower yield and only moderate stereoselectivity (Table 15, entry 10). On the other hand, replacing the *tert*-butyl (*t*Bu) substituents R<sub>1</sub> for methyl groups did not change the yield and stereoselectivity of the reaction significantly (Table 15, entry 11). Next we turned our attention to the aldehyde scope. A series of aldehydes **2c-i** bearing differently substituted aromatic rings was tolerated and furnished products **3m-s** in good yield under high stereocontrol (Table 15, entries 12-18).

Interestingly, an aliphatic aldehyde such as pentanal **2a** afforded a slightly decreased but still decent diastereoselectivity, while the enantioselectivity remained excellent (Table 15, entry 19). This indicates that bulky substituents at the aldehyde, such as a phenyl ring, contribute to the diastereocontrol of the reaction. Finally, the aldehyde scope was expanded to the brominated *para*-quinone methide **1e**. Also in these cases the reactions proceeded smoothly, delivering compounds **3u-x** in good yield and high stereoselectivity (Table 15, entries 20-23).

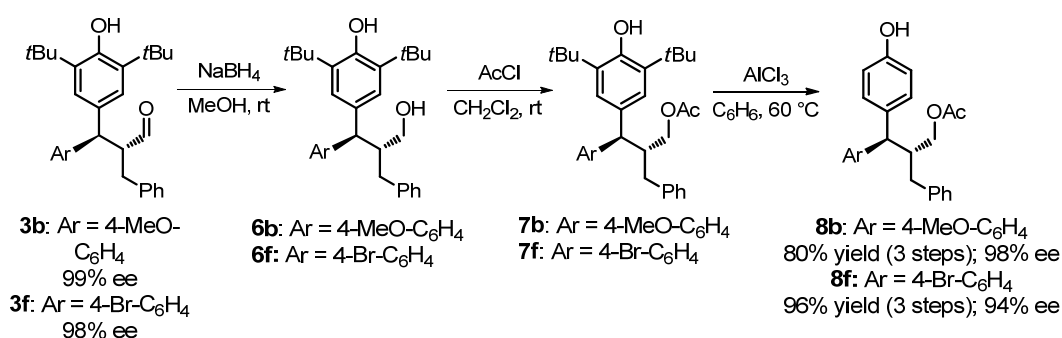
**Table 15.** Scope of the organocatalytic  $\alpha$ -alkylation of aldehydes via 1,6-conjugated addition of enamine-activated aldehydes to *para*-quinone methides.



Entry	1	2	3-yield <sup>b</sup> (%)	dr <sup>c</sup>	ee <sup>d</sup> (%)
1	<b>1a</b> ( <i>t</i> Bu, 4-(MeO)C <sub>6</sub> H <sub>4</sub> )	<b>2b</b> (C <sub>6</sub> H <sub>5</sub> )	<b>3b</b> -79	7.9:1	99
2	<b>1b</b> ( <i>t</i> Bu, C <sub>6</sub> H <sub>5</sub> )	<b>2b</b> (C <sub>6</sub> H <sub>5</sub> )	<b>3c</b> -84	9.4:1	99
3	<b>1c</b> ( <i>t</i> Bu, C <sub>6</sub> D <sub>5</sub> )	<b>2b</b> (C <sub>6</sub> H <sub>5</sub> )	<b>3d</b> -78	8.3:1	99
4	<b>1d</b> ( <i>t</i> Bu, 4-(NO <sub>2</sub> )C <sub>6</sub> H <sub>4</sub> )	<b>2b</b> (C <sub>6</sub> H <sub>5</sub> )	<b>3e</b> -71	7.0:1	98
5	<b>1e</b> ( <i>t</i> Bu, 4-BrC <sub>6</sub> H <sub>4</sub> )	<b>2b</b> (C <sub>6</sub> H <sub>5</sub> )	<b>3f</b> -83	10.2:1	98
6	<b>1f</b> ( <i>t</i> Bu, 3,5-(Me) <sub>2</sub> -C <sub>6</sub> H <sub>4</sub> )	<b>2b</b> (C <sub>6</sub> H <sub>5</sub> )	<b>3g</b> -90	11.0:1	99
7	<b>1g</b> ( <i>t</i> Bu, 2-furanyl)	<b>2b</b> (C <sub>6</sub> H <sub>5</sub> )	<b>3h</b> -55	2.0:1	92
8	<b>1h</b> ( <i>t</i> Bu, 2-thiophenyl)	<b>2b</b> (C <sub>6</sub> H <sub>5</sub> )	<b>3i</b> -72	3.7:1	99
9 <sup>e</sup>	<b>1i</b> ( <i>t</i> Bu, 4-pyridyl)	<b>2b</b> (C <sub>6</sub> H <sub>5</sub> )	<b>3j</b> -67	8.2:1	99
10 <sup>f</sup>	<b>1j</b> ( <i>t</i> Bu, Me)	<b>2b</b> (C <sub>6</sub> H <sub>5</sub> )	<b>3k</b> -40	5.5:1	80
11	<b>1k</b> (Me, C <sub>6</sub> H <sub>5</sub> )	<b>2b</b> (C <sub>6</sub> H <sub>5</sub> )	<b>3l</b> -76	7.5:1	99
12	<b>1b</b> ( <i>t</i> Bu, C <sub>6</sub> H <sub>5</sub> )	<b>2c</b> (4-(MeO)C <sub>6</sub> H <sub>4</sub> )	<b>3m</b> -80	8.2:1	99
13	<b>1b</b> ( <i>t</i> Bu, C <sub>6</sub> H <sub>5</sub> )	<b>2d</b> (4-MeC <sub>6</sub> H <sub>4</sub> )	<b>3n</b> -90	9.8:1	98
14	<b>1b</b> ( <i>t</i> Bu, C <sub>6</sub> H <sub>5</sub> )	<b>2e</b> (4-FC <sub>6</sub> H <sub>4</sub> )	<b>3o</b> -81	7.8:1	99
15	<b>1b</b> ( <i>t</i> Bu, C <sub>6</sub> H <sub>5</sub> )	<b>2f</b> (3,5-(Me) <sub>2</sub> C <sub>6</sub> H <sub>4</sub> )	<b>3p</b> -83	8.5:1	96
16	<b>1b</b> ( <i>t</i> Bu, C <sub>6</sub> H <sub>5</sub> )	<b>2g</b> (2-naphtyl)	<b>3q</b> -82	8.3:1	96
17	<b>1b</b> ( <i>t</i> Bu, C <sub>6</sub> H <sub>5</sub> )	<b>2h</b> (2-thiophenyl)	<b>3r</b> -82	7.5:1	95
18	<b>1b</b> ( <i>t</i> Bu, C <sub>6</sub> H <sub>5</sub> )	<b>2i</b> (Bn)	<b>3s</b> -72	5.8:1	98
19	<b>1b</b> ( <i>t</i> Bu, C <sub>6</sub> H <sub>5</sub> )	<b>2a</b> (Et)	<b>3t</b> -64	4.0:1	98
20	<b>1e</b> ( <i>t</i> Bu, 4-BrC <sub>6</sub> H <sub>4</sub> )	<b>2c</b> (4-(MeO)C <sub>6</sub> H <sub>4</sub> )	<b>3u</b> -80	8.5:1	88
21	<b>1e</b> ( <i>t</i> Bu, 4-BrC <sub>6</sub> H <sub>4</sub> )	<b>2d</b> (4-MeC <sub>6</sub> H <sub>4</sub> )	<b>3v</b> -79	10.0:1	97
22	<b>1e</b> ( <i>t</i> Bu, 4-BrC <sub>6</sub> H <sub>4</sub> )	<b>2f</b> (3,5-(Me) <sub>2</sub> -C <sub>6</sub> H <sub>4</sub> )	<b>3w</b> -86	8.7:1	99
23	<b>1e</b> ( <i>t</i> Bu, 4-BrC <sub>6</sub> H <sub>4</sub> )	<b>2h</b> (2-thiophenyl)	<b>3x</b> -79	8.3:1	92

(a) Reaction conditions: **1a-k** (0.05 mmol), **2a-i** (0.075 mmol), **4h** (0.005 mmol), **5** (0.015 mmol), dichloromethane (0.200 mL), 4°C, reaction time: 48 h. (b) Isolated yield (c) Determined by <sup>1</sup>H NMR of the crude reaction mixture. (d) Determined by Chiral Stationary Phase UPC<sup>2</sup> and referred to the major diastereoisomer. (e) Performed at RT, reaction time: 72 h. (f) Performed at -35°C.

In most of these examples the bulky *tert*-butyl groups were installed to stabilize the *para*-quinone methide. Actually, the *t*Bu is often used as a bulky protecting group in the syntheses of aromatic compounds.<sup>169</sup> Importantly, utilizing a three steps procedure, consisting of the reduction of the aldehyde, acetyl-protection of the corresponding alcohol and AlCl<sub>3</sub> mediated *de-tert*-butylation<sup>168,169</sup> the stereomerically pure aldehydes **3b** and **3f** were converted into the *de-tert*-butylated compounds **8b** and **8f** in high yield and without loss of stereoinformation (Scheme 77). Notably, in product **8b** we were able to obtain a stereocenter which is only derived from a methyl substituent at one of the hydroxy functionalities of the diphenolmethine scaffold.



Scheme 77. *De-tert*-butylation reaction sequence.

### 6.3.1. Determination of the absolute and relative configurations of compounds **3**

The absolute and relative configurations of products **3** were unambiguously assigned by single-crystal X-ray analysis<sup>82</sup> of derivative **7f**. The observed *2R,3S* configuration is in agreement with the predicted stereochemical outcome of the reaction (Scheme 76). This evidence confirms the hypothesized model for the stereinduction, consisting in the approach of the *para*-quinone methide to the enamine in the way minimizing the steric clash with the bulky pendant placed at C4-position of the catalyst **4h** (see § 6.3.2).

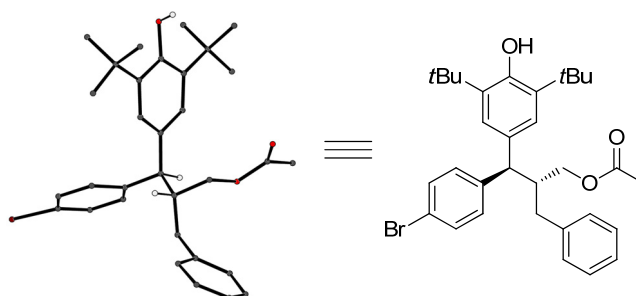
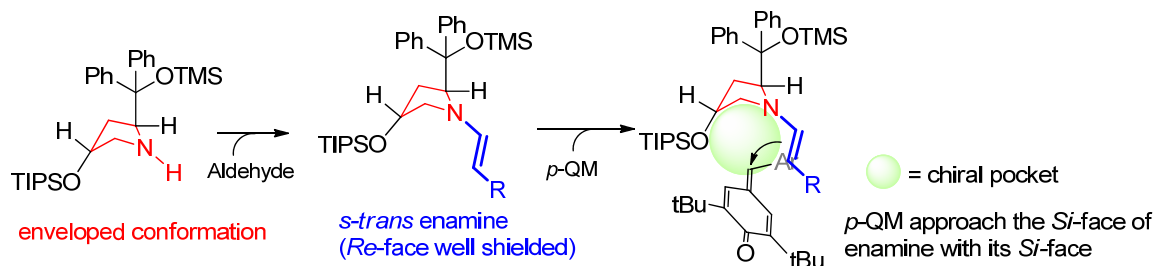


Figure 42. Crystallographic data for **7f** (hydrogen atoms are omitted).

### 6.3.2. Mechanistic proposal

To account for the observed  $2R,3S$  absolute configuration, we referred to the model depicted in Scheme 78.



**Scheme 78.** Model accounting for the observed  $2R,3S$  absolute configuration.

The pyrrolidine-based aminocatalysts are known to possess high flexibility, which induces an increased number of possible transition states; however, the stabilization of one or other conformer by insertion of specific substituents in the 4-position is well documented.<sup>170</sup> Possibly the insertion of a bulky silyloxy group in the 4-*trans*-position forces the pyrrolidine ring to assume an envelope conformation, in which the bulky substituents at C2 and C4 point towards opposite directions, in order to minimize the steric hindrance. Condensation of an aldehyde on this secondary amine catalyst results in the formation of an *s-trans* enamine, whose *Re*-face is effectively shielded by the (diphenyl)-trimethylsilyloxy group. The concomitant presence of an OTIPS group on C4-position generates a kind of “chiral pocket” in which the electrophile may approach

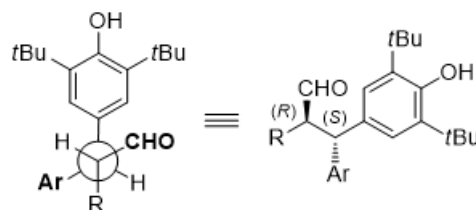


**Figure 43.**  $\alpha$ -Diarylmethine alkylated aldehyde showing  $2R, 3S$  stereochemistry

only from its own *Si*-face, namely in a *like* approach. This will lead to the observed  $2R,3S$  diastereoisomer in which the aldehyde moiety and the aryl group are placed in an *anti*-configuration (Figure 43). Other approaches of the electrophile would be too sterically congested, hence not favored.

## 6.4. Experimental details

### 6.4.1. General methods and materials

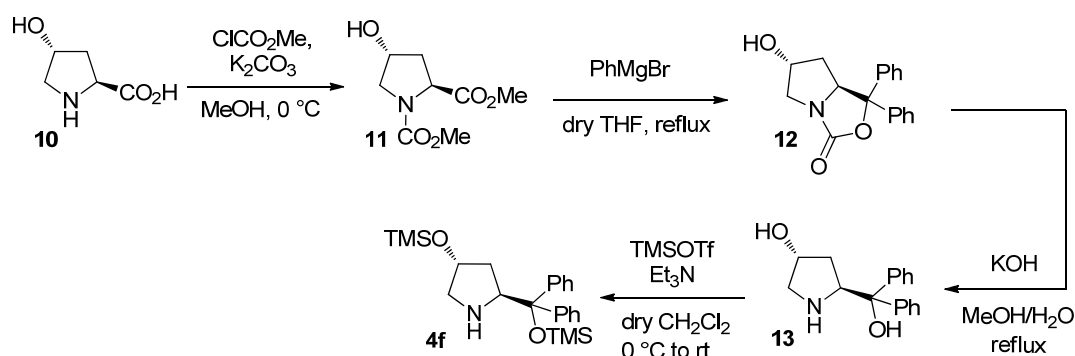
NMR spectra were acquired on a Varian AS 400 spectrometer running at 400 MHz for  $^1\text{H}$  and 100 MHz for  $^{13}\text{C}$ . Chemical shifts ( $\delta$ ) are reported in ppm relative to residual solvent signals.<sup>84</sup> The following abbreviations are used to indicate the multiplicity in

NMR spectra: s, singlet; d, doublet; t, triplet; q, quartet; m, multiplet; br s, broad signal. For characterization of isomeric mixtures \* denotes minor isomer, + denotes overlap of signals of both isomers, whereas no sign denotes signal of major isomer. The number of protons given in parenthesis is the sum over both isomers  $^{13}\text{C}$  spectra were acquired in broad band decoupled mode. Mass spectra were recorded on a micromass LCT spectrometer using electrospray ( $\text{ES}^+$ ) ionization (referenced to the mass of the neutral species) or on a Bruker Maxis Impact mass spectrometer using electrospray ( $\text{ES}^+$ ) ionization (referenced to the mass of the charged species). Dry solvents were obtained from a MBraun MB SPS-800 solvent purification system. Analytical thin layer chromatography (TLC) was performed using pre-coated aluminium-backed plates (Merk Kieselgel 60 F254) and visualized by UV radiation,  $\text{KMnO}_4$ , *p*-anisaldehyde or 2,4-dinitrophenylhydrazine stains. For flash chromatography (FC) silica gel (Silica gel 60, 230-400 mesh, Sigma-Aldrich) was used. Optical rotations were measured on a Perkin-Elmer 241 polarimeter,  $\alpha$  values are given in  $\text{deg}\cdot\text{cm}^3\cdot\text{g}^{-1}\cdot\text{dm}^{-1}$ ; concentration *c* in  $\text{g}\cdot(100\text{ mL})^{-1}$ . The diastereomeric ratio (dr) of products was evaluated by  $^1\text{H}$  NMR analysis of the crude mixture. The enantiomeric excess (ee) of products was determined by chiral stationary phase HPLC (Daicel Chiralpak) or chiral stationary phase Waters ACQUITY UPC<sup>2</sup> (Daicel Chiralpak). Organocatalytic reactions were performed by employing catalyst **4h** (see S14), however the preparation of *ent*-**4h** would have been uneconomical due to long synthetic procedures. Racemic samples were prepared using racemic ( $\pm$ )- $\alpha,\alpha$ -diphenyl-2-pyrrolidinemethanol trimethylsilyl ether **4a** as catalyst. Here, the dr was poor and sometimes the diastereoisomers could not be well separated by FC. In these cases the diastereoisomeric mixture was characterized by means of chiral stationary phase HPLC or UPC<sup>2</sup> in which all four peaks of both diastereoisomers were present; the correct correspondence of the peaks was confirmed by the juxtaposition of the UV spectra, recorded by the PDA detector of the HPLC or UPC<sup>2</sup> system, respectively.

#### 6.4.2. Syntheses of starting materials 1 and 2

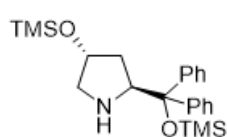
According to reported literature procedures,<sup>168</sup> *para*-quinone methides **1** were synthesized by refluxing 2,6-di-*tert*-butyl phenol, the appropriate aldehyde and piperidine in a Dean-Stark apparatus for 16 h. Then the crude mixture was treated with acetic anhydride for 1 h. After work up the *p*-QM was purified by flash chromatography on silica gel.

The aldehydes that were not commercially available were synthesized according to reported procedures.<sup>171</sup> Pentanal **2a** was distilled before using; hydrocinnamaldehyde **2b** was purified by FC on silica gel ( $\text{CH}_2\text{Cl}_2$ ) before using; all the aldehydes were stored at  $-35\text{ }^\circ\text{C}$  in a vial filled with argon.

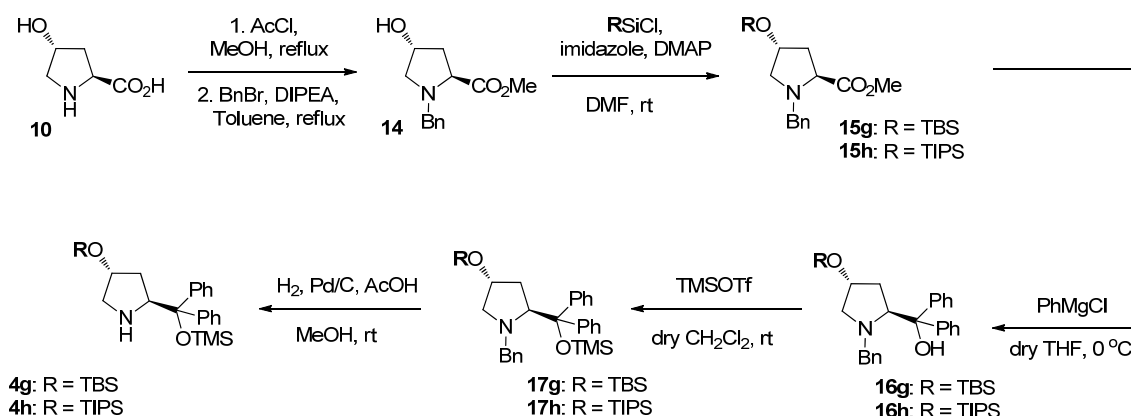
6.4.3. Synthesis of catalyst **4f**Scheme 79. Synthesis of catalyst **4f**

The synthesis of catalyst **4f** started from the commercially available *trans*-4-hydroxy-*L*-proline **10**. Esterification and *N*-carbomoylation of the starting material,<sup>172</sup> followed by Grignard reaction led to the bicyclic adduct **12**.<sup>173</sup> The subsequent hydrolysis afforded 4-hydroxy diphenyl prolinol **13**.<sup>173b</sup> Spectral data of these intermediates are according to the corresponding literature.<sup>172,173</sup>

**(2*S*,4*R*)-2-(Diphenyl((trimethylsilyl)oxy)methyl)-4-((trimethylsilyl)oxy)pyrrolidine, **4f****



In a round bottom flask equipped with a magnetic stirring bar, (3*R*,5*S*)-5-(hydroxydiphenylmethyl)pyrrolidin-3-ol (1.10 mmol, 1 equiv.) and Et<sub>3</sub>N (4.18 mmol, 3.8 equiv.) were suspended in dry CH<sub>2</sub>Cl<sub>2</sub> (5 mL). The flask was filled with argon and placed in an ice bath, then TMSOTf (3.88 mmol, 3.5 equiv.) was slowly added over 15 min. The reaction was then allowed to reach rt and was stirred for 24 h until full conversion was confirmed by TLC analysis. The reaction was quenched with water, the product was extracted three times with CH<sub>2</sub>Cl<sub>2</sub> and dried over Na<sub>2</sub>SO<sub>4</sub>. After removal of solvent the catalyst was isolated by FC (CH<sub>2</sub>Cl<sub>2</sub>/EtOAc, 9/1) in 67% yield. <sup>1</sup>H NMR (400 MHz, CDCl<sub>3</sub>) δ = 7.45-7.15 (m, 10H), 4.38 (t, *J* = 7.53 Hz, 1H), 3.92-3.86 (m, 1H), 2.79-2.71 (m, 2H), 1.85-1.70 (m, 2H), 1.65-1.50 (m, 1H) 0.04 (s, 9H), -0.11 (s, 9H). <sup>13</sup>C NMR (100 MHz, CDCl<sub>3</sub>) δ = 146.5, 145.4, 128.5 (2C), 127.8 (2C), 127.6 (2C), 127.4 (2C), 126.9, 126.8, 82.9, 72.2, 63.5, 55.8, 37.5, 2.1 (3C), 0.1 (3C) HRMS calculated for [M-TMS+H]<sup>+</sup>: 342.1884; found: 342.1889. [α]<sub>D</sub><sup>22</sup> = -42.1 (c = 0.427 in CH<sub>2</sub>Cl<sub>2</sub>).

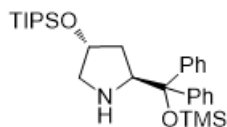
6.4.4. Syntheses of catalysts **4g** and **4h**Scheme 80. Syntheses of catalysts **4g** and **4h**.

The synthesis of catalysts **4g** and **4h** began with the conversion of *trans*-4-hydroxy-*L*-proline **10** into its methyl ester and *N*-benzylated derivative **14**. Next, the first silyloxy moiety was installed through the protection of the hydroxyl group at C4. Grignard reaction and subsequent TMS-protection of the hydroxyl group furnished the *N*-protected precursor of catalysts **17g** and **17h**. Spectral data of these intermediates are according to the corresponding literature.<sup>174</sup>

**(2*S*,4*R*)-4-((*tert*-Butyldimethylsilyloxy)-2-(diphenyl((trimethylsilyloxy)methyl)pyrrolidine, **4g****

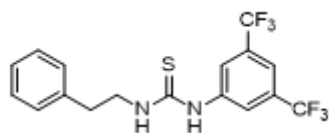
In a flame dried round bottom flask equipped with a magnetic stirring bar, (2*S*,4*R*)-1-benzyl-4-((*tert*-butyldimethylsilyloxy)-2-(diphenyl((trimethylsilyloxy)methyl)pyrrolidine (0.61 mmol, 1 equiv.) and concentrated acetic acid (0.73 mmol, 1.2 equiv.) were dissolved in methanol (3 mL). Palladium on activated charcoal was added (10 wt.-%). The mixture was subsequently saturated with hydrogen gas and stirred under hydrogen atmosphere overnight. Hereafter, the reaction mixture was filtered through a short bed of celite and the solution was evaporated under reduced pressure. The residue was suspended in 20 mL of a saturated aqueous solution of NaHCO<sub>3</sub> and extracted with Et<sub>2</sub>O (3x20 mL). The combined organic layers were dried over MgSO<sub>4</sub>. After filtration and evaporation of the solvent catalyst **4g** was isolated by FC (pentane/EtOAc, 10/1) in 54% yield (0.15 g, 0.33 mmol). <sup>1</sup>H NMR (400 MHz, CDCl<sub>3</sub>) δ = 7.46 (d, J = 8.32 Hz, 2H), 7.35 (d, J = 8.45 Hz, 2H), 7.29-7.18 (m, 6H), 4.36 (t, J = 7.92 Hz, 1H), 3.95-3.90 (m, 1H), 2.73 (dq, J = 19.52, 11.23, 4.63 Hz, 2H), 1.76-1.64 (m, 2H), 1.58-1.50 (m, 1H), 0.85 (s, 9H), -0.02 (s, 6H), -0.12 (s, 9H). <sup>13</sup>C NMR (100 MHz, CDCl<sub>3</sub>) δ = 146.7, 145.5, 128.4, 127.8, 127.6, 127.3, 126.8, 126.7, 82.9, 72.5, 63.5, 56.0, 37.8, 25.9, 18.1, 2.1, -4.8. HRMS (ESI +) m/z calculated for [M+H]<sup>+</sup>: 456.2696; found: 456.2793. [α]<sub>D</sub><sup>20</sup> = -31.2 (c = 0.633 in CH<sub>2</sub>Cl<sub>2</sub>).

**(2*S*,4*R*)-2-(Diphenyl((trimethylsilyl)oxy)methyl)-4-  
((triisopropylsilyl)oxy)pyrrolidine, **4h****



In a flame dried round bottom flask equipped with a magnetic stirring bar, (2*S*,4*R*)-1-benzyl-2-(diphenyl((trimethylsilyl)oxy)methyl)-4-((triisopropylsilyl)oxy)pyrrolidine (1.20 mmol, 1 equiv.) and concentrated acetic acid (1.40 mmol, 1.2 equiv.) were dissolved in methanol (10 mL). Palladium on activated charcoal was added (10 wt.-%). The mixture was subsequently saturated with hydrogen gas and stirred under hydrogen atmosphere overnight. Hereafter, the reaction mixture was filtered through a short bed of celite and the solution was evaporated under reduced pressure. The residue was suspended in a saturated aqueous solution of NaHCO<sub>3</sub> (30 mL) and extracted with Et<sub>2</sub>O (3x30 mL). The combined organic layers were dried over MgSO<sub>4</sub>. After filtration and evaporation of the solvent catalyst **4h** was isolated by FC (pentane/EtOAc, 19/1) in 50% yield (0.30 g, 0.60 mmol). <sup>1</sup>H NMR (400 MHz, CDCl<sub>3</sub>) δ = 7.58 (d, J = 7.57 Hz, 2H), 7.47 (d, J = 8.00 Hz, 2H), 7.40-7.30 (m, 6H), 4.50 (t, J = 7.70 Hz, 1H), 4.15-4.09 (m, 1H), 1.92 (br s, 1H), 1.85-1.69 (m, 2H), 1.12 (s, 22H), -0.01 (s, 9H). <sup>13</sup>C NMR (100 MHz, CDCl<sub>3</sub>) δ = 144.5, 143.3, 126.4 (2C), 125.8 (2C), 125.6 (2C), 125.2 (2C), 124.8, 124.7, 80.8, 70.5, 61.5, 54.2, 36.1, 15.9 (6C), 10.0 (3C), 0.0 (3C). HRMS calculated for [M+H]<sup>+</sup>: 498.3218, found: 498.3244. [α]<sup>20</sup><sub>D</sub> = -26.3 (c = 1.03 in CH<sub>2</sub>Cl<sub>2</sub>).

**6.4.5. Synthesis of 1-(3,5-bis(trifluoromethyl)phenyl)-3-phenethylthiourea, **5****



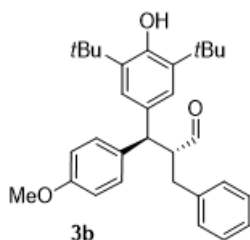
In a round bottomed flask 3,5-bis(trifluoromethyl)phenyl isothiocyanate (1.0 mmol, 271 mg) and phenylethylamine (1.0 mmol, 121 mg) were mixed in CH<sub>2</sub>Cl<sub>2</sub> (4 mL) at rt. After 2 h the solvent was evaporated and the residue was purified by crystallization from *n*-hexane and acetone to afford thiourea **5** in quantitative yield. <sup>1</sup>H NMR (400 MHz, CDCl<sub>3</sub>) δ = 7.92 (br s, 1H), 7.69 (s, 1H), 7.59 (s, 2H), 7.33-7.15 (m, 5H), 5.96 (br s, 1H), 3.92 (br d, J = 5.68 Hz, 2H), 2.96 (t, J = 6.69 Hz, 2H). <sup>13</sup>C NMR (100 MHz, CDCl<sub>3</sub>) δ = 180.4, 138.5, 137.9, 128.9, 128.6, 127.0, 124.3, 124.0, 121.3, 119.7, 46.3, 34.6. HRMS calculated for [M+Na]<sup>+</sup>: 415.0674, found: 415.0679.

**6.4.6. General procedure for the organocatalytic reactions.**

A glass vial equipped with a magnetic stirring bar was charged with catalyst **4h** (0.005 mmol, 0.1 equiv.), thiourea **5** (0.015 mmol, 0.3 equiv.), the appropriate *para*-quinone methide **1a-k** (0.05 mmol, 1 equiv.) and CH<sub>2</sub>Cl<sub>2</sub> (200 μL). The vial was placed into an ice bath and stirred for few minutes, then the corresponding aldehyde **2a-i** (0.075 mmol,

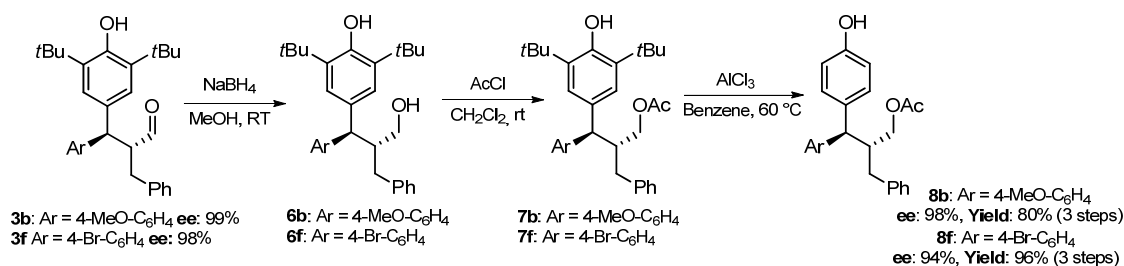
1.5 equiv.) was added in one portion. The resulting mixture was stirred at 4 °C for 48 h, then it was filtered through a short plug of silica gel and the plug was washed several times with CH<sub>2</sub>Cl<sub>2</sub>. After removal of solvent, the crude mixture was analyzed by <sup>1</sup>H NMR in order to evaluate the dr. Finally the mixture was purified by FC on silica gel (pentane/CH<sub>2</sub>Cl<sub>2</sub> mixtures).

**(2*R*,3*S*)-2-Benzyl-3-(3,5-di-*tert*-butyl-4-hydroxyphenyl)-3-(4-methoxyphenyl)propanal, 3b**



Following the general procedure, the title compound was isolated by FC on silica gel (pentane/CH<sub>2</sub>Cl<sub>2</sub> 1:1) in 74% yield as yellowish oil. <sup>1</sup>H NMR (400 MHz, CDCl<sub>3</sub>) δ = 9.52 (d, *J* = 3.40 Hz, 1H), 7.27-7.15 (m, 5H), 7.05-7.00 (m, 4H), 6.89 (d, *J* = 8.66 Hz, 2H), 5.05 (s, 1H), 4.05 (d, *J* = 10.7 Hz, 1H), 3.80 (s, 3H), 3.50-3.41 (m, 1H), 2.89 (dd, *J* = 9.47, 14.0 Hz, 1H), 2.71 (dd, *J* = 3.73, 14.1 Hz, 1H), 1.38 (s, 18H). <sup>13</sup>C NMR (100 MHz, CDCl<sub>3</sub>) δ = 204.4, 158.3, 152.5, 139.0, 136.0 (2C), 134.9, 132.1, 129.1 (2C), 129.0 (2C), 128.4 (2C), 126.3, 124.6 (2C), 114.2 (2C), 58.1, 55.3, 51.9, 34.8, 34.3 (2C), 30.3 (6C). HRMS calculated for [M-H]<sup>-</sup>: 457.2821; found: 457.2755. [α]<sub>D</sub><sup>26</sup> = +20.5 (*c* = 0.80 in CH<sub>2</sub>Cl<sub>2</sub>). The dr was evaluated by <sup>1</sup>H NMR of the crude mixture and was found to be 7.9/1. The ee was determined by UPC<sup>2</sup>, using Chiralpack IB-3 column [1% *i*-PrOH (0.5 min), then linear gradient from 1% to 25% (3%/min), 120 bar, 40 °C] flow rate: 3 mL/min, *t*<sub>major</sub> = 4.22 min *t*<sub>minor</sub> = 4.38 min, ee = 99%.

**6.4.7. General procedure for the de-*tert*-butylation reaction sequence**



**Scheme 81.** De-*tert*-butylation reaction sequence.

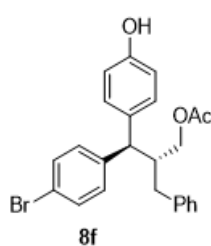
a) In a glass vial equipped with a magnetic stirring bar, compound **3b** or **3f** (0.17 mmol) was dissolved in 660 μL of MeOH, then NaBH<sub>4</sub> (0.66 mmol) was added at 0 °C and the mixture was allowed to reach rt. After 30 min. the reaction was quenched with brine and extracted twice with Et<sub>2</sub>O. The organic layers were combined and dried over Na<sub>2</sub>SO<sub>4</sub>. After removal of solvent, the corresponding alcohol **6b** or **6f** was isolated without further purifications.

b) In a glass vial equipped with a magnetic stirring bar, compound **6b** or **6f** (0.13 mmol) was dissolved in 400 μL of dry CH<sub>2</sub>Cl<sub>2</sub>, then AcCl (0.26 mmol) was added in one portion

and the mixture was stirred at rt overnight. After removal of solvent, compound **7b** or **7f** was isolated without further purifications.

c) In a flame dried vial equipped with a magnetic stirring bar, compound **7b** or **7f** (0.056 mmol) was dissolved in 3 mL of dry benzene and the vial was filled with nitrogen.  $\text{AlCl}_3$  (0.33 mmol) was quickly added and the mixture was stirred at 60 °C for 1 h. The mixture was then quenched with water and extracted twice with EtOAc, the organic layers were combined and dried over  $\text{Na}_2\text{SO}_4$ . The residue obtained was purified by FC on silica gel (pentane/EtOAc mixtures) to afford the de-*tert*-butylated compound **8b** or **8f**.

#### (2*R*,3*R*)-2-Benzyl-3-(4-bromophenyl)-3-(4-hydroxyphenyl)propyl acetate, **8f**



Following the part c) of the general procedure, the title compound was isolated after FC on silica gel (pentane/EtOAc 3:1) in 96% yield.  $^1\text{H NMR}$  (400 MHz,  $\text{CDCl}_3$ )  $\delta$  = 7.45 (d,  $J$  = 8.42 Hz, 2H), 7.29-7.22 (m, 4H), 7.20-7.15 (m, 1H), 7.08 (d,  $J$  = 8.69 Hz, 2H), 7.05 (d,  $J$  = 7.22 Hz, 2H), 6.70 (d,  $J$  = 8.69 Hz, 2H), 5.13 (br s, 1H), 3.91 (dd,  $J$  = 3.15, 11.29 Hz, 1H), 3.82 (d,  $J$  = 10.98 Hz, 1H), 3.74 (dd,  $J$  = 4.75, 11.44 Hz, 1H), 2.78-2.66 (m, 2H), 2.50 (dd,  $J$  = 10.30, 14.18 Hz, 1H), 1.99 (s, 3H).  $^{13}\text{C NMR}$  (100 MHz,  $\text{CDCl}_3$ )  $\delta$  = 171.1, 154.3, 142.6, 139.7, 134.4, 131.9 (2C), 129.7 (2C), 129.0 (2C), 129.8 (2C), 128.4 (2C), 126.2, 120.2, 115.6 (2C), 63.7, 52.4, 43.1, 35.6, 20.8. **HRMS** calculated for  $[\text{M}+\text{Na}]^+$ : 461.0723; found: 461.0723.  $[\alpha]_{\text{D}}^{28}$  = -31.8 ( $c$  = 0.67 in DCM). The *ee* was determined by UPC<sup>2</sup> using Chiralpack IB-3 column [1% *i*-PrOH (0.5 min), then linear gradient from 1% to 30%, (6.0%/min), 120 bar, 40 °C] flow rate: 3 mL/min,  $t_{\text{maj}}$  = 5.63 min,  $t_{\text{min}}$  = 5.80 min, *ee* = 94%.

#### 6.4.8. Crystallographic data

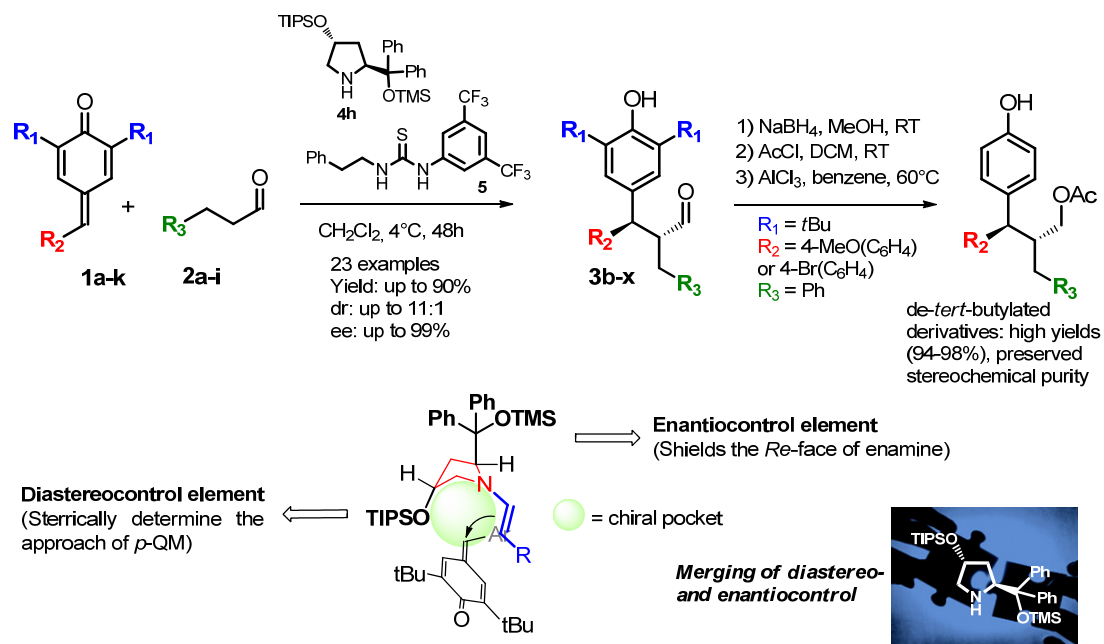
Crystal data for **7f**:  $\text{C}_{32}\text{H}_{39}\text{BrO}_3$ ,  $M$  = 551.57, monoclinic, space group P21 (no. 6),  $a$  = 16.508(6) Å,  $b$  = 9.0189(4) Å,  $c$  = 20.058(8) Å,  $\beta$  = 104.827(4)°, Flack parameter = -0.025,  $V$  = 2886.9(2) Å<sup>3</sup>,  $T$  = 100 K,  $Z$  = 4,  $d_c$  = 1.2689 g cm<sup>-3</sup>,  $\mu(\text{Mo K}\alpha, \lambda = 0.71073 \text{ \AA})$  = 1.453 mm<sup>-1</sup>, 31301 reflections collected, 6034 unique [ $R_{\text{int}}$  = 0.1298], which were used in all calculations. Refinement on  $F^2$ , final  $R(F)$  = 0.0974,  $R_w(F2)$  = 0.135. CCDC number 1019855.

## 6.5. Conclusion

In conclusion, we have developed a new and easy-to-conduct organocatalytic strategy for the  $\alpha$ -alkylation of aldehydes. For the first time, enamine-activated aldehydes have been added to *para*-quinone methides, providing  $\alpha$ -diarylmethine-substituted aldehydes with

two contiguous stereocenters in high yield and broad substrate scope. The control of the stereochemical outcome, particularly the diastereoselectivity, of the proposed transformation has been an intriguing challenge. Having identified in the uncontrolled approach of the *p*-QM to the enamine-activated aldehyde the reason of the low dr, we have synthesized a new class of C4-substituted TMS-protected diphenyl prolinol. Indeed the bulky silyloxy moiety placed at the peripheral C4-position was found to control the approach of the electrophile through steric repulsion, leading to highly diastereo- and enantioenriched product.

The presence of the electron-donating *tert*-butyl groups on the C2 and C6 position of the cyclohexatriene core was almost a mandatory requirement for the stabilization of the *p*-QM. Being aware that this could limit the scope and the applicability of our synthetic protocol, we developed a de-*tert*-butylation reaction sequence that led to the corresponding de-*tert*-butylated diaryl derivatives in high yield and preserved enantioselectivity.



**Scheme 82.** Organocatalytic diastereo- and enantioselective  $\alpha$ -Alkylation of aldehydes performed via 1,6-conjugated addition of enamine-activated aldehydes to *para*-quinone methide. A novel chiral secondary amine catalyst was the key to the success of this reaction.



## 7. Bibliography

- <sup>1</sup> IUPAC, Compendium of Chemical Terminology, 2<sup>nd</sup> ed., 1997.
- <sup>2</sup> Gal, J. *Chirality* **2012**, *24*, 959
- <sup>3</sup> Noyori, R. *Adv. Synth. Catal.* **2003**, *345*, 15
- <sup>4</sup> Seebach, D. *Angew. Chem. Int. Ed.* **1990**, *29*, 1320.
- <sup>5</sup> Schmid, A.; Dordik, J. S.; Hauer, B.; Kiener, A.; Wubbolts, M.; Witholt, B. *Nature* **2001**, *409*, 258
- <sup>6</sup> Heitbaum, M.; Glorius, F.; Escher, I. *Angew. Chem. Int. Ed.* **2006**, *45*, 4732.
- <sup>7</sup> Blaser, H. U.; Federsel, H. J. *Asymmetric Catalysis on Industrial Scale*. Wiley VHC, Weinheim, **2011**.
- <sup>8</sup> Gawley, R. E.; Aubé, J. *Principles of Asymmetric Synthesis* 2<sup>nd</sup> edition. Elsevier, Amsterdam, **2012**.
- <sup>9</sup> Selected reviews on asymmetric organocatalysis: (a) Dalko, P. I.; Moisan, L. *Angew. Chem. Int. Ed.* **2004**, *43*, 5138; (b) List, B. *Asymmetric Organocatalysis*. Wiley VHC, Weinheim, **2005**; (c) List, B. *Chem. Rev.* **2007**, *107*, 5413; (d) Pellissier, H. *Tetrahedron* **2007**, *63*, 926; (e) Gaunt, M. F.; Johansson, C. C. C.; McNally, A.; Vo, N. T. *Drug Discovery Today* **2007**, *12*, 8. (f) MacMillan, D. W. C. *Nature* **2008**, *455*, 304; (g) Dondoni, A.; Massi, A.; *Angew. Chem. Int. Ed.* **2008**, *47*, 4638.
- <sup>10</sup> Bernardi, L.; Fochi, M.; Comes Franchini, M.; Ricci, A. *Org. Biomol. Chem.* **2012**, *10*, 2911.
- <sup>11</sup> (a) Haios, Z. G.; Parrish, D. R. German patent DE 2102623, **1971**; (b) Eder, U.; Sauer, G.; Wiechert, R. *Angew. Chem. Int. Ed.* **1971**, *10*, 496; (c) Hajos, Z. G.; Parrish, D. R. *J. Org. Chem.* **1974**, *39*, 1615.
- <sup>12</sup> Source: ISI-web of Science until December 2014, using the keyword “organocatalysis” and refining the research area to “Chemistry”. A more realistic research has been conducted by using also the keyword “organocatalytic” together with “organocatalysis”; this search is unlikely to have found all publications on organocatalysis, nonetheless the estimation is lying around more than 15000 manuscripts so far.
- <sup>13</sup> Tu, Y.; Wang, Z.; Shi, Y. *J. Am. Chem. Soc.* **1996**, *118*, 9806.
- <sup>14</sup> Denmark, S. E.; Wu, Z.; Crudden, C.; Matshuhashi, H. *J. Org. Chem.* **1997**, *62*, 8288.
- <sup>15</sup> Yang, D. *J. Am. Chem. Soc.* **1996**, *118*, 491
- <sup>16</sup> Sigman, M.; Jacobsen, E. N. *J. Am. Chem. Soc.* **1998**, *120*, 4901
- <sup>17</sup> Corey, E. J.; Grogan, M. J. *Org. Lett.* **1999**, *1*, 157.
- <sup>18</sup> (a) List, B.; Lerner, R. A.; Barbas, C. F. III. *J. Am. Chem. Soc.* **2000**, *120*, 1629; (b) List, B. *J. Am. Chem. Soc.* **2000**, *122*, 9336.
- <sup>19</sup> Ahrendt, K. A.; Borths, C. J.; MacMillan, D. W. C. *J. Am. Chem. Soc.* **2000**, *122*, 4243.
- <sup>20</sup> Marqués-López, E.; Herrera, R. P.; Christmann, M. *Nat. Prod. Rep.* **2010**, *27*, 1138
- <sup>21</sup> Rouhi, M. A.; *Chem. Eng. News.* **2004**, *82*, 41.
- <sup>22</sup> (a) Akiyama, T.; Itoh, J.; Fuchibe, K. *Adv. Synth. Catal.* **2006**, *348*, 999. (b) Taylor, M. S.; Jacobsen, E. N. *Angew. Chem. Int. Ed.* **2006**, *45*, 1520; (c) Doyle, A. G.; Jacobsen, E. N. *Chem. Rev.* **2007**, *107*, 5713; (d) Zhang, Z.; Schreiner, P. R. *Chem. Soc. Rev.* **2009**, *38*, 1187.
- <sup>23</sup> Melchiorre, P.; Marigo, M.; Carlone, A.; Bartoli, G. *Angew. Chem. Int. Ed.* **2008**, *47*, 6138.
- <sup>24</sup> (a) Grondal, C.; Jeanty, M.; Enders, D. *Nat. Chem.* **2010**, *2*, 167; (b) Volla, C. M. R.; Atodiresei, I.; Rueping, M. *Chem. Rev.* **2014**, *114*, 2390.
- <sup>25</sup> Du, Z.; Shao, Z. *Chem. Soc. Rev.* **2013**, *42*, 1337
- <sup>26</sup> Nicewicz, D.; MacMillan, D. W. C. *Science* **2008**, *322*, 77
- <sup>27</sup> Warshel, A. *Angew. Chem. Int. Ed.* **2014**, *53*, 10020 and references therein.
- <sup>28</sup> Wenzel, A.G.; Jacobsen, E.N. *J. Am. Chem. Soc.* **2002**, *124*, 12964.
- <sup>29</sup> (a) Kacprzak, J.; Gawroński, J. *Synthesis* **2001**, 961; (b) Marcelli, T.; Hiemstra, H. *Synthesis* **2010**, 1229.
- <sup>30</sup> Lippert, K.M.; Hof, K.; Gerbig, D.; Ley, D.; Hausmann, H.; Guenther, S.; Schreiner, P. R. *Eur. J. Org. Chem.* **2012**, 5919
- <sup>31</sup> Okino, Y.; Hoashi, Y.; Takemoto, Y.; *J. Am. Chem. Soc.* **2003**, *125*, 12672.
- <sup>32</sup> Okino, Y.; Hoashi, Y.; Xu, X.; Takemoto, Y. *J. Am. Chem. Soc.* **2005**, *127*, 119.
- <sup>33</sup> Hamza, A.; Schubert, G.; Soós, T.; Pápai, I. *J. Am. Chem. Soc.* **2006**, *128*, 13151.
- <sup>34</sup> Malerich, J. P.; Hagihara, H.; Rawal, V. H. *J. Am. Chem. Soc.* **2008**, *130*, 14416.
- <sup>35</sup> Alemán, J.; Parra, A.; Jiang, H.; Jørgensen, K. A. *Chem. Eur. J.* **2011**, *17*, 6890.
- <sup>36</sup> Akiyama, T.; Itoh, J.; Yokota, K.; Fuchibe, K. *Angew. Chem. Int. Ed.* **2004**, *43*, 1566.
- <sup>37</sup> Uraguchi, D.; Terada, M. *J. Am. Chem. Soc.* **2004**, *126*, 5356.

- <sup>38</sup> For reviews on chiral phosphoric acids see: (a) Akiyama, T. *Chem. Rev.* **2007**, *107*, 5744; (b) Terada, M. *Synthesis* **2010**, 1929; (c) Kampen, D.; Reinsinger, C. M.; List, B. *Top. Curr. Chem.* **2010**, *291*, 395; (d) Rueping M.; Kuenkel A.; Atodiresei, I. *Chem. Soc. Rev.* **2011**, *40*, 4539. (e) Parmar, D.; Sugiono, E.; Raja, S.; Rueping, M. *Chem. Rev.* **2014**, *114*, 9047.
- <sup>39</sup> Simón, L.; Goodman, J. M. *J. Org. Chem.* **2010**, *75*, 589.
- <sup>40</sup> Jakab, G.; Tancon, C.; Zhang, Z.; Lippert, K.M.; Schreiner, P. R. *Org. Lett.* **2012**, *14*, 1724.
- <sup>41</sup> Christ, P.; Lindsay, A. G.; Vormittag, S. S.; Neudörfl, J.-M.; Berkessel, A.; O'Donoghue, A. C. *Chem. Eur. J.* **2011**, *17*, 8524.
- <sup>42</sup> Fleischmann, M.; Drettwan, D.; Sugiono, E.; Rueping, M.; Gschwind, R. *Angew. Chem. Int. Ed.* **2011**, *50*, 6364.
- <sup>43</sup> Review on aminocatalysis, besides ref. 23: (a) Bertelsen, S.; Jørgensen, K. A. *Acc. Chem. Res.* **2009**, *38*, 2178; (b) Nielsen, M.; Worgull, D.; Zwifel, B.; Bertelsen, S.; Jørgensen, K. A. *Chem. Commun.* **2011**, *47*, 632; (c) Jensen, K. L.; Dickmeiss, G.; Jiang, H.; Albrect, L.; Jørgensen, K. A. *Acc. Chem. Res.* **2012**, *45*, 248.
- <sup>44</sup> For historical perspective: (a) Barbas III, C.F. *Angew. Chem. Int. Ed.* **2008**, *47*, 42; (b) List, B. *Angew. Chem. Int. Ed.* **2010**, *49*, 1730.
- <sup>45</sup> Earliest reports: (a) Bertelsen, S.; Marigo, M.; Brandes, S.; Dinér, P.; Jørgensen, K. A. *J. Am. Chem. Soc.* **2006**, *128*, 12973; (b) Jia, Z. -J.; Gschwend, B.; Li, Q. -Z.; Yin, X.; Grouleff, J.; Chen, Y. -C.; Jørgensen, K. A. *J. Am. Chem. Soc.* **2011**, *135*, 5053.
- <sup>46</sup> Marigo, M.; Wabnitz, T. C.; Fielenbach, D.; Jørgensen, K. A. *Angew. Chem. Int. Ed.* **2005**, *44*, 794.
- <sup>47</sup> Hayashi, Y.; Gotoh, H.; Hayashi, T.; Shoji, M. *Angew. Chem. Int. Ed.* **2005**, *44*, 4212.
- <sup>48</sup> Austin, J. F.; MacMillan, D. W. C. *J. Am. Chem. Soc.* **2002**, *124*, 1172.
- <sup>49</sup> (a) Komisaraska-Patora, K.; Benohoud, M.; Ishikawa, M.; Seebach, D.; Hayashi, Y. *Helv. Chem. Acta* **2011**, *94*, 719; (b) Burés, J.; Armstrong, A.; Blackmond, D. G. *J. Am. Chem. Soc.* **2011**, *133*, 8822; (c) Seebach, D.; Sun, X.; Sparr, C.; Ebert, M.-O.; Schweizer, W. B.; Beck, A. K. *Helv. Chem. Acta* **2012**, *95*, 1064; (d) Burés, J.; Armstrong, A.; Blackmond, D. G. *J. Am. Chem. Soc.* **2012**, *134*, 6741, corrigendum: *J. Am. Chem. Soc.* **2012**, *134*, 14264; (e) Sahoo, G.; Rahaman, H.; Madarász, Á.; Pápai, I.; Melarto, M.; Valkonen, A.; Pihko, P. M. *Angew. Chim. Int. Ed.* **2012**, *51*, 13144.
- <sup>50</sup> (a) Figueiredo, R. M.; Christmann, M. *Eur. J. Org. Chem.* **2007**, 2575; (b) Busacca, C. A.; Fandrick, D. R.; Song, J. J.; Senanayake, C. H. *Adv. Synth. Catal.* **2011**, *353*, 1825; (c) Alemán, J.; Cabrera, S. *Chem. Soc. Rev.* **2013**, *42*, 774 and references therein.
- <sup>51</sup> (a) Katritzky, A. R.; Rachwal, S.; Rachwal, B.; *Tetrahedron* **1996**, *52*, 15031 (b) Sridharan, V.; Suryavanshi, Menéndez, J. C. *Chem. Rev.* **2011**, *111*, 7157.
- <sup>52</sup> (a) Povarov, L. S.; Mikhailov, B. M. *Izn. Akad. Nauk SSSR, Ser. Khim.* **1963**, 953; (b) Povarov, L. S.; Grigos, V.I.; Mikhailov, B. M. *Izn. Akad. Nauk SSSR, Ser. Khim.* **1963**, 2039.
- <sup>53</sup> Povarov, L. S. *Russ. Chem. Rev.* **1967**, *36*, 656.
- <sup>54</sup> Selected review on Povarov reaction: (a) Glushkov, V. A.; Tolstikov, A. G. *Russ. Chem. Rev.* **2008**, *77*, 137; (b) Kouznetsov, V. V. *Tetrahedron* **2009**, *65*, 2721; (c) Fochi, M.; Caruana, L.; Bernardi, L. *Synthesis* **2014**, *46*, 135.
- <sup>55</sup> (a) Lucchini, V.; Prato, M.; Scorrano, G.; Stivanello, M.; Valle, G. *J. Chem. Soc. Perkin Trans. 2* **1992**, 259; (b) Hermitage, S.; Jay, D. A.; Whiting, A.; *Tetrahedron Lett.* **2002**, *43*, 9633; (c) Hermitage, S.; Howard, J. A. K.; Jay, D.; Pritchard, R. G.; Probert, M. R.; Whiting A. *Org. Biomol. Chem.* **2004**, *2*, 2451; (d) Alves, M. J.; Azoia, N. G.; Fortes, A. G. *Tetrahedron* **2007**, *63*, 727.
- <sup>56</sup> Sridharan, V.; Avendano, C.; Menéndez, J. C. *Synthesis* **2008**, 1039.
- <sup>57</sup> For recent examples see: (a) Maiti, S.; Menéndez, J. C. *Synlett* **2009**, 2249; (b) Vicente-García, E.; Catti, F.; Ramón, R.; Lavilla, R. *Org. Lett.* **2010**, *12*, 860
- <sup>58</sup> Ishitani, H.; Kobayashi, S. *Tetrahedron Lett.* **1996**, *37*, 7357.
- <sup>59</sup> Connon, S. J. *Angew. Chem. Int. Ed.* **2006**, *45*, 3909.
- <sup>60</sup> Akiyama, T.; Morita, H.; Fuchibe, K. *J. Am. Chem. Soc.* **2006**, *128*, 13070.
- <sup>61</sup> Yamanka, M.; Itoh, J.; Fuchibe, K.; Akiyama, T. *J. Am. Chem. Soc.* **2007**, *129*, 6756.
- <sup>62</sup> Liu, H.; Dagousset, G.; Masson, G.; Retailleau, P.; Zhu, J. *J. Am. Chem. Soc.* **2009**, *131*, 4598.
- <sup>63</sup> Dagousset, G.; Zhu, J.; Masson, G. *J. Am. Chem. Soc.* **2011**, *133*, 14804.
- <sup>64</sup> (a) Čorić, I.; Müller, S.; List, B. *J. Am. Chem. Soc.* **2010**, *132*, 17370; (b) Xu, F. X.; Huang, D.; Han, C.; Shen, W.; Lin, X.; Wang, Y. G. *J. Org. Chem.* **2010**, *75*, 8675.
- <sup>65</sup> Huang, D.; Xu, F.; Chen, T.; Wang, Y.; Lin, X. *RSC Adv.* **2013**, *3*, 573.
- <sup>66</sup> Lin, J.-H.; Zong, G.; Du, R.-B.; Xiao J.-C.; Liu, S. *Chem. Commun.* **2012**, *48*, 7738

- <sup>67</sup> Purser, S.; Moore, P.R.; Swallow, S.; Gouverneur, V. *Chem. Soc. Rev.* **2008**, *37*, 320.
- <sup>68</sup> Dagousset, G.; Retailleau, P.; Masson, G.; Zhu, J. *Chem. Eur. J.* **2012**, *18*, 5869.
- <sup>69</sup> Bergonzini, G.; Gramigna, L.; Mazzanti, A.; Fochi, M.; Bernardi, L.; Ricci, A. *Chem. Commun.* **2010**, *46*, 327.
- <sup>70</sup> Cheng, H.-G.; Chen, C.-B.; Tan, F.; Chang, N.-J.; Chen, J.-R.; Xiao, W.-J. *Eur. J. Org. Chem.* **2010**, 4976.
- <sup>71</sup> (a) He, L.; Bekkaye, M.; Retailleau, P.; Masson, G. *Org. Lett.* **2012**, *14*, 3158; (b) Shi, F.; Xing, G.-J.; Tao, Z.-L.; Luo, S.-W.; Tu, S.-J.; Gong, L.-Z. *J. Org. Chem.* **2012**, *77*, 6970.
- <sup>72</sup> (a) Hermitage, S.; Howard, J. A. K.; Jay, D.; Pritchard, R. G.; Probert, M. R.; Whiting, A. *Org. Biomol. Chem.* **2004**, *2*, 2451; (b) Alves, M. J.; Azoia, N. G.; Fortes, A. G. *Tetrahedron* **2007**, *63*, 727; (c) Sridharan, V.; Ribelles, P.; Estévez, V.; Villacampa, M.; Ramos, M. T.; Perumal, P. T.; Menéndez, J. C. *Chem. Eur. J.* **2012**, *18*, 5056; for definition and systematisation of vinylogous Povarov reaction see: (d) Sridharan, V.; Avendaño, C.; Menéndez, J. C. *Synlett* **2007**, 1079.
- <sup>73</sup> Caruana, L.; Fochi, M.; Ranieri, S.; Mazzanti, A.; Bernardi, L. *Chem. Commun.* **2013**, *49*, 880.
- <sup>74</sup> (a) Overman, L. E.; Jessup, P. J. *J. Am. Chem. Soc.* **1978**, *100*, 3182; (b) Momiyama, N.; Konno, T.; Furiya, Y.; Iwamoto, T.; Terada, M. *J. Am. Chem. Soc.* **2010**, *133*, 19294.
- <sup>75</sup> (a) Fuson, R. C. *Chem. Rev.* **1935**, *16*, 1; (b) Krishnamurthy, S. *J. Chem. Educ.* **1982**, *59*, 543.
- <sup>76</sup> (a) Matsubara, R.; Kobayashi, S. *Acc. Chem. Res.* **2008**, *41*, 292; (b) Goplaiah, K.; Kagan, H. B. *Chem. Rev.* **2011**, *111*, 4599.
- <sup>77</sup> (a) Terada, M.; Machioka, K.; Sorimachi, K. *Angew. Chem. Int. Ed.* **2006**, *45*, 2254; (b) Terada, M.; Machioka, K.; Sorimachi, K. *J. Am. Chem. Soc.* **2007**, *129*, 10336; (c) Lu, M.; Lu, Y.; Zhu, D.; Zheng, X.; Li, X.; Zhong, G. *Angew. Chem. Int. Ed.* **2010**, *49*, 8588; (d) Alix, A.; Lalli, C.; Retailleau, P.; Masson, G. *J. Am. Chem. Soc.* **2012**, *134*, 10389.
- <sup>78</sup> Blackmond, D. G.; *Angew. Chem. Int. Ed.* **2005**, *44*, 4302.
- <sup>79</sup> Karplus, M. *J. Am. Chem. Soc.* **1963**, *85*, 2870.
- <sup>80</sup> Stott, K.; Stonehouse, J.; Keeler, J.; Hwang T.-L.; Shaka A.J. *J. Am. Chem. Soc.* **1995**, *117*, 4199.
- <sup>81</sup> (a) Polavarapu, P. L. *Chem. Rec.* **2007**, *7*, 125; (b) Special Issue: *Chirality* **2008**, *20*, 605-759; (c) Mazzanti, A.; Casarini, D. *WIREs Comput. Mol. Sci.* **2012**, *2*, 613.
- <sup>82</sup> Bijvoet, J. M.; Peerdeman, A. F.; Van Bommel, A. J. *Nature* **1951**, *168*, 271.
- <sup>83</sup> Terada, M.; Sorimachi, K. *J. Am. Chem. Soc.* **2007**, *129*, 292.
- <sup>84</sup> Gottlieb, H. E.; Kotlyar, V.; Nudelman, A. *J. Org. Chem.* **1997**, *62*, 7512.
- <sup>85</sup> Jessup, P. J.; Petty, C. B.; Ross, J.; Overman, L. E. *Organic Syntheses Coll.* **1988**, *6*, 95.
- <sup>86</sup> (a) Rueping, M.; Nachtsheim, B. J.; Koenigs, R. M.; Ieawsuwan, W. *Chem. Eur. J.* **2010**, *16*, 13116; (b) Bartoszek, M.; Beller, M.; Deutsch, J.; Klawonn, M.; Köckritz, A.; Nemat, N.; Pews-Davtyan, A. *Tetrahedron* **2008**, *64*, 1316.
- <sup>87</sup> Hooft, R. W. W.; Scémo, C. L.; Stravera, L. H.; Spek, A. L. *J. Appl. Cryst.* **2008**, *41*, 96.
- <sup>88</sup> (a) Schardl, C. L.; Panaccione, D. G.; Tudzynki, P. *The alkaloids*. Ed. G. A. Cordell, Elsevier, Amsterdam. **2006**, *63*, 45; (b) Somei, M.; Yokoyama, Y.; Murakami, Y.; Ninomiya, I.; Kiguci, T.; Naito, T. *The Alkaloids*. Ed. G. A. Cordell, Academic Press, San Diego. **2000**, *54*, 191.
- <sup>89</sup> Selected reviews: (a) Humphrey, G. R.; Kuethe, J. T.; *Chem. Rev.* **2006**, *106*, 2875; (b) Krueger, K.; Tillack, A.; Beller, M. *Adv. Synth. Catal.* **2008**, *350*, 2153. (c) Barluenga, J.; Rodríguez, F.; Fañanas, F. J. *Chem. Asian J.* **2009**, *4*, 1036; (d) Taber, D. F.; Tirunahari, P. V. *Tetrahedron* **2011**, *65*, 7195; (e) Bartoli, G.; Dalpozzo, R.; Nardi, M. *Chem. Soc. Rev.* **2014**, *43*, 4728.
- <sup>90</sup> Recent reviews: (a) Bandini, M.; Eichholzer, A. *Angew. Chem. Int. Ed.* **2009**, *48*, 9608; (b) Bartoli, G.; Bencivenni, G.; Dalpozzo, R. *Chem. Soc. Rev.* **2010**, *39*, 4449; (c) Shiri, M. *Chem. Rev.* **2012**, *112*, 3508; (d) Dalpozzo, R. *Chem. Soc. Rev.* **2015**, *44*, 742.
- <sup>91</sup> Baeyer, A.; *Justus Liebigs Ann. Chem.* **1866**, *140*, 295.
- <sup>92</sup> Hofmann, A. *LSD – My problem child*. Ed. Mc-Graw-Hill book company, **1980**.
- <sup>93</sup> Shulgin, A.; Shulgin, A. *TiHKAL*. Ed Berkeley: Transform press, **1997**.
- <sup>94</sup> First total synthesis of lysergic acid: (a) Kornfeld, E. C.; Fornefeld, E. J.; Kline, G. B.; Mann, M. J.; Morrison, D. E.; Jones, R. G.; Woodward, R. B. *J. Am. Chem. Soc.* **1956**, *78*, 3087. Recent examples with references therein: (b) Somei, M.; Yokoyama, Y.; Murakami, Y.; Ninomiya, I.; Kiguci, T.; Naito, T. *The alkaloids*. Ed. G. A. Cordell, Academic Press, San Diego, **2000**; (c) Yamada, F.; Makita, Y.; Somei, M. *Heterocycles* **2007**, *72*, 599; (d) Baran, P. S.; Maimone, T. J.; Richter, J. M. *Nature* **2007**, *446*, 404. (e) Liu, Q.; Jia, Y. *Org. Lett.* **2011**, *13*, 4810 (f) Inuki, S.; Iwata, A.; Oishi, S.; Fujii, N.; Ohno, H. *J. Org. Lett.* **2011**, *76*, 2072; (g) Umezaki, S.; Yokoshima, S.; Fukuyama, T. *Org. Lett.* **2013**, *15*, 4230; (h) Liu, Q.; Zhang, Y.-A.; Xu, P.; Jia, Y. *J. Org. Chem.* **2013**, *78*, 10885 (i) Ohno, H.; Chiba, S.; Inuki, S.; Oishi, S.; Fujii, H.; *Synlett* **2014**, 179; (h) Wang, W.; Lu, J.-T.; H.-L. Zhang, Shi, Z.-F.; Wen, J.; Cao, X.-P. *J. Org.*

*Chem.* **2014**, *79*, 122; (j) Jabre, T.; Watanabe, T.; Brewer, M. *Tetrahedron Lett.* **2014**, *55*, 197;; (k) Bartoccini, F.; Casoli, M.; Mari, M.; Piersanti, G. *J. Org. Chem.* **2014**, *79*, 3255.

<sup>95</sup> Selected examples: (a) Greshick, T. J.; Funk, R. L.; *J. Am. Chem. Soc.* **2006**, *128*, 4946; (b) Park, I.-K.; Park, J.; Cho, C.-G.; *Angew. Chem. Int. Ed.* **2012**, *51*, 2496; (c) Shan, D.; Gao, Y.; Jia, Y. *Angew. Chem. Int. Ed.* **2013**, *52*, 4902; (c) Breazzano, S. P.; Poudel, Y. B.; Boger, D. L. *J. Am. Chem. Soc.* **2013**, *135*, 1600; (d) Miura, T.; Funakoshi, Y.; Murakami, M. *J. Am. Chem. Soc.* **2014**, *136*, 2272. One of the few examples of organocatalytic mediated 3,4-annulation of indoles: (e) Cheng, D.-J.; Wu, H.-B.; Tian, S.-K. *Org. Lett.* **2011**, *13*, 5636.

<sup>96</sup> Raushel, J.; Fokin, V. V. *Org. Lett.* **2010**, *12*, 4952.

<sup>97</sup> (a) Huang, Y.; Walji, A. M.; Larsen, C. H.; MacMillan, D. W. C. *J. Am. Chem. Soc.* **2005**, *127*, 15051; (b) Walji, A. M.; MacMillan, D. W. C. *Synlett* **2007**, 1477

<sup>98</sup> For the application of cascade reaction in the construction of heterocyclic compounds see: Liu, L.-Q.; Chen, J.-R.; Xiao, W.-J. *Acc. Chem. Res.* **2012**, *45*, 1278.

<sup>99</sup> Selected examples in which organocascade reactions are involved in the synthesis of indole-containing compounds: (a) Austin, J. F.; Kim, S.-J.; Sinz, C. J.; Xiao, W.-J.; MacMillan, D. W. C. *Proc. Nat. Acad. Sci.* **2004**, *101*, 5482; (b) Jones, S. B.; Simmons, B.; MacMillan, D. W. C. *J. Am. Chem. Soc.* **2009**, *131*, 13606; (c) Enders, D.; Greb, A.; Deckers, K.; Selig, P.; Merckens, C.; *Chem. Eur. J.* **2012**, *18*, 10226; (d) Loh, C. C. J.; Raabe, G.; Enders, D. *Chem. Eur. J.* **2012**, *18*, 13250; (e) Horning, D. B.; MacMillan, D. W. C. *J. Am. Chem. Soc.* **2013**, *135*, 6442; (f) Laforteza, B. N.; Pickworth, M.; MacMillan, D. W. C. *Angew. Chem. Int. Ed.* **2013**, *52*, 11269.

<sup>100</sup> Jones, B. S.; Simmons, B.; Mastracchio, A.; MacMillan, D. W. C. *Nature* **2011**, *475*, 183 and references therein

<sup>101</sup> To our knowledge, the only example of asymmetric organocatalytic reaction generating a seven-membered-nitrogen-containing 3,4-ring fused indole is: Cheng, D.-J.; Wu, H.-B.; Tian, S.-K. *Org. Lett.* **2011**, *13*, 5636.

<sup>102</sup> (a) Bernardi, L.; Ricci, A. *Catalytic asymmetric Friedel–Crafts alkylation*, chapter 2.3. Ed Bandini, M.; Umami Ronchi, A. Wiley-VCH, Weinheim, **2009**, 67. Recent reviews on Friedel–Crafts alkylation with therein useful references: (b) Terrason, V.; Marcia de Figuerideiro, R.; Campagne, J. M. *Eur. J. Org. Chem.* **2010**, 2635; (c) Zeng, M.; You, S.-L. *Synlett* **2010**, 1289; (d) Rueping, M.; Nachtsheim, B. J. *Beilstein J. Org. Chem.* **2010**, *6*, 6; (e) Lu, H.-H.; Tan, F.; Xiao, W.-J.; *Curr. Org. Chem.* **2011**, *15*, 4022.

<sup>103</sup> Organocatalytic Michael addition reactions have been already applied in the synthesis of chromenes, thiochromenes and 1,2-dihydroquinilines, see: Bhanja, C.; Jena, S.; Nayak, S.; Mohapatra, S. *Beilstein J. Org. Chem.* **2012**, *8*, 1668.

<sup>104</sup> The preparation of 4-substituted indoles usually requires multistep synthesis. The synthetic difficulties are due to the fact that electrophiles prefer reaction at either 5- or 7- position of indole; for example see: Bronner, S. M.; Goetz, A. E.; Garg, N. K. *J. Am. Chem. Soc.* **2011**, *133*, 3832.

<sup>105</sup> For selected examples of iminium ion promoted Friedel–Crafts reactions see ref. 48 and: (a) Hong, L.; Wang, L.; Chen, C.; Zhang, B.; Wang, R. *Adv. Synth. Catal.* **2009**, *351*, 772; (b) Wang, Z.-J.; Yang, J.-G.; Jin, J.; Lu, X.; Bao, W. *Synlett* **2009**, 3994; (c) Enders, D.; Wang, C.; Mukanova, M.; Greb, A. *Chem. Commun.* **2010**, *46*, 2447; Riguet, E. *J. Org. Chem.* **2011**, *76*, 8143.

<sup>106</sup> Selected examples: (a) Hechavarria Fonseca, M. T.; List, B. *Angew. Chem. Int. Ed.* **2004**, *43*, 3958; (b) Hayashi, Y.; Gotoh, H.; Tamura, T.; Yamaguchi, H.; Masui, R.; Shoji, M. *J. Am. Chem. Soc.* **2005**, *127*, 16028. For reviews see: (c) Vicario, J. L.; Badía, D.; Carillo, L. *Synthesis* **2007**, 2065

<sup>107</sup> (a) Ranganathan, D.; Rao, C. B.; Ranganathan, S.; Mehrotra, A. K.; Iyengar, R. *J. Org. Chem.* **1980**, *45*, 1185; application of nitroethene in asymmetric catalysis: (b) Wiesner, M.; Revell, J. D.; Tonazzi, S.; Wennemers, H.; *J. Am. Chem. Soc.* **2008**, *130*, 5610; (c) Chi, Y.; Guo, L.; Kopf, N. A.; Gellman, S. H. *J. Am. Chem. Soc.* **2008**, *130*, 5608; (d) Bui, T.; Syed, S.; Barbas III, C. F.; *J. Am. Chem. Soc.* **2009**, *131*, 8758; (e) Mitsunuma, H.; Matsunaga, S.; *Chem. Commun.* **2011**, *47*, 469; (f) Mitsunuma, H.; Shibasaki, M.; Kanai, M.; Matsunaga, S. *Angew. Chem. Int. Ed.* **2012**, *51*, 5217.

<sup>108</sup> Selected examples of H-bond catalysis in Friedel–Crafts addition of indoles to nitroalkenes: (a) Herrera, R. P.; Sgarzani, V.; Bernardi, L.; Ricci, A. *Angew. Chem. Int. Ed.* **2005**, *44*, 6576; (b) Zhuang, W.; Hazell, R. G.; Jørgensen, K. A. *Org. Biomol. Chem.* **2005**, *3*, 2566; (c) Ganesh, M.; Seidel, D. *J. Am. Chem. Soc.* **2008**, *130*, 16464; (d) Wang, X.-F.; Chen, J.-R.; Cao, Y.-J.; Cheng, H.-G.; Xiao, W.-J. *Org. Lett.* **2010**, *12*, 1140; (e) Chen, L.-A.; Tang, X.; Xi, J.; Xu, W.; Gong, L.; Meggers, E.; *Angew. Chem. Int. Ed.* **2013**, *52*, 14021; (f) Loh, C. C. J.; Atodiresei, I.; Enders, D. *Chem. Eur. J.* **2013**, *19*, 10822; (g) ref. 100c; (h) ref. 100d.

<sup>109</sup> Selected examples of chiral phosphoric acid catalyzed Friedel–Crafts reactions of indoles with nitroalkenes: (a) Itoh, J.; Fuchibe, K.; Akiyama, T.; *Angew. Chem. Int. Ed.* **2008**, *47*, 4016; (b) Mori, K.; Wakazawa, M.; Akiyama, T. *Chem. Sci.* **2014**, *5*, 1799.

- <sup>110</sup> Selected examples in which acrolein takes part in organocatalytic cascade reaction: (a) Enders, D.; Wang, C.; Mukanova, M.; Greb, A. *Chem. Commun.* **2010**, 46, 2447; (b) Wang, C.; Yang, X.; Raabe, G.; Enders, D. *Adv. Synth. Catal.* **2012**, 354, 2629.
- <sup>111</sup> Schreiner, P. R.; Wittkopp, A. *Org. Lett.* **2002**, 4, 217.
- <sup>112</sup> Mayr, H.; Lakhdar, S.; Maji, B.; Ofial, A. R.; *Beilstein J. Org. Chem.* **2012**, 8, 1458.
- <sup>113</sup> López-Alvarado, P.; Steinhoff, J.; Miranda, S.; Avendaño, C.; Menéndez, J. C. *Tetrahedron* **2009**, 65, 1660.
- <sup>114</sup> Bal, B.S.; Childers, W.E.; Pinnick, H. W. *Tetrahedron* **1981**, 37, 2091.
- <sup>115</sup> Lindgren, B. O.; Nilsson, T.; Husebye, S.; Mikalsen, Ø.; Leander, K.; Swhan, C.-G. *Acta Chem. Scand.* **1973**, 27, 288.
- <sup>116</sup> Patchornik, A.; Lawson, W. B.; Gross, E.; Witkop, B.; *J. Am. Chem. Soc.*, **1960**, 82, 5923.
- <sup>117</sup> Ohnuma, T.; Kimura, Y.; Ban, Y. *Tetrahedron Lett.*, **1981**, 22, 4969.
- <sup>118</sup> Labroo, R. B.; Labroo, V. M.; King, M. M.; Cohen, L. A. *J. Org. Chem.*, **1991**, 56, 3637
- <sup>119</sup> A phosphoric acid catalyzed aza-Henry reaction involving a nitronate intermediate has been reported, however in the presence of an imine as basic component: Rueping, M.; Antonchick, A. P. *Org. Lett.* **2008**, 10, 1731.
- <sup>120</sup> For catalytic enantioselective intramolecular nitro-Michael reactions see: a) Nodes, W. J.; Nutt, D. R.; Chippindale, A. M.; Cobb, A. J. A. *J. Am. Chem. Soc.* **2009**, 131, 16016; b) Vicario, J. L.; Badia, D.; Carrillo, L.; Reyes, E. *Organocatalytic Enantioselective Conjugate Addition Reactions*, RSC, **2010**; c) Dai, D.; Arman, H.; Zhao, J. C.-G. *Chem. Eur. J.* **2013**, 19, 1666; d) Quintavalla, A.; Lombardo, M.; Sanap, S. P.; Trombini, C. *Adv. Synth. Catal.* **2013**, 355, 938.
- <sup>121</sup> Vakulya, B.; Varga, S.; Soós, T. *J. Org. Chem.* **2008**, 73, 3475.
- <sup>122</sup> (a) Anderson, J. C.; Koovits, P.J. *Chem. Sci.* **2013**, 4, 2897; for a Lewis acid variant see: (b) Lu, L.-Q.; Li, F.; An, J.; Cheng, Y.; Chen, J.-R.; Xiao, W.-J. *Chem. Eur. J.* **2012**, 18, 4073; for a discussion on the relevance of the protonation in different type of organocatalytic cycles see: ref. 49a,b,e
- <sup>123</sup> Hirata, T.; Yamanaka, M. *Chem. Asian. J.* **2011**, 6, 510.
- <sup>124</sup> Zheng, C.; Sheng, Y.-F.; Li, Y.-X.; You, S.-L. *Tetrahedron* **2010**, 66, 2875.
- <sup>125</sup> Muchowski, J. M. *J. Heterocyclic Chem.* **2000**, 37, 1293.
- <sup>126</sup> Antoine, M.; Marchand, P.; Le Baut, G.; Czech, M.; Baasner, S.; Gunther, E. *J. Enzyme Inhib. Med.* **2008**, 23, 686.
- <sup>127</sup> Chen, H. et al. *J. Med. Chem.* **2013**, 56, 685
- <sup>128</sup> Relevant reviews on the application *ortho*-quinone methide in organic synthesis: (a) Van De Water, R. W.; Pettus, T. R. R. *Tetrahedron* **2002**, 58, 5367; (b) Weinert, E. E.; Dondi, R.; Colloredo Melz, S.; Frankendield, K. N.; Mitchell, C. H.; Freccero, M.; Rokita, S. *J. Am. Chem. Soc.* **2006**, 128, 11940. (c) Pathak, T.P.; Sigman, M. *J. Org. Chem.* **2011**, 49, 5957; (d) Willis, N. J.; Bray, C. D. *Chem. Eur. J.* **2012**, 18, 9160; (e) Singh, M. S.; Nagaraju, A.; Anand, N.; Chowdhury, S. *RSC Adv.* **2014**, 4, 55924; (f) Bai, W.-J.; David, J. G.; Feng, Z.-G.; Weaver, M. G.; Wu, K.-L.; Pettus, T. R. R. *Acc. Chem. Res.* **2014**, 47, 3655; (g) S. Cao, X. Peng, *Curr. Org. Chem.* **2014**, 18, 70.
- <sup>129</sup> Reports accounting for the chemistry of quinone methides: (a) Chiang, Y.; Kresge, A. J.; Zhu, Y. *Pure Appl. Chem.* **2000**, 72, 2299; (b) Rokita, S. E. *Quinone Methides* Ed., Wiley, New York, **2009** (b) Toteva, M. M.; Richard, J. P. *Adv. Phys. Org. Chem.* **2011**, 45, 39.
- <sup>130</sup> Fries, K.; *Liebigs Ann. Chem.* **1907**, 339, 350.
- <sup>131</sup> McIntosh, C. L.; Chapman, O. L.; *J. Chem. Soc. D* **1971**, 383.
- <sup>132</sup> Amouri, H.; Besace, Y.; Le Bras, J.; Vaisserman, *J. Am. Chem. Soc.* **1998**, 120, 6171.
- <sup>133</sup> Significant reports in which stabilized *o*-QMs were employed in asymmetric settings: (a) Alden-Danforth, E.; Scerba, M. T.; Leckta, T. *Org. Lett.* **2008**, 10, 4951; (b) Lv, H.; You, L.; Ye, S. *Adv. Synth. Catal.* **2009**, 351, 2822; (c) Lv, H.; Jia, W.-Q.; Sun, L.-H.; Ye, S. *Angew. Chem. Int. Ed.* **2013**, 52, 8607; (d) Chu, W.-D.; Zhang, L.-F.; Bao, X.; Zhao, X.-H.; Zeng, C.; Du, J.-Y.; Zhang, G.-B.; Wang, F.-X.; Ma, X.-Y.; Fan, C.-A. *Angew. Chem. Int. Ed.* **2013**, 125, 9399. (e) Caruana, L.; Kniep, F.; Johansen, T. K.; Poulsen, P. H.; Jørgensen, K. A. *J. Am. Chem. Soc.* **2014**, 136, 15929; (f) Adili, A.; Tao, Z.; Chen, D.; Han, Z. *Org. Biomol. Chem.* **2015**, 13, 2247.
- <sup>134</sup> Lv, H.; Jia, W.-Q.; Sun, L.-H.; Ye, S. *Angew. Chem. Int. Ed.* **2013**, 52, 8607.
- <sup>135</sup> Luan, Y.; Schaus, S. E. *J. Am. Chem. Soc.* **2012**, 134, 19965.
- <sup>136</sup> Grayson, M. N.; Godman, J. M. *J. Org. Chem.* **2015**, 80, 2056.
- <sup>137</sup> (a) Zhang, Y.; Sigman, M. *J. Am. Chem. Soc.* **2007**, 129, 3076; (b) Jensen, K. H.; Pathak, T. P.; Zhang, Y.; Sigman, M. *J. Am. Chem. Soc.* **2009**, 131, 17074; (c) Jensen, K. H.; Webb, J. D.; Sigman, M. S. *J. Am. Chem. Soc.* **2010**, 132, 17471; (d) Pathak, T. P.; Glicorich, K. M.; Welm, B. E.; Sigman, M. S. *J. Am. Chem. Soc.* **2010**, 132, 7870; (e) Pathak, T. P.; Sigman, M. S. *Org. Lett.* **2011**, 13, 2774.

- <sup>138</sup> (a) Izquierdo, J.; Orue, A.; Scheidt, K. A. *J. Am. Chem. Soc.* **2013**, *135*, 10634; (b) Lee, A.; Scheidt, K. A. *Chem. Commun.* **2015**, *51*, 3407.
- <sup>139</sup> Yeung, C. S.; Ziegler, R. E.; Porco Jr, J. A.; Jacobsen, E. N.; *J. Am. Chem. Soc.* **2014**, *136*, 13614.
- <sup>140</sup> Rueping, M.; Uria, U.; Lin, Y.-M.; Atodiresei, I. *J. Am. Chem. Soc.* **2011**, *133*, 3732.
- <sup>141</sup> (a) El-Sepelgy, O.; Hasseloff, S.; Alamsetti, S. K.; Schneider, C. *Angew. Chem. Int. Ed.* **2014**, *53*, 7923; (b) Saha, S.; Schneider, C. *Chem. Eur. J.* **2015**, *21*, 2348; (c) Saha, S.; Alamsetti, S. K.; Schneider, C. *Chem. Commun.* **2015**, *51*, 1461; (d) Saha, S.; Schneider, S. *Org. Lett.* **2015**, *17*, 648.
- <sup>142</sup> Hsiano, C.-C.; Liao, H.-H.; Rueping, M. *Angew. Chem. Int. Ed.* **2014**, *53*, 13258.
- <sup>143</sup> Zhao, W.; Wang, Z.; Chu, B.; Sun, J. *Angew. Chem. Int. Ed.* **2015**, *54*, 1461.
- <sup>144</sup> Quasdorf, K. W.; Overman, L. E. *Nature*, **2014**, *516*, 181.
- <sup>145</sup> Chen, M.-W.; Cao, L.-L.; Ye, Z. S.; Jiang, G.-F.; Zhou, Y.-G. *Chem. Commun.* **2013**, *49*, 1660.
- <sup>146</sup> (a) Fochi, M.; Gramigna, L.; Mazzanti, A.; Duce, S.; Fantini, S.; Palmieri, A.; Petrini, M.; Bernardi, L. *Adv. Synth. Catal.* **2012**, *354*, 1373; for recent reviews on alkylideneindolenines from sulfonyl indoles see: (b) Palmieri, A.; Petrini, M.; Shaik, R. R. *Org. Biomol. Chem.* **2010**, *8*, 1259; (c) Wang, L.; Chen, Y.; Xiao, J. *Asian. J. Org. Chem.* **2014**, *3*, 1036; for reviews on in situ generated imines from  $\alpha$ -amido sulfones see: (d) Petrini, M. *Chem. Rev.* **2005**, *105*, 3949; (e) Yin, B.; Zhang, Y.; Xu, L.-W. *Synthesis* **2010**, 3583.
- <sup>147</sup> Ellis, G. P. *The chemistry of Heterocycles, Vol. 31, Chromenes, Chromanones and Chromones*. Wiley-VCH, Weinheim, **2007**
- <sup>148</sup> This proposal was in agreement with previous findings dealing with the formation of *N*-carbamoyl imines from  $\alpha$ -amido sulfones in reactions catalyzed by *Cinchona* derived catalysts or related phase-transfer catalysts: (a) Lou, S.; Dai, S.; Schaus, J.; *Org. Chem.* **2007**, *72*, 9998; (b) Marianacci, O.; Micheletti, G.; Bernardi, L.; Fini, F.; Fochi, M.; Pettersen, D.; Sgarzani, V.; Ricci, A. *Chem. Eur. J.* **2007**, *13*, 8338; (c) Gomez-Bengoia, E.; Linden, A.; López, R.; Mùgica-Mendiola, I.; Oiarbide, M.; Palomo, C. *J. Am. Chem. Soc.* **2008**, *130*, 7955.
- <sup>149</sup> See for exaples: (a) Bissel, P.; Nazih, A.; Sablong, R.; Lepoittevin, J.-P. *Org. Lett.* **1999**, *1*, 1283; (b) McGuire, M. A.; Shilcrat, S. C.; Sorenson, E. *Tetrahedron Lett.* **1999**, *40*, 3293; (c) Chen, G.; Tokunaga, N.; Hayashi, T. *Org. Lett.* **2005**, *7*, 2285; (d) Ulgheri, F.; Marchetti, M.; Piccolo, O. *J. Org. Chem.* **2007**, *72*, 6056 (e) Gallagher, B. D.; Taft, B. R.; Lipshutz, B. H. *Org. Lett.* **2009**, *11*, 5374; (f) Su, Q.; Wood, J. L.; *Tetrahedron Lett.* **2010**, *51*, 4237.
- <sup>150</sup> (a) Kemnitzer, W.; Kasibhatla, S.; Jiang, S.; Zhang, H.; Zhao, J.; Jia, S.; Xu, L.; Crogan-Grundy, C.; Denis, Barriault, N.; Vaillancourt, L.; Tseng, S. B.; Drewe, J.; Cai, S. X. *Bioorg. Med. Chem. Lett.* **2005**, *15*, 4745; (b) Semenova, M. N.; Tsyganov, D. V.; Malyshev, O. R. *Bioorg. Med. Chem. Lett.* **2014**, *24*, 3914.
- <sup>151</sup> Barancelli, D.-A.; Salles Jr., A.-G.; Taylor, J.-G.; Correia, C.-R. D. *Org. Lett.* **2012**, *14*, 6036.
- <sup>152</sup> Modifications: reaction time 18 h, product isolated by standard work up (Et<sub>2</sub>O/H<sub>2</sub>O) and chromatography on silica gel. Maes, D.; Vervisch, S.; Debenedetti, S.; Davio, C.; Mangelinckx, S.; Giubellina, N.; De Kimpe, N. *Tetrahedron* **2005**, *61*, 2505.
- <sup>153</sup> (a) Yang, W.; Du, D.-M. *Org. Lett.* **2010**, *12*, 5450; (b) Cassani, C.; Martín – Rapún, R.; Arceo, E.; Bravo, F.; Melchiorre, P. *Nat. Protoc.* **2013**, *8*, 325.
- <sup>154</sup> (a) Wang, Z.; Ai, F.; Wang, Z.; Zhao, W.; Zhu, G.; Lin, Z.; Sun, J. *J. Am. Chem. Soc.* **2015**, *137*, 383; (b) Dai, W.; Lu, H.; Jiang, X.-L.; Gao, T.-T.; Shi, F. *Tetrahedron Asymm.* **2015**, *26*, 109; (c) Li, M.-L.; Chen, D.-F.; Luo, S.-W.; Wu, X. *Tetrahedron Asymm.* **2015**, *26*, 219; (d) Guo, W.; Wu, B.; Chen, P.; Wang, X.; Zhou, Y.-G.; Liu, Y.; Li, C. *Angew. Chem. Int. Ed.* **2015**, early view DOI: 10.1002/anie201409894; (e) Zhao, J.-J.; Sun, S.-B.; He, S.-H.; Wu, Q.; Shi, F. *Angew. Chem. Int. Ed.* **2015**, early view DOI: 10.1002/anie201500215; (f) Wu, B.; Gao, Chen, M.-W.; Zhou, Y.-G. *Tetrahedron Lett.* **2015**, *56*, 1135.
- <sup>155</sup> Recent reviews on  $\alpha$ -alkylation of aldehydes: (a) Vesely, J.; Rios, R. *ChemCatChem* **2012**, *4*, 942; (b) Hodgson, D. M.; Charlton, A.; *Tetrahedron* **2014**, *70*, 2207.
- <sup>156</sup> Selected examples: (a) Cozzi, P.G.; Benfatti, F.; Zoli, L. *Angew. Chem. Int. Ed.* **2009**, *48*, 1313; (b) Benfatti, F.; Capdevila, M. G.; Zoli, L.; Benedetto, E.; Cozzi, P. G. *Chem. Commun.* **2009**, 5919; (c) Benfatti, F.; Benedetto, E.; Cozzi, P. G. *Chem. Asian J.* **2010**, *5*, 2047; (d) Zhang, L.; Cui, L.; Li, X.; Li, J.; Luo, S.; Cheng, J.-P. *Chem. Eur. J.* **2010**, *16*, 2045; (e) Stiller, J.; Marques Lopez, E.; Herrera, R. P.; Fröhlich, R.; Strohmam, C.; Christmann, M. *Org. Lett.* **2011**, *13*, 70; (f) Xiao, J.; *Org. Lett.* **2012**, *14*, 1716. (g) Xiao, J.; Zhao, K.; Loh, T.-P. *Chem. Commun.* **2012**, *48*, 3548; (h) Trifonidou, M.; Kokotos, G. C. *Eur. J. Org. Chem.* **2012**, 1563. For a review on the employment of diary alcohol for the  $\alpha$ -alkylation of aldehydes see: (i) Gualandi, A.; Cozzi, P.G. *Synlett* **2013**, 281.
- <sup>157</sup> Brown, R. A.; Kuo, W. H.; Jacobsen, E. N. *J. Am. Chem. Soc.* **2010**, *132*, 9286.
- <sup>158</sup> The example shown in Scheme 68 can be found in: (a) Oppolzer, W.; Moretti, R.; Thomi, S.; *Tetrahedron Lett.* **1989**, *30*, 5603. For a review exemplifying the use of SAMP and RAMP chiral

- auxiliaries in the alkylation of carbonyl compounds see: (b) Job, A.; Janeck, C. F.; Bettray, W.; Peters, R.; Enders, D. *Tetrahedron* **2002**, *58*, 2253.
- <sup>159</sup> Alba, A.-N.; Viciano, M.; Rios, R. *ChemCatChem* **2009**, *1*, 437.
- <sup>160</sup> Nicewiz, D. A.; MacMillan, D. W. C. *Science* **2008**, *322*, 77.
- <sup>161</sup> For other relevant examples in which  $\alpha$ -alkylated aldehydes are obtained by means of a combination of organocatalysis and photoredox catalysis see: (a) Arceo, E.; Jurberg, I. D.; Álvarez-Fernández, A.; Melchiorre, P. *Nat. Chem.* **2013**, *5*, 750; (b) Arceo, E.; Bahamonde, A.; Bergonzini, G.; Melchiorre, P. *Chem. Sci.* **2014**, *5*, 2438.; (c) Riente, P.; Adams, A. M.; Albero, J.; Palomares, E.; Pericàs, M. A. *Angew. Chem. Int. Ed.* **2014**, *53*, 9613; for a review see: (d) Prier, C. K.; Rankic, D. A.; MacMillan, D. W. C. *Chem. Rev.* **2013**, *113*, 5322.
- <sup>162</sup> Vignola, N.; List, B. *J. Am. Chem. Soc.* **2004**, *126*, 450.
- <sup>163</sup> List, B.; Čorić, I.; Grygorenko, O. O.; Kaib, S. J. P.; Komarov, I.; Lee, A.; Leutzch, M.; Pan, S. C.; Tymtsunik, A. V.; Van Gemmeren, M. *Angew. Chem. Int. Ed.* **2014**, *53*, 282
- <sup>164</sup> Shaik, R. R.; Mazzanti, A.; Petrini, M.; Bartoli, G.; Melchiorre, P. *Angew. Chem. Int. Ed.* **2008**, *47*, 8707.
- <sup>165</sup> Mayr, H.; Patz, M. *Angew. Chem. Int. Ed.* **1994**, *33*, 938.
- <sup>166</sup> Streidl, N.; Denegri, B.; Kronja, O.; Mayr, H. *Acc. Chem. Res.* **2010**, *43*, 1537.
- <sup>167</sup> For a review see: Csáký, A. G.; de La Herrán, G.; Murcia, M.C. *Chem. Soc. Rev.* **2010**, *39*, 4080.
- <sup>168</sup> Chu, W.-D.; Zhang, L.-F.; Bao, X.; Zhao, X.-Y.; Zeng, C.; Du, J.-Y.; Zhang, G.-B.; Wang, F.-X.; Ma, X.-Y.; Fan, C.-A. *Angew. Chem. Int. Ed.* **2013**, *52*, 9229.
- <sup>169</sup> Saleh, S. A.; Tashtoush, H. I. *Tetrahedron* **1998**, *54*, 14157.
- <sup>170</sup> Quintard, A.; Langlois, J.-B.; Emery, D.; Mareda, J.; Guénée, L.; Alexakis, A. *Chem. Eur. J.* **2011**, *17*, 13433 and references therein.
- <sup>171</sup> Aldehydes **2d-h** were synthesised according to: (a) Gualandi, A.; Emma, M.G.; Giacoboni, J.; Mengozzi, L.; Cozzi, P.G. *Synlett* **2013**, *4*, 449. Aldehydes **2i** was synthesised according to: (b) Henninger, T.C.; Macielag, M. J.; Tennakoon, M. A.; Xu, X. *US2003/220272 A1*, **2003**.
- <sup>172</sup> Martínez, J.; Reyes, E.; Uria, U.; Carrillo, L.; Vicario, J. L. *ChemCatChem* **2013**, *5*, 2240.
- <sup>173</sup> Uria, U.; Vicario, J. L.; Badia, D.; Carrillo, L.; Reyes, E.; Pesquera, A. *Synthesis* **2010**, *4*, 701. (b) Tsuda, T.; Senba, N.; Uratani, T. *US2013/253228 A1* **2013**.
- <sup>174</sup> (a) Alza, E.; Sayalero, S.; Kasapar, P.; Almaşi, D.; Pericàs, M. A. *Chem. Eur. J.* **2011**, *17*, 11585; (b) García-García, P.; Ladépêche, A.; Halder, R.; List, B. *Angew. Chem. Int. Ed.* **2008**, *47*, 4719.